University of Strathclyde

A Mechatronic Design Synthesis for Very Low Flow Control Valves

by

Rémi C. Zante

This thesis is submitted to the University of Strathclyde in fulfilment of the requirement for the Degree of

Doctor of Philosophy

Department of Design, Manufacture and Engineering Management

2008

Acknowledgements

Many People have contributed to the successful completion of this thesis and I would first of all like to thank my supervisor Dr. Xiu-Tian Yan for giving me the opportunity to undertake this work in the first place and for his continued support and guidance over the course of my research and not least for ensuring that I was adequately funded for the duration. Thanks also go to all those at Scottoiler for supporting this research and particularly Rory for the time spent on the industrial oiler and ensuring that this research will be put to future use and to Rachel for her knowledge on the inner workings of the RMV and asking all the right questions.

I would also like to extend particular thanks to Dr William Dempster of the Department of Mechanical Engineering for his invaluable guidance and advice at a critical points in this research and particularly for his help in developing the analytical model of valve flow described in this thesis.

Hearty thanks are extended to all the technicians who contributed to the successful trial of the prototype oiler systems and flow measurement rig, in a particular Mr Donnie Macleod, Mr Barrie Hunter and Mr Dino Bertolaccini.

Thanks also go to all the other researchers who I have worked alongside for providing a welcome distraction when necessary and also practical advice on how to complete a PhD. Thanks to Colin for providing a sympathetic ear concerning the difficulties of conducting practical based research.

Lastly I would like to thank my wife Susan for her unfaltering support over the duration of my study and for managing to stay awake while proof reading this thesis after a long day at work.

Abstract

The means by which the control of very low flows in the region of 0.1-400ml/hr using valves with microchannels (<250μm) is not well defined. This work presents a review of existing literature that contributes to the understanding of controlling very low flows. Mechatronic principles are used to bring new understanding to the field of very low flow control using needle valves. Flow rate experiments were conducted using a mechatronically controlled needle valve and a novel flow measurement device constructed for the purpose, from which an analytical flow model is developed. Details of a linear actuated needle valve are given along with open loop and closed loop control systems developed for the purpose of accurately controlling very low flows. The open loop system is derived from the valve operating principles enabling an efficient method of modelling the valve flow characteristics for the purpose of control. The closed loop method, incorporating gain scheduling is capable of controlling flows to within 0.0016ml/hr at low flows. A prototype lubricant dispensing system using a low flow needle valve was tested in an industrial environment. A design synthesis is developed by consolidating the knowledge gained from these studies is presented. This discusses the all main factors affecting the design and operation of needle valves for the control of very low flows while describing practical solutions to the problems commonly encountered.

Contents

List of Figures

List of Tables

Common Symbols

In general the following symbols have been standardised throughout this thesis. In the case where equations have been quoted from other authors' work and their definitions vary from those here, the symbol definitions are quoted directly after the equation. The units quoted are for the purpose of calculations. Other units may be used during discussion where convenient. In most cases the SI unit system is used.

Symbol	Quantity	Dime-nsion	Unit
General values			
A	Area, cross section of flow channel	L^2	m^2
b	Distance between centres of eccentric annular flow. The level of eccentricity of a core in a pipe.	L	m
C	Generally denotes a form of flow coefficient for a valve although definition varies according to use. e.g. C_v	n/a	n/a
C_i	A temporary value of C used in iterative calculations of C_v	n/a	n/a
C_v	the number of US gallons of water, within a temperature range of 40 ºF to 100 ºF, that will flow through a valve in 1 min when a pressure drop of 1 psi exists	L^3T^{-1}	US Gal/min
D_h	Hydraulic diameter. $=4A/p$	L	m
dP	Differential pressure	$ML^{-1}T^{-2}$	kPa
dh	Refer to h	L	m
E	Engagement length. The length of valve needle of working diameter engaged in the valve orifice.	L	m
f	Fluid friction	$ML^{-1}T^{-2}$	kPa
g	Gravitational constant	LT^{-2}	m/s^2
G_v	Valve coefficient for gravity fed needle valve. Defined as the gradient of the Q/dP plot.	n/a	n/a
GG_v	Gradient of the G_v as a function of valve position. G_v/VP or G_v/E	n/a	n/a

h	Fluid column height. Also known as *dh*, the differential height between reservoir surface and nozzle outlet	L	m
K	Flow coefficient for the generic form of the orifice flow equation	n/a	n/a
K_v	Metric version of C_v. $K_v=0.865C_v$	n/a	n/a
m	mass	M	kg
nl	Nano litre	L^3	litre
p	Perimeter of flow channel	L	m
P	Pressure	$ML^{-1}T^{-2}$	kPa
Q	Volume flow rate (use of 'flow rate' in this thesis refers to volume flow rate).	$L^3\ T^{-1}$	l/s
Q_c	Flow rate though a concentric annular channel	$L^3\ T^{-1}$	l/s
Q_m	Mass flow rate	$M\ T^{-1}$	kg/s
Re	Reynolds number	n/a	n/a
Re_c	Reynolds number for concentric annular flow	n/a	n/a
t	Temperature	n/a	°C
T	time	T	s
T_p	Drip period (Time Period). The time interval between drips	T	s
u	Mean fluid velocity	LT^{-1}	m/s
v	Kinematic Viscosity		cSt
V_d	Drip Volume	L^{-3}	m^3
VP	Valve position, position of adjuster dial	n/a	n/a
ρ	Density of fluid	ML^{-3}	Kg/m^3
σ	Surface tension	MT^{-2}	N/m
μ	Dynamic Viscosity	$ML^{-1}T^{-1}$	kg/ms

Flow Channel Geometry Definitions

d_a	Needle diameter	L	m
d_m	Hydraulic Mean Diameter. Used in the calculation of Reynolds number for non-circular conduits.	L	m
d_o	Orifice Diameter	L	m
h_1	Channel height = r_o- r_a	L	mm
r_a	Radius of valve needle in section A of profile	L	mm
r_b	Radius of valve needle in section B of profile	L	mm

r_n	Radius of drop nozzle diameter. Used for the estimating drop volume.	L	mm
r_o	Radius of orifice	L	mm
W	Channel Width equivalent to the circumference of channel midpoint.	L	mm

Spring Force Calculation Definitions

A_a	Cross sectional area of air gap	L	m
I	Current through coil	n/a	Ampere
F	Spring force	MLT^{-2}	N
F_S	Solenoid force	MLT^{-2}	N
k_{RMV}	Spring constant, RMV	MT^{-2}	N/m
k_C	Spring constant, solenoid spring	MT^{-2}	N/m
N	Number of turns of coil	n/a	n/a
x_C	Centre spring travel	L	m
x_{RMV}	RMV travel	L	m
x_T	Total travel	L	m
X	Solenoid extension	L	m
ξ	Permeability of air	n/a	N/A

Flow Control Definitions

T_pa	Actual flow in terms of drip interval
T_pd	Desired flow in terms of drip interval
S_na	Actual step number. The number of stepper motor steps from datum.
S_nd	Desired step number. The number of stepper motor steps from datum.
S_nk	Step correction
G	Gain.

Glossary

Active Channel	The narrowest point of the valve flow stream. Controls flow rate.
Analytical Model	A representation of a physical system built up from first principles and mathematical symbols.
CFD	Computational Fluid Dynamics. A numerical finite element method of studying fluid flow.
Computational Model	A computer based simulation of a physical system. In this case CFD.
cSt	Centi-Stokes. 100 Stokes
Data Model	A mathematical equation that represents or fits a set of experimentally derived data. An empirical model.
Frustum cone	A cone with the top portion removed to leave a circular plane.
ISO VG	International Standards Organisation Viscosity Grade
LARMV	Linear Actuated Reservoir Metering Valve
Mechatronics	A product, or the discipline of, integrating Mechanical, Electronic and Computer systems into a single system.
MEMS	Micro Electrical Mechanical Systems
Needle	See Plug
Orifice	See Seat
PIC	Programmable Intelligent Computer. A microcontroller chip produced by Microchip Technology Inc.
Plug	The variable portion of a valve that controls the flow. i.e. the needle in a needle valve
Seat	The stationary part or orifice against which the plug acts to control flow. In a traditional valve it is also the surface against which the plug fits to seal the valve shut.
Trim	Refers to the Plug and Seat combination; e.g. equal percentage shaped plug, or needle. or Valve type; e.g. Gate, butterfly, ball etc
RMV	Reservoir Metering Valve
St	Stoke, unit of measurement of Kinematic viscosity
VI	Virtual Instrument. National Instruments proprietary file format for LabVIEW
VMM	Vision Measuring Machine. An optically based precision measuring machine.
μm	Micron or Micrometer. 1/1000,000 of a meter

Key Values

The following key values help place the context of this work in terms of the physical dimensions of the key components and also the resulting flow rates.

Channel Height	17-250µm
Channel Width	~4.68mm
Channel Length	0-3.2mm
Mechanical displacement	~2mm
Needle Step Size	6.25µm

Drip interval flow measurement:				
	T_p Seconds	**ml/hr**	**months /litre**	**Note**
Minimum	<1500 sec	0.0045	312	Actual lower limit has not yet been determined
Maximum	0.2	400	2.5	
Range	>3500:1			
RMV controllable flow rates:				
Minimum	700	0.1	14	As achieved by automatic control
Maximum	0.2	400	2.5	Limited by measurement device
Range	900:1			

1 Introduction

1.1 Need for controlled flow

The need for this research program stems from the industrial partner involved in the research. Scottoiler Ltd. is a world leader in motorcycle chain lubrication systems. Their Reservoir Metering Valve (RMV) is an automatically activating needle valve triggered by a connection to the air inlet manifold of the motorcycle engine. It was first launched over twenty five years ago and has benefited from continual improvement ever since. However, while the RMV in its original form is well suited to the purpose for which it was conceived it is ill-suited to serving emerging markets in the industrial domain such as chain driven machinery and plant equipment.

With the new markets comes a much wider variety of operational environments requiring a more flexible actuation and flow adjustment mechanism and the ability to dispense lubricants of varying viscosity. Using a mechatronic approach to redesigning the RMV offers the potential to significantly increase the flexibility and stability of lubricant flow. Mechatronics is more than the combination of mechanical and electronic elements as the name suggests. It encompasses an integrated approach to solving complex problems through the intelligent control of simple mechanical elements rather than increasing mechanical complexity. This centres on modelling the physical systems to be controlled and simultaneously designing the mechanical elements and control systems on the basis of the models.

While this research is centred on a solution to a particular application, there are wider flow control domains that can benefit from this research. Efficient lubricant flow is characterised by a continuous low flow of a viscous fluid [1]. Controlling very low

flows in turn requires very small geometric features, which generates a common ground with microfluidic devices and microelectromechanical systems (MEMS). Micro fluid control is required for micro heat exchangers for cooling electronic circuits, reactors for separating biological cells, blood analysers, drug delivery and cell based analysers to name but a few applications [2, 3]. What differentiates this problem from MEMS is the combination of scales. While MEMS tend to focus on reducing the scale of the whole system, this research focuses on the fusion of two scales. In this way macro-scale technology is used to control microscale geometries and in doing so controls micro-scale fluid flow. In this way, the advancements made by this study in the modelling of flow in micro-channels is directly applicable to microfluidic devices and the research as a whole benefits applications that require the control of very low flows.

Much of what makes this problem interesting is that it stands at the juncture of two different scales; the macro world where objects can be seen, touched and understood directly by a person as they are clearly visible to the naked eye, and the micro world were the sizes that become important are often a fraction of the width of a human hair. The term *micro* can be applied to any device with prominent features below 100μm [4]. In this case we have a macro-mechatronic system used to control micro-scale geometry for the purpose of controlling fluid flow. This study looks at the ability of a valve with minimum flow channel dimensions of 17-250μm to be able to accurately control extreme levels of fluid flow; in the region of 0.1 to 400ml per hour. This is the equivalent to a flow of 14months/litre to 2.5hours/litre.

1.2 Need to understand flow parameters

The key to being able to accurately and consistently control low fluid flows is to establish the link between valve geometry and the flow characteristics of the valve. Once this has been accomplished it is then possible to develop the mechanical and control elements required to manipulate the valve geometry to achieve the desired flow rate. What makes this problem such a rich source of research subject matter is that there are many other factors that conspire to adversely affect the flow rate, in which case, these factors need to be identified, quantified and accounted for in the mechanism and control system. The models that describe the relationships between the various factors are described in detail in this thesis and form the basis of the contribution to knowledge of this work.

Although needle valves have been around a long time there is very little literature available that explains the critical functions of a needle valve and how one might not only create a correctly functioning valve, but one that is optimised for its intended use. This is especially the case for very low flow valves. This thesis goes some way towards filling the gap in current literature. While the understanding that would allow a fully optimised valve is still some way off, this thesis explores the critical factors affecting gravity fed needle valve performance and describes various means of achieving levels of flow control desirable for a variety of commercial uses.

This new understanding builds on existing ideas developed in a variety of fields in literature combined with the detailed study and adaptation of an existing flow control-valve. A comprehensive review of literature has identified concepts and ideas from a wide range of fields that can be brought to bear on the problem at hand. It has also highlighted the crucial areas where the existing literature is deficient.

Recent studies [5, 6] show that although the flows and geometries involved are very small, they are still within the continuum range of fluid mechanics and so there is no need to resort to molecular level fluid principles. As such the problem lies within a boundary of the fluid mechanics field that is well understood. However, what is not known, is how to apply the standard theory and what form the solution should take. Much of this thesis is devoted to defining the problem and investigating what tools are appropriate for analysing the problem. Through extensive testing and measurement undertaken as part of this study, a great deal of understanding has been accumulated regarding the factors affecting valve performance. An attempt has been made to convey the most relevant aspects, particularly where there are implications to the generic performance of valves and also where there is a knock on effect in subsequent testing or analysis. Presenting raw data has been avoided in favour of analysis and conclusions that are judged to be of greater significance. Many graphs are included as a means of illustrating particular performance characteristics and can be seen as a visual representation linking physical characteristics (such as geometry, pressure or temperature) with the subsequent performance. These are then interpreted such that an overall picture can be built up of the factors affecting flow performance. Where possible particular characteristics have been investigated and described using a variety of modelling techniques including computational fluid dynamics (CFD) and mathematical modelling.

1.3 Thesis Outline and Contribution

The following chapters of this thesis includes a comprehensive literature review in Chapter 2, a description of the methodological approach to the research in Chapter 3, a description of the experimental equipment used for the analysis in Chapter 4, details

of the development of the theoretical models that govern flow rate in Chapter 5, a description of the hardware and control systems developed to control low flow rates in Chapter 6, the consolidation of the knowledge gained to develop a design syntheses for low flow control valves in Chapter 7 and finally conclusions in Chapter 8.

The literature review (Chapter 2) describes the problems with traditional control valve theory and why it is not applicable to very low flows. Also covered is the lack of theory relating flow channel geometry to valve flow characteristics. Existing flow channel models are investigated as a means of contributing to a solution for controlling the valve flow and finally the means of measuring very low flows is reviewed.

The research methodology and research tools are discussed in Chapter 3. The contribution that a model based methodology can make to a mechatronic development is highlighted along with the model types that are required in order to be able to meet the multiple requirements of a mechatronic system.

The reservoir metering valve (RMV) is introduced in Chapter 4 along with a description of the development of a novel flow measurement device capable of measuring very low flows. The development of a temperature controlled chamber for conducting temperature related experiments is also described. This is followed by a description of the detailed measurements made of each valve to ensure compliance with the theoretical flow models.

The valve flow models are developed in Chapter 5. This includes models for fluid viscosity, pressure head and most significantly the channel geometry. Various possible channel configurations are explored using analytical models and

computational fluid dynamics (CFD) simulation and verified against experimental test data.

A number of mechatronic developments are described in Chapter 6. This includes the development of two prototype automatic oiler systems, their installation and testing in an industrial setting. The design and build of a mechatronically controlled version of the RMV is described followed by performance testing. Two control systems are developed based on open and closed loop control. The former makes use of the novel flow measurement device described in Chapter 4, while the latter describes a system for characterising valve flow for the purpose of flow sensorless control.

Chapter 7 consolidates the knowledge developed in the previous sections in a design synthesis. All the relevant parameters relating to the accurate control of low flow fluids are explored. Particular attention is given to describing the effects flow channel geometry has on the mechanical aspects of valve design and the subsequent control issues. A factor analysis is performed as a means of highlighting the relative sensitivity of the design to changes in the most important influencing factors. Recommendations are made to aid designers to create robust designs and insulate the design from unwanted noise while at the same time boosting desired characteristics. The formulas developed can be used to change the flow characteristics of a valve for different application requirements without the need to redevelop control systems.

The contributions of this thesis are detailed below:

1. **Literature review Chapter 2:** A review of the state of the art and related disciplines that shed light on very low flow control. This consolidates all existing literature that can be brought to bear on the problem of very low flow in control valves.

2. **Very low flow measurement Chapter 4:** The development of a novel low flow measurement system, including testing and calibration. This novel low cost device can be used to measure extremely low flow rates and is unique in its ability to continuously measure flows of 0.0045-400ml/hr thereby showing exceptional rangeability. The linear relationship between volumetric flow rate and drip interval is a critical part of the functionality of the drip interval measurement device and as far as the author is aware is previously unpublished.
3. **Development of valve theory-Chapter 5:** Valve theory is developed to include very low flow of viscous fluids. There is no published literature linking valve geometry with flow characteristics. Valve style modifiers are used for valve size calculations, but no published literature on how to create specific flow characteristics exists. However this should be relatively straight forward as it is solely dependant on orifice area if the flow is in the turbulent domain, as such; this is what existing theory focuses on. However, there is no indication how one might go about designing a valve shape for a low flow laminar conditions. This thesis extends valve flow theory to cover the laminar regime and makes a link between valve geometry and flow characteristics.
4. **Flow control model Chapter 6:** The means by which a valve flow characteristics can be efficiently modelled with the minimum of testing and implemented in a flow control model. This flow sensorless open loop system is inherently more efficient and more flexible than other feed forward control models such as data mapping and neural networks. The reliability of the model is such that is it sufficient for most lubricant dispensing applications.
5. **Mechatronic Developments Chapter 6:** Whilst linear actuated valves are undoubtedly not novel, there is currently no comprehensive description of the design, build and evaluation of a linear actuated microflow control valve. This extends to the design, evaluation and description of the mechatronic system in which the valve operates.
6. **Design synthesis Chapter 7:** There is no literature discussing the critical parameters of needle valve design or explanation of their characteristics. For example, why they can be so temperamental and difficult to control and why they are still in use despite this. This thesis brings to bear all relevant current knowledge on the design of needle valves. The characterisation of valve flow

for the purposes of the design of needle valves based on practical test results, computational analysis & mathematical analysis. This incorporates all the knowledge relating to the function of valves and the inherent factors that affect flow rate.

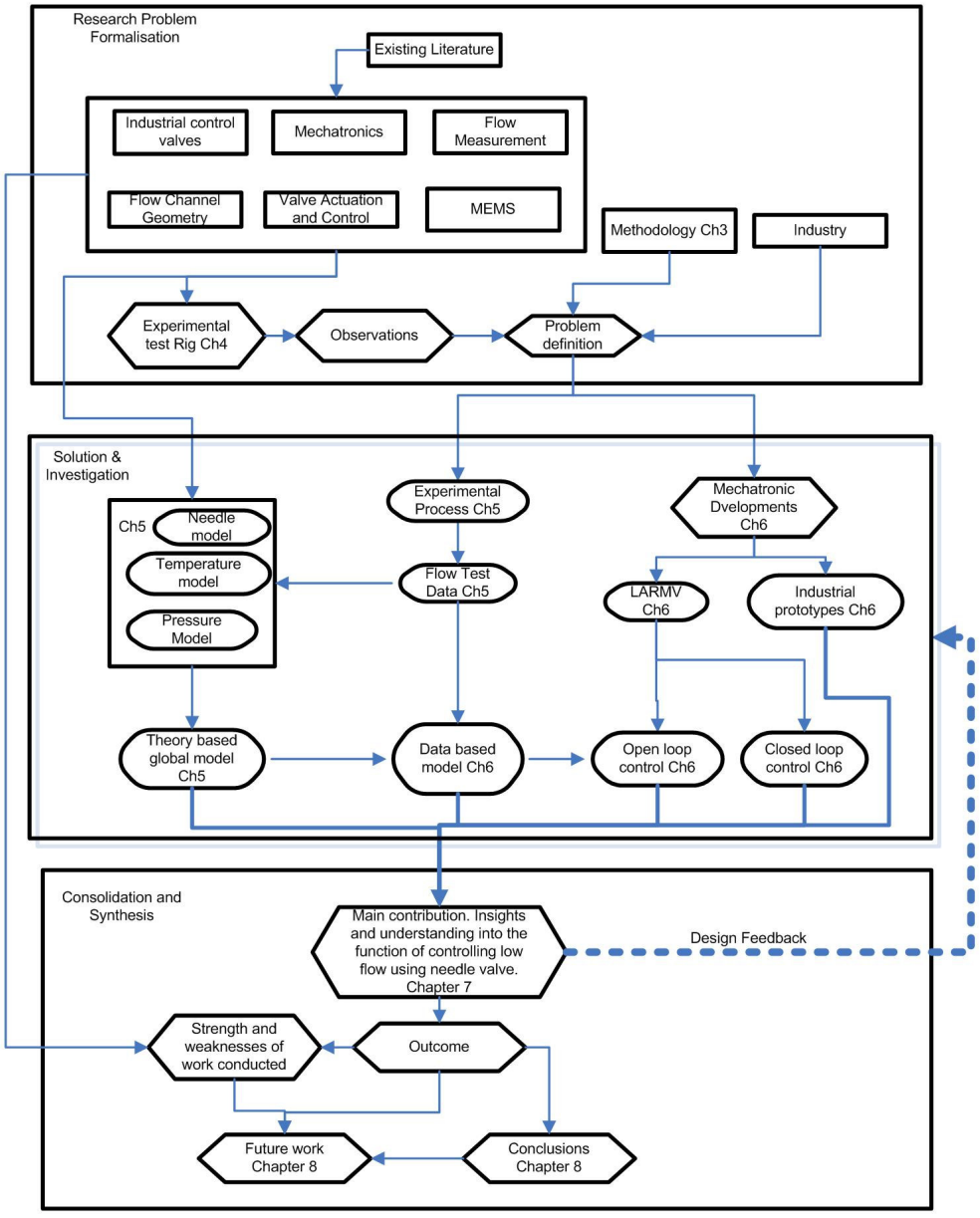

Figure 1-1 Thesis structure diagram

2 Literature Review

2.1 Introduction

There is a trend towards intelligent functionality through increased use of mechatronic concepts [7]. One of the key elements to mechatronic systems engineering is the use of physical/mathematical models, defined as the physical understanding of systems and component behaviour. [7].

While there is no universally accepted definition of mechatronics, it can generally be described as the synergistic integration of electronic engineering, mechanical engineering, control engineering, information technology and informatics, with the keywords being "synergistic integration" [8]. Simultaneous design is required of mechatronic systems because the mechanical system influences the design of the electronic system, and vice versa [9].

There are different ways of dividing up the constituent domains of mechatronics such as that proposed by Cetinkunt [10] who divides the domains into; Mechanical Technology, Electrical Technology and Computer Technology. Alternatively Isermann [9] uses the divisions; Mechanics and Electro-mechanics, Electronics and Information Technology.

In addition to the traditional mechatronic domains just described, there are the physical domains specific to intelligently controlled valve flow. The interface of each must be accounted for if the whole system is to function correctly. This is split into three main system interfaces:

- Mechanical-Fluid
- Electronic-Mechanical
- Fluid-Electronic

Whilst the literature review encompasses all domains that have a bearing on the current problem, all topics investigated add insights into at least one of these three interfaces. Roughly speaking, the three interfaces selected can be represented by the following physical entities:

- Mechanical-Fluid: The valve body. The means by which the fluid flow is controlled by altering the flow channel geometry and is common to nearly all control valve types. This is normally achieved through some form of linear or rotational movement. A critical part of valve design and operation is the understanding of the relationship between mechanical movement and the resultant effect on flow rate. This movement may be achieved manually (normally through some form of gearing system) or via an actuator in a mechatronic system.

- Electronic-Mechanical: Valve control. There are two stages to the next step of flow control. The first is the ability to change the mechanical position of the valve via the actuator to a known position. The second is the ability to intelligently control the actuator position in response to the user command of desired flow rate whilst considering other variables such as current flow rate, pressure and temperature. This is normally embodied by programmable logic control and the electrical circuits associated with controlling the valve actuator.

- Fluid-Electronic: Flow measurement transducer. In order for a system to respond dynamically or to be able to investigate system dynamics, it is normally necessary to be able to directly measure the flow variable. In this study, the transducer is able to convert flow directly in to electrical signal form using a piezo-electric disc.

The nature of a mechatronic problem is such that it crosses traditional functional disciplines and because of this there is a wide variety of sources of information that relate to problem of controlling very low viscous flows. The relevant aspects of these disparate areas are contained within this literature review. This includes previous investigations carried out by students within the department and Scottoiler's expertise gained from many years of developing the product. Other sources of information include existing control valve theory, particularly relating to industrial control valves and hydraulic control valves. Due to the scale of the flow channel geometry involved in controlling very low flows there are significant synergies with Micro Electrical Mechanical Systems (MEMS) and the study of flows in very small channels. A review is also undertaken of the mathematical analysis of flow within channel geometries that have a bearing on the analysis of flow within the valve.

A significant aspect of investigating the control of very low flows is the ability to accurately measure very low flow rates and so the review includes a survey of measurement methods. Through the course of this research, a flow rate measurement method was devised based on timing the intervals of drips issuing from a nozzle. As a result, the dynamics of drip formation relating to drip volume

is covered here as well as the relevant aspects of drip formation research equipment.

2.2 Previous studies

In addition to the ongoing development conducted at Scottoiler, there have been three significant studies investigating the flow properties of the RMV in relation to oil valve position, viscosity and temperature. As these were the first documented attempts at systematic study of flow properties, much can be learnt from the methods used and the problems faced, although the results generated are of limited use, for reasons that will be described.

The first was conducted by Crosson in early 2002 [11] and was principally concerned with the CAD modelling of the RMV using the open source modelling software Open CASCADE, however as part of the study an investigation of the flow properties of the valve was conducted for three different oil viscosities at 5°C, 10°C and 15°C. This data gathering exercise must have required considerable patience and determination as it consisted of manually timing over 800 data points with some drip intervals over six minutes, while located at a commercial drinks' cooler in a pub.

The second was a study conducted by Casey in late 2002 [12] whose main aim was RMV flow rate prediction through the use of computational techniques. He conducted a study into the feasibility of using both computational fluid dynamics and neural networks through the use of simplified cases. As part of this study he also measured the drip intervals in a similar vein to Crosson but at 30°, 35°C, 40°C, and 45°C.

The third study by Du in September 2003 [13] is a continuation of Casey's CFD and neural network study and includes a more detailed analysis. Neural network training

and CFD verification is based on Crosson and Casey's data. The study aims to provide design information for reducing the effects of viscosity changes on flow rate by using the neural network to predict flow rate as a function of fluid temperature and orifice area. The study concluded that neural network flow rate prediction is possible but that the actual results were inconclusive mainly due to the quality of the data.

Poor understanding of the main variables affecting experiment performance means that the data produced by Casey and Crosson is of limited use and can be summarised as:

-The experimental procedure was not closely defined. There are a number of variables which are known to affect drip intervals but which were not noted for the experiments. Of particular importance is the fluid gravity head which has a direct effect on flow rate and the drip nozzle geometry which affects drip size and therefore the drip interval for a given flow rate.

- Unknown valve tolerancing including valve mechanism and needle geometry. Although "identical" valves were used, individual units are known to have different flow characteristics depending on their construction. Component tolerance is important, particularly that of the needle where tolerances are especially tight.

-The temperature control environment was fairly crude and acknowledged to have affected flow results. Both the refrigerator and the oven were prone to significant temperature fluctuation due to the simple inbuilt thermostatic control.

-The manual method of timing drip intervals is especially laborious and tedious, and so is prone to human error. With drip intervals ranging from one second to over six minutes accurate timing requires a high level of patience and concentration.

While these results are good at highlighting qualitative trends, the deficiencies in the experimental process mean that it is not possible to use the data in a quantitative analysis. However, these studies are valuable sources of information when designing further experiments and the methods used in this study are based on the above works with each of the deficiencies addressed.

2.3 Flow Channels and Control

Flow control can be achieved in a number of ways, the most common of which are, the modulation of the active pumping mechanism or alternatively, restricting the flow from a positive pressure source such as a pump or a higher pressure area of the system, such as caused by a boiler or gravity head.

2.3.1 Valves & Valve Flow Theory

A valve can be defined as any device that shuts off, starts, regulates, or controls the flow of a fluid and as such includes a vast range of devices designed to perform one of these functions in innumerable applications. The common functions for valves are [14]:

1- Starting and stopping flow

2- Preventing reverse flow

3- Changing flow direction

4- Regulating flow volume

5- Limiting fluid pressure.

Many valves are bi-state, in that under normal operation they are in one of two states and therefore affect fluid flow in one of two ways. This includes on/off control valves, pressure relief valves and flow direction control valves. An important distinction must be made between bi-state valves and those that require proportional control. Proportional control valves are required to function at the bi-state positions as well as positions in between, which may be either at discrete values or infinitely an infinite number of values. This research is primarily focused on regulating flow volume by variable constriction of the flow in a conduit and so falls into the second category. For the purpose of intelligent control it is necessary to establish the relationship between the variable geometric parameters of the constriction and the corresponding effects on flow rate.

The governing equations for valve flow of both process control-valves [15] and spool type hydraulic control systems [16] are based on the flow through an orifice which can be derived directly from Bernoullli's equation [17] or from dimensional analysis Schashcke [18]. The physical representation of the orifice is a narrowing of the flow channel in a circular pipe, the section with the smallest cross sectional area being the orifice. There is no definitive form of the orifice flow equation as it depends on how the problem is structured but the form given by Schaschke is perhaps the most generic of an incompressible fluid as it is derived from the dimensional analysis:

$$Q = Kd_o^2\sqrt{\frac{dP}{\rho}}$$

Equation 1

Where Q is the volumetric flow rate, dP is the difference in pressure between the upstream and downstream side of the orifice, ρ represents the fluid density, d_0 represents the orifice length scale or diameter if the orifice is circular, as it is squared,

represents the cross sectional area of the orifice. *K* is a flow coefficient that is particular to the specific problem. It corresponds to a form of the Reynolds number and so accounts for viscosity effects, as the Bernoulli equation is related to inviscid flow. *K* takes a different form depending on the field of application. It is normally determined experimentally but can be calculated in some cases as will be discussed later.

In most problems involving fluid flow it is necessary to establish if the flow is laminar or turbulent. The Reynolds number is used to define the flow type that dominates a particular flow problem and is a function of channel size and viscosity. For simple cases, this can be defined as [19]:

$$\mathrm{Re} = \frac{u d_o \rho}{\mu} = \frac{4 Q_m d_o}{A \mu} = \frac{4 Q_m}{\pi d_o \mu}$$

Equation 2

Where Re is the Reynolds number, u is the mean fluid velocity, μ is the dynamic viscosity, Q_m is the mass flow rate and A is the cross sectional area of the flow channel. The transition from laminar to turbulent flow has been experimentally observed to occur in the range 2000<Re<4000. Below Re=2000 the flow is always laminar; above Re=4000 the flow is usually, but not always turbulent [16].

In this way there is a direct link between channel dimensions and flow turbulence. Other versions of the Reynolds number exist, for example the valve Reynolds number Re_v is used to determine if the flow through a valve is turbulent. From the calculations and discussions in Appendix A: BS EN 60534-2-1 Sample Calculation and Appendix F: Reynolds Number Calculation for Concentric Annular Flow, it is clear that the flow characteristic of this study is firmly in laminar regime.

Equation 1 represents flow through an orifice and accounts for viscosity effects through the use of the flow coefficient. While the orifice flow equation (Equation 1) can be derived from Bernoulli's equation, the formula for viscous flow through a conduit can be derived directly from the Navier-Stokes equations. Viscous flow through a pipe called the Hagen-Poiseuille law can be defined as [20]:

$$Q = \frac{\pi d^4 dP}{128 \mu l}$$

Equation 3

In this way, if the flow is known to be laminar, the volumetric flow rate through a conduit can be expressed directly in terms of the conduit dimensions, pressure differential and viscosity. The implications of Equation 1, Equation 3 and their variants on valve flow control will be discussed through this thesis.

2.3.1.1 Needle Valve specific studies

Other than the previous studies detailed in Section 2.2 which relate to the RMV, the literature relating specifically to low flow control through the use of needle valves is limited despite their widespread use. Bryant's investigation into the characteristics of commercial needle valves in 1962 [21] and Takemura in 1975 [22] are two of the few papers dealing specifically with needle valves. Bryant's short study focuses on the "small" quantities of water flowing through needle valves in industrial and laboratory applications. In fact the flow rates studied are in the vicinity of 72000ml/hr, well above the 400ml/hr maximum flow rate considered in this study and certainly well above what could be considered a microflow. His investigation concluded that the sensitivity of a valve could be regulated by varying the inlet and outlet diameters and is largely independent of the valve chamber geometry. The results were obtained

empirically and there is no theoretical basis offered so it is not known if the flow regime was laminar or turbulent.

Takemura [22] found that even with pressure and temperature compensation, needle valves used in hydraulic circuits of machine tools were unable to consistently control fluid flows of less than 200ml/min whereas a positive displacement device using motor driven pistons was able to control flows from 30ml/min up to 3000ml/min. He notes that needle valves have the disadvantage of being influenced by temperature induced viscosity changes in the fluid and that these effects increase as the flow rate decreases.

Takemura mentions needle valve flow calculations in passing. He states that at regular flow levels the standard valve equation can be used while at very low flow rates, an annular flow model should be used although there is no mention of the source or derivation of this model:

$$Q = 1.67x10^{9}.\frac{\Delta P h_1^3 d_o}{vL}$$

Equation 4

Where h_1 is the gap between the core and pipe wall, d_o is the pipe diameter, v is the kinematic viscosity and L is channel length. Flow rate characteristics are shown but no actual values are given.

The very small geometries required for control of small flows means that needle valves are susceptible to dirt and other environmental interferences [23]. This study focuses on the flow reduction effects of oil particle sizes and flow experiments were conducted using a 50μmx10μmx12mm channel. The study does not address the issue of valve flow characteristics in relation to channel geometry.

2.3.1.2 Industrial Control-valves

There are many types of valve used to control liquid flow by restricting a fluid under pressure. On a large scale this includes valves used in the chemical processing industry including ball, gate and butterfly valves [15].

Most literature relating directly to controlling valve sizing dates from the early 60's and may be influenced by the boom in the oil and chemical processing industry as it relates directly to the problems encountered in industrial processing. The work of George Stiles from the early 60' to the late 70's is particularly notable for contributions to the understanding of cavitation and valve sizing [24-28]. Indeed the long standing ISA 75.01 Flow Equations for Sizing Controlling Valves standard is based on his work (BS EN Equivalent: BS EN 60534). However, the standards are not definitive. They are biased towards the large scale and for viscous fluids. H.D. Baumann's work in the field of valve design and analysis started around the same time as Stiles [29] and continuously refined the standards developed by Stiles up until the late 90's [30, 31] as well as a great deal of work on valves in general [32-35]. Contributions were also made on the subject of valve sizing and valve coefficients by Rahmeyer in 1986 [36] and George in 1989 [37].

Essentially simple pipe flow problems can be solved using simple constant mass flow and constant energy principles until the introduction of a complex variable such as a valve is placed in the flow. Here valve weighting factors in the form of the valve coefficient C_v and valve style modifier F_d have to be taken into account. It is because these coefficients are based on experimental procedures and include factors that are references against predetermined experimental curves that they require progressive refinement. The valve coefficient is determined by the pressure drop across the valve

for a given flow rate. This causes particular problems for a gravity fed valve as the pressure on either size of the valve system is atmospheric. The small scale and low pressure involved make measuring low pressures difficult or costly.

The BS EN 60534 test and calculation procedure assumes turbulent flow. Calculations for non-turbulent flow are based on those for turbulent flow with a modifier (Reynolds number factor F_R) to take into account non-turbulent flow. This is most likely to happen with low flow and high viscosities; exactly those of the relating to this study.

BS EN 60534-2-1:1998 and associated standards BS EN 60534-1:2005 and BS EN 60534-2-3:2005 define the process of classifying the flow properties of industrial-process control-valves. The main components comprise of:

- BS EN 60534-1:2005 Control Valve terminology and general considerations [38]
- BS EN 60534-2-1:1998 Flow capacity- Sizing equations for fluids under installed conditions [39]
- BS EN 60534-2-3:2005 Flow capacity-Test procedures.[40]

The purpose of these standards is to "identify the relationships between flow rates, flow coefficients, related installation factors and pertinent service conditions for control valves handling incompressible fluids." BS EN 60534-2-1:1998. The relevant coefficients and factors can be found experimentally or calculated using the equations defined in the standard. Flow rate is defined in terms of the flow coefficient C_v and pressure differential. Therefore in order to be able to specify a valve for an application it is necessary to define C_v. The strict definition of C_v is "represented as the number of

US gallons of water, within a temperature range of 40ºF to 100ºF, that will flow through a valve in 1 min when a pressure drop of 1 psi exists." [38]. The experimental definition of C_v is:

$$C_v = Q\sqrt{\left(\frac{\Delta P_{Cv}}{\Delta P}\right)\left(\frac{\rho}{\rho_w}\right)}$$

Equation 5

Where Q is the measured volumetric flow rate in US gallons per minute, ρ is the density of the flowing fluid in pounds per cubic foot, ρ_w is the density of water within a temperature range of 40ºF to 100ºF in pounds per cubic foot, ΔP is the measured static pressure loss across the valve in psi and ΔP_{cv} is equal to 1 psi. The British Standard and European Norm, specifies a metric equivalent K_v, but this is little used in practice and it is more normal to use a conversion factor of K_v=0.865C_v.

Although there are no stated limits to the applicability of the theory, there are a number of problems when trying to apply this to very small valves. The basic assumption of the standard is that the flow through the valve is turbulent, and while there are correction factors for laminar flow, it is still normally required to determine the turbulent flow parameters before applying the correction factor for laminar flow. The small scale low differential pressures and high viscosities involved in the current study make it impractical to achieve turbulent flow. So while it is impossible to define C_v experimentally, it is at least in theory possible to follow a calculation procedure to define the flow rate using predetermined coefficients and factors.

The main factors involved are:

- Valve Reynolds number Re_v: The Reynolds number for the valve.

- Reynolds number factor F_R: Takes into account the low Reynolds numbers that result from low pressure differentials, viscous fluids and low values of C. As such it applies to cases of non-turbulent flow. If experimentally derived, this is defined as:

$$F_R = \frac{\text{C Laminar Flow}}{\text{C Turbulent Flow}}$$

- Valve style modifier F_d: Takes into account the effect of trim geometry on the Reynolds number. (The trim is the actual valve mechanism. Gate, butterfly needle etc.)

An example showing why the standard valve sizing calculations do not work for very small valves with viscous fluids can be found in Appendix 10.1.The example shows that the negative F_R value results in a negative C_v value which is clearly impossible. The cause of the negative value can be traced to the extremely low Re_v value. Assuming F_L and n_2 are constant Re_v would need to be above 5.21 to generate a positive C value. Therefore the C_v calculation method described in EN 60534-2-1:1998 is only valid for Reynolds Valve numbers above 5.21.

The valve coefficient described above only determines the flow rate at a single valve position and so must be recalculated for each position in the full range of valve travel. As such it does not determine the flow characteristics of the valve. For valve flow control purposes it is important to establish the flow rate at each of the possible valve positions.

A study by Sondh et al. [41] approaches this problem from a slightly different perspective, that of a variable area orifice meter. A valve is subject to the same physical principles as an orifice meter with a variable orifice; therefore a variable area

orifice meter works on exactly the same principle as a control valve except the purposes are reversed. It is worth noting that they state "very little information is available on the design methodology of these meters due to the proprietary nature of the design". The same has been found of valve design. The problem with a traditional fixed orifice meter is that it causes a permanent pressure drop in the system that is proportional to flow rate. Using a variable orifice decouples the pressure drop from the flow rate. Flow measurements are then taken from the movement of the body within the orifice rather than pressure differential (this does beg the question why an orifice is then needed at all and why flow is not just measured from movement of the body?). Their work is based on the differential pressures generated for different flow rates for a frustum cone within a circular orifice. However an important omission in this work is the link between "plug" geometry and flow rate. There is no explanation as to why a frustum cone was used as the basis of the variable orifice. Three types of cone were investigated; a bluff body, one with a hemispherical base and a third with a parabolic top.

The basic theory they present is based on the following equation [41]:

$$Q = \frac{C}{\sqrt{1-\beta^4}} \frac{\pi d^2}{4} \sqrt{2\rho\Delta P}$$

Equation 6

where the discharge coefficient *C* is equal to actual mass flow rate divided by theoretical mass flow rate. The $\frac{\pi d^2}{4}$ term represents the orifice area and the main difference from valve theory is the β value, which represents the ratio of pipe diameter to orifice diameter.

Firstly the flow rates for a range of pressure differentials were plotted for various positions of the cone. It was found that the relationship between pressure and flow rate was non-linear and that the position of the different plots for cone position were not equally spaced. They concluded from this that there was a non-linear relation between flow rate and cone position. It was noted that the frustum cone with hemispheric base and parabolic apex had a more even distribution; no analysis was presented to quantify this relationship. Further plots indicate that there is a generally linear relationship between plug position and flow rate.

Following on from Sondh et al, Singh et al [42] conducted a similar study, but this time making the link between plug geometry and plug displacement. They used a frustum type plug but with parabolic sides such that when the flow equation:

$$Q = \frac{C.A}{\sqrt{1-\beta^4}}\sqrt{2\rho\Delta P}$$

Equation 7

is used, the differential pressure-flow rate relationship remains constant due to the automatic adjustment of the discharge coefficient such that $\frac{CA}{\sqrt{1-\beta^4}}$ remains constant.

The results presented show flow rate against differential pressure for various positions of the plug. The curves for 0-40% engagement are co-located. Above 40% sees a gradual displacement of the $Q/\Delta P$ curve.

Although neither Sondh or Singh define the specific Reynolds numbers for which their work is valid, it is clear from their use of the orifice equation as the basis of their investigation that it is only valid for high Reynolds number problems. However these are two of the few studies to explicitly define the relationship between plug movement and flow rate although in the context of an orifice flow meter.

The only study to define flow rate in terms of valve position in the context of a valve is by Thananchai [43], who investigated the effects of valve area on flow rate and valve constant for a ball valve. Although the traditional coefficient C_v is explained in some detail, it is not actually used for the work and the formula described is for gas flow through a valve despite water being used as the test medium. Instead of using the classical C_v value, Thananchai uses his own simplified derivation of valve constant designated C. Where:

$$\mathrm{Q} = \mathrm{C}(\alpha)\sqrt{\Delta \mathrm{P}}$$

Equation 8

or

$$C(\alpha) = Q/\sqrt{\Delta P}$$

Equation 9

and the valve constant is dependant on the orifice area α.

He found that there was a direct relationship between lnQ and $ln\Delta P$ for each different orifice area.

$$\ln Q = \ln(C(\alpha)) + 1/2\ln(\Delta P)$$

Equation 10

Where the gradient was consistently found to be 0.5 and the y-intercept is equal to the logarithmic value of the valve constant C for each orifice area, α. Comparing Equation 8 and Equation 10 it can be seen that they contradict each other. Equation 8 gives C as the gradient of the line, while in Equation 10, C corresponds to the intercept. From plotting α against C for the experimental data, it can be determined that there is not a linear relationship between C and α. However, it is not clear how Equation 8 is used to advance the understanding of theory. A cross-check against the data shows that it does not accurately predict C values when experimental Q and ΔP

are used. Although the study determines the change in valve constant for the change in orifice area, there is no explicit determination of the reason for this and what orifice shape would be required to linearise the flow characteristic of the valve. However the method for defining the flow characteristics of the valve using the *ln(Q)/ln(ΔP)* plot is worth noting and is adapted for use in this study.

2.3.1.3 Hydraulic Valves

Hydraulic control valves operate on a similar principle to that of regular high volume process control valves in that the fluid medium is assumed to have a significant kinetic or velocity component and the control is affected by means of the orifice area. The governing equation is the same as that used for control-valves [16]

Although the flow calculations for hydraulic valves share the same basis as that of flow control-valves, there is a significant difference in terms of control requirements, in that spool movement is dynamic. Its purpose is to transmit power to an actuator and the fluid is used as an energy transport mechanism, therefore the spool is required to respond in real time. Conversely, flow control-valves tend to control mass flow rate for process purposes and therefore aim to maintain a steady state or a relatively gradual change in state.

Borghi [44] conducted an analytical investigation of hydraulic lock-in of spool type valves. While the solution does not look directly at the relationship of the valve geometry to flow rate, there is an interesting formulation of flow in an eccentrically aligned tapered annular duct and is therefore of a similar flow channel to a needle valve. However the solution relates to the lateral forces on the core that induce lock-in of the spool. In contrast Eryilmaz and Wilson model spool valve flow rate in terms of

valve displacement but do not directly model the valve flow in terms of the valve orifice [45]. Ruan et al. model both the spool displacement [46] and the flow rate[47], but like Thanananchai [43] and all other macro flow control studies, the solution is based solely on orifice area. Their treatment of the valve control relates only to the positional accuracy of the valve spool using a stepper motor and digital displacement feedback, rather than establishing the link between stepper motor control and fluid flow.

2.3.1.4 MEMS and Micro Mechatronic devices

Micro technology in the form of Micro Electro-Mechanical Systems and very small mechatronic technology has the potential of providing very low controlled flow rates. This could be in the form of micro pumps [48-52]or through the use of microvalves for controlling the flow [53-56]. The prefix *micro* is considered appropriate for devices with prominent features having length scales in the order of 100μm or less [4].

Oh's recent in-depth review [57] of microvalve developments since Terry's microvalve was first reported in 1979 [58] describes and catalogues all the latest technologies associated with microvalves. Micro pumps are also included in the survey for their ability to control flow rate and in many cases their function and structure are very similar. Some forty five studies and devices are catalogued, of which only six meet the dual criteria of working with a liquid medium as opposed to gas and regulating the flow rather than on/off switching.

Wailbel et al [59] developed a microfluidic fountain pen capable of dispensing ink in arduous conditions. Flow is limited to 0.006ml/hr. The device developed by Goettsch et al [60] developed for the controlled delivery of minute amount of drugs uses an

elastomeric membrane to restrict the flow of fluid in a capillary. Flow rates are limited to 0.004-4ml/hr. Peirs et al [61] developed a self propelled colonoscope using hydraulic actuators as means of manoeuvring within the human colon. The hydraulic actuators are controlled by means of micro hydraulic valves located within the colonoscope. Two types of microvalves with 15x3.5x5mm dimensions were developed; piezo actuated and electromagnetic. Flow rates for the piezo version were 0-3.6ml/hr at 300-600kPa using low viscosity silicon oil and for the electromagnetic version was 0-648ml/hr at 100-600kPa using water. Bae et al [54] tested an electromagnetic diaphragm pressure relief valve to treat abnormally high intraocular pressure (Glaucoma). Although the experiments included it as part of a closed-loop control system with pressure feedback, only the valve itself is micro sized. Flow rates are in the region of 1.5ml/hr. Oh et al [62] created an electromagnetically driven in-line ball valve. The design relies on the fluid pressure to seat the ball securely and therefore suffers from leakage problems at low pressures. Flow rates were 0-8.4ml/hr and controllability and range issues are not discussed. With the exception of Peirs [61], the flow of viscous fluids are not discussed and in the case of Peirs, although a viscous oil was used for one experiment, this was at high pressure and it was noted that a lower viscosity fluid would be preferred due to the lower power losses. In summary, none of the designs were able to operate and control a variety of viscous fluids.

Microvalve arrays offer a method of accurate control of very small flows due to the inherent linearity of an array structure. [63, 64]. A single valve structures' flow will vary at low Reynolds numbers with the cube of the channel height, whereas an array structure scales linearly with the number of microvalves open. However, the linear scaling nature of valve arrays means that the rangeability of the valve is inherently

limited. A combination of micro valve arrays with pulse width modulation has been developed for controlling gas flow. [64]. The flow range is fairly limited at 50:1 and limited to maximum flow rates of 30 SCCM (Standard Cubic Centimetres per Second). The device is also limited to gas flows.

From this review, the following general points can be noted concerning microvalves and microvalve studies. Microvalves in general suffer from low rangeability. Control accuracy is rarely specified in articles detailing the valve development, although many valves are still in the early stages of development and are yet to realise their full potential. Although some microvalves have been integrated into full working mechatronic systems, generally the microvalve subsystems have been developed in isolation and the technology has still to mature before being applied.

MEMS based micropumps found in micro-fluidic systems such as print heads and drug infusers are able to pump volumes in the sub-nano litre range to several ml/min [48]. Laser conducted an in-depth review of micro pump research and technology [4] and divided the results in to positive displacement technologies such as diaphragm pumps and dynamic micropumps that use electrohydrodynamic and electroosmosis principles. Of the forty six positive displacement systems only four offered maximum flow rates above 160ml/hr [65-67] and all but one used water as the flow medium [68]. It was also noted that in general, the pumps reviewed had high voltage requirements with most requiring over 100V for operation [66-69], although some were as low as 20V [65]. Laser also remarked how few reports included the power consumption of the pumps and associated components. This has obvious implications for power supply and management as additional power regulation components would

be required for any industrial application especially if the device is to be powered by battery.

Although many micro pumps use a similar technology to microvalves, there are some important differences, especially when potential applications are considered. If for example a continuous very small flow rate is required over a long period, such as in a chain lubrication application. Valves are passive in the sense that they are able to make use of a gravity head to create the pressure differential required for flow. Therefore they can control fluid flows using relatively small mechanical displacements as they are not required to impart energy to the fluid. Conversely a pump would be required to operate continuously over a long period and although a pump would have the advantage of being able to act against an unfavourable pressure head this would not be a particularly efficient mode of operation. This potentially makes it easier to reach the design requirements of durability and lifespan using a microvalve rather than a micropump, where reliability and power consumption are particular issues [4].

There is a general lack of studies using viscous fluids such as the high ISO grade oils required for lubrication applications. This makes it difficult to determine the suitability of using MEMS devices for lubricant dispensing purposes.

2.3.1.5 Valve Actuation and Control

If a valve is considered as the mechanical means by which the orifice of a flow channel is altered to affect a change in flow rate, it is normal to have some means by which the valve is controlled; in most cases this would be an actuator of some description. The actuator must in turn be controlled in some intelligent manner such

that the relationship between control signal and actuation is understood and the relationship between valve position and flow rate is understood. In some cases there may be sensors that help establish the dynamic relationship between valve position and flow rate. This section describes the common actuator types and means of control for industrial control-valves, hydraulic valves, microvalves and describes some micro actuators that may be relevant in developing a micro actuated control-valve. In the context of this work the term control-valve is reserved for industrial control valves while those used for hydraulic control purposes are referred to as hydraulic valves or spool valves.

Industrial Control-valves: The industrial control-valve is the final control element of a process loop consisting of a sensing device, controller (actuator) and final control element (valve) [15]. Industrial process control-valves can be actuated by various means, the most common being pneumatic systems due to their low cost and robustness. However, where higher accuracy or actuation force is required, electrical power (ac or dc) or hydraulic power is used. Actuation signals can be sent pneumatically but there is a growing trend towards electropneumatic systems, with the control power supplied by compressed air, but with the greater accuracy associated with electrical signals and digital control.

The latest generation of industrial control-valves are available with fully integrated mechatronic control. However their current use is limited as there is extensive fragmentation of control system architectures, largely due to the number and diversity of legacy systems that still exist in current use. Legacy systems include pneumatic and low current analogue control signals, mechanical feedback control systems for valve position and electropneumatic signal converters. The primary form of valve actuation

power is still pneumatic, but the latest generation of controllers are now able to communicate with the distributed control system (DCS-the central plant control system) via field bus. Functions and components normally located in other parts of the flow system such as flow sensors can be integrated into the control-valve along with temperature sensors, valve position sensors and pneumatic actuator sensors. This allows closed loop control to be devolved locally to the control-valve while the DCS can be freed to deal with wider plant control issues. The integrated function sensing and control allows a high level of flexibility, safety and diagnostic functions to be built into the valve. Fully integrated control-valves are called Smart valves and are intelligently controlled valves that can compensate for deficiencies inherent in a manual control system. Non-linearity can be removed or compensated for, as well as hysteresis effects [70].

Hydraulic Valves: The control issues affecting hydraulic valves are different to those of control-valves. While a certain level of responsiveness is desirable in a control-valve, the primary concern is stability. Conversely hydraulic valves are often used in high performance applications that require a high level of responsiveness and high power as they are often controlling real time applications [45]. Solenoid activation is common, [71, 72] although stepper motor control is also possible [73]. Many valve spools behave in a nonlinear manner and coupled with nonlinear actuators such as solenoids, can create significant nonlinearities. Fortunately it is possible to design controllers that account for the nonlinearities in a similar fashion to the Smart control-valves. However before a nonlinear control can be designed it is first necessary to create a model of the valve and actuator [45].

Micro Actuators: Current needle valves use macro scale actuators to achieve microscale flows [11, 12, 21]. It is conceivable that control may be improved and cost reduced by matching the actuator technology to the scale of the valve mechanism through the use of MEMS technology. Micro linear actuators of a similar configuration to macro linear motors [74] can be built using electrostatic principles for actuation, were the maximum length of the slider movement depends only on the design requirements [75, 76]. A micro magnetic flap using electromagnetic micro technology can produce tip displacements of more than 2mm [77] while thermopneumatic devices can produce higher forces than that of the electromagnetic devices with displacements of over 1mm [53]. However with relatively inexpensive macro scale linear actuators able to achieve micro scale steps, this may not be necessary for some time. There is great scope inherent in the MEMS manufacturing technology to be able to match the cost of micro linear actuators to their size.

Mechatronic Control: Of crucial importance to any mechatronic development is the simultaneous design of the mechanical and control elements [9, 10, 78]. One of the typical characteristics of mechatronic design is the integration of onboard control [9, 78, 79]. However as mechanical and electronic systems need to be developed concurrently in order to ensure good integration, this is sometimes difficult as on-board systems are often difficult to program quickly and so are not suited to the development process. In this case Rapid Control Prototyping (RCP) which consists of a *simulated controller* made up of high-speed hardware and software is used as a substitute for the final electronic control unit (ECU) [9] .

Control Options: There are two control options that have a significant effect on the mechanical aspects of the valve, the control program and also how the mechatronic valve is developed.

Open Loop: The control input of an open loop system is not affected by the system output and the system itself is not affected by the output. Open loop systems are generally stable and not prone to uncontrolled movement or oscillations, however they do require calibration and are often unable to cope with parameter variations outside the initial control criteria [80]. An open loop system is only effective when the performance characteristics of the control components are exactly known, which is rarely the case in real situations [81]. Sensors may be used as an input of the control process but do not include monitoring of the control variable itself. An open loop system is inherently stable whilst not being able to adapt to changes in input variables it has not been trained for [9]. A open loop system may be implemented through simple proportional or proportional-derivative algorithms or through the use of look up tables [9].

Closed loop: In contrast to Open loop systems, closed loop control systems are affected by the system output, indeed this forms the basis of the control system but are susceptible to instability and potentially damaging undesired motion [70, 80, 81]. Therefore, while closed loop control has the advantage of being adaptive, there is the inherent risk of instability [9]. A closed loop system requires a sensor for the control variable, a logic control system for comparing the actual flow rate with desired flow rate and to send a signal to the final control element (or valve in this case) in order to affect a change in the flow rate.

It is normal to implement a closed-loop system for complex control applications due to the adaptive nature of feedback systems. However if an appropriate sensor to measure the controlled variable does not exist, it is necessary to use an open loop control system [9].

System response is an important parameter in control design. Systems requiring fast responses typically have high gains that are a potential source of stability problems. However the system needs to be balanced. Specifically referring to control-valve control, Lipták states "the positioner will normally improve control, but will do that only if the loop response is slow when it is compared with the control-valve response." [70] Otherwise the control response will always lag the system and is likely to lead to instability or at least lower accuracy.

Conclusions: From the examples of industrial control-valves and hydraulic spool valves, it is clear that control systems implemented for a particular problem must be tailored to that specific system. This requires simultaneous design of the mechanical aspects and control system. For example, while high tech fully integrated control-valves are available to the process control industry, penetration is low due to the limitations of existing infrastructure. The development of a control system for microflows is therefore dependent on the specific hardware used.

Although the end goal of this research is a fluid control system, this is focused towards the ability to be able to implement one, rather than focusing on the control logic itself. In this way it is deemed sufficient to show that a reasonable level of control is possible. This is logical considering the considerable effort required to refine a control system is only really justified if there is a specific end requirement or set of operational conditions that must be achieved. As there is no specific application

in this case, the control aspects are left at a generic level. Also a mechatronic system is characterised by a fixed set of hardware whose functionality can be flexibly modified through programming [79].

2.3.1.6 Valves & Valve Flow Theory Conclusions

The existing literature is polarised between macro and micro domains. The specific needle valve studies cover flow ranges well in excess of those studied here and are not covered in-depth, while the small flow rates are covered by micro technology. This study is unique in current literature in that it spans the gap between macro and micro technology by using macro technology to achieve micro flows. Table 2-1 summarises the studies investigating very low flow or the relationship between valve geometry and flow rate covered by the literature review.

Although there are procedures for defining the flow coefficient through industrial valves for the purpose of valve sizing calculations [31, 36, 39, 82], the relationship between valve geometry and the flow characteristics of the valve are not defined. Because the flow calculations are based on the orifice flow equation (Equation 1) there is an implied link between the orifice area and flow rate, in which case the link between flow rate and valve position is relatively straight forward. However this relationship is not discussed explicitly in literature and it is assumed that in an operational environment there are many other influencing factors and that the valve profiles are in fact developed through a process of trial and error. Only Thananchai [43] directly addresses the issue of the relationship between valve geometry and valve flow characteristic, although this is still based on the orifice area. Other studies such as those by Sondh et al. [41] and Singh et al [42] tackle a related issue by establishing the link between flow rate and plug geometry for the purpose of a variable area orifice

meter. However as with Thananchai, the theory is based on orifice area which is not valid for very low Reynolds numbers.

Source	Application/ Valve type	Flow rate as stated	Flow rate ml/hr
Bryant 1962 [21]	Commercial needle valves	5-25 cm3/sec	1800-90,000
Takemura 1975 [22]	Hydraulics. Power fluid control-valve	30-3000 cm3/min	1,800-180,000
Baumann 1991 [30]	Generic control-valves	0.6 minimum l/min	3600 minimum
Nguyen 1998 [51]	Micropump	0.04-0.08 ml/min	2.4-4.8
Thielicke 2000 [48]	MEMS in general	"sub-nanolitre up to several" ml/min	<0.06-600 approx
Xi 2001 [23]	Needle valve	0.3-0.6 ml/sec	18-36
Singh 2004 [42]	Variable orifice meter	12 kg/sec	43,200,000 (water)
This work	*Needle valve*	*0.45-400 ml/hr*	*0.45-400*

Table 2-1 Previous flow rate studies as found in literature with corresponding flow rates involved in respective studies. Note 1 cubic centimetre c.c. or cm^3=1 ml

Control mechanisms and strategies must be developed at the same time as the mechanical aspects of the solution and are therefore hardware and application dependent. While general control mechanisms can be developed to tie in with mechanical aspects, a mechatronic approach should allow flexibility to fine tune the control systems to specific applications as they become known.

2.3.2 Flow Channel Geometry

It is important to establish the correct flow regime for this study in order to be able to select the appropriate analysis techniques. The potential flow analysis methods

appropriate to micro channels are reviewed followed by analysis methods appropriate to specific flow channel geometries associated with a needle valve.

2.3.2.1 Microflow and Microchannels

Sharp et al. [83] define the microchannel domain of fluid flow as channels with dimensions between 1μm and 1mm. While flow channels of this order of magnitude are normally associated with MEMS or microfluidic devices, it is also true that macroscopic devices such as valves regulating very small flows necessarily have channel dimensions of this order of magnitude.

Ho and Tai (1998) [84] conducted one of the first reviews of micro-electrical-mechanical systems and fluid flows. Quoting a study by Pfahler et al. [85] it was found that the value of the viscosity of polar isopropanol decreases from the nominal value for a channel height smaller than 40 microns and reaches an asymptotic value at a channel height of about 10 microns. For the equivalent results for non-polar silicon oil, the data did not show a clear trend of viscosity variation in the same range of channel size.

Following on from this Gad-El-Hak (2001) [86] and Sharp et al. (2001) [83] in The MEMS Handbook review eleven flow resistance experiments conducted by other research groups between 1983 and 2000. They conclude that at some point in the diminishing scale of flow, from macroflow to microflow, the traditional macro-scale flow analysis techniques become unreliable and that there is no consistency with rational theory. Some studies find there is no difference with rational theory while others find there is an increase or a decrease in fRe (friction factor Reynolds number). In some cases there is an increase or decrease in fRe depending on a particular

parameter such as temperature or channel diameter. Gad-El-Hak describes macro scale theory as comprising of Continuum models such as Euler, Navier-Stokes and Burnett, where the fluid is considered as continuous and indefinitely divisible. This contrasts with molecular models that consider the fluid at a molecular level and therefore as a number of discreet bodies. It is often unclear if the discrepancies between flows predicted by macroscopic continuum theory and experimental results are due to microscopic flow effects or the inherent inaccuracies involved with apparatus of this scale. In the microscopic scale, where the surface to volume ratio is many factors higher than macroscopic applications, microscopic effects such as boundary slip can become proportionally significant, in contrast to traditional analysis where it is discounted as insignificant. Most significant is the lack of consistency in the deviation from traditional macro scale theory.

However Judy et al. (2002) [5] reviewed eleven studies involving flow in microchannels of various sizes and fluids, some of which were the same as those reviewed by Sharp et al. [83]. They also conducted their own experiments and concluded that discrepancies between theory and experimental results are due to experimental deficiencies and that if standard flow theory is correctly applied, any deviations with test data results are within the bounds of experimental error.

Hetsroni et al (2005) [6] conducted a critical evaluation of a large number of previous studies in the microflow domain in an attempt to establish the effects of experimental accuracy on the results. The aim was to clarify if the strange effects experienced by previous studies were 'real' effects of microfluid flow or due to experimental deficiencies. They concluded that for hydraulic diameters D_h=15 to D_h=4010μm and Reynolds numbers Re=10^{-3} to Re=Turbulent that conventional Newtonian theory is

correct when the experimental conditions are consistent with the theoretical conditions.

The critical works on this subject are summarized in Table 2-2.

Source	**Position adopted in article**	**Source**
Ho Tai 1998 [84]	Viscosity variations in micro channels	Migun & Prokhorenko 1987 [87] Pfahler et al 1990, 1991 [85, 88]
Gad-El-Hak 2001 [86]	Stokes breakdown. Point unknown	Sharp et al. [83]
Judy 2002 [5]	No deviation from theory 15-150μm	Review of other works with, and without, discrepancies and verified by own study.
Hetsroni et al 2005 [6]	No deviation from theory d_h=15-150μm	Re-analysis of other researchers data

Table 2-2 Position on deviation of liquid flow in microchannels from Navier-Stokes theory.

The well known Knudsen [86, 89, 90] number helps define the appropriate analysis regime (continuum, molecular or other), by comparing an appropriate length scale to the mean free path of the fluid particles or molecules. It is however used to distinguish between dense and dilute gas flows and is not applicable to the analysis of liquids [86]. Liquids do not have as well-advanced molecular-based theory as dilute gases and the concept of mean free path for liquids is not a very useful one as in essence the molecules are always in a collision state.

From this it can be concluded; the scale at which the continuum based Navier-Stokes equations are no longer valid is not well defined and not well understood largely because of the experimental complexity and uncertainty inherent with working at such small scales. Further more, once the Navier-Stokes equations become invalid; there is no appropriate analysis technique other than the extremely computationally expensive

molecular model. However recent analysis [6] suggests that the limit for Navier-Stokes theory is below channel sizes of d_h <15μm and that above this level, deviations from theory can be attributed to experimental conditions.

It is critical to establish the correct flow regime for the present study to ensure the appropriate analysis techniques are used. As this study has a hydraulic diameter of approximately 25μm and Reynolds number of Re=0.0093 to 80 (see Appendix F: Reynolds Number Calculation for Concentric Annular Flow for calculation) it falls within the standard laminar flow theory.

2.3.2.2 Annular Flow Channels

The flow through the critical portion of a needle valve is annular, bounded by the walls of the orifice and the needle itself. If the axis of the needle is not coincident with the axis of the orifice, this then becomes an eccentric annular flow.

There are different means of deriving a solution for annular flow. One method is derived from the basic flow theory as used to solve the circular cross section pipe [17]. Another means is to approximate an annular flow with a flow between parallel plates. This works well for cases where the difference between the inner and outer radii is small in relation to the cylinder diameter [91].

The seminal work on eccentric annular flow was conducted by Piercy, Hooper and Winny [92]and published in a paper entitled Viscous Flow through Pipes with Cores in 1933. In it, an analytical solution based on an infinite series is presented for eccentric annular flow with an approximation as a simpler alternative. Extensive experimentation was also conducted. The approximation suggested is a factor of a

well known analytical solution for concentric annular flow Q_c (although this is misquoted in the paper- *log* should be *ln* as shown in Equation 12).

$$\frac{Q}{Q_c} = 1 + \frac{3b^2}{2(r_o - r_a)^2}$$

Equation 11

Where Q is the eccentric flow, b is the distance between centres (eccentricity), r_o is the pipe radius and r_a is the core radius. The standard equation for concentric annular flow is (Munson [17]):

$$Q_c = \frac{\pi \Delta P}{8\mu l}\left[r_o^4 - r_a^4 - \frac{(r_o^2 - r_a^2)^2}{\ln(r_o / r_a)} \right]$$

Equation 12

Where μ is the dynamic viscosity, ΔP the pressure differential and l the length of the conduit. It is clear from Equation 11 that flow rate increases significantly as eccentricity increases up to a maximum increase of 150%. Note also that there is no channel length term in the eccentricity approximation meaning that it is based solely on Q_c and channel diameters, therefore for a given pipe with parallel core with maximum eccentricity, the percentage increase is constant regardless of initial flow rate Q. They propose that the approximation is sufficiently accurate for diameter ratios of r_a/r_o>0.5. In general the radius ratios considered in this study are in the region of 0.95-0.98.

Heyda 1957 [93] developed a solution for the locus of maximum velocity for laminar flow in an eccentric annulus on which Redberger and Charles 1962 [94] based their numerical study. They present a procedure for obtaining the velocity profiles and flow rates as a function of pressure gradient and conduit geometry based on a finite difference version of the differential equations. Of particular interest is the general discussion of the results and the graphical representation of the relationship between

flow rate to geometry in dimensionless form. In contrast to Piercy et al, they suggest that the maximum percentage increase for flow rate for a conduit with a diameter ratio of 0.9 is 240%.

They state that "although small displacements from the concentric position do not significantly affect the flow rate at small diameter ratios (<0.5), at large diameter ratios the flow rate is very sensitive to small displacements from the concentric position. For example, for a diameter ratio of 0.9, a 5% displacement would produce a 40% increase in the flow rate." So highlighting the significance of eccentricity in applications with high diameter ratios.

Related to the work of Redberger and Charles and also based on Heyda's work is that of Snyder and Goldstein 1965 [95] who present a solution for the local shear stress around the inner and outer surfaces of the annulus.

An alternative analytical solution exists for Equation 12 whereby if $(r_o\text{-}r_a)/r_o$ is small the flow channel can be approximated by a flat channel:

$$Q = \frac{W h_1^{\,3} \Delta P_A}{12 l \mu}$$

Equation 13

Where W is the channel width equivalent to the circumference of the annular channel and h_1 is the gap between the inner core and inner piper radius $(r_o\text{-}r_a)$ [91]. It is often useful to rearrange Equation 13 in terms of ΔP:

$$\Delta P = \frac{12 Q l \mu}{W h_1^3}$$

Equation 14

Through this work a comprehensive solution exists for the case of laminar flow in eccentric annuli with parallel core. However as it is necessary to use a profiled core in

order to modify the valve flow characteristics, the solutions presented cannot be used directly in design of valve geometries, rather it is one tool amongst many that can be used to help understand the principles behind flow in needle valves.

It has been established in Section 2.3.1.2 that the valve Reynolds number Re_v is not appropriate for very low flow valve. However a simpler calculation can be performed to determine the Reynolds number in a concentric annulus by adapting Equation 2 to take account of alternative channel cross sections [19].

$$\mathrm{Re} = \frac{4Q_m}{\pi\mu(d_o - d_a)}$$

Equation 15

For non-circular cross sections, replace d_o by the *hydraulic mean diameter* d_m, which for an annular flow is [19]:

$$d_m = \frac{4\pi(r_o^2 - r_a^2)}{2\pi(r_o + r_a)} = d_o - d_a$$

Equation 16

This is sufficient to give an indication of the level of turbulence to be expected in a very low flow needle valve. As can be seen from the calculation in Appendix 10.6, it is clear that this problem falls well within the laminar regime. The principle of laminar flow is critical to the development of understanding the flow of the needle valve.

2.3.2.3 Tapered Flow Channel Geometry

So far only a cylindrical needle profile has been considered. In practice the needle or core would need to be profiled in some way to provide the type of flow characteristics required. This is consistent with existing control-valves. It means that the flow

analysis problem will deviate from the relatively simple approximation just discussed to one where the cross sectional area of the conduit varies along its length.

The flow can be characterised as slow viscous laminar flow through a small tapered channel. Schlichting describes a solution to a similar problem related to the hydrodynamic theory of lubrication and describes the flow of separating fluid in the small gap between bearing surfaces [96]. Schlichting describes very slow motion as being when the Reynolds number is below 1, and is sometimes described as creeping motion. In this case, the viscous forces are considerably greater than the inertia forces. Schlichting's solution is for a variant of Couette flow [97] where two plates slide past each other separated by a viscous laminar fluid except in his case, one of the plates is at a small angle. Critical to the function of the solution is the concept of small angle and parallel flow. The assumption is that while the angle is small the vertical component of fluid flow (normal to direction of plate movement) is small in relation to the horizontal flow in the same direction as the plate movement. The solution can be adapted to current use by altering the boundary conditions and assuming that the two surfaces are stationary relative to each other and that the fluid flows by means of a pressure differential. The adaption of Schlichting's solution to the current problem is described in Section 5.1.3.7.

2.3.2.4 Flow Channel Geometry Conclusions

Despite the conflicting evidence [5] [6] [84] [86] as to the applicability of standard theory to flow in microchannels it is clear that there are significant challenges to experimentation at this small scale that clearly affect the results of many attempts to study microflows. The studies by Judy et al. [5] and Hetsroni et al. [6] certainly suggest that standard theory is applicable and that deviation from theory is often

attributable to experimental factors. There are existing flow theories in the form of annular and eccentric annular flow equations that can be brought to bear on the problem for needle valve control of very small flows. Additionally, small laminar tapered flow can be adapted from Schlichting's hydrodynamic theory of lubrication.

2.4 Flow Measurement

Flow measurement is an integral part of any flow control investigation. A custom flow measurement system was developed as part of this research and it is easy to explain why this was necessary with a survey of existing systems. A summary by the authoritative Béla G. Lipták, a leading industry figure on process control and automation in Flow Measurement [98] catalogues the characteristics of all the main sensor technologies. Each sensor type is rated against a number of criteria, the most relevant of which are; the ability to detect the flow of viscous liquids, rangeability, flow range and accuracy. Flow range indicates the total flow range that a type of sensor can be applied to, while rangeability describes how much of that range can be covered with a single sensor.

Table 2-3 shows highlights the ranges for critical characteristics for a selection of sensors technologies as summarised in from Flow Measurement [98]. Only the methods that come closest to meeting the requirements for this application have been listed. Cost and complexity is not covered and units have been converted to ml/hr for ease of comparison using a density of 824kg/m^3 equivalent to the mineral oil used in this study.

Sensor type	Viscous Liquids	Rangeability	Flow Range ml/hr		Accuracy
			Min	Max	
Valve study requirement	*yes*	*2000:1*	*0.2*	*400*	*±0.5% rate*
Mass flow meters (general)	yes	100:1	1200	>1.28	±0.5% rate
Coriolis	yes	20:1	1200	>1.27	±0.5% rate
Weirs, Flumes	limited	100:1	105	>1010	±2-5% Full Scale
Metering Pumps	yes	20:1	10	109	±0.1-1% Full Scale
Orifice (plate)	limited	3:1	10	109	±2% Full Scale, ±0.5% rate

Table 2-3 Flow sensor characteristics comparison [98].

It is clear that none of the sensors described meet the requirements of this study. While some sensors such as the mass flow meters and weirs have relatively high rangeability, it is still far short of requirements and none meet the minimum flow requirements. It is possible that the source of this information may have a bias towards industrial process control, and therefore emphasise more generic technology at the expense of equipment with a more scientific or laboratory purpose. To reduce the possibility that a suitable flowmeter already exists, a comprehensive search was conducted into commercially available flowmeters, Table 2-4 gives details of these. The most important parameters are the minimum and maximum flow rates and the rangeability, calculated from the given min/max flow values. It is clear that there is no single flow measurement device that covers the full range required.

There are other methods by which general flow measurement can be achieved. Perhaps the simplest would be to have a graduated reservoir, where the change in fluid level over time can be directly related to the flow rate. However, this is not

practical for low flow gravity fed systems as this method requires a significant change in fluid level for a given volume in order that an accurate reading may be taken. This necessarily means that there would be a significant change in pressure head which has a significant effect on flow rate.

Device	Technology	Seller	Cost	Min flow ml/hr	Max flow ml/hr	Range-ability	Min pressure	Accuracy (Resolution)
Piezo ultrasonic wave	concurrent transit time - CTT technology	EESIFLO	-	fraction of a ml per min	-	-	-	(Resolution 0.3ml/min [flight path dependant])
LMX Series	Extreme Low Flow Liquid Pelton Wheel Flowmeter	jlc international	-	180	3900,000	20000:1	-	± 2% of actual reading for 10 - 100% of range
OG1	Oval gear meter	Titan Enterprises Ltd.	£243	1800	240,000	130:1	10 bar	±0.5% full scale deflection
OG2	Oval gear meter	Titan Enterprises	£243	600	60,000	100:1	10 bar	±0.5% full scale deflection
Electromag 500 Series	Electromagnetic flowmeter	Litremeter	-	850	250,000	294:1	-	Dependent on converter;
LF2M	Coriolis	Emerson (Micro Motion)	-	1.21	461	380:1	-	+/-0.5% of rate
SLG1430-025	Thermal	Sensiron	-	0.015	0.42	28:1	1 bar	(1.5nl)

Table 2-4 Commercially available extreme low flow meters.

2.4.1 Dripping

An early objective of the research project was to develop an automated means of measuring the drip interval. This would build on the research methods used by Scottoiler and by the previous valve flow investigations described in Section 2.2. It was Du [13] who first attempted to establish the link between drip interval and flow rate for the purpose of valve flow rate investigation and it was through the need to develop a means of accurately measuring the drip interval and determining the drip volume that an investigation into dripping phenomenon was undertaken.

Although investigations into the free flow properties of liquids have been conducted for the last three hundred years [99], the modern study of dripping behaviour, or the 'dripping faucet' problem as it is now known, can be traced back to Rossler's [100] suggestion in 1977, that drops falling from a leaking faucet could be a naturally occurring form of chaos. Since the late eighties there have been a great number of studies into the chaotic behaviour of the system [101-114].

2.4.1.1 Drip Formation

Investigations into the reasons for the chaotic behaviour led to the renewed popularity of research into the dynamics of drip formation and finding a model for drip formation. D'Innocenzo studied the effects of nozzle geometry and drip formation in relation to the onset of chaotic behaviour [115, 116] using the classic drip period method coupled with high speed videography. This may prove useful during future product developments, as it may be possible to maintain a set flow rate but control drip frequency using nozzle geometry to suit a particular chain lubrication application or, as described later, to adjust the parameters of a drip interval based flow

measurement method. Rayleigh's work over a century ago [99] laid the basis for much of the work undertaken in the last decade, indeed his formula for estimating drop size is still relevant to work carried out in the last ten years [117] and his theories on drip jets are still compared alongside more modern work [99, 118, 119]. The Rayleigh drop mass approximation is [117]:

$$m = 3.8\sigma\left(\frac{r_n}{g}\right)$$

Equation 17

Where m is the mass of the drop, σ is surface tension, r_n is the radius for the drop nozzle and g is the gravitational constant.

There are a number of studies concerned merely with the topic of drop formation, including the satellite drop formed by the break-up of the liquid thread that joins the drop to the nozzle while falling. These studies are often centred on the dynamics of a single drop formation, assuming zero or near zero flow, but also with predicting the formation of several drops in sequence [107, 120-122]. Studies also include generalised formations of a large number of drops over an extended period in line with chaos studies [101, 103, 110, 114, 123, 124].

In recent years there has been a diversification of study area. Including dripping with ants Bonabeau et al 1998 [104], drop ejection from an oscillating rod Wilkes and Basaran 2001 [125] and drop formation in a co-flowing ambient fluid Cramer et al 2004 [126]. These studies are generally concerned with the effects of flow rate, and other parameters, on drop formation, whereas the current study is less concerned with drop formation, but rather on the flow rate itself. While the effect of flow rate on drop volume is to be determined, there is no indication that the drop formation affects flow

rate, however it is hoped to infer some understanding of the flow rate from studying the drop frequency.

As this study uses the drip interval and drip volume as a means of measuring flow rate, it is important to establish the flow conditions under which drip volume is stable.

Neda et al [117] suggest that the Rayleigh approximation of drop mass (Equation 17) is reasonable for very slow flow rates, although very slow is not quantified. As this formula is not flow-rate dependent this suggests that drop mass is constant for slow flow rates. Their experimental study is performed at relatively high flow rates 1692-4410ml/hr and was designed to chart the onset of chaos and the subsequent change in drop volume. Flow rates in their study are one to four orders of magnitude higher than in this study.

Zhang [119] conducted an in-depth study of the effects of nozzle diameters and thickness, flow rates, viscosity modifiers and surfactants on drop volume. It also includes a comparison with a popular drip volume prediction formula by Scheele and Meister [127].

$$V = F\left[\frac{2\pi\sigma R}{g\rho} - \frac{4Q^2}{3\pi R^2 g} + 7.14\left(\frac{Q^2R^2\sigma}{g^2\rho}\right)^{1/3}\right]$$

Equation 18

Where R is the outer radius of the nozzle and F, the Harkins-Brown correction factor. It was shown to deviate up to 25% from experimental results and is thought to be due to the F, the Harkins-Brown correction factor and deficiencies in the basis of the formula, namely the assumption of static conditions during the first stage of drop formation. Drop volume is measured optically by integrating the profile of the drop as recorded by a digital camera.

He confirms that under stable conditions, the volume of successive drops is uniform and does not vary under slow flow conditions. Worth noting is "For common liquids, viscosity is well known to have little effect on the volume of primary drops."

It must be noted that the measurement of drop volume and comparison with the formula was conducted under very strict experimental conditions using highly sophisticated equipment. Even then, the experiment disagrees with the popular empirical formula by up to 25%. While there are undoubtedly more sophisticated formulas they are likely to be highly complex and still rely on very strict experimental conditions. In this sense there is no appropriate drip volume prediction technique especially if the drip conditions are less than ideal.

In conclusion it can be noted that it is possible to determine the drop volume by analytical means, but in order for the analytical result to correspond to the physical test results, the experimental conditions would require very close control. In this way it is difficult to make any practical use of the analytical model due to the requirement to control the drip formation conditions. Simpler approximations exist but the accuracy and conditions in which they are valid are uncertain. Under these circumstances it is considered more practical to determine the drip volume experimentally using the fluids and apparatus specific to the valve flow experiments of this study.

2.4.1.2 Measurement Equipment

The equipment for studying chaotic behaviour and drop formation is of particular interest for its ability to detect drop time intervals (also known as the drop period). The dripping studies described in the previous section use measured flow rates to

study the corresponding effects on flow rate. However it should be possible to reverse the process and use the same equipment to measure flow rate by measuring the drop period for known drop volumes.

Wu et al [101] published one of the first studies in this area and so describe their apparatus in detail. The most significant difference between studies of chaotic behaviour of fluid flow and the study of the RMV is the volume flow rate. The onset of chaotic behaviour occurs when the drop frequency is close to becoming a constant flow, or jet as it is termed. This means the drop rate intervals are in the millisecond range. Due the very low flows being investigated, the drip intervals for this study cover a range of 0.2 seconds to over 1500 seconds. The higher frequency drip rates require a correspondingly more accurate timing system. The microphone based timing method adopted in this study is much simpler than the laser based method but has proved sufficient for detecting the drip intervals used in conjunction with the RMV. Laser based systems can be used to measure the duration the fluid particle interrupts the beam, and so estimate the size of the drop [117]. The latest studies tend to use a combination of emitter detector methods (ie laser) and high speed video. Buch et al [128] describes some of the limitations of the emitter detector method and how high speed video techniques can be used to visualise drop formation but also analyse drop formation quantitatively and thus complementing emitter detector methods.

These high precision studies use complex flow stabilising equipment. This often comprises of a system for stabilising the pressure head and involves a continuous stream to top up the feed reservoir with an overflow to maintain a constant level. This normally feeds a second reservoir used to buffer flow fluctuations from the first. A variety of other control measures are normally added to this base setup. This includes

needle valves or a tank hoisting system to vary the flow rate, capillary tubes and heat exchangers to stabilise the flow still further. Pumping mechanisms are isolated to remove vibration effects. There is no need for these complex flow stabilising measures in this study, as it is the valve itself that is the source of the flow instability and is itself the target of study. Methods and equipment for the current study will be discussed in detail in future chapters.

2.4.1.3 CFD Review: Valves and Microflow

While small needle valves have been in use for many years there is very little information in literature that describes flow characteristics in terms of critical geometry. There are a number of classical methods for solving flow problems, which include experimentation, analytical and more recently, numerical methods. This work comprises a mixture of all three with an aim of generating a robust understanding of fluid flow in very low flow needle valves. The finite element method (FEM) is also an important method for validating the analytical models of microfluidic systems [129] .

As discussed in the earlier section on control-valves, much work has been conducted in characterising valve flow in terms of C_v for a given pressure differential. As this is determined experimentally, determining the C_v value can be an expensive process. Davis and Stewart [130, 131] successfully predicted C_v values for a selection of industrial globe valves using CFD by assuming the flow field in the region of the plug is axisymmetric. In this way they were able to predict the C_v value in a computationally inexpensive manner and avoid the cost of expensive physical testing. While the axisymmetric approximation is useful for reducing the computational cost in a turbulent flow such as found in a globe valve, it was found to only be valid for smaller valve openings. The discrepancy was thought to be due to the flow turbulence

becoming three-dimensional at higher valve openings. Low viscous flow through a needle valve is laminar and inherently axisymmetric. Moreover, due to the very small gap in the needle valve, further simplification should be possible such as the annular approximation described by Equation 13.

Singh et al [42] used experimental apparatus and the CFD program FLUENT to determine the drag force on the plug core of a variable area orifice meter. They used a similar process to that of Davis and Stewart except their 3D solution was able to account for three-dimensional turbulence. Their analysis was not used to develop the shape of the plug, merely to determine the drag force on the pre-determined plug profile.

These examples have all been in the macro scale, using high flow rates and turbulent flow. Micro-flows are becoming increasingly a source of study as microfluidic devices and MEMS devices develop. This is because of the difficulty of developing apparatus that can accurately measure the salient parameters of flow at the micro scale. It should be noted that computational techniques suffer the same problem as analytical methods, in that it is difficult to ensure that the experimental conditions are equivalent to the theoretical conditions. Section 2.3.2.1 covering Microflow and Microchannels concludes that the standard fluid dynamics theory based on the Navier-Stokes equations is valid for channels with a hydraulic diameter above d_h=15μm. In this case, any commercial CFD package based on the Navier-Stokes equations should provide good accuracy. Indeed, Zhang et al. [129] state that comparison of analytical and computational results is a common model validation technique and many microfluid studies use CFD as part of the modeling process including: Townsend et

al. [132], Iancu and Muller [133], Kobayashi et al. [134], Ng et al. [135], Maruyama et al. [136] and Klank et al. [137].

2.4.2 Flow Measurement Conclusions

Existing commercial flow measurement devices are not suitable for this study and existing technologies do not offer the minimum flow measurement and range required. It is theoretically possible to create a drip interval based flow measurement device for the measurement of very low flows based on similar equipment to that used for drip formation and the leaky faucet experiments. CFD is an important method for determining flow rates in microchannels and a means of verifying the flow model.

2.5 Literature Review Conclusion

There is a gap in existing literature of valve flow studies between industrial control-valves and MEMS type microvalves. This is applicable to both the scale of the flow rates and the scale of the valve geometry. Other than the study by Thananchai [43] there is no theory that describes the tuning of valve flow characteristics through the use of valve geometry and any reference to valve flow rate calculations are based on orifice area which is not applicable to low Reynolds number flows. There is no general discussion or theory available on which to base the design of very low flow needle valves in the macro domain.

It is essential as part of a mechatronic development to simultaneously design the control program, actuator and final control mechanism and is best achieved through the use of component modelling.

Microflows in micro channels are adequately served by standard fluid dynamics theory despite the difficulties faced by previous studies to match experiment results to theory. CFD tools and current flow theories play an important part in developing a model for very low flow needles valves. The geometric scale of this study is such that the model results are applicable to the microflow domain.

A suitable low flow measurement device that meets the needs of this study does not exist. However it is possible to create a drip interval based measurement device based on similar equipment to that used for drip formation experiments described in literature. CFD can be a useful tool for determining flow rates in microchannels and a means of verifying the flow model.

3 Methodology and Research Tools

3.1 Modelling

The aim of this research is to generate understanding through the use of modelling and by following the basic principles described by Giordano and Weir [138]. They describe a framework with which to investigate phenomena through modelling.

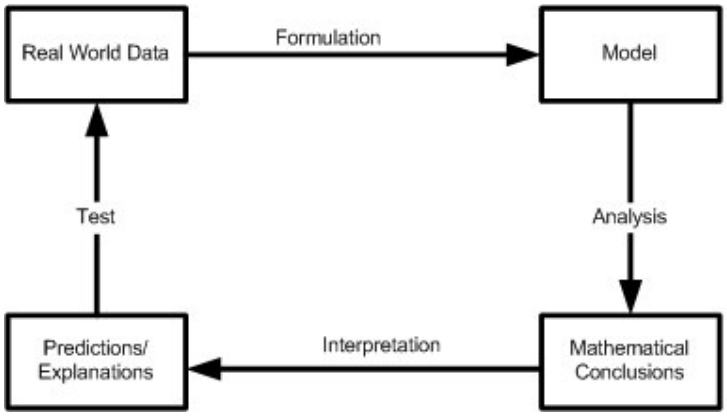

Figure 3-1 The modelling process. Adapted from Giordano and Weir [138]

The general method described is as follows:

- Through observation, identify the primary factors involved in the real world behaviour, possibly making simplifications.
- Conjecture tentative relationships among the factors.
- Apply mathematical analysis to the resultant "model".
- Interpret mathematical conclusions in terms of real-world problem.

Observation is particularly important when first approaching a new subject for modelling, and may consume a considerable amount of time in the initial iteration of the model. If, as in this case, the system under consideration has many interacting influencing factors it may be required to undertake some basic testing or further observation in order to add weight to a conjectured relationship before seeking a mathematical model. This could be considered a 'sub-loop' within the iteration

process. The work described in this thesis is the result of many iterations, although each iteration is not described as such. Rather, each variation explored or alternative way of formulating the problem is the result of an iteration of the modelling process. Many iterations have not been described that required significant rework of the conjectured relationships. This would often require a considerable rework of test pieces and effort in collecting data in order that the next iteration of the model may proceed. As the final models presented here were developed through an evolutionary process, it is no doubt possible to refine the models further through further evolution. As the model building process is circular rather than linear, each loop through the process is important as a means of justifying the conclusions drawn and the result achieved. In this way, failed modelling attempts are important contributions to why a model is how it is. Therefore it is sometimes necessary in order to explain what some thing is, to also explain what it is not. When there is a mismatch between model and reality it is important to find out why. For example, has a wrong assumption been made for the analytical model or is there a problem with the test equipment?

The iterative model building process can be said to be complete when it is sufficiently accurate for its intended purpose. As part of this, it is necessary to define the limits of function of the model. For empirical or data driven models the bounds are normally defined by the extent of the initial data, however, for an analytical model, the bounds may not be so clear and require verification through testing. This thesis presents two models relating to the flow rate of the valve. The first, an analytical model for the purpose of aiding the design process, can be deemed sufficiently accurate if it captures the general flow characteristics of the valve as a function of channel geometry, pressure differential and fluid viscosity. The second empirical model is used as the basis of a closed loop control program and the ultimate accuracy

requirement is application dependant. In this case is used for demonstration purposes and deemed accurate enough for general lubricant control requirements.

One of the principle aims of this research is to create a model of the valve flow properties that can be used as a vehicle to generate understanding of the function of the valve and as a means of driving future changes. As with any model process there is a trade-off between simplicity and precision of the model, so that in order to increase the precision of the model, more factors have to be taken into account, thereby increasing complexity. The aim therefore is to achieve a model that achieves the required precision with the minimum complexity [138]. Subsequently no useful model has absolute validity, whereas its strength lies in the insight gained into the key factors that affect behaviour [78].

In order to determine if the model has achieved the necessary precision it is first necessary to define the aims of the model.

Is the RMV able to provide a predetermined flow rate using its available adjustment range for a given set of operating conditions? This is to allow a complete lubrication system to be specified for a specific installation on the basis of an inspection of a proposed installation site and knowledge of basic operating conditions.

Does the model account for the main factors affecting flow rate and capture the trends involved for the purpose of understanding factor interaction? This is to aid future design and system specification by understanding all the relevant factors that contribute to variable flow rate.

Throughout this work, an important distinction is made between predictive models and explicative models. In general it is desirable to develop an explicative model. This

is normally a mathematical analysis based on a number of assumptions. As such it is the most flexible, so well suited to system design, but suffers from low fidelity due the assumptions made in the construction [138]. By contrast, the predictive model allows accurate predictions because it is based on observed data and so is well suited to forming the basis of a control system. The aim of this research is to provide understanding of the flow phenomenon and also the ability to control the flow.

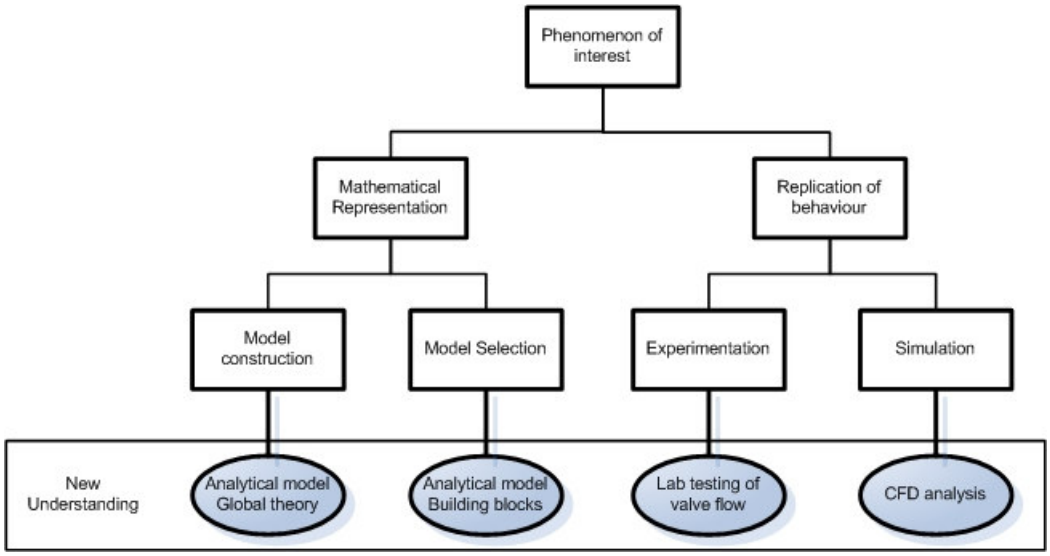

Figure 3-2 Nature of the model. Ovals depict how each model type is implemented within this thesis. Adapted from Giordano and Weir.

In practice a mix of modelling methods are required to be able to fulfil the model goals described previously. The breakdown of the model types is shown in Figure 3-2. The intention is to construct a global mathematical model that describes the overall performance of the system. This in turn is made up of sub-models, covering aspects such as pressure head, fluid viscosity and valve expansion. Formula describing the sub-models may exist already in literature, be developed form first principles or be derived from experimental data. CFD is used as a means of triangulation between the analytical model and test data. Where there is a discrepancy between the analytical

model and the test data it is often useful to have a third source to help indicate which value is the source of error. It could be argued that the test data is always the correct value but in reality, the test values may not represent the intended conditions due to experimental error or as the flow rate is a derived value, there could also be an error in the calculation.

Through the course of the investigation three main types of model are used.

- **Mathematical or Analytical solution**. This incorporates assumptions and possibly some simplification of the flow channel geometry followed by fluid flow analysis based on fundamental fluid flow principles. This generally results in an equation that will define the flow rate in terms of channel geometry, pressure, viscosity and any other relevant factors. This type of model is explicative in nature and offers insights into what parameters can be changed in order to achieve desired performance characteristics. It is normal to find that explicative models are able to follow the overall trends of a system, and so are a powerful aid to design, but are often not accurate enough for control purposes.

- **CFD model**. Any CFD analysis requires assumptions to be made regarding the physical characteristics of the system, such as the channel geometry, characteristics of the fluid and flow characteristics within the channel. An attempt is then made to replicate this in a computer environment. The three parts to this include; the physical representation in the form of the CAD model, the generation of the mesh from the CAD model, i.e. how the flow space is divided up for flow calculation and finally the assumptions of the flow calculation such as pressure differential, viscosity etc. To have a good

level of confidence in the model, it must be validated in some way. This can be through validating the calculation assumptions or by comparing the results with a physical test. Where it is difficult to conduct physical experiments, CFD analysis can be used as a substitute for the physical case where there is high confidence that the CFD accurately represents the physical case. From this is possible to build confidence in the accuracy of the analytical model to predict flow rates outside the experimental data range. Judicious use of CFD models is required due to the time and computational expense required to run them. A single result is also of little use for investigative or design purposes as it only provides a single 'snapshot' of the phenomenon under investigation. In order to capture trends in response to varying parameters, a series of results are needed. This can be a long process, even for the simplest CFD models.

- **Data model**. This type of model uses test data to describe the performance of the subject. It is normal to try to find some form of mathematical function that approximates the form of the data (curve fitting). This type of model can only be used to predict performance (e.g. for valve control purposes) but does not explain the reason for the performance and is therefore possibly less useful for design purposes. The model created is only as good as the data gathered, and although it is possible to achieve a very close fit to the data the resultant model is sometimes considered less robust than an analytical solution as the data can be influenced by noise factors (such as tolerances or temperature fluctuations) that means the model would be inaccurate in other similar situations.

The methodology described is not specific to mechatronic applications, but is well suited to the mechatronics design process. Firstly, models form an integral part of a

mechatronic system as they are required as part of the mechanical design and for optimisation of the mechanical aspects of the design. Essentially any decision that is based on a calculation is based on some form of model as they form the basis for defining the form and function of any physical object. Secondly, just as models are an integral part of the physical embodiment of a mechatronic design, they also form the basis of any control system, although the models will often take a different form.

As can be seen from Figure 3-1and Figure 3-2, testing and experimentation forms an integral part of the modelling process and is used as means of validating theoretical models and as a source of data on which to base descriptive or data driven models.

It is worth noting at this point that it was decided not to pursue the neural network method of modelling the flow as investigated by Casey [12] and Du [13] because it is essentially a particular form of curve fitting as described above. It adds an extra level of complexity and potentially provides even less opportunities for understanding the reason of performance than traditional curve fitting. If there were a large number of factors of a complex nature involved it could potentially be used in future valve control developments as a method of controlling the valve function as described by Thananchai [139].

Statistical methods such as Orthogonal Array type experiments were also discounted for the experimental stages despite close consideration for similar reasons to the neural networks. The orthogonal array method of experimental analysis such as described by Lochner [140] and Box [141], are not explicative in nature in that it does not explain the fundamental principles governing the phenomenon of interest. Array experiments can help identify relevant parameters and interaction effects, but require a large number of readings to be made. This is particularly significant as in order to

comply with the rigorous statistical method; each reading must be made by conducting the experiments in random order. This is not practical for experiments with a large set up time. For example, the orthogonal array method is intended to be able to highlight the interaction effects between different variables and is considered an investigative tool for this purpose. However, if, as in this case, there are five relevant variables, and a two factorial approach is used, this requires 32 readings to be taken with the variables altered in a random fashion. This means that each experiment requires a full set up procedure i.e., it is not possible to vary one variable at a time. It is likely that due to the variables involved it would require a full day to obtain a single reading, meaning it would take approximately one month to gather a basic data set. The purpose of randomising the order of the experiments is to "neutralise" the effects of uncontrolled variables and thus statistically eliminate a potentially significant source of error.

For this study it is considered more useful to chart the flow characteristics across the whole range of a variable (as opposed to two factorial experiments that only use high and low values of each variable). As this is significantly faster, it allows much larger and more varied data sets to be gathered. The overall number of tests can be reduced by arranging tests to explore specific phenomenon. This allows better interpretation for developing an explicative model as well as generating data to be used for predictive modelling.

3.1.1 Sources of Modelling Error

Analytical mathematical models are by nature explicative. That is they are based on fundamental principles of physics and so are able to give an insight into the process at work. However in order to be able to build an analytical model it is necessary to first

gain a good understanding of the physical process of the problem at hand. If there is a discrepancy between the model and results gained through testing, the error must come from either the use of the wrong theory, or through the poor interpretation of the problem. For example the error could arise from applying the wrong principle such as the difference between applying a turbulent flow model or laminar flow model or it could arise from applying the correct principle wrongly such as by incorrect measurement for flow, viscosity or geometry. This highlights the importance of understanding the source of error when using an iterative modelling process so that the model can be improved with each generation of model. In all cases, all test data generated must be under strictly controlled conditions in order that there are no extraneous effects on the data. In the case of flow through a valve there are many sources of potential error, the exact location of the needle in the orifice is one of the greatest unknowns and there are many factors involved that can affect its location. This includes the mechanical setup of the valve including tolerances, backlash, and even temperature effects. In some cases the source of error is far from obvious and may require substantial investigation. If the source of error is not identifiable, an alternative theory may be required, or even an alternative modelling method.

3.1.2 CFD Methodology

The use of CFD tools in complex fluid flow problems is almost universal; however, the way in which it is used is extremely important. Whilst computational tools are extremely powerful, they also have some significant drawbacks to be considered. First of all, the data generated by any analysis is only as good as the definition of the problem by the user. This includes input parameters as well as any simplifications to geometry or approximations used. It is also dependant on the meshing and solvers

used in the calculation. This means that for any one problem there can be a multitude of answers, some of which may differ significantly from reality. Which in itself leads to the question of "which reality"? CFD as with any model is an approximation of the subject of interest. It is therefore prudent and necessary to have some idea as to the accuracy of the model. It is for this reason that where possible, computational results are validated using experimental data. CFD does allow the investigator to explore a range of scenarios that would be either, impractical or impossible to achieve by experimental means.

The second drawback of CFD is computational expense. The combination of computer power and time taken for complex problems can be prohibitively high, especially if pre-processing time is also considered. Generating geometry and meshing can exceed the computational time.

Just as there are a number of possible analytical solutions, there are a corresponding number of ways of formulating a CFD solution. In both cases it is necessary to verify the solution against test data to ensure a good level of accuracy. However the strength of using CFD is that it is possible to explore cases that are difficult to replicate physically or analytically. While it is relatively easy to use CFD to gain an idea of relative performance from one concept to another, the absolute values may differ greatly from reality. In order to achieve a measure of confidence in results where it is not possible to verify with test data, it is necessary to build on a method and set of results that have been verified. In this way the knowledge of the problem can be built up using simple easily verified problems and then expanded to more complex cases and then finally to cases where verification with test results is not possible.

3.2 Scale

One of the important features of this research is the crossing of the scale boundary between macro and micro domain. This applies to the time scale in the form of drip intervals varying between 0.2 seconds to several hours in some cases, the dimensions of the controlling hardware are generally in centimetres and millimetres but the critical flow channel the hardware is interfacing with is measured in microns and the maximum and minimum flow rates which can vary from 400ml/hr to much less than 0.1ml/hr in some cases. Clearly viewing data that represents several orders of magnitude can be problematic. The log scale is used extensively when representing data in this thesis for its ability to provide detailed microscopic views alongside the macro data. However, while this tool is excellent for the analytical examination of data, there is a particular drawback. As the Log scale effectively distorts the real world scale that we are used to working with, it makes it difficult to see what the real world implications of features that may appear in a Log plot. In light of this, both regular scale and Log scale figures are used in this thesis, depending on the particular point being made.

3.3 Data Management

Due to the nature of the investigation, a considerable amount of data was generated for a variety of test pieces over a range of conditions and because if this, traceability was a significant issue. It is imperative to know when comparing sets of data what the differences are between them and whether it is in fact possible to draw direct comparisons. If the details of the test are not recorded, it is impossible to know what the differences between data sets could be due to, thereby making any comparison irrelevant. This also applies to results generated using CFD.

To alleviate this problem, a comprehensive data tracking system was implemented; allowing any analysis to be traced directly to its source, including the conditions of any test and the exact geometry of any pertinent components. The process starts with numbering needles and orifice sets, which are then measured and the results converted into a 2D CAD representation of the measurement results. All valve assemblies are then numbered and measured as they are built, so that if any components are reused for future assemblies they can be differentiated. Reusing needle sets saves the effort of re-measuring a new needle set, but also may be required as a common parameter in a particular test.

All flow data can then be linked to a specific valve assembly and then any subsequent analysis can then be linked to a specific set of flow data. The conditions from all tests are recorded including the valve number used. Each test is numbered and the corresponding test conditions recorded along with the valve number and can be cross-referenced with any particular flow data or flow analysis. CFD data is logged in a similar fashion so that the source geometry can be traced (e.g. a theoretical channel or replicating an actual needle) and linked to the CAD model, mesh and analysis results. Each analysis can be run in a variety of ways including variations on input parameters.

3.4 Conclusion

A model based methodology is proposed as the basis of the mechatronic investigation due to the fundamental role that models pay in mechatronic developments. A mix of models is required to fulfil the different roles within the product and the development process.

Three forms of model have been identified that cover all the modelling requirements: analytical model, CFD simulation and data driven model. Between these three forms of model and in conjunction with experimentation it is possible to validate and describe any phenomena in a form that suits the mechatronic design process. Testing and experimentation forms and integral part of the model building process, both as validation for theoretical models and as a source of data for descriptive models.

4 Experimental Test Rig

4.1 Introduction

There were two requirements for developing an experimental test rig. The first was to create a means of measuring valve flow rate under controlled conditions in order to be able to establish a link between the flow rate and the characteristics of the valve. This includes identifying and quantifying all the main factors that affect the flow rate through the valve. The second purpose for developing an experimental rig was to develop appropriate control systems once the valve characteristics had been defined. An integral part of this was to develop a means of accurately measuring very low flow rates. The novel drip interval based method developed as a consequence of this is one of the contributions of this thesis.

A general layout of the experimental equipment is shown in Figure 4-1 and a detailed view of the Reservoir Metering Valve is shown in Figure 4-2. A brief description of the system is given here with details of each of the components described below.

The control valve (termed a Reservoir Metering Valve, RMV) is fed by a variable height reservoir, allowing the differential pressure to be altered. The valve is opened and closed using a solenoid attached to the needle mount via a cable. The fluid flow is regulated by limiting the displacement of the valve needle. The flow is regulated by the user via a rotational dial that linearly adjusts the position of the stopper via a screw thread. The rotational dial is adjusted manually, while the solenoid can be remotely activated via a control program.

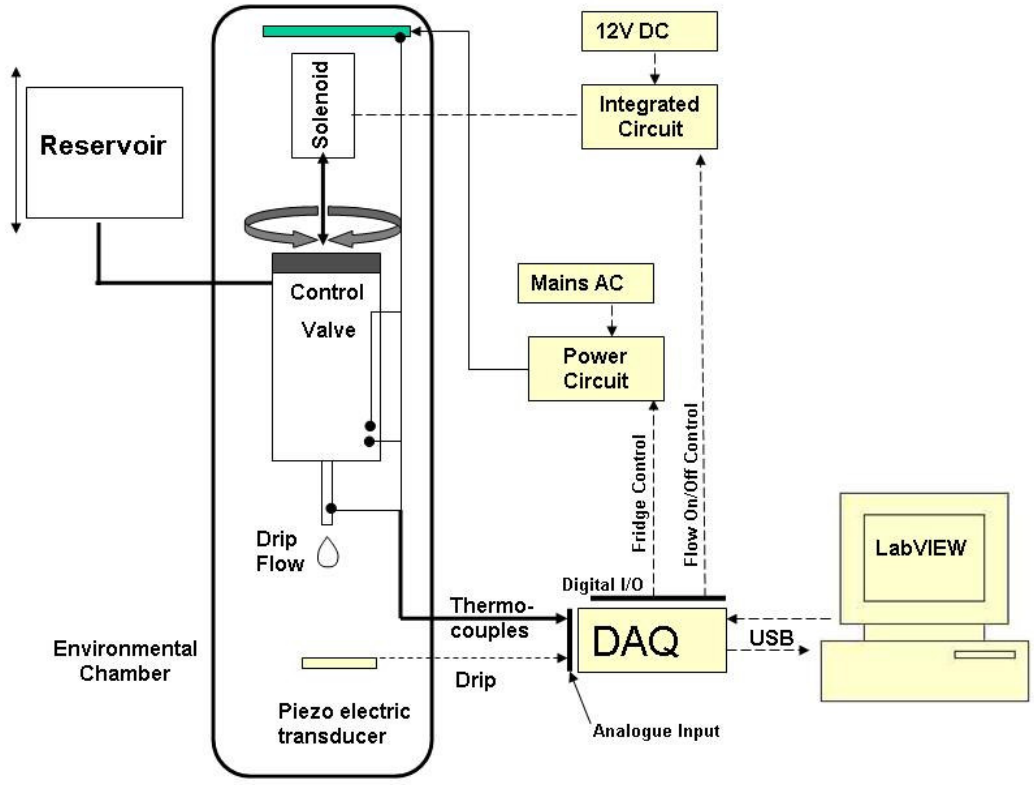

Figure 4-1 Test rig architecture

Central to the test rig operation is the data acquisition and control function consisting of an analogue to digital converter with digital output interfaced with the LabVIEW control program. The digital output controls the solenoid operation and also the environmental temperature by cycling a refrigerator pump. The analogue to digital converter captures the pulses generated by the control fluid dripping onto a piezo-electric disc and converts the time interval into an equivalent flow rate. Thermocouple temperatures are also monitored, including; the refrigerator element for temperature control purposes, the temperature at various points within the RMV as well as the temperature of the outer surface of the valve body. There is also a thermocouple inserted as near to the drip nozzle exit as possible. The drip nozzle is kept constant throughout all experiments and kept at constant height above the piezoelectric transducer. The reservoir height is altered relative to the nozzle position to control the

differential pressure in the system. Various LabVIEW programs were developed to integrate particular functions or to allow functions to be run separately.

The system is modular allowing different functions to be put to use depending on the requirements of the particular test being undertaken.

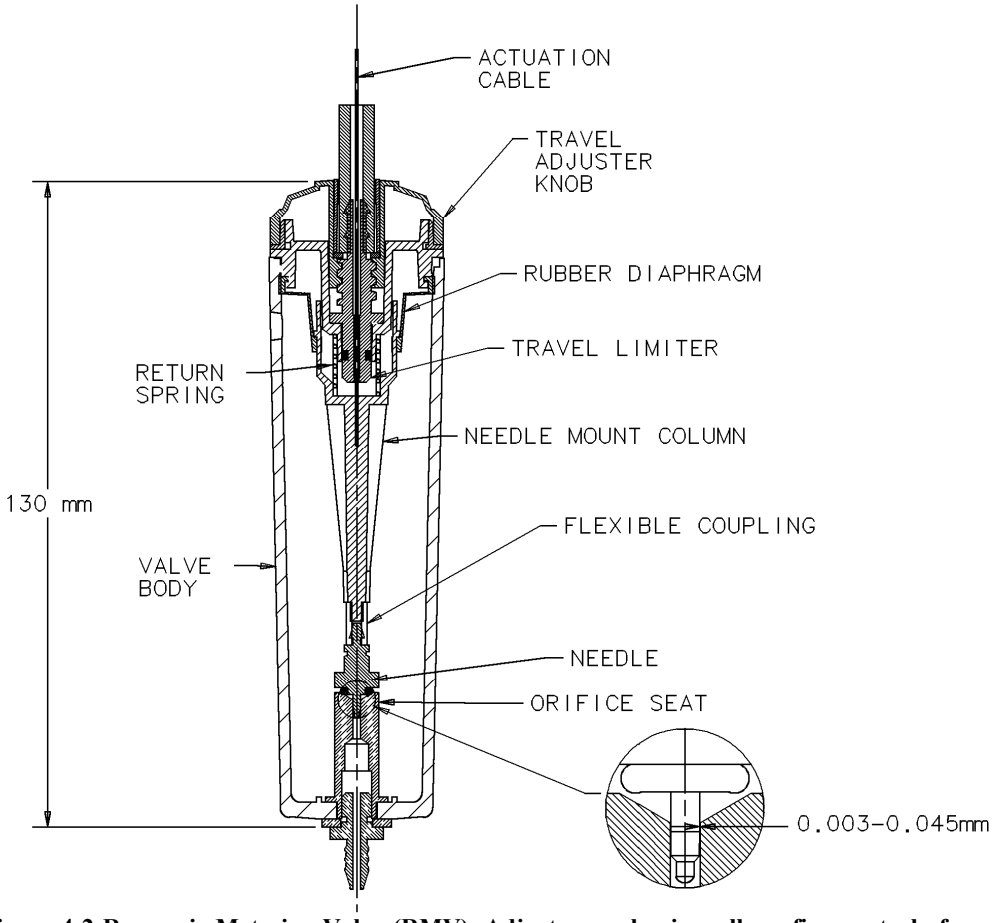

Figure 4-2 Reservoir Metering Valve (RMV). Adjuster mechanism allows fine control of needle position over a range of 2mm. Needle clearances in the orifice are 0.003-0.045mm.

4.1.1 RMV Test Valve

This research is structured around a particular commercial needle valve (RMV) one of the aims being to expand the functionality of the valve in terms of mechatronic control. The original valve design as currently being produced by Scottoiler is not conducive to mechanical control as it is designed to be activated by a vacuum. With

the exception of the actuation cable, the valve shown in Figure 4-2 is identical to the original valve configuration. The valve is opened by a diaphragm and is normally connected to the intake manifold of a motorbike engine. The needle position is controlled by a rotational dial (travel adjuster knob) that limits the needle lift so that when the vacuum is applied, the needle mount column is lifted via the diaphragm and its movement limited by the position of the rotational dial. As the standard valve is activated by a vacuum, the test valves required modification in order to facilitate activation by other means. Two types of interface modifications were made, both of which were simple in concept but required persistence to ensure they operated correctly.

The valve needle is mounted on the end of a shaft that runs the length of the valve which in turn is mounted on a diaphragm which allows the needle to move in the orifice while maintaining a sealed unit. Fixing a mechanical attachment required solidly fixing a length of nylon cable to the needle mount. This was easily achieved by drilling a hole through the needle mount and passing the cable through so that the cable would act directly on the needle mount. Subsequent trial and error established a method for sealing the hole in the needle mount to ensure a sealed valve unit. This is particularly important as any leak path results in fluid escaping from the system which has particular repercussions when measuring the effects of pressure head on valve flow. However having the needle mounted on the end of a shaft which in turn is mounted on a flexible diaphragm has some disadvantages. For example, a misaligned actuation cable can cause the needle mount to rotate about the diaphragm, due to the length of the needle mount column this causes a significant radial displacement of the needle mount relative to the orifice.

There are significant implications for the valve model due to the needle mount system and alignment of the needle within the valve orifice. This will be discussed in the channel geometry modelling stage in Section 5.1.3.

The second modification was to allow a linear actuator to connect directly to the needle mount. This too required some experimentation in order to achieve the necessary performance. The initial prototype used a flexible coupling between the needle mount column and the linear actuator. However it was found that at high differential pressures, the needle was forced to retract from the orifice, altering the follow rate. This altered the inherent flow characteristics of the valve and an alternative system was investigated. Modelling of the valve flow based on needle position and differential pressure is described in the following chapter.

4.1.2 Labview

As with all mechatronic systems, the experimental test rig created for the purpose of investigating the flow behaviour of the needle valve requires a software control system that complements and works in conjunction with (and within the limitations of) the physical hardware that makes up the rest of the same system. Some form of logic control is required for a diverse range of tasks including; data acquisition of timing and temperature data, temperature control, control of valve actuation through a solenoid or linear actuator, and control of a conveyor simulator. National Instruments program and control application LabVIEW version 7.1 was used as the controlling software. Several reasons contributed to its selection, including; availability, the relative ease at which an inexperienced programmer such as the author is able to achieve required functionality and the advertised ability to be able to interface with numerous types of hardware. The ability to be able to create programs built up of

blocks of code (known as Virtual Instruments or VIs) was seen as being of particular benefit. While some of the functions just mentioned are specific to the laboratory environment, some functions such as valve actuation and potentially temperature and timing acquisition are intended to be incorporated into some form of integrated commercial product. From this point of view it is acknowledged that a final product would require some form of embedded control rather than a computer based control program, however, a computer based system allows for much faster development of complex functions through the sophisticated user interface; a process known as Rapid Control Prototyping (RCP) [9]. Once the necessary data has been captured and analysed and the control parameters suitably refined, it should be entirely feasible to incorporate this knowledge into an onboard integrated chip. The important point at this stage is to develop the relevant knowledge for the application and that the control medium, PC or integrated chip, is of secondary importance.

In practice it was found that it was relatively easy to develop specific functions, such as timing measurements, temperature measurement and control data recording etc, but it was found that it became increasingly difficult to integrate new functions into a single program that could fulfil the needs of different types of experiment. As new functions were added or combined, problems would appear that became increasingly difficult to solve. The most common serious problem that was often the hardest to detect and solve was that of timing. It could also be manifested in several different modes. As timing is central to the experimental process as a means of determining flow rate, particular care must be taken to avoid sources of timing errors. Timing errors are not always immediately obvious and many experimental results were generated before realising there may be errors. Additionally, any changes to the program can introduce errors. As there was a range of different experiments to

perform, this necessitated different uses of hardware and therefore different software configurations, each of which needed to be verified for reliability.

As an example, a typical timing problem involved the simultaneous recording of temperature and drip intervals. The Pico thermocouple logger has a maximum sample rate of 10 samples per second. If temperature sampling is integrated within the drip timer VI, this creates a timing error of around 0.1 second for each drip period. This is clearly not acceptable considering drip intervals may be as small as 0.4 seconds. This therefore necessitates a separate data stream that then needs to be cross-referenced with the drip timing data.

Ultimately it was necessary to develop a number of smaller, simpler VIs built up from functional modules that are dedicated to each experiment rather than a single complex program that that would be able to conduct most experiments.

4.2 Flow rate Q

As discussed in the literature review, using drip intervals as an indication of flow rate is the standard practice at Scottoiler and has been used in a number of previous studies into the flow properties of the Scottoiler valve [11-13]. There is also evidence of drip intervals being measured as part of flow studies, although not necessarily as a measure of flow rate. It was on this basis that it was decided to construct an automated drip counter to allow more accurate time intervals to be recorded and to aid in the timing of very long drip intervals. It follows that if the drip volume is known, it is possible to calculate the volumetric flow rate, which is a much more useful parameter to work with than drip interval when investigating valve flow properties.

The use of the drip interval method of flow rate measurement is convenient as it allows the construction of a highly accurate flow measurement rig capable of measuring a wide range of flow rates, including very low flows. It is possible to do this using inexpensive general-purpose lab equipment at a fraction of the cost of purpose built equipment; especially as the flow rates being studied are in the region of 0.1-400ml/hr. In fact, using the drip interval method there is no theoretical lower limit for flow measurement, although there becomes a practical limit as the drip intervals become too long for practical use. The other problem with long intervals between discreet measurements is that there is more likely to be a variation in operating conditions over this time, that may affect readings, and that instantaneous flow rates are not being measured but in effect the aggregate flow over the drip interval period.

The basis of flow rate measurement is $Q=V_d/T_p$, where V_d is the drip volume in ml and Tp is the time interval between drips in seconds. The volumetric flow rate Q is normally expressed in terms of ml/hr as this suits the general flow rates being studied. In order to accurately measure flow rate using this method, it necessarily follows that the time interval and drip size need to be accurately accounted for. Figure 4-3 shows the breakdown of the parameters that need to be accounted for in order to make an accurate flow measurement.

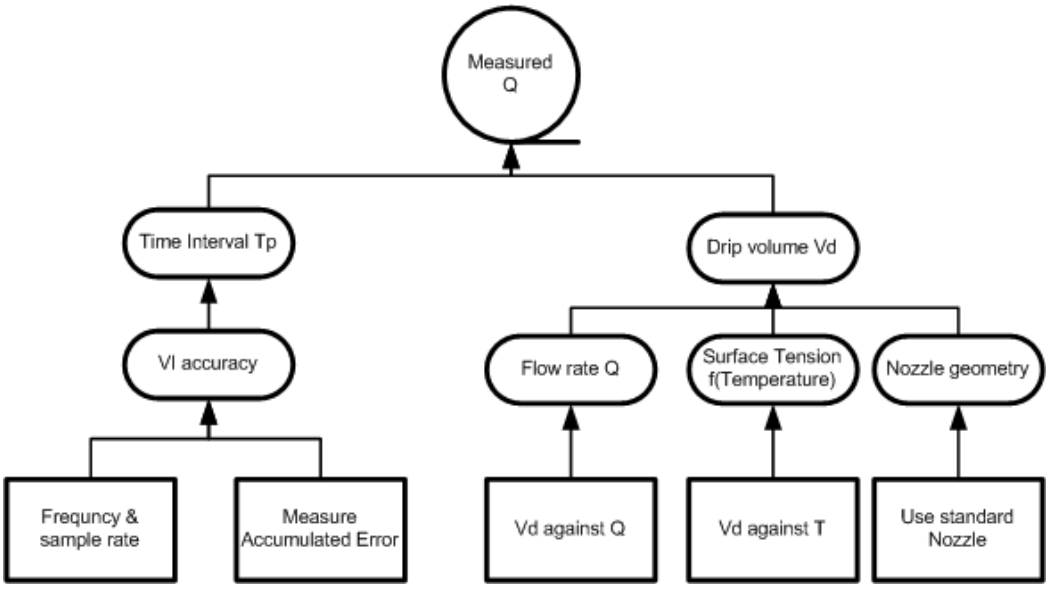

Figure 4-3 Drip time interval based flow measurement structure

4.2.1.1 Timing

Measurement of the drip interval T_p is achieved through the use of a piezo disc and analogue to digital data recorder. As the drip impinges on the disc from a height, an analogue signal is generated by the piezo disc that can be analysed by a PC. Figure 4-4 describes the process of converting a pulse signal into Boolean output with the time lapse between pulses corresponding to the drip interval.

A National Instruments USB-6008 was used to convert the analogue signal to digital to be processed by Labview. This inexpensive device has eight 12bit analogue inputs, two analogue outputs and twelve digital in/outputs. Maximum sample rate is 10k samples/second. The Labview program was set to detect the pulse generated by the drip hitting the disc and used a real-time clock to compare the time interval between drips.

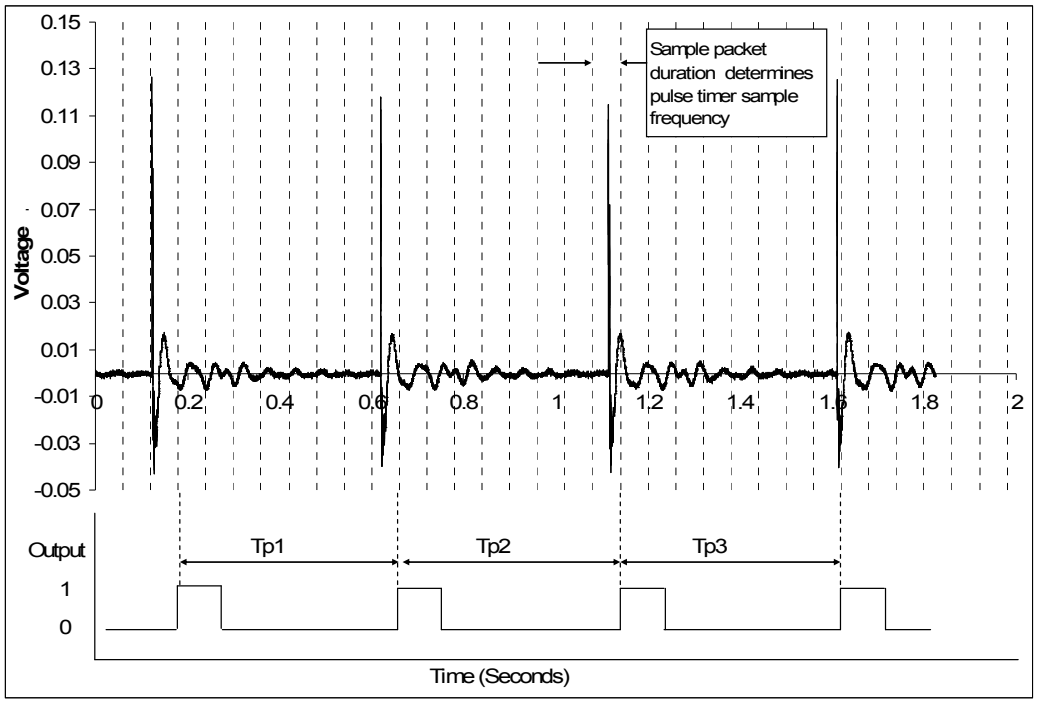

Figure 4-4 Drip voltage input pulse (top) with corresponding Boolean output (bottom). Real time clock starts and stops at the leading edge of each pulse to generate the time interval T_p.

It should be noted that Figure 4-4 is an example of the signal to be measured and that it is not necessary to capture the drip signal in such high definition for the purpose of drip interval timing. The system takes consecutive snapshots of the incoming signal and determines if a drip pulse event has occurred. If an event is detected, the drip interval timer is activated. The snapshot or packet time (T_d) is determined by:

$$Packet\,Time\,(T_d) = \frac{Device\,Maximum\,Sample\;Rate\,(f_{\max})}{Number\;of\;Samples\,(N_S)}$$

Equation 19

The drip timer frequency is set by the timing of the consecutive packets as depicted in Figure 4-4. Because of this, the packet time (T_d) determines the drip interval sample rate:

$$Drip\,interval\,sample\ \ rate\,(f_{Tp}) = \frac{1}{Packet\,Time\ \ (T_d)}$$

Equation 20

The drip sample rate (f_{Tp}) determines the resolution of the timer. In this way, the number of samples used for a packet has a direct bearing on the resolution of the timer.

A test was conducted in order to determine the minimum packet time (T_d) that will reliably detect the pulse and to establish the effect of the packet time on the drip interval timer (T_p). The test consisted of timing the drip interval for a constant stream of drips with an interval of approximately 1.06 seconds.

Figure 4-5 shows the effect of the packet time on measured drip interval (T_p) as controlled through the number of samples (N_S), following Equation 19. It can be seen in the first section for the chart that as the packet consists of 1000 samples, the duration is 0.1 second and this translates to a timing resolution of 0.1 seconds as shown by the T_p value bouncing between 0.99 and 1.09 seconds. Similarly, 500 sample packets have a duration of 0.05 seconds and the timer resolution is 0.05 seconds with T_p values being rounded to 1.04 and 1.09 seconds. Finally, when the snapshot consists of 50 samples, corresponding to a duration of 0.005 seconds, the timer begins to pick up background noise indicating a timer resolution higher than the background noise levels. It was noted that the maximum peak to trough duration of the drip pulse is just short of the 0.005 packet time and that shorter packets of less than 50 samples did not allow the software to reliably detect the rising edge of the pulse.

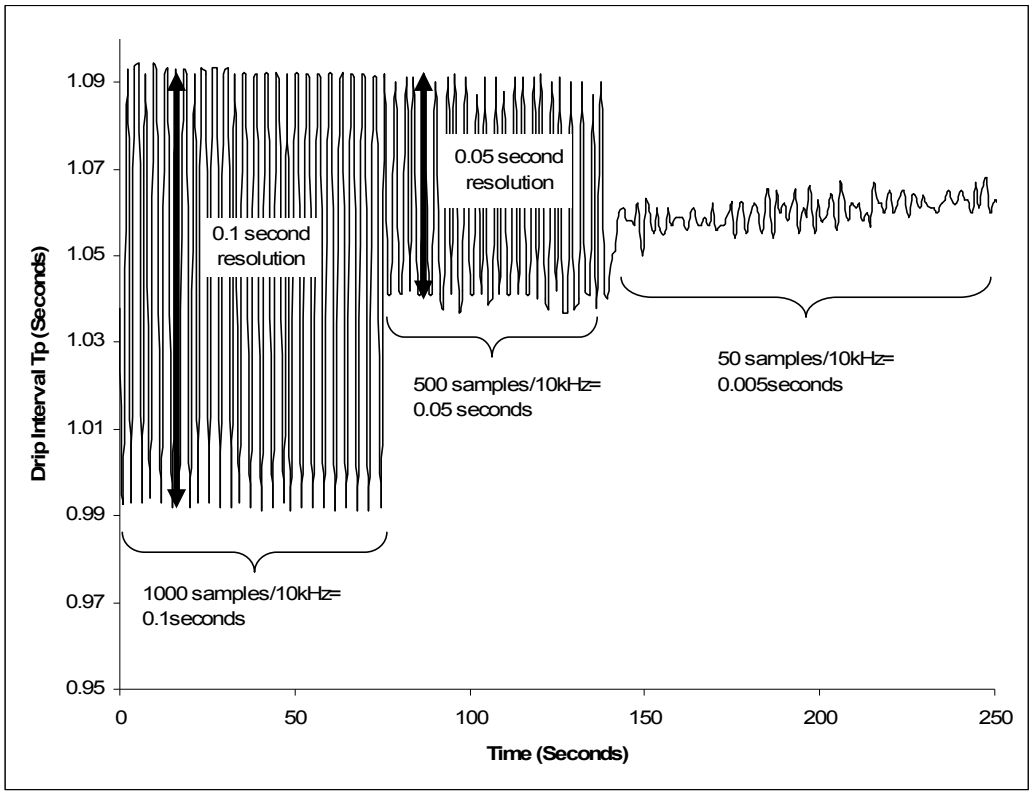

Figure 4-5 shows the effect of packet size on timing accuracy of drip interval T_p with a drip interval of approximately 1.06 s and sample frequency of 10kHz.

Nyquist-Shannon sampling theory states that the sample frequency must be at least twice that of the source frequency in order to be able to accurately reproduce the signal [142]. In this case our maximum drip interval timer sample frequency (and therefore also resolution) is 0.005seconds or 200Hz. Therefore theoretically the maximum frequency the timer is able to capture is 10Hz.

4.2.1.2 Timer Calibration

During initial development of the timing VI, it was found that certain program structures could cause the VI to miscalculate the drip time interval (T_p). Because of this, it was necessary to verify as far as possible that the system was indeed accurately capturing the time interval.

A synthesised function generator; GFG-2004 by ISO-TECH, was used to simulate the signal generated by the drip impinging on the piezo transducer. The rising edge trigger of the timer VI was able to detect the synthesised signal in the same manner as the drip signal and there was no difference in the ability to detect the sine, square or triangular waveforms from the function generator. The generator's range is 0.1Hz to 1MHz, while the drip frequency of this study is approximately $1x10^{-3}$Hz to 5Hz. The overlap is sufficient to cover the most critical timing area as any timing errors will have the greatest impact at high frequencies as the relative error is larger. In this way, if the timing error is acceptable at high frequencies it will also be acceptable at the lower frequencies. The high frequency outputs that can be produced by the generator also allow the upper limit of the timer system to be explored although it should be noted that it is generally the lower flows that are of interest in this study.

Hz	**0.1**	**0.2**	**1**	**5**	**10**	**100**
T_p (Sec)	**10**	**5**	**1**	**0.2**	**0.1**	**0.01**
Mean Measured Value	9.9998	4.999324	0.998983	0.198358	0.084671	n/a
Standard Deviation Absolute Error	0.00119	0.001248	0.001261	0.001761	0.015329	n/a
Standard Deviation Relative Error (%)	0.0119	0.0249	0.126	0.880	15.32	n/a

Table 4-1 Timer calibration results. Mean and standard deviation for a range of drip period values. Accuracy reduces significantly above 10Hz and fails at 100Hz.

Over one hundred time interval readings were taken at a selection of frequencies increasing from 0.1Hz until the drip internal timer no longer functioned. The mean measured value is given for each of the frequencies in Table 4-1. Also shown is the standard deviation of the absolute error and the standard devotion of the relative error.

It can be seen that in the 0.1 to 5Hz range the mean measured value is very close to the input signal value and that the absolute error small and fairly constant at approximately 0.001 second. However at frequencies above 0.2Hz, the measured mean value is further from the input signal value and the absolute error increases significantly. By 100Hz the timer is no longer able to operate. The reliable working range of the drip timer is most clearly illustrated by the relative error. This increases as the drip interval reduces to the point where the error is no longer acceptable. From this it can be concluded that a drip interval of 0.2seconds or 5Hz is the top limit of the flow measurement timer and that the error level is acceptable for values below this. This is lower than the theoretical maximum discussed in the previous section.

4.2.2 Drip Volume

The other half of accurate flow measurement using the drip interval method relies on knowing the drip volume (V_d). This entails a more involved process than that of interval timing and requires calibration. While there is a substantial body of work investigating the dynamics of a dripping liquid, there remains a lack of practical analytical solution for determining the volume of a drip. The Rayleigh formula describing drip mass; $m \approx 3.8.\sigma.(r/g)$ is somewhat simplistic and does not account for the variety of influences encountered in a typical experimental situation (m = the mass of a drop, σ = surface tension, r = radius of the nozzle and g = gravitation constant). More recent developments tend to focus on experimental and numerically derived results or other models based on the mass spring model [99, 103, 121]. Previous work not withstanding, it is still a significant endeavor to predict drip volume given an initial set of conditions, hence the need to determine volume experimentally over a range of experimental conditions.

In this case the controlled variables are flow rate Q as a function of fluid head dh, and valve setting VP, ambient temperature t and viscosity grade of oil. The nozzle is constant across all experiments.

The drip volume was measured manually using a 5ml measuring cylinder in order to calibrate the drip volume over the working range of variables. Care was taken to ensure that the manually measured volume was a true reflection of actual volume; this was done by averaging two hundred drips over a period of time. Tests conducted at temperatures below ambient room temperature necessitated the use of an environmental chamber from which it is not possible to manually count drip numbers and so the automatic drip counter was used. The LabVIEW controlled valve meant that a precise number of drips could be counted into the measuring cylinder. Investigations were conducted to ensure that the residual fluid remaining on the sensor did not affect the volume measurements. It was found that by priming the sensor with a residual oil film, that there was no measurable difference in overall measured volume compared to manually counting drips. Care was also taken to ensure that there was no splashing as the drip hit the sensor. As relatively high viscosity fluids were used, it was possible to channel the fluid off of the sensor directly into the measuring cylinder. With these precautions in place it was then possible to measure the drip volume over different time periods and at different temperatures.

As can be seen from Figure 4-6, drip volume V_d, is stable above T_p=10 and increases significantly below this value, with particular effect below T_p=5. It can also be seen that V_d follows the same trend for different temperature ranges.

Using regression, it is possible to approximate the curve with a function of the form $V_d = a + be^{-Tp}$. In this case a=0.018814 and b=0.005749. Using the approximated value

of V_d it is possible to calculate a value for Q and compare this with the measured value of Q (see Figure 4-7). A very close correlation can be observed with slightly greater differences appearing at very low T_p values. It can also be seen that using a constant value for V_d significantly under predicts at low T_p values indicating that an average drip volume value does not predict the flow rate well over the full drip interval range. For example if the drip volume is assumed to be constant across all flow ranges at V_d=0.018814ml as an average value, the flow rate at T_p=0.22sec is given as Q=307ml/hr. In comparison, the modelled drip volume is V_d=0.02342ml at T_p=0.22sec which results in a calculated flow rate of Q=383ml/hr and so much closer to the manually measured flow rate of Q=392ml/hr. This demonstrates the benefits of using a modelled value for drip volume over an over the assumption that drip volume is constant for all flow rates.

Overall, the drip size model contributes to a good approximation of flow rate, however there are problems with this when it is necessary to express the drip interval in terms of flow rate. As $Q=V_d/T_p$ and $V_d = a+be^{-Tp}$, this means that $Q=(a+be^{-Tp})/T_p$, and so it is not possible to express T_p in terms of Q. It is therefore useful to be able to convert directly between drip interval and flow rate. Fortunately this is made particularly easy due to the extremely linear relationship between the two parameters when the relationship is displayed on a logarithmic scale (Figure 4-8). The author is not aware of this relationship between drip interval and flow rate in any existing literature. The straight line in Figure 4-8 can be approximated by an equation of the form:

$$lnQ = m.lnT_p + c$$

Equation 21

In this case m= 1.033 and c=4.381. It can be seen from Figure 4-8 that the measured data, drip volume model (Modelled V_d) and the model based on Equation 21 (Tp-Q Model) are all very close and only the model based on the assumption of a constant drip volume (V_d=0.018814) deviates from the measured data. Using Equation 21, it now becomes a much simpler process to convert between the two parameters, especially when working with control programs where the working parameter is T_p but the user parameter is normally Q.

Due to the accuracy of the timing system, the resolution of the flow measurement is such that discernable differences in flow rate can be immediately identified from sub-millimetre changes in pressure head and temperature changes as small as 0.1°C. As the LabVIEW program uses a real-time clock for timing, the timing error is not proportional to the drip interval. This means the proportion of timing error to total drip interval time reduces as drip interval increases; this has the positive effect of increasing measurement accuracy as flow reduces. If timing resolution is taken as equal to noise amplitude (0.01sec), Table 4-2 shows that flow rate errors range from 20ml/hr at T_p = 0.2 sec to $6x10^{-5}$ml/hr at T_p=100. This equates to 4.762% and 0.01% of flow rate respectively. The range and accuracy of this flow measurement system is unique and as such makes a significant contribution to this thesis.

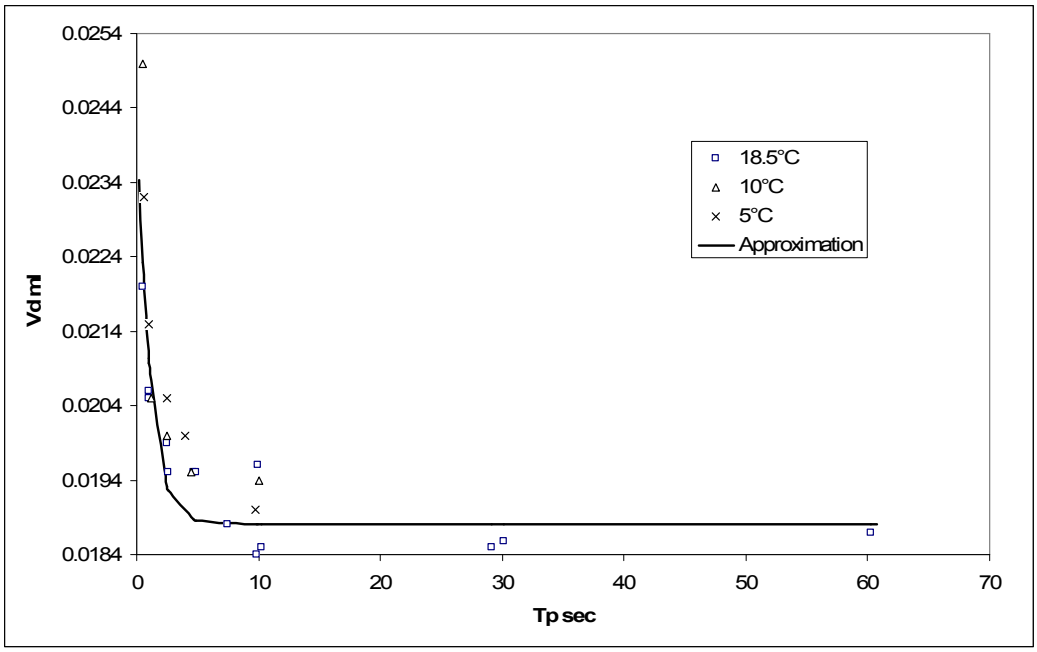

Figure 4-6 Drip volume (Vd) increases as drip interval decreases (flow increases) over different temperature ranges.

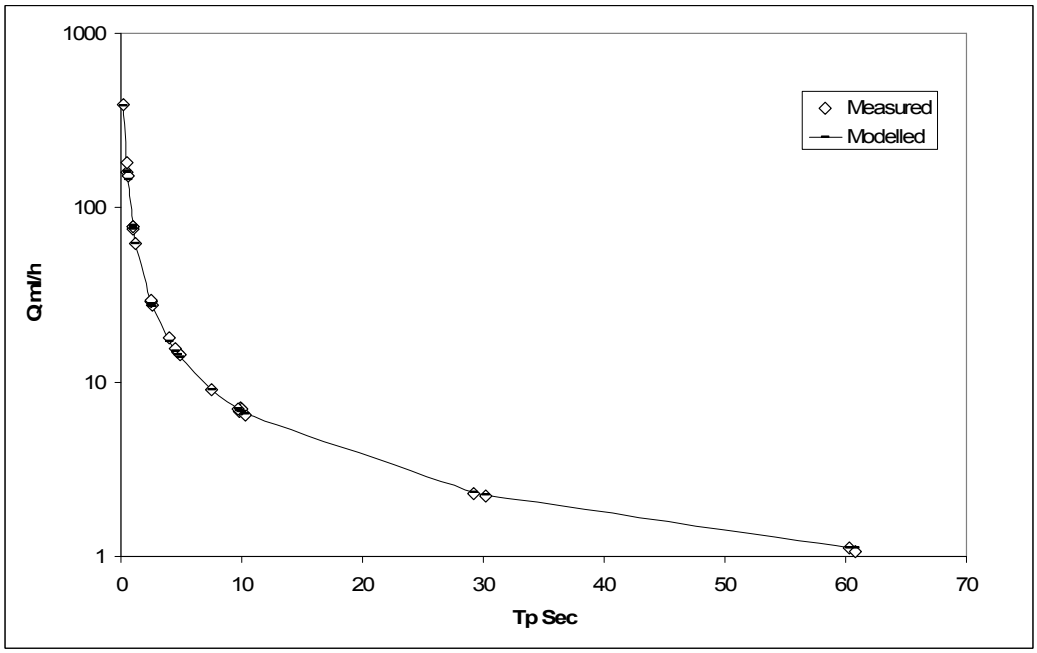

Figure 4-7 Measured and modelled flow rate compared.

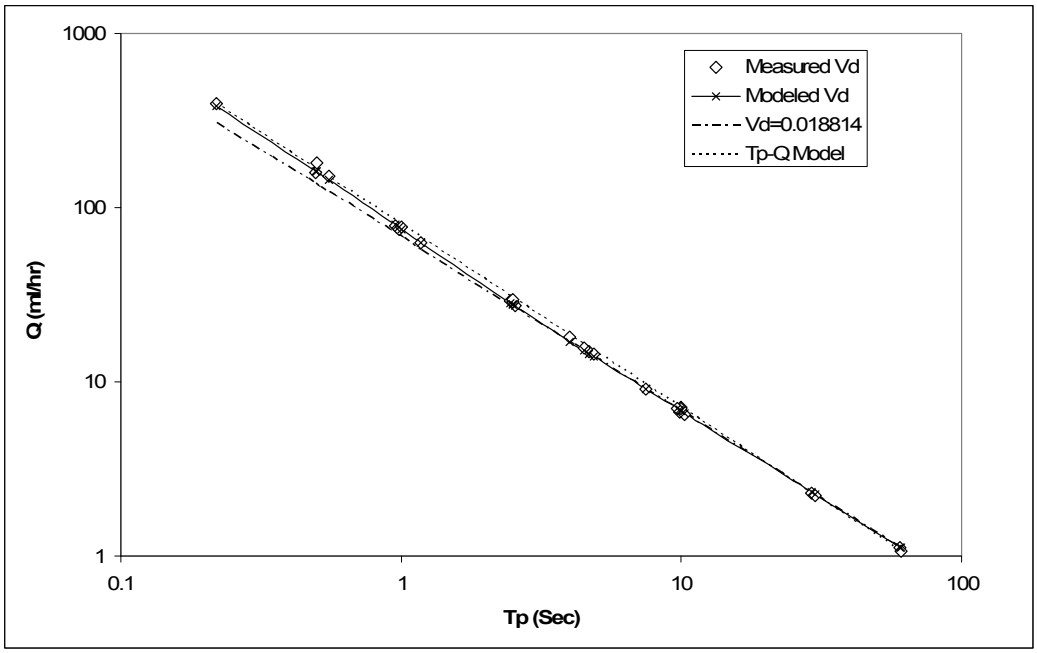

Figure 4-8 A direct linear relationship can be made between drip interval (T_p) and flow rate (Q).

T_p sec	Vd ml	Q ml/hr	Error ml/hr	% of Q
0.2	0.0235	423.38	20.161	4.762
10	0.0188	6.77	0.007	0.100
60	0.0188	1.13	1.880E-04	0.017
100	0.0188	0.68	6.767E-05	0.010

Table 4-2 Effects of 0.01sec timing error on flow rate including percentage error

4.3 Temperature

Experience from the industrial partner and previous academic investigations [11-13] into the flow properties for the valve acknowledged a significant influence of temperature on the flow rate of the valve. The susceptibility of needle valves to temperature fluctuations was confirmed in the literature review [22]. The studies conducted by Crosson and Casey used commercial ovens and refrigerators to control ambient temperatures where they noted that the control systems used by the refrigerator and oven caused significant fluctuations in temperature that probably affected test results. It was decided to investigate the effects of temperature on valve flow rate, with the expectation that it would be necessary to develop some form of

environmental control for the test rig to improve on the existing refrigerator bang-bang temperature controller.

A Pico Technology USB TC-08 device was purchased for the purpose. It is a USB device that allows data recording from eight thermocouples using standard miniature thermocouple connectors. It also comes with its own logging software but is able to interface with LabVIEW. This is particularly important as the temperature data needs to be synchronised with the flow data in order to be able to investigate a possible link. Using the VIs supplied by Pico it was possible to integrate the temperature data logger into the drip timer VI. This included setting thermocouple types and channels. Channel zero is reserved for the cold junction compensation and is built into the logger unit. One of the reasons for choosing thermocouples over other temperature logging methods such as RTDs (Resistive Temperature Detector) and thermistors is that they are easily fabricated and are very small and can therefore be incorporated inside working devices. Their small size also makes them extremely responsive to small changes in temperature with a particularly small time constant.

Up until this point it had always been assumed that the variation in flow rate of the valve while in use in the field was due to a temperature induced change in viscosity of the lubricant. As discussed in section 5.1.1, mineral oils are highly susceptible to temperature induced changes in viscosity. It is for this reason that the first explorative experiments used a thermocouple inside the RMV near the orifice entrance in direct contact with the fluid. A second thermocouple was placed on the outside as a means of monitoring ambient conditions. It quickly became apparent that whilst there was a correlation between flow rate and fluid temperature, there is a much stronger link with the temperature of the valve body. Figure 4-9 demonstrates the close link between

flow rate and valve body temperature. The lag in the flow rate response to changes in valve body temperature is very small. Fluid temperature would seem to play a less dominant role in affecting flow rate.

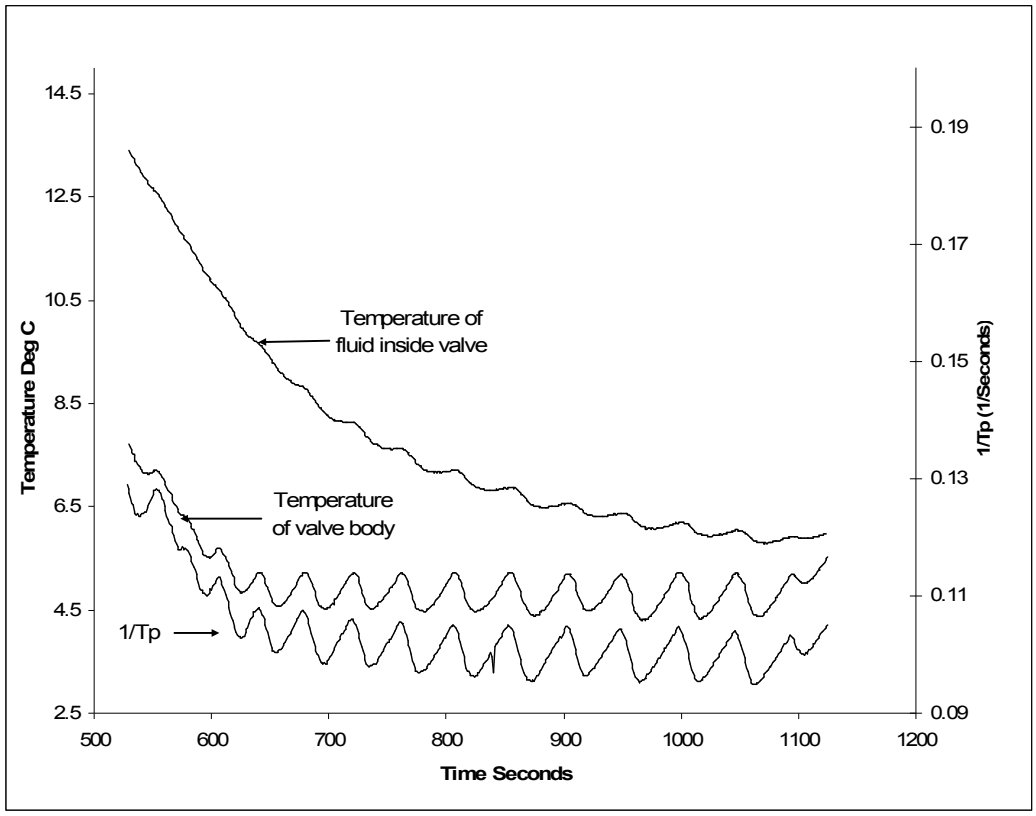

Figure 4-9 there is a very close correlation of flow rate with the valve body temperature while the correlation with the fluid temperature is much weaker. Flow rate is represented by 1/drip interval ($1/T_p$).

4.3.1.1 Temperature control

From these observations it can be concluded that temperature has a compound effect on flow rate through the expansion of the valve and change in viscosity of the fluid. This makes it essential to have a controlled environment in which to conduct flow testing. A temperature-controlled environment would allow:

1. Accurate testing of flow rate in a stable temperature for investigation of properties not related to temperature, such as needle position, needle shape and pressure differential.

2. Investigation of dynamic effects of temperature change on the valve through continuous variation of temperature.

3. Investigation of changes in viscosity by setting temperature at specific values within the temperature range. This relies on knowing the temperature-viscosity properties of the fluid and allowing temperatures to stabilise through the whole valve and fluid.

It was felt that the first reason alone was the minimum requirement for temperature control and that cases 2 and 3 would allow a more detailed analysis of temperature effects.

An investigation of the temperature control methods used in the previous studies [11, 12](a commercial refrigerator and an industrial oven) highlighted some serious flaws in the temperature control, demonstrating that the methods used are not suitable for accurate flow rate experiments. The study revealed that regular refrigerator control units will maintain the temperature inside the fridge to ±0.75°C at a low temperature of 5°C but fluctuated significantly, in the region of ±5°C, when set to maintain a temperature of 15°C. See Figure 4-10. Likewise, the oven used for the previous studies [12] was able to maintain a temperature within ±0.5°C at 100°C, but fluctuated significantly when set to temperatures closer to what would be expected in a warm climate. Essentially, as these machines are designed to operate at temperatures

beyond regular ambient temperatures, they do not cope well when set to maintain temperatures close to ambient.

It was decided to replace the control system of a domestic refrigerator with a LabVIEW based system that would be able to maintain the interior temperature within the bounds required for this experimentation. The aim was to create a system at least equal to the general accuracy of thermocouples at ±1°C.

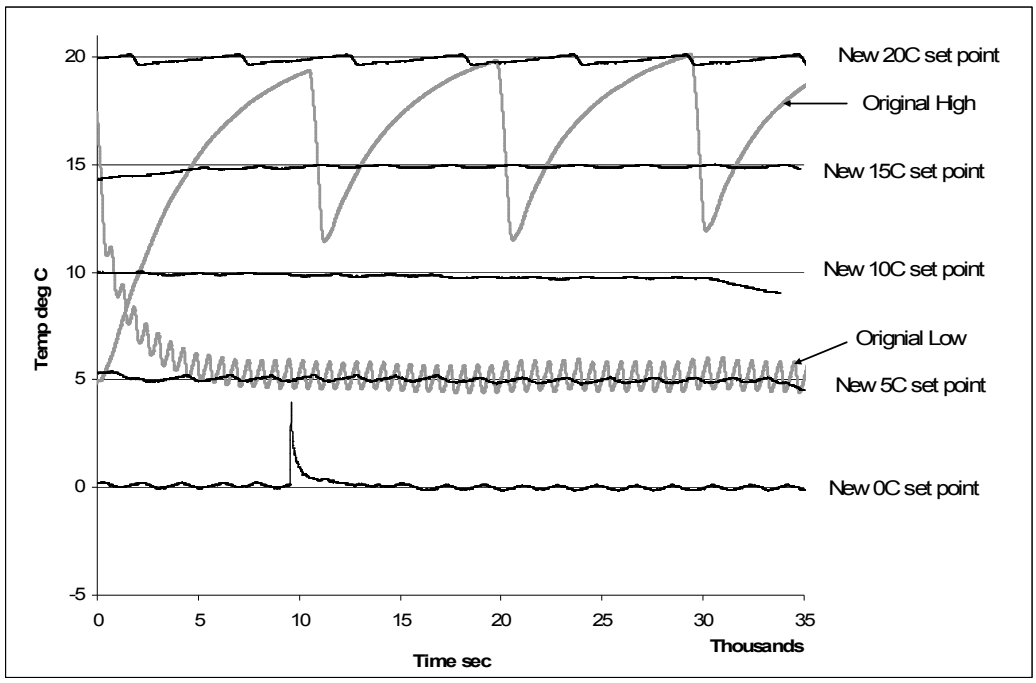

Figure 4-10 Automatic temperature control for unmodified refrigerator (Original) and with the new control system (New).

The power control circuit was connected directly to the refrigerator pump bypassing the existing control circuit. The new power control system is activated by the digital output port of the same National Instruments USB-6008 unit used to sample drip intervals. The only means of controlling the temperature of the fridge is by turning the pump on or off in response to a measured temperature reading. The very basic level of control can lead to a number of problems, which were overcome satisfactorily.

The basic on/off function of the refrigerator pump means that the cooling level cannot be made proportional to the difference between actual temperature and desired temperatures. On top of this there is no active warming, so that if the fridge element or interior drops below the required temperature, there is no means of raising the temperature other than by equalisation with room temperature. A basic level of control can be achieved by setting upper and lower limits around a desired temperature. In this way the pump can be turned on if the interior temperature rises above the upper limit and will switch off below the lower limit. Simple logic control can be used to maintain a steady command while in between limits, meaning that if the temperature is rising it will continue to do so until it clears the upper limit and vice versa for the lower limit. This creates a steady oscillation based on, but not limited to, the preset limits. The steady oscillation can be closely controlled and prevents the pump from flipping between the on and off states.

There can be a large lag between the temperature of the cooling element and the interior of the fridge, especially when initiating large temperature changes. This means unless the system is damped, it suffers from severe overshoot and may take a considerable time to reach a stable temperature. The interior temperature settling time is reduced if the difference between the desired temperature and the temperature of the cooling element is limited. This is proportional to the difference between the actual interior temperature and the desired temperature.

In conclusion, the temperature effects on the valve necessitate a stable testing environment and the ability to change the ambient temperature to test the temperature effects on the valve. To this end, an environmental chamber was created using a

domestic refrigerator with a bespoke control system that is able to maintain a stable temperature to within ±1° and normally ±0.5°.

4.4 Valve Details and Setup

While the previous section described the apparatus necessary to study very low flows and to take account of temperature effects, the object of study is the needle valve itself as this is the means by which the control for the flow is achieved. As such any valve used for a flow study must be strictly defined in terms of physical characteristics in order that they may be accurately related to the experimental conditions. The most critical valve parameter is the needle geometry.

4.4.1 Defining Needle Geometry Characteristics

The valve is only one part of a whole flow control system. One that is influenced by many controlled and uncontrolled factors, however, the primary means of adjusting flow rate is through altering the position of the valve needle relative to the valve orifice. This is because it forms the narrowest flow channel in the whole system; it therefore exerts the greatest influence. As such, the narrowest point of the flow system, which has a cross sectional area many times smaller than any other part of the system, is termed the *Active Channel* for the purposes of this thesis.

In order to understand the effects of needle and orifice geometry on the flow characteristics of a valve, it is necessary to define the flow channel geometry and understand how the channel geometry is affected by needle movement. It is also important to have a reliable means of defining the position of the needle relative to the orifice without which it is not possible to define the channel geometry. The process of understanding the flow channel geometry and needle positioning was an iterative

process that consumed a significant portion of the overall time spent on experimentation and analysis and involved considerable observation, flow measurement and geometrical measurements.

Initial attempts to model the channel geometry were based on models constructed from the theoretical shape of the valve based on the manufacturing drawings of the valve components. This allowed the calculation of the channel geometry as a function of needle movement in line with standard valve theory and was initially centred on the channel area rather than the whole channel. However it was found that at the scales involved, it was not sufficient to rely on the dimensional tolerances specified in the drawings and that a greater level of certainty of the needle geometry is required in order to be able to link flow models and theory with test results. In essence, once accurate flow measurement equipment was developed, it was necessary to ascertain the integrity of the samples being tested. Some characteristics can be directly measured, while others can only be assumed or observed. For example it is possible to quantify the geometry of the needle and its linear relationship to the valve seat, while it is not possible to determine the level of concentricity.

Defining the precise needle geometry and any assumptions made is essential for the integrity of subsequent analysis. The effects of the investigation and definition of the valve geometry on model structure is explained in Section 5.1.3. For the purposes of analysis the needle was split into sections. This also facilitates communication by labelling the various features of the needle. Figure 4-11 shows the breakdown of geometrical features. The geometry is exaggerated to make it easier to see subtle and small details.

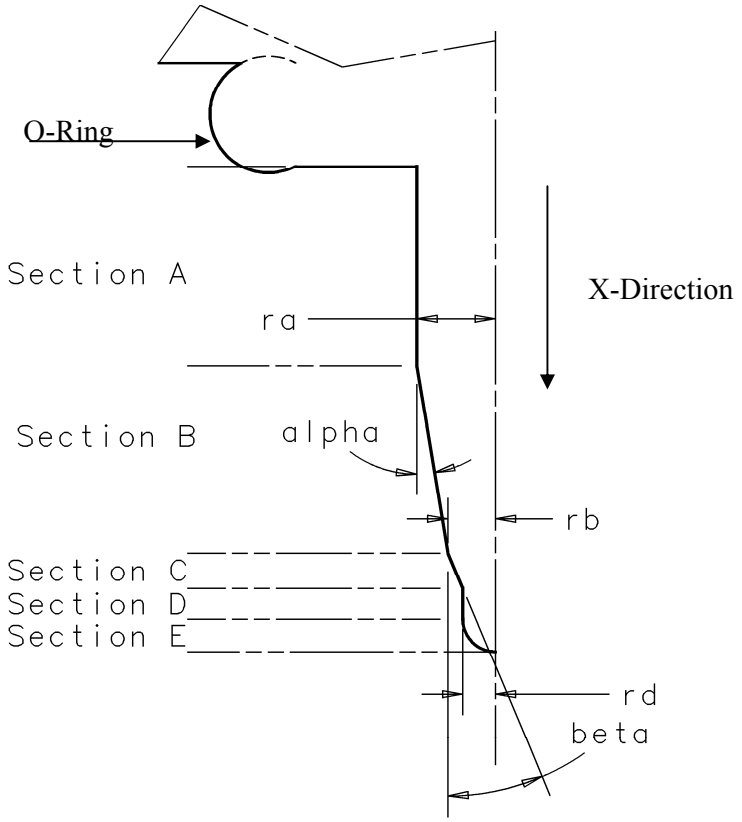

Figure 4-11 Valve needle basic geometry

Points to note about the needle shape are:

- Only sections A and B have an affect on flow through the valve as they form the narrowest point of the flow channel and as such are used to define the active channel, see Figure 4-12.
- The angle Alpha forms a shallow angle taper of approximately 1° between section A and Section B. A zero degree taper results in a parallel sided needle. A limited number of tests were also conducted on 2°, 3° and 4° taper-angles.
- Sections C, D and E form a feature used to develop high flow rates (in the region of 400ml/hr) for the purpose of priming delivery conduits downstream of the valve while maintaining needle location within the orifice. This section is not used for flow control, merely for priming the system.
- In reality, Section E is not the dome described in the manufacturing drawing, but a flat end with rounded corners.
- It can be seen from Figure 4-12 the o-ring has very little effect on restricting the flow of fluid through the valve onve it has moved a short distance for its

seat. There is a very large sudden increase in area in proportion to the area of the needle orifice for a small displacement of the needle. However, in practice is was found that due to the axial misalignment and o-ring deformation there is a transition zone were it seems the o-ring does affect flow rate before a full seal is made.

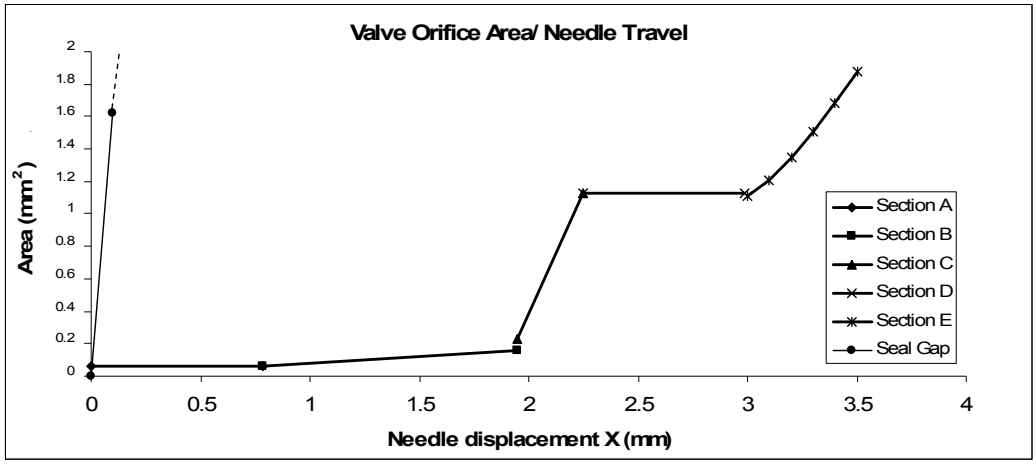

Figure 4-12 Valve flow channel area as a function of needle travel. The series of lines representing the change in orifice area due to profile of the needle as it exits the orifice is denoted by the bold lines with the Section label. The change in orifice area caused by the o-ring interacting with the sealing surface is shown by Seal Gap line.

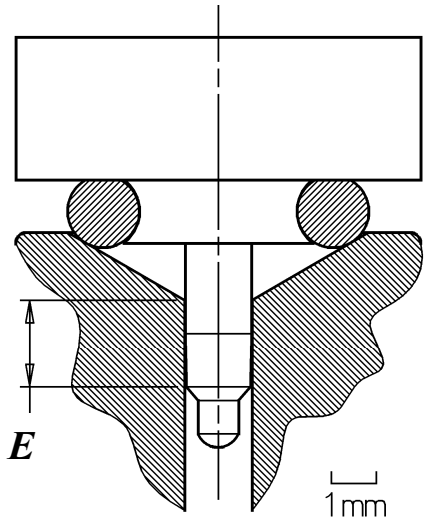

Figure 4-13 Engagement Length *E* defined by the needle in the orifice. Note how the clearance between the needle and the orifice is barely visible even at this scale.

The engagement length, *E*, is defined as the length of the active channel portion of the valve geometry and is the distance from the mouth of the orifice to the end of the

needle, excluding the nipple end of the needle as shown in Figure 4-13. Needle displacement is zero at maximum *E*.

According to the design specification, there is a clearance of 0.005-0.045mm between the needle diameter and the orifice wall (Table 4-3). As the needle is mounted on the end of a shaft, which in turn is mounted on a flexible diaphragm and because there is no specific alignment mechanism for the needle, it should be assumed that the needle is always in contact with the orifice wall.

	Nominal	**Min**	**Max**
Orifice D (ro) mm	1.5	1.49	1.51
Pin d (ra) mm	1.475	1.465	1.485
Needle Clearance mm	0.025	0.005	0.045

Table 4-3 Valve orifice clearance based on design tolerance.

An investigation was conducted using CAD to determine the extent of axial misalignment. An assumption that takes into account the working conditions of the valve would be that the needle mount column rotates about the stop mechanism, but not to the extent that the flexible coupling becomes distorted. In effect, it assumes that the needle mount column, flexile coupling and needle are a rigid member. If the needle-mount assembly is assumed to be rigid, it can be assumed to be flexibly located at both ends. The maximum angulation permitted at the needle end is restricted by the diaphragm, and the rotation caused by unevenness in the diaphragm is restricted by the needle in the orifice. By restricting the movement at either end of the needle and mount assembly, rotational movement is minimal, in the order of 0.01°.

To back up this assumption, a heavily used valve was examined with the expectation that there may be signs of wear on the needle to indicate contact with the orifice wall. On disassembling the needle and valve, the first observation is that the normally

bright brass surfaces have become an almost uniform dull brown. The cause of this is likely to be some form of mineral deposit from the oil. Where the needle has been in contact with other parts, the needle is clean and bright.

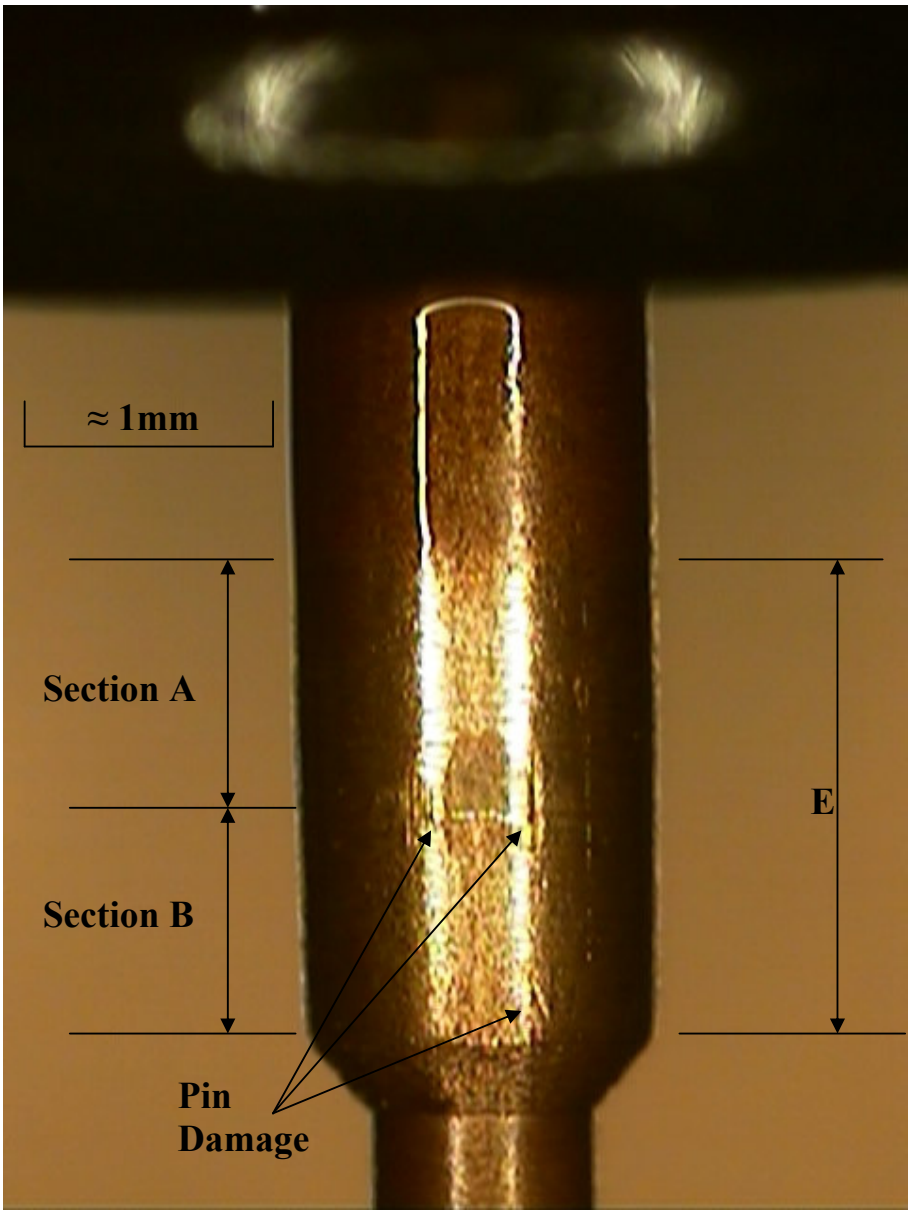

Figure 4-14 The bright white reflections of the light give an indication of surface roughness. It is thought that the slightly pitted bright surface is more representative of the original surface and that the duller smoother finish is due to deposits from the oil. The surface grooves made during manufacturing are just visible

As can been seen from Figure 4-14, where the needle has been in contact with the orifice wall, it has been rubbed bright with the base of the pin retaining the dull colour

of the rest of the needle. The bright section was measured and found to be approximately 1.85mm. This corresponds very closely with maximum *E*, as indicated in the Figure 4-14. It was noted that the bright part of the needle was all the way round, indicating that the needle changes position relative to the seat producing an even contact area. There was not, for instance, a single burnished strip indicating a regular contact in one area, or a flattened area indicating heavy contact in a single rotational position.

There were however some blemishes on the surface of the needle. It is not possible to tell if this is scoring caused by needle movement or damage to the needle prior to assembly. Although the photograph does not show clearly, there may be an element of both.

4.4.2 Needle Geometry Measurement

In order to be able to correlate the geometrically based analytical solution with the flow test experimentation it is necessary to establish the geometry of the needles being tested. This can be split into two types of measurement. There are the component measurements which cover the geometry of the component in isolation and the assembled geometry of the valve that identifies the spatial relationship between the components. The first covers the needle and orifice dimensions and is covered in this section; the second is largely restricted to defining the engagement length E relative to the adjuster mechanism and is covered in Section 4.4.3.

The main areas of focus for detailed measurement were the features that interact with the fluid flow for control purposes. This is essentially everything below the level of

the o-ring. Specific attention was given to sections A and B, which are considered to have the most critical effect on fluid flow.

Detailed measurements were made using a Mitutoyo Quick Scope 359 3D CNC Vision Measuring Machine (VMM) which has a resolution of 0.5µm and an accuracy of 2.5µm in the XY plane and 5µm in the Z axis over the distances measured. It uses a visual graphic interface displayed on a PC to define features to be measured. The interface allows features such as straight edges, arcs or circles and points to be defined as a coordinate and vector or coordinate and radius. Measurements such as the distance between lines and the position of the intersection of two lines are calculated from the definition of the lines involved. While it is possible for the software to define intersects and distances for the user, it can also be done manually using the line definitions. As the latter method was generally found to be more convenient, the measured geometry was drawn to scale in a CAD environment where it is easier to visualise the interactions between the needle and orifice and to measure the geometric relationships, e.g. the engagement length or channel size with an eccentrically orientated needle.

It should be noted that while the VMM is extremely accurate at measuring in profiles, and can also measure in the Z-axis, it is not able to determine the 3D geometry of a cylinder as there are no features on the surface to provide a reference. As such it is not possible to determine the true concentricity of the needle regardless of the number of profiles measured.

There were some features that were difficult to define accurately or consistently. These included:

-Shallow taper: Due to the shallow taper-angle of section B, it is very difficult to define the junction between the tapered section B and the parallel section A (see Figure 4-14). A small change in taper-angle or the way in which the angle is defined can result in a relatively large change in the axial location of the intersection. The axial position of the transition from parallel to tapered sections (sections A to B) is important due to the effect of the change in needle profile on the flow rate when the needle position is varied. In general the analytical solutions developed in this thesis assume certain geometries.

-O-ring: This is due to the soft edge that the o-ring presents to the lens. The combination of rough surface and curved form creates a blurred edge and the deformable nature of the material means that the edge is not a true circle. There are tools that automatically pick up multiple points on the edge of a circle, but this was found to produce a high variability as the o-ring surface is made up of many varying arcs. In this case a simple three point tool was used to define the circle in the most critical area, this being the arc that comes into contact with the valve seat and influences the fluid flow. See Figure 4-15. The position of the o-ring has implications on the valve needle control program and can affect flow rates in the near-closed position.

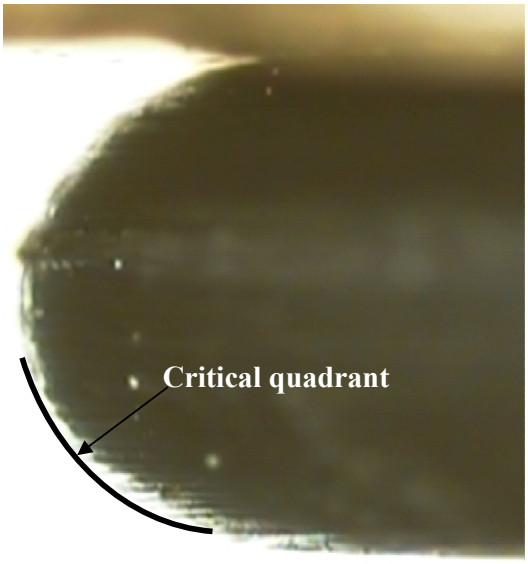

Figure 4-15 Image of O-ring shows surface irregularities. The distortion of the O-ring is clear from the flash line which should normally be through the centre of the arc and at the lowest point in the curve.

-Machined radius: The small radius at the tip of the needle was subject to distortion from a true circle, making it hard to define consistently. Generally this is not a critical dimension as long as the tip of the needle relative to the active profile is known.

It was possible to define some geometry more consistently, including the diameter of section A. This is particularly important due to the role section A plays in the control of fluid flow. While manufacturing tolerances allow the needle clearance in the orifice to be 0.003-0.045mm, it was found to be 0.030-0.036mm and the repeatability of the needle diameter was in the region of 0.002-0.005mm.

The surface roughness of a number of needles were also measured but as these were not used in subsequent analysis they are not presented here. The results are available for reference in 10.3 Appendix C: Surface Measurement.

4.4.3 Needle Positioning

Having determined the geometry of the needle, it is necessary to determine its spatial relationship with the orifice bore. This consists of defining a known relative position or datum for the needle and orifice entrance, then determining the subsequent displacement of the needle in the X direction for a known control input. It is the axial position of the needle relative to the orifice that affects the engagement length *E*. The maximum engagement length is limited by the relative position of the o-ring to the needle shaft and valve seat. The o-ring is also the only form of axial location of the needle relative to the valve orifice. However, this is not a fixed point due to the flexibility of the o-ring and so cannot be used as a positional reference point for the needle.

A number of systems were tried and the method evolved as solutions were sought to accurately define the needle position. Initial methods were based on the theoretical geometric sizing of the valve. This model assumes that the valve is closed when the o-ring contacts the valve seat and displacements based on the pitch of the adjuster mechanism. Using the theoretical closing point of the valve proved inadequate because while this point exists in theory, it is not possible to define in practice due to the deformation of the O-ring. It is possible to measure the point at which the valve seat becomes airtight, but this still does not correspond to a known needle position due to the o-ring deformation. Also, it was found that using the adjuster pitch to calculate needle displacement was unreliable due to the backlash in the system and possible irregularities in the thread form.

As it is not possible to define the needle position theoretically, calibration for each valve must be used to ensure the needle is in a known position for testing. It is

possible to measure the relative positions through the use of a gauge rod inserted into the valve so that it contacts the needle end (see Figure 4-18). This allows the needle movements to be externalised and are therefore visible for inspection. The same method can be used to define the orifice seat position and so the relative positions can be calculated. In order to maintain consistency, each valve used for flow testing had the factory fitted scale removed and a new scale marked on the control knob that sets zero to the valve closed position as determined when the valve seals against a small vacuum pressure.

Figure 4-16 shows the variation of engagement length in relation to the valve dial position, VP. A reading was taken for each position in the open (up) and closed (down) direction, and repeated in order to determine the level of consistency. This clearly shows the backlash inherent in the system shown by the difference between the Up and Down values. Although the readings are largely linear excluding the start and ends, repeating the measurements maintained the slight wave found in the middle. It is assumed that this is caused by inconsistencies in the form of the screw thread, however this can be accounted for in subsequent analysis and the accuracy is solely dependent on being able to position the adjuster knob accurately. In practice the knob is always moved in a single direction to avoid problems with backlash. Moving in the Down direction allows the tests to be carried out with high flows first moving towards low flows. In this way tests can be stopped once flow is judged to be negligible.

The screw thread has a measured pitch of 3.15mm; this gives a theoretical needle displacement of 0.166 mm per mark on the adjuster scale. Figure 4-17 shows the actual displacement per mark in comparison to the theoretical. It can be seen that if

the extremities of travel are excluded, the actual needle displacement is fairly consistent about the theoretical line.

Having determined the needle geometry in Section 4.4.2 and characterised the valve travel in this section, it is possible to combine the results to generate a theoretical flow channel for a given valve. Unfortunately these results are not generic as each valve has slightly different component and assembly tolerances and because of this, each valve used for flow testing must undergo a full needle measurement and controlled build procedure. Due to the individual nature of each valve it is difficult to compare flow test results with the generic analytical model of CFD results, and so theoretical models must be tailored to suit the experimental conditions by taking into account the actual valve geometry.

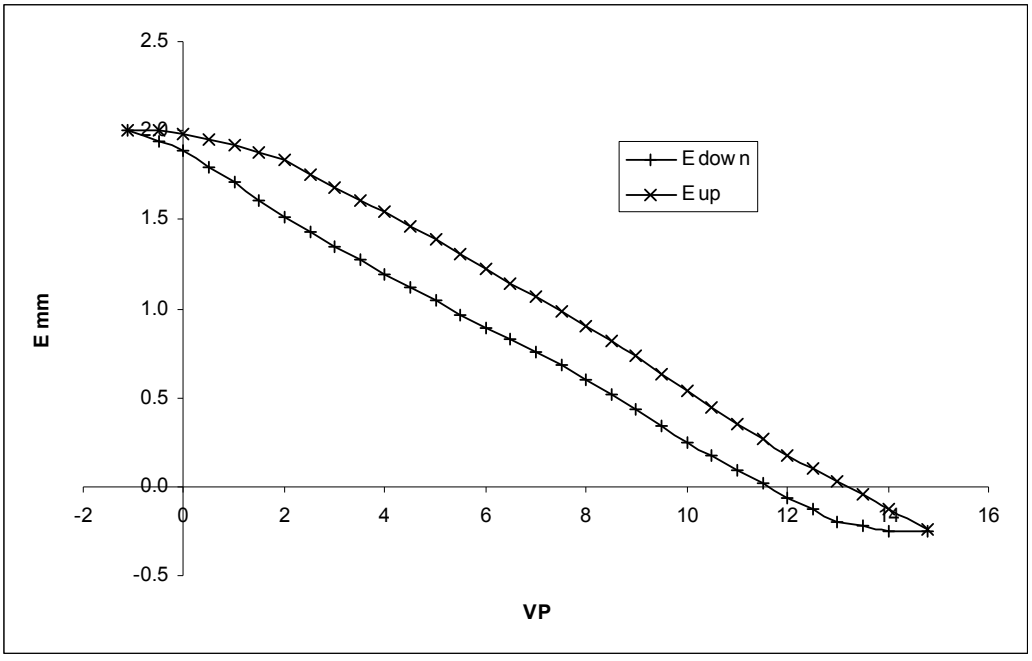

Figure 4-16 Needle engagement *E*, in relation to the valve position VP as measured on an optical measuring machine.

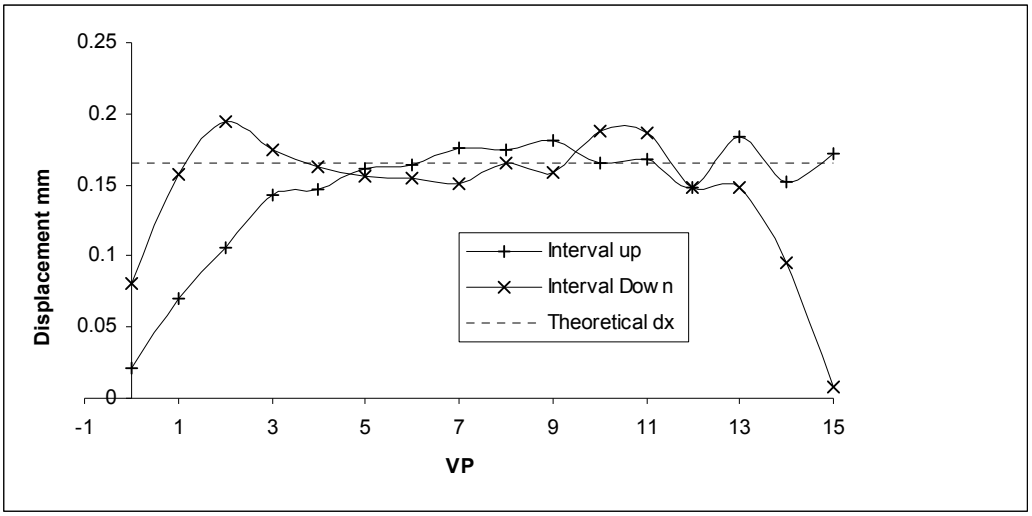

Figure 4-17 Linear displacement step sizes of the valve needle per valve position VP.

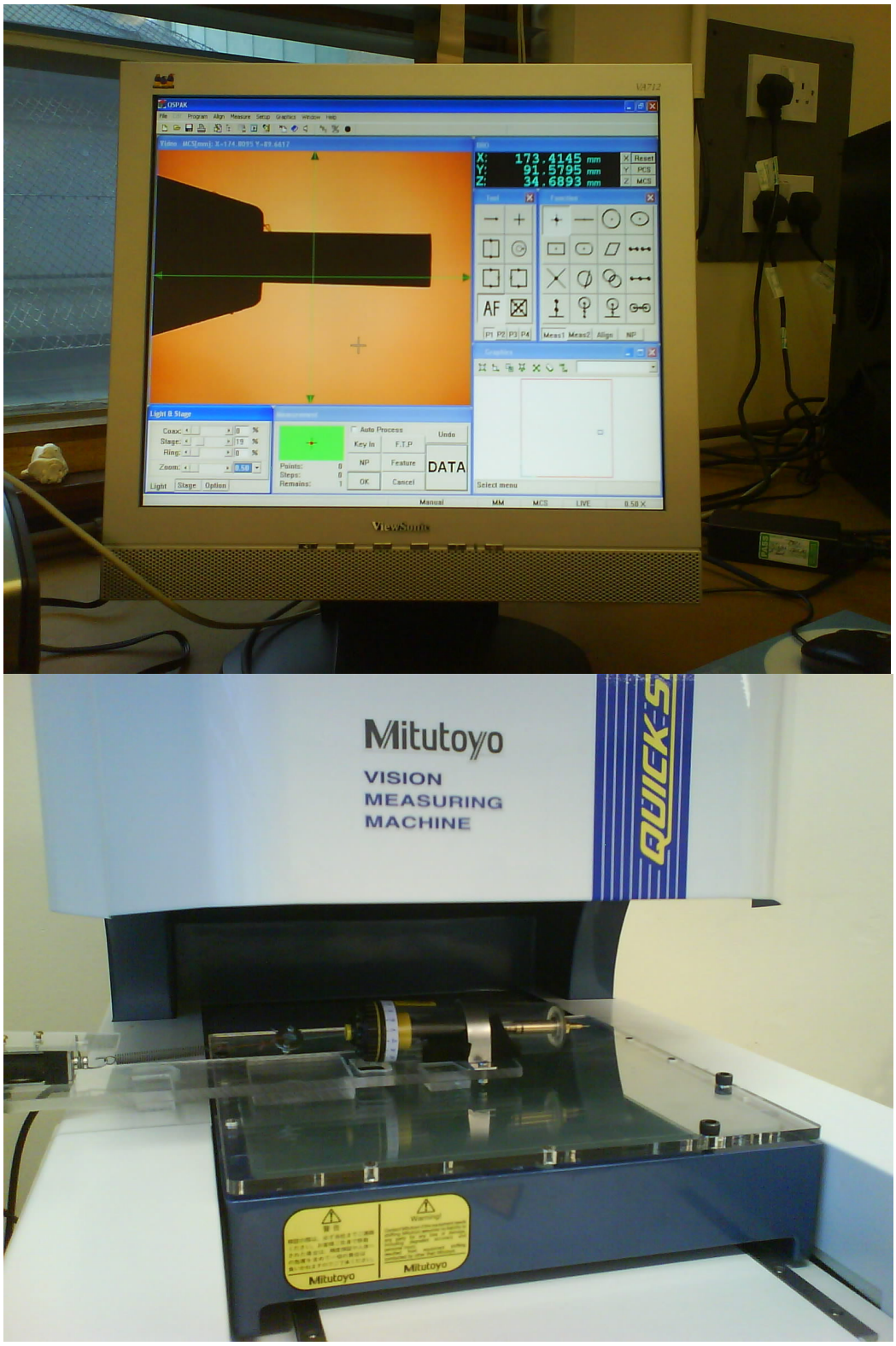

Figure 4-18 Measuring valve needle displacement using a Vision Measuring Machine, VMM. The top image shows the gauge rod inserted into the valve so that contact is made with the needle.

4.5 Conclusion

As with any experimental approach, it is crucial to adequately control the relevant variables that may affect the test results. From this point of view it is important to have appropriate test facilities. Coupled to this it is important to accurately define the test conditions and test samples in order to be able to make an accurate theoretical representation for modelling purposes. A novel high accuracy very low flow measuring method has been developed in response to the specific requirements of this investigation.

In order to be able to compare experimental test results with theoretical equivalents, it is necessary to accurately define the flow channel geometry. The significant elements of the critical components have been identified and labelled. These elements have been quantified by measuring the needle profile and the valve travel through the use of a highly accurate vision measuring machine with a resolution of 0.5μm and accuracy of 2.5μm.

A system has been devised that allows the specific needle and valve geometry to be linked to the flow results of a particular valve. This allows accurate reproduction of the valve geometry for use in the theoretical models.

5 Valve Flow Modelling

5.1 Introduction to Model Structure

Most physical systems can be broken down into a number of discrete sub-systems, as such; a corresponding model of a system needs to account for each subsystem through the use of a sub-model. The number of subsystems and sub-models is dictated by the level of accuracy required of the model and limited by the increasing complexity generated by each sub model.

The sub-system structure as shown in Figure 5-1 was developed through an iterative process in the course of the research and is a result of close observation of the physical system and analysis of data gathered through extensive testing and application of theoretical principles. Although the structure in Figure 5-1 is relatively simple, generating the model is far from obvious as it is not clear what the relevant variables are, what interaction effects might be in effect and each sub model is potentially very complex in its own right. However correctly formulating the problem structure is important for future analysis as it is often difficult to isolate the individual effects of each contributing factor. Each branch of the structure has been investigated and will be described in subsequent analysis, with the emphasis placed on the areas of greater complexity or uncertainty.

The main factors affecting flow rate are; *Fluid Viscosity, Pressure Head* and *Channel Geometry*. Temperature is potentially another important variable and can have a profound affect on flow rate. Temperature is considered a secondary effect, as its effects are expressed in terms of changes in viscosity and needle displacement due to the expansion and contraction of the valve body. It is therefore important to fully

understand the effects of displacement and viscosity on flow rate before tackling the subject of temperature effects. Once these are known then temperature affects will be described in terms of displacement and viscosity rather than on flow rate.

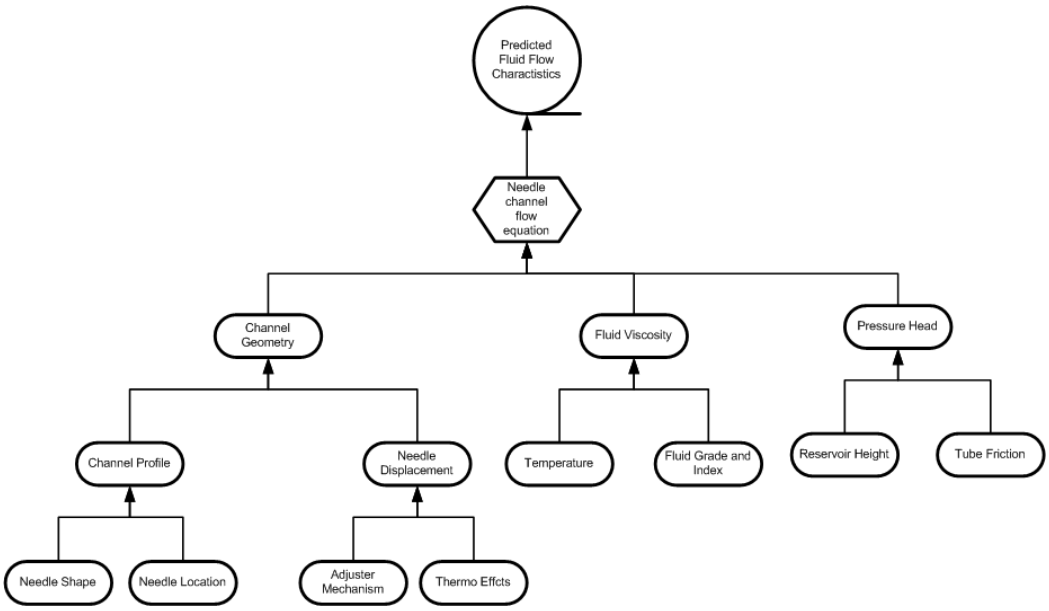

Figure 5-1 Subsystem model structure

5.1.1 Viscosity

Viscosity is a critical parameter in many fluid flow problems. It is critical in determining if the flow in question is turbulent or laminar, which determines the methods used to analyse the flow properties of a system. It will invariably then play a role in the subsequent analysis and has particular repercussions on flow rate when the geometry of the flow channel is taken into account.

Once the flow regime has been established, the viscosity term is used directly in the flow rate equations which define a direct relationship between channel geometry and flow rate. The existing flow rate equations for simple geometries such as for annular flow channels (Equation 12 and Equation 13) are discussed in detail in section 2.3.2.2.

There are two commonly used definitions of viscosity:

Dynamic Viscosity, μ, units of Pascal-second (Pa.s), is used in most flow calculations.

Kinematic Viscosity, v, units of centistokes (cSt) is often used by lubricant manufactures to define fluid properties

The equation $\mu=\rho v$ can be used to convert between the two when expressed in SI units (meters, seconds, kg) and ρ is density.

Temperature has a direct affect on viscosity, and therefore the flow properties of the valve, and there are various theoretical and empirical equations to describe the relationship between temperature and viscosity [143]. Some of which claim to be more accurate than others, however, the most widely used by industry for Newtonian liquids is the Walther equation [143] and forms the basis of the standard ASTM D314:

$$Log_{10}log_{10}(v+0.7)=A-B.log_{10}T$$

Equation 22

Where v is kinematic viscosity in centistokes (cSt), T is the temperature in Kelvin, and A and B are constants that can be calculated if two data points are known. Strictly speaking, the 0.7 value is a third constant C that can be determined by a third data point however it is common to assume a value of 0.7 or 0.8. This is useful as most data provided by oil manufacturers only includes viscosities at 40°C and 100°C. Figure 5-2 shows an example viscosity-temperature relationship generated using the above method for values 32cSt at 40°C and 6cSt at 100°C and is representative of an ISO32 grade oil. It is worth noting that the temperature effects increase significantly as the temperature reduces.

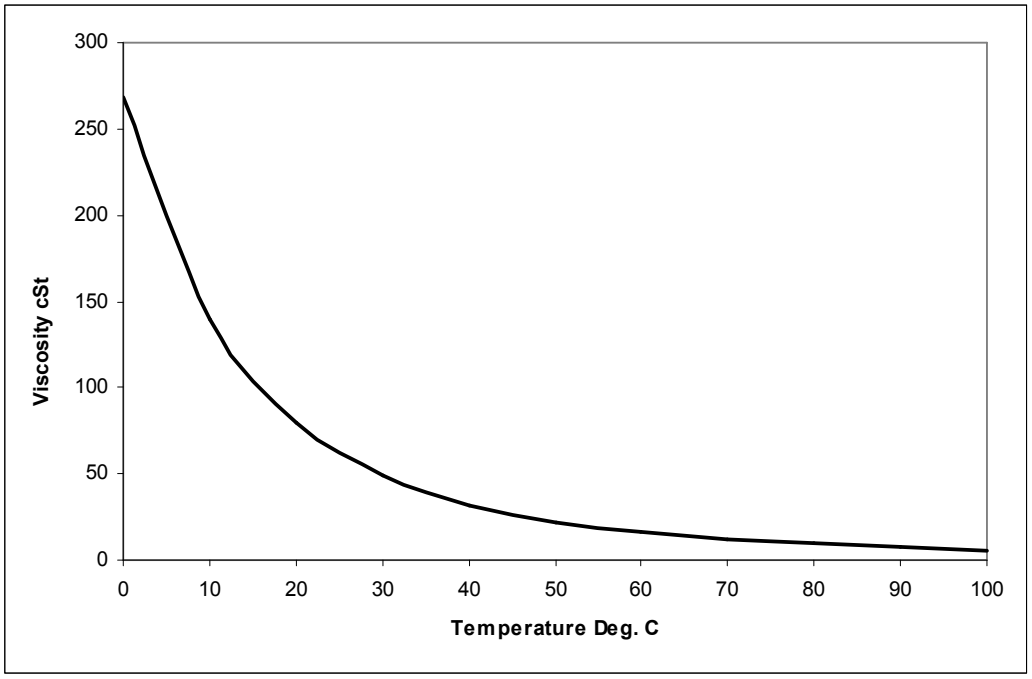

Figure 5-2 Viscosity-Temperature chart generated from two known points using Walther equation for ISO32 grade oil.

The viscosity grade or ISO viscosity grade (ISO VG) is the nominal viscosity of the oil at 40°C as defined by the standard ISO3448:1992 [144]. There are a number of discrete grades available starting at ISO VG 2, up to ISO VG 3200. Typical values for the oils within this study are 32, 46 and 68. ISO 220 has also been used during industrial testing. Charts plotting the temperature/viscosity relationship for all the oils use in this study including the Scottoiler proprietary oils are shown in 10.8Appendix H: Viscosity Comparison Charts. Typically manufacturers supply the viscosity index number for an oil as an indication of sensitivity to temperature. However as this is an arbitrary value derived from the two viscosity-temperature points that are normally also supplied, then it is of little use for the purpose of scientific study. It is more useful to plot the viscosity temperature relationship using the Equation 22.

5.1.2 Pressure Differential

Pressure differential has a very close relationship with flow rate and is present in most forms of flow equation (Equations: Equation 4, Equation 5, Equation 7, Equation 12, Equation 13). The critical parameter is often the differential pressure across the item of interest (such as a valve or length of tubing) rather than the absolute pressure. Pressure differential forms the basis of the standard valve sizing equations, as discussed in Section 2.3.1 of the literature review. Fortunately the definition and calculation of differential pressure for gravity fed systems is very simple, as the differential pressure is directly proportional to the difference in vertical height between the fluid inlet and outlet from atmosphere [145] when tube friction is neglected;

$$\Delta p = \rho g h$$

Equation 23

Where the differential pressure is Δp, ρ is the fluid density, h is the height of the fluid column. As many flow equations are expressed in terms of pressure differential, across the channel of interest, flow rate Q is directly proportional to Δp which in turn is directly proportional to h as shown in Equation 23. Loss of pressure due to the conduit tubing can be discounted as it is very small in relation to the pressure drop caused by the needle channel. This is explored in more detail in Section 7.5.

5.1.3 Channel Geometry

Establishing the link between flow rate and channel geometry is by far the most challenging of the three flow control factors and hence occupies the greatest part of this thesis. The reason for this is twofold; firstly, defining the flow properties for a given channel geometry is a far from simple task and secondly, it is extremely

difficult to precisely define the physical geometry of the active flow channel of the valve in use for any given flow rate experiment. Defining the link between channel geometry and flow characteristics is one of the main contributions of this work. Doing this requires a mix of techniques involving testing flow calculations with estimations of the valve geometry.

5.1.3.1 Model Types

Two main types of needle geometry were investigated, a needle with a 1° taper as described in section 4.4.1 and a needle with zero taper termed a parallel needle. As it is not possible to quantify the level of eccentricity of the needle in the orifice, or if eccentricity was actually effecting flow rate, it was necessary to examine both concentric and eccentric cases and compare the results with experimental test data to determine the best fit. Mathematical modelling and CFD analysis was performed for each of the cases to provide a level of verification.

As the permutations to be explored increases with each variable added to the problem domain, so the number of cases increases dramatically. For this research two different needle geometries and two radial positions with various needle engagement lengths were explored using three different methods; experimental testing, mathematical modelling and CFD.

5.1.3.2 Model Abstraction

Existing literature is focused on turbulent flow through valves and suggests, through the use of the valve style modifier equation, that flow characteristics are linked solely to the orifice area. It is clear that this is not the case where viscous flow is dominant and can be demonstrated by the change in flow rate for a parallel needle where the

flow varies while the area remains constant. This means that a length of flow channel must be considered rather than just the cross sectional area.

The actual flow control channel of the valve is likely to be a complex shape, even if the relatively simple parallel needle is used. The task of accurately centering a needle within the orifice where the clearance is in the order of several microns is a mechanically complex task. As such there is no specific needle alignment mechanism for the valves in this study. Because of this, the most likely actual position of the needle is that there is a single point of contact between the needle and the inside of the orifice and a level of axial misalignment between the two. This however would make any kind of meaningful analytical solution extremely difficult and any CFD analysis particularly laborious. It is therefore necessary to find some level of abstraction of the problem that makes analysis possible while still representing the problem sufficiently closely to provide accurate results. Therefore the greater level of abstraction makes analysis easier but is also the furthest from reality, lower levels of abstraction are potentially more accurate but harder to analyse.

A number of different levels of abstraction are used depending on the analysis being performed and the needle geometry under investigation.

5.1.3.3 CFD Approach to Modelling

CFD requires benchmarking in order to be able to have confidence in the results. Starting with the simpler forms of the flow problem allows the CFD solution to be developed as the analytical problem is developed. Testing various forms of CFD solution in the early stages allows different forms of the solution to be developed that

can be used according to the mathematical model and needle geometry under investigation.

The simpler forms of the flow channel as shown in Figure 5-3, can be modelled as a 2D problem, however by formulating it as a 3D problem it allows the solution to be expanded to more complex geometries. For this reason, simple needle geometries are modelled as flattened 3D channels as it is simpler and quicker to generate the mesh. As the flow channel geometry for an eccentric needle is more complex, it is simpler to model the channel in its natural form as seen in Figure 5-5. The geometry and mesh generation for this form of problem takes significantly longer than for a flattened 3D channel due to the nature of the geometry.

It is necessary to modify the geometry to remove features that may cause problems for the solver. In this case it is necessary to remove the infinitely small area caused by the needle touching the orifice wall. It can be seen from Figure 5-5 that there is a continuously reducing gap between the orifice wall and the needle that becomes a theoretical point. It is necessary to truncate this and provide an actual surface for the channel to end with. Although this is effectively reducing the cross sectional area of the channel, the effects should be minimal as the flow in the small gap is negligible compared to the flow in the larger part of the channel. Truncating the channel causes additional problems as the dimensions of the truncated face are actually too small to model directly in most CAD packages as it is far below the tolerance levels available. The channel geometry must be scaled up when it is being generated in I-DEAS and while meshing in GAMBIT. The mesh can then be scaled down once imported to the CFD package Fluent. A good correlation with the analytical solution demonstrates that a suitable mesh density has been used for the CFD solution. In general, as the

volumes under investigation for the concentric models (parallel and tapered) are simple and the flow domain strictly laminar, the mesh can be quite course. Mesh density is less critical for simple laminar flows than for turbulent flows or geometries with sudden flow- interrupting features where the mesh density must be scaled to take into account sudden changes of the flow characteristics. Even if relatively high grid densities are used, the simple geometry of the flow volume means that the CFD results are solved quickly; typically in under a minute. The pre-processing time is in fact far greater than the solution time.

The following Fluent settings were used; 3D segregated, laminar models. Pressure inlet and pressure outlet boundary conditions; with 10909Pa normal to the inlet boundary corresponding to a fluid column height of 1.35m and the outlet was atmospheric. Fluid flux was measured form the outlet boundary.

5.1.3.4 Flow Model Overview

The ideal scenario in product development is to have a working model that can be used as a tool in developing new variants of a product. In this case, a mathematical model describing the flow properties of the valve would be ideal, but, as in many flow problems, it becomes difficult to develop an accurate mathematical model of flow for anything other than the simplest scenarios. Any flow model also needs to be compared to relevant experimental data in order to give an indication of its accuracy and suitability for intended purpose. The model type for the following flow channel configurations is:

- Parallel concentric-Analytical model and CFD.
- Parallel eccentric- Approximation model based on parallel concentric model and CFD.
- Tapered concentric- Analytical model and CFD.
- Tapered eccentric- Data driven empirical model.

5.1.3.5 Parallel Concentric Needle Model

Concentric Annular Flat structure: This model type offers the greatest simplicity as well as the greatest level of abstraction by assuming the needle is concentric with the orifice. It is created by 'unravelling' the annular flow channel to create a flattened channel and is a good approximation when the gap between the inner (r_a) and outer (r_o) diameters is small in relation to the circumference [17], as is true in this case. In the case of the parallel needle, it turns a circular channel into a cuboid where the opposing pairs of faces are the inlet and outlet, valve surfaces and faces created by splitting the annular channel (Figure 5-3). The channel length (E) is the equal to the engagement length as described in section 4.4.1. The width of the channel (W) is equal to the circumference of the mid point between the r_o and r_a as expressed by $Ws=2\pi(r_o + r_a)/2$. Channel height is simply $h_1=r_o-r_b$. It should be noted that the diagram is not to scale and that h_1 must be small in relation to W for the approximation to be valid. Also for most cases W is also larger than E.

As the simplest of the scenarios listed in the previous section, the parallel concentric needle problem can be analysed using a number of different techniques. This makes it ideal as a test bed to refine the techniques required to solve the more complex variants of the problem. This involves a comparison of two versions of the analytical solution (circular and flattened) with their corresponding CFD solution as represented in Figure 5-3. The theoretical results are also compared with test data.

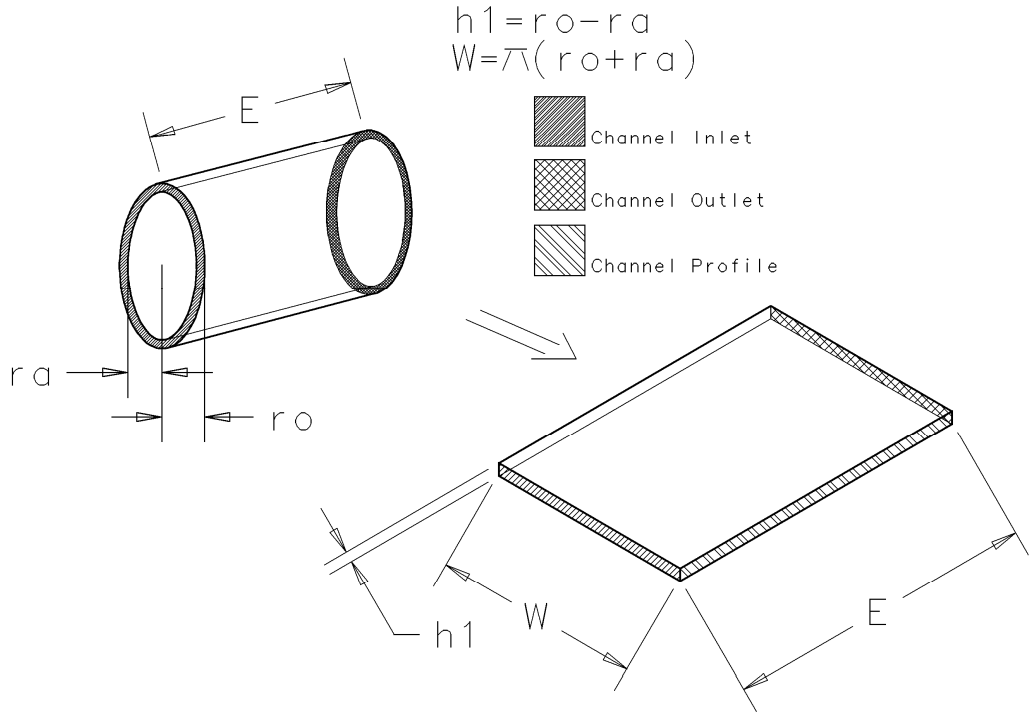

Figure 5-3 Parallel needle annular channel (right) shown with flat channel approximation (left).

The first analytical solution is of a concentric annular channel as described by Equation 12 (page 42) and the second is the corresponding flattened channel and is represented by Equation 13 (page 43). It was found that there is negligible difference between the two forms of analytical solution. The CFD solution was also tested in both forms of the problem and the differences were again negligible. This confirms that the flattened channel approximation is valid.

Figure 5-4 compares the results of flow models created from the analytical model and CFD solutions. As the differences between the concentric annular and flattened approximations are negligible, they have been merged. The CFD data is within 5% of the analytical solution validating the CFD mesh and input values used. The similarity with the test data is apparent, showing that the CFD and analytical models are accurate to at least an order of magnitude.

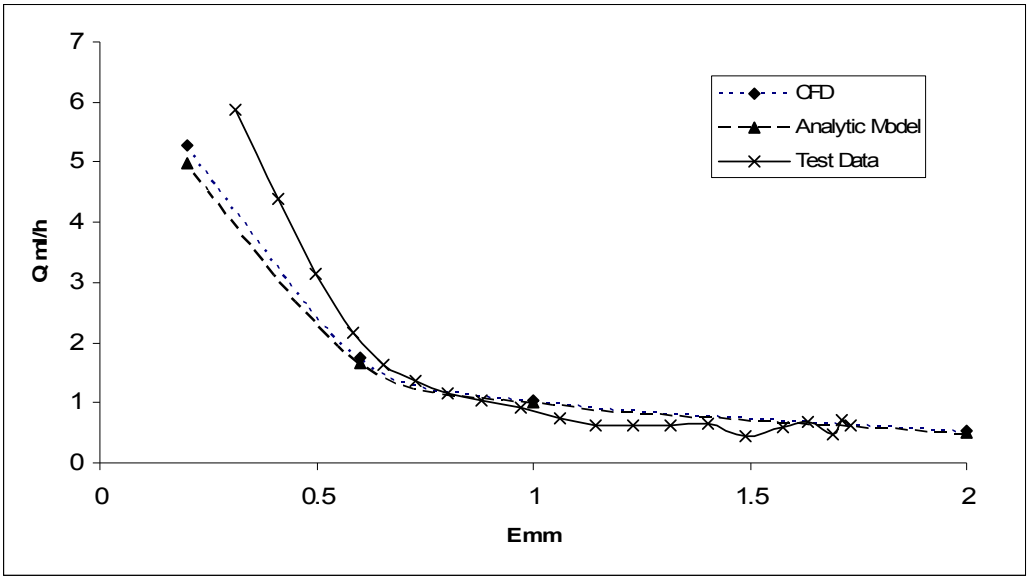

Figure 5-4 Comparison of flow rate *Q*, with engagement length *E* for CFD is in close agreement with the analytical model and both are in general agreement with test data. Test conditions: ISO32 grade oil at 20°C, parallel needle and fluid column height of 1.35m (10909Pa).

Validating the analytical solution allows a number of flow rate parameters to be explored in detail. An idea can be built up of the effects and sensitivity to changes in channel geometry, fluid viscosity and pressure head.

5.1.3.6 Parallel Eccentric Needle Model

Eccentric Annular: The previous model assumes that the needle is concentric in the orifice. However, this is unlikely to reflect the experimental conditions, so an eccentric model is required. The simplest eccentric model assumes that the needle is at its maximum off-centre position but still aligned axially with the orifice as shown in Figure 5-5. This now becomes a 3D problem, as there is no longer a uniform profile across the width of the channel. This now makes a 2D analysis impossible and so makes it less attractive to 'flatten' the channel (Figure 5-5). The added complexity of the eccentricity means that CFD techniques become more prominent.

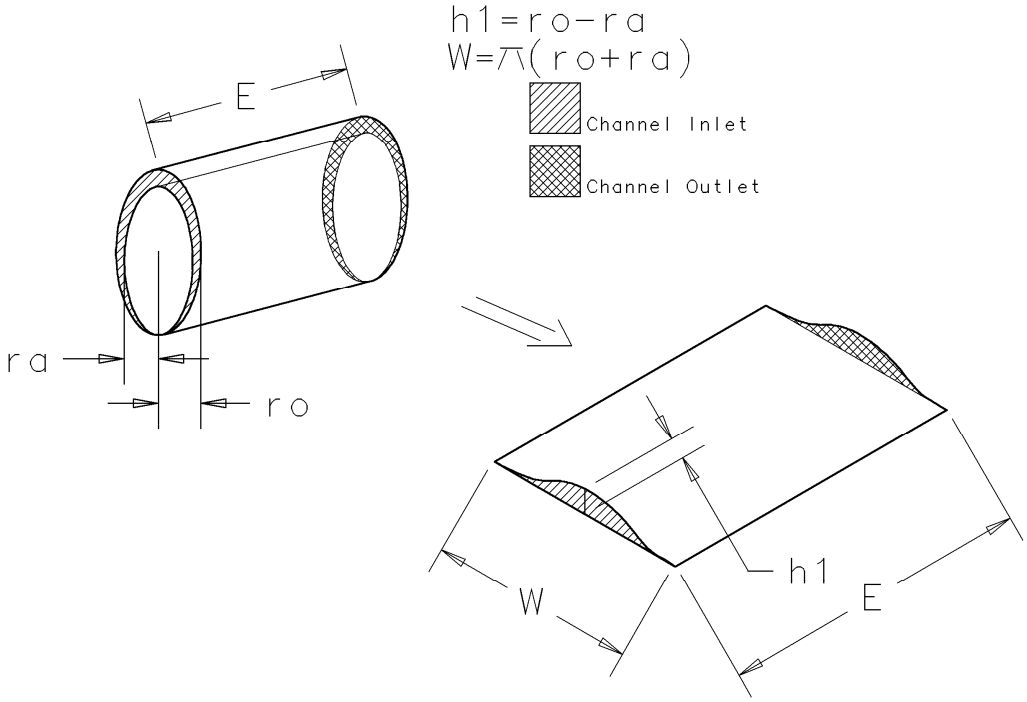

Figure 5-5 Eccentric Annular channel representing a parallel needle

The eccentric flow problem can be set up a number of different ways for both the CFD analysis and when constructing an analytical model. It is possible to use a flat structure similar to the concentric parallel problem described previously. Figure 5-6 shows the profile of the orifice channel, a derivation of which can be found in the appendices in section 10.7. The orifice height (*l*) is given in terms of the arc length of the needle, where the total arc length corresponds to the needle circumference. Note the exaggerated vertical scale in relation to the arc length. Profiles are shown for the maximum and minimum clearance within drawing tolerance as well as the nominal value. Also note how the arc length on the x-axis varies according to the circumference of the needle. Converting the flow channel to a flat equivalent creates a 3D problem. In this case it is simpler to create the CFD model directly in 3D.

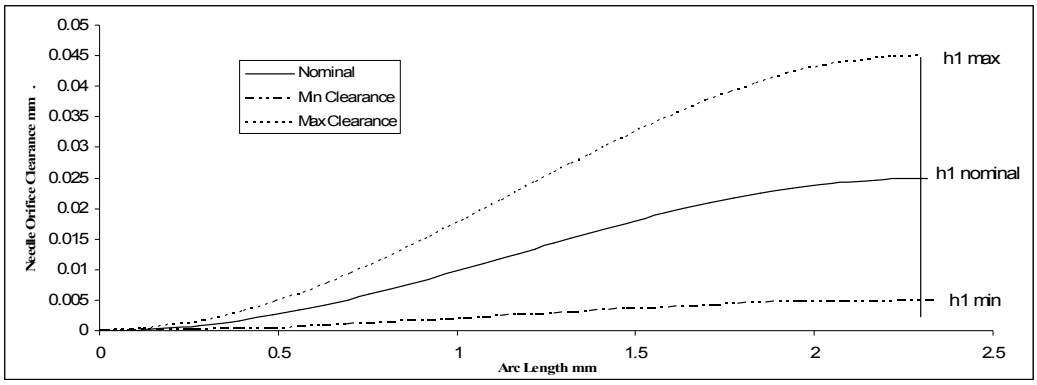

Figure 5-6 The clearance between the needle and orifice for nominal, maximum and minimum conditions. The maximum value for each curve represents the h1 value. The area under the curve represents the valve orifice area and the arc length represents the needle circumference.

Theory suggests there should be a significant difference in flow rate through concentric and eccentric annular flow conduits. The use of Piercy and Rebergers models is explained in Section 2.3.2.2 of the literature review.

CFD results showed that there is a very consistent relationship between the eccentric annular flow and the concentric analytical model. The CFD analysis predicts a 163.3% increase for eccentric flow over the concentric case. This can be compared with the percentage increase from the concentric case predicted by the Piercy and Redbereger models which predict increases of flow rate of 150% and 240% respectively. The results are displayed in Table 5-1.

	Q ml/hr						
E mm	Concentric Analytic Model Q	CFD Eccentric Q	% *ΔQ*	Piercy Model Q	% *ΔQ*	Redberger model Q	% *ΔQ*
2	0.262	0.69	163.3%	0.655	150%	0.891	240%
0.6	0.873	2.3	163.3%	2.184	150%	2.970	240%
0.4	1.310	2.45	163.3%	3.275	150%	4.454	240%
0.2	2.620	6.9	163.3%	6.551	150%	8.909	240%

Table 5-1 Comparison of concentric and eccentric flow models with the analytical model flow results.

The highly consistent CFD results mean that only a relatively small number of cases need be run as it is possible to extrapolate other results by adding 163.3% to the concentric analytical results.

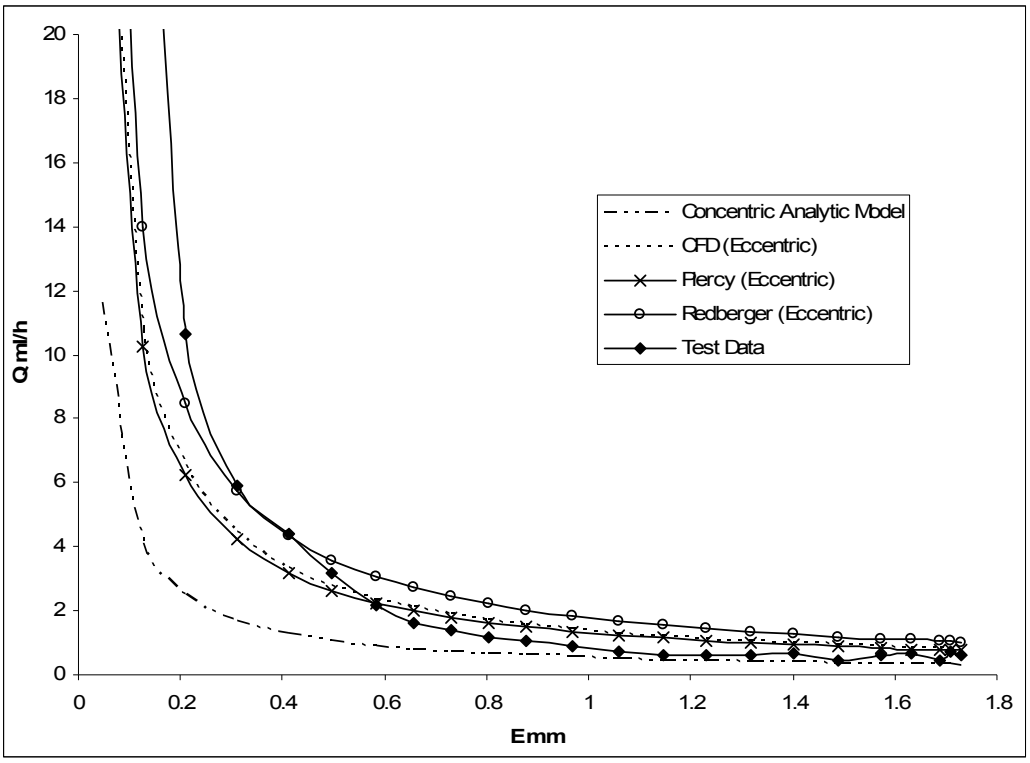

Figure 5-7 Comparison of eccentric flow models with test data.

It can be seen from Figure 5-7 that the difference between the Piercy model and the CFD results is very slight. Also, the eccentric models capture the general trend of

flow rate better than the concentric model, confirming the likelihood that the needle is in fact eccentrically located in the orifice bore. While none of the models are an exact match for the test data, the general trend is sufficient for an explicative model and a valuable tool for understanding the function of the valve. In this way informed design decisions can be made when considering the performance of the valve.

5.1.3.7 Concentric Tapered Needle Model

The same principle as used for the concentric parallel needle can be applied to a tapered needle where the tapered portion, section B (see Figure 4-11), is accounted for by an equivalent tapered section in the flat model to form a polyhedron (Figure 5-8).

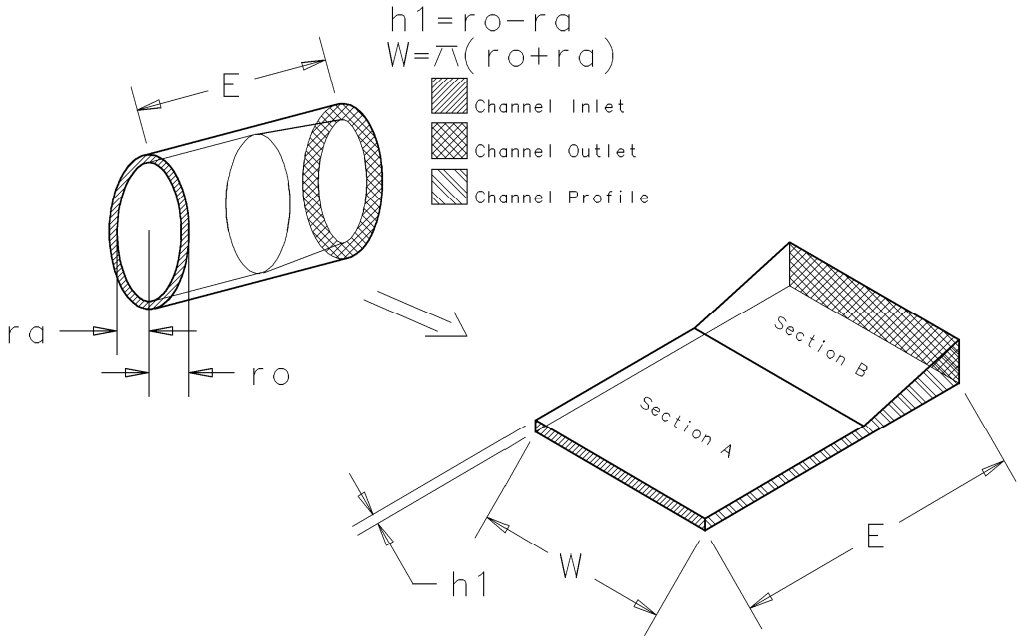

Figure 5-8 Tapered needle annular channel (right) with flat channel approximation (left). Also refer to Figure 4-11 Valve needle basic geometry for section definitions.

This type of model can be considered a 2D problem as the channel profile is uniform across the entire width (*W*). It can also be termed a composite profile as the active

profile is made up of two distinct geometries, different proportions of which are in use depending on the engagement length. I.e. at low engagement lengths, only section B is active.

A generic analytical solution can be derived from the underlying Navier-Stokes equations provided the flow and flow channel are not too complex. An analytical solution would provide a great deal of flexibility in terms of exploring the design space. Approximating the annular flow channel by a flat equivalent simplifies the geometry and aids development of the analytical solution.

The analysis of the flow channel is divided according to the two geometry types. The first, corresponding to the parallel section of the needle, can be analysed in the same manner as the parallel concentric needle described in section 5.1.3.5 using Equation 13 (page 43) rearranged in terms of pressure differential. It is represented by l_1 in Figure 5-9 and corresponds to the active portion of Section A of the needle as described in Figure 4-11. Given x,y,z represents the geometric coordinate system and u,v,w are the corresponding fluid velocity vectors, p is the fluid pressure and μ is the fluid dynamic viscosity.

The tapered section B corresponding to l_2 in Figure 5-9 requires a different analysis approach and can be based on Schlichting's hydrodynamic theory of lubrication [96]. His analysis is of an oil film between a bore and rotating shaft where the viscous forces are predominant which can be approximated by the case of two plates moving past each other whilst inclined at a small angle. This principle can be applied to l_2 with modifications to the boundary conditions to account for the current circumstances. When considered in conjunction with the theory of flow between

parallel plates applied to l_1, a general solution to flow in a needle valve with a composite profile needle can be generated.

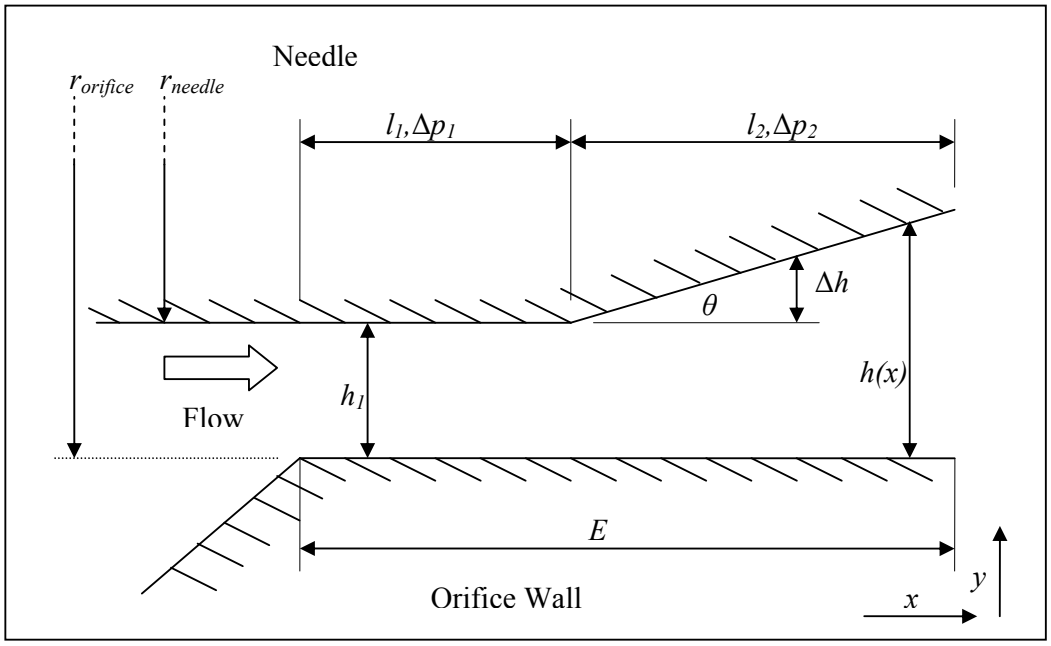

Figure 5-9 Problem diagram for solving the flow equations for a composite needle concentric in the valve orifice. l_1 and l_2 corresponds to the active portion of section A and section B of the needle respectively.

Note the use of l_1 and l_2 corresponding to sections A and B of the needle. This subscript notation is used to highlight the difference between the dimensions as measured on the needle (alphabetical) and how these portions of the needle correspond to the active channel dimensions (numeric).

Schlichting's analysis involves a number of assumptions; that one plane slides past another inclined at a small angle and that the surfaces are very large in the transverse direction (W) with respect to l_2 so that the problem is two dimensional, the distance between the two planes, $h(x)$, is small compared to the length (l_2), and the pressure distribution must satisfy the condition that $p=p_0$ at both ends of the channel. From this problem formulation it is assumed that the v component of the fluid velocity is

negligibly small in relation to the *u* component or in other words, that the flow is primarily parallel with very little flow perpendicular to the channel walls. The differences between Schlichting's hydrodynamic theory of lubrication and a valve micro channel is that in this case, the plates are stationary relative to each other and that fluid flow is generated by a pressure differential rather than plate movement.

Based on the above assumptions, Schlichting's simplification of the Navier-Stokes equation is:

$$\frac{dp}{dx} = \mu \frac{d^2u}{dy^2}$$

Equation 24

And the equation of continuity replaced by the condition that the volume of flow in every section must be constant:

$$Q = \int_0^{h(x)} u \, dy$$

Equation 25

This analysis differs from Schlichting's in that in this case both plates are stationary and so the boundary conditions are:

$$y=0: \quad u=0; \quad x=0: \quad p=p_0$$

$$y=h: \quad u=0; \quad x=l: \quad p=p_0$$

Equation 26

The solution of Equation 24 which satisfies the boundary conditions of Equation 26 gives:

$$u = -\frac{h^2}{2}\frac{p'}{\mu}\frac{y}{h}\left(1-\frac{y}{h}\right)$$

Equation 27

Note that p' is the pressure gradient term, $\frac{dp}{dx}$, and by inserting Equation 27 into Equation 25 we obtain;

$$Q = -\frac{h^3 p'}{12\mu}$$

Equation 28

Or solving for p':

$$p' = 12\mu\left(\frac{u}{2h^3}\right)$$

Equation 29

Integrating Equation 29 gives:

$$p(x) = p_0 - 12\mu Q\int_0^x \frac{dx}{h^3}$$

Equation 30

Using the limits p_0, $x = 0$ and $p(x)$, $x = x$:

$$\Delta p_2 = \left(p_{x=l} - p_{x=0}\right) = -12\mu Q\int_0^x \frac{dy}{h^3}$$

Equation 31

defines the differential pressure in the tapered section in terms of varying l_2. However in order to take into account the variation of h with respect to x;

$$h(x) = h_1 + \Delta h = h_1 + x\tan\theta$$

Equation 32

Substitute the h term in Equation 31 for the $h(x)$ term in Equation 32 to give:

$$\Delta p_2 = -12\mu Q \int_0^{l_2} \frac{dx}{(h_1 + x\tan\theta)^3}$$

Equation 33

Integrating Equation 33 using the form:

$$\int \frac{dx}{(a+bx)^3} = \frac{-1}{2(a+bx)^2\, b}$$

Equation 34

Gives, using some simplification:

$$\Delta p = \frac{12\mu Q}{2\tan\theta}\left(\frac{1}{(h_1 + l_2\tan\theta)^2} - \frac{1}{(h_1)^2}\right)$$

Equation 35

Equation 35 now gives us the pressure differential for the tapered part of the valve in terms of the volume flow rate Q per unit width W, dynamic viscosity μ, length of channel l_2 and taper-angle θ.

Where W is the channel width corresponding to the orifice circumference. While Equation 35 gives an exact solution to flow in tapered channel, a level of approximation is required to convert the two dimensional solution to the three dimensional equivalent. The orifice circumference can be taken from the mid point of the channel:

$$W = 2\pi \frac{(r_{orifice} + r_{needle})}{2}$$

Equation 36

And while this is constant for l_1 it becomes a variable in l_2 due to the varying radius of the needle. As the flow rate is directly proportional to W, any error in defining W translates to a corresponding error in Q. If the taper effect on W is taken into account for a needle profile with a short shallow taper of 1° over 1.2mm, this translates to a difference in W of approximately 2.7% over the case where W is assumed constant. In

comparison, a needle with a 4° taper over 3mm this would have a 28% effect on flow rate. It should be noted that even 28% is a relatively small amount compared to the effects of changing *E* which will create changes in flow in the region of $x10^4$.

It should also be noted that Equation 35 is only valid for flows that are predominantly parallel. There is a point at which taper-angles are such that this would no longer hold true and will be investigated further later in this section.

Combining Equation 35 and Equation 14 (page 43) gives a solution for the total pressure drop across the valve in terms of flow rate:

$$\Delta p = \frac{l_1 12\mu Q}{W h_1^3} - 12\mu \frac{Q}{W 2\tan\theta}\left[\frac{1}{(h_1 + \tan\theta l_2)^2} - \frac{1}{h_1^2}\right]$$

Equation 37

Equation 37 can be rearranged to give:

$$Q = \frac{1}{6}\Delta p W h_1^3 \frac{h_1^2 + 2h_1.\tan\theta.l_2 + \tan\theta^2.l_2^2}{\mu(2l_1h_1^2 + 4l_1l_2h_1\tan\theta + 2l_1\tan\theta^2 l_2^2 + 2l_2h_1^2 + l_2^2 h_1\tan\theta)}$$

Equation 38

Where Δp can be substituted with Equation 23, $\Delta p = \rho g h$ to give flow rate in terms of fluid column height, allowing flow rate to be predicted for a given set of initial conditions. Equation 38 represents a significant contribution to low flow valve development in that it provides a model that links valve geometry to flow rate, from which the valve flow characteristics can be derived.

It should be noted at this point that it would be normal to produce a series of results corresponding to a series of engagement lengths E. In this case a set of logic statements help to define the geometric parameters as the channel changes from a composite profile to a single profile.

Referring to Figure 5-9:

$E_{max} = l_{1max} + l_{2max}$

IF $E \geq l_{2max}$ then;

$l_1 = E - l_{2max}$; $l_2 = l_{2max}$; $h_1 = r_{orifice} - r_{needle}$

otherwise;

$l_1 = 0$; $l_2 = E$; $h_1 = r_{orifice} - r_{needle} + \tan\theta(l_{2max} - E)$

From the statements above it can be seen that h_1 is constant while the parallel and tapered sections are engaged in the orifice, but becomes a variable dependant on E, when only the tapered section is engaged. It is possible to formulate the problem in terms of h_1 for the parallel section and h_2 for the tapered section, but the method described above is deemed slightly simpler and is essentially a question of semantics.

The model described above, centred on Equation 38, assumes 'parallel' flow conditions. That is, that the vertical component of the flow stream is small in relation to the horizontal. This holds true for needle profiles with a small taper-angle, but this assumption must fail at some point as the taper-angle increases by allowing a greater vertical flow component. It is possible to test the analytical model for non-parallel flow errors by comparing it against CFD results which will inherently take into account non-parallel flow.

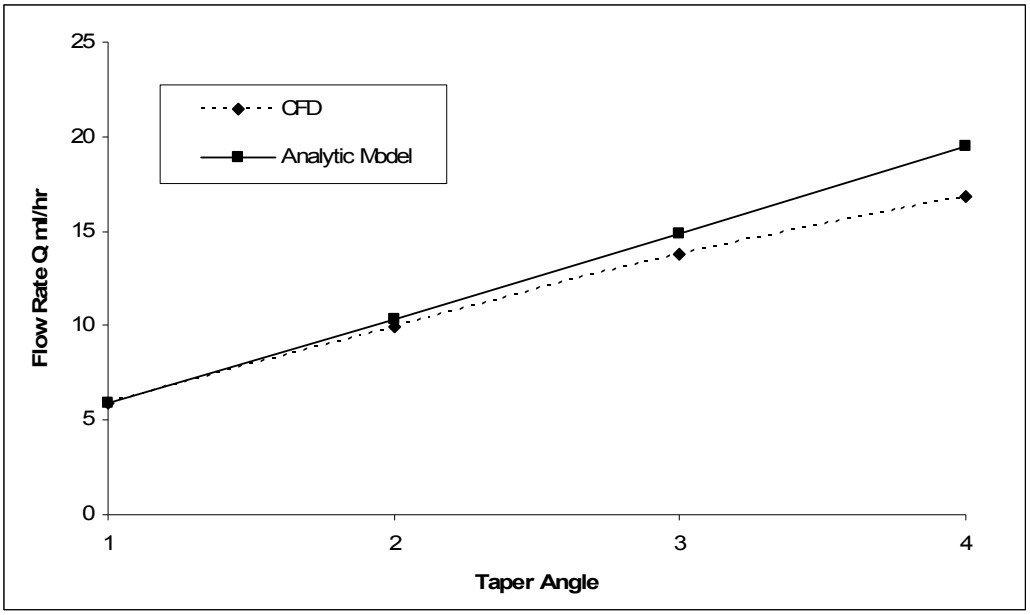

Figure 5-10 A comparison of analytical model results and CFD for a selection of taper-angles.

It can be seen from Figure 5-10 that the CFD result starts to diverge from the analytical model as the taper-angle increases confirming that the accuracy of the analytical model reduces as the taper angel increases. It holds therefore that the analytical model accuracy should increase for any set of conditions that increases the portion of parallel flow. Because the analytical model assumes parallel flow, any geometrical feature of the flow channel that increases the magnitude of the y (perpendicular) component of the flow (Q) in relation to the magnitude of the x (parallel) component, reduces the validity of the model. In this case it is possible to observe the effect of varying the initial flow channel height (h_1) for the taper-angle values used above. Figure 5-11 uses the ratio of taper-angle and initial channel height (h_1) plotted against the percentage error between the CFD and analytical results. There is a clear trend that shows that as the ratio increases, so does the error, so that the accuracy of the analytical model is related to not just the taper-angle or channel height, but a combination of both.

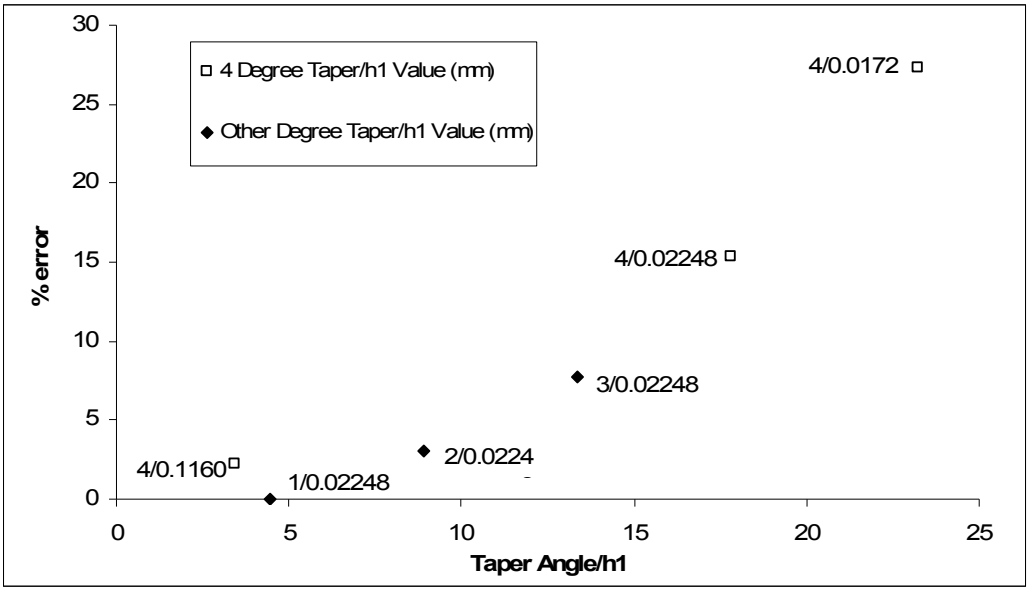

Figure 5-11 The ratio of taper-angle and initial channel height (h_1) against the percentage error between the CFD and analytical results.

It is most accurate for low taper-angles with high h_1 values, and least accurate for high taper-angles with low h_1 values. This may also be influenced by viscosity, but it is suggested that under the conditions used here an angle/ h_1 ratio of 10-15 when h_1 is measured in mm should be sufficiently accurate.

As with all models, the validity needs to be verified in some way. In this case, a direct comparison with test data and CFD analysis is possible. Figure 5-12 shows that the CFD analysis is in very close agreement with the analytical model for a 1° taper-angle for the full range of needle travel. There is also good agreement with the test data. It would be expected that some level of correction would be required to account for the eccentricity of the needle as was the case for the parallel needle. Although the eccentricity effects of a tapered annulus are not known, it is possible to apply the standard Piercy correction factor of 150%. However when this is used, the model significantly over predicts indicating that it is not appropriate for a profiled needle.

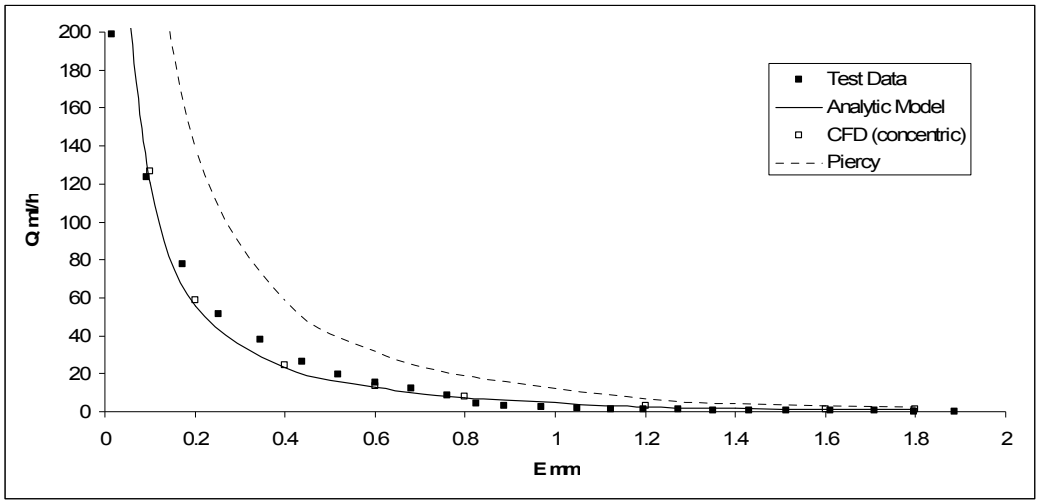

Figure 5-12 A comparison of experimental test data with the analytical model and CFD analysis. Also included is the Piercy correction factor for flow past an eccentric annulus.

In order to further explore the limits of the model, a further set of experiments covering a range of needle profiles were performed.

The flow characteristics for a number of needle shapes are plotted for two different pressure heads, corresponding to dh=1.35m and dh=0.45m. It should be noted that although the needles are referred to by their taper-angle, this is only a nominal value and that other geometric parameters may vary significantly. This particularly applies to the Section A and Section B lengths and also to the absence of nipple end for 3° and 4° needles. This is reflected in the E values on the x-axis of the graphs.

The following Figures show the Engagement/Flow rate relationship for needles with 1°, 2°, 3° and 4° taper-angles. The test results are compared with the analytical solution generated from the specific measurements of the needle and valve.

The results as shown by Figure 5-13, Figure 5-14, Figure 5-15 and Figure 5-16 are mixed. Generally the analytical predictions capture the magnitude and trend of the flow rate correctly. However, when considering the 2° (Figure 5-14) and 4° (Figure 5-16) needles, the correlation is only close at higher *E* values. For these test results it

is possible that there is some unknown geometrical interaction occurring that has not been accounted for in the analytical model. It is also possible that there are additional fluid dynamic effects occurring at low E values that are not captured by the analytical model as it is based solely on the engagement length. The model as described by Equation 38 tends towards infinity as E becomes small and as the needle disengages from the orifice, negative E values produce a negative flow rate. This is clearly not possible in reality so it shows that there is a point at which the model deviates from reality at small E values.

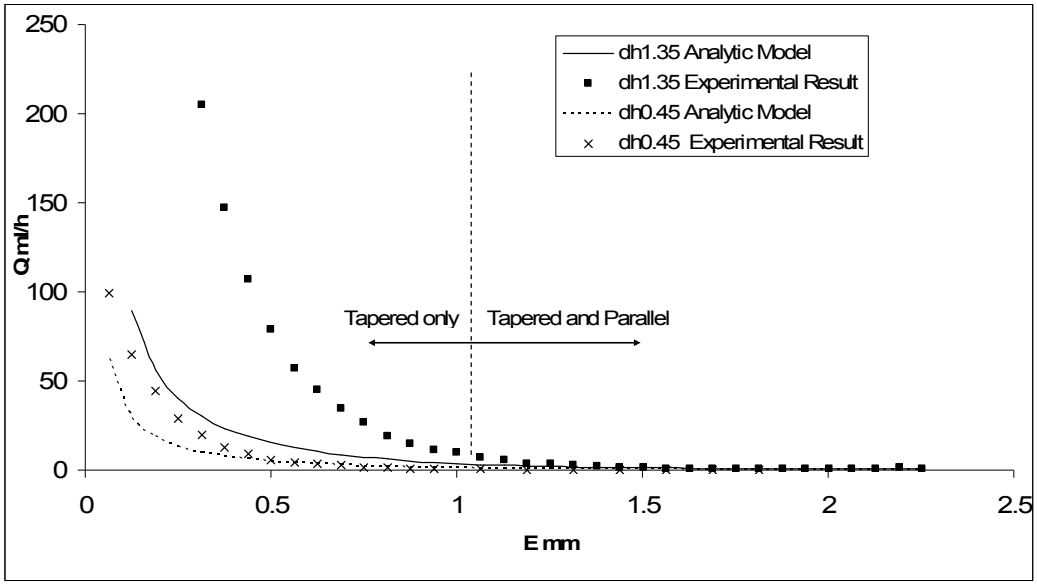

Figure 5-13 1° taper-angle. Transition from parallel to tapered section begins as E=1.08mm.

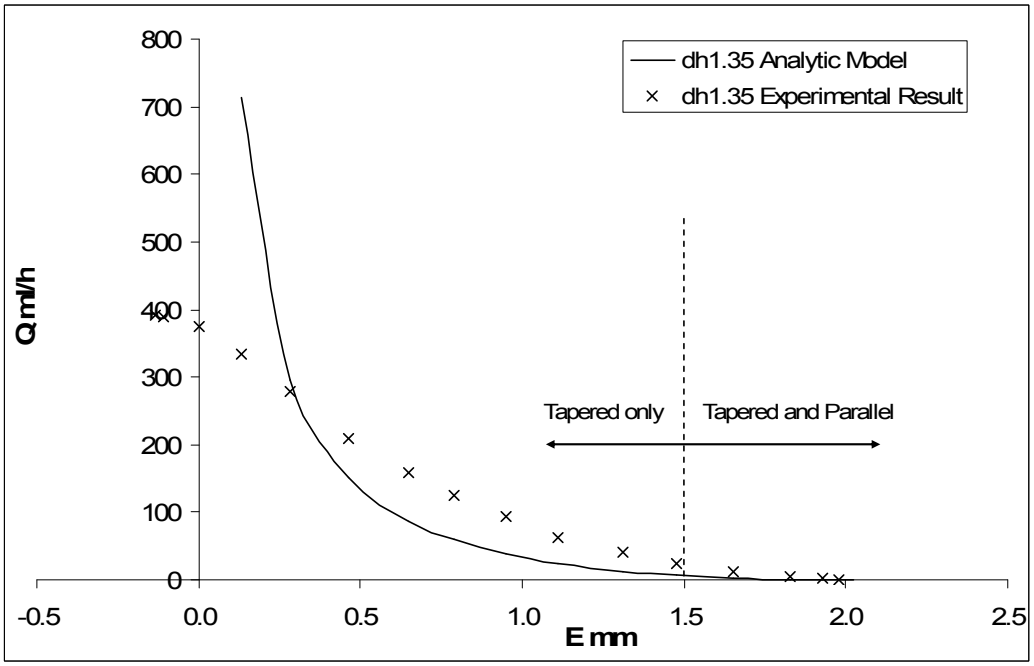

Figure 5-14 2° taper-angle. Transition from parallel to tapered section begins as E=1.5mm.

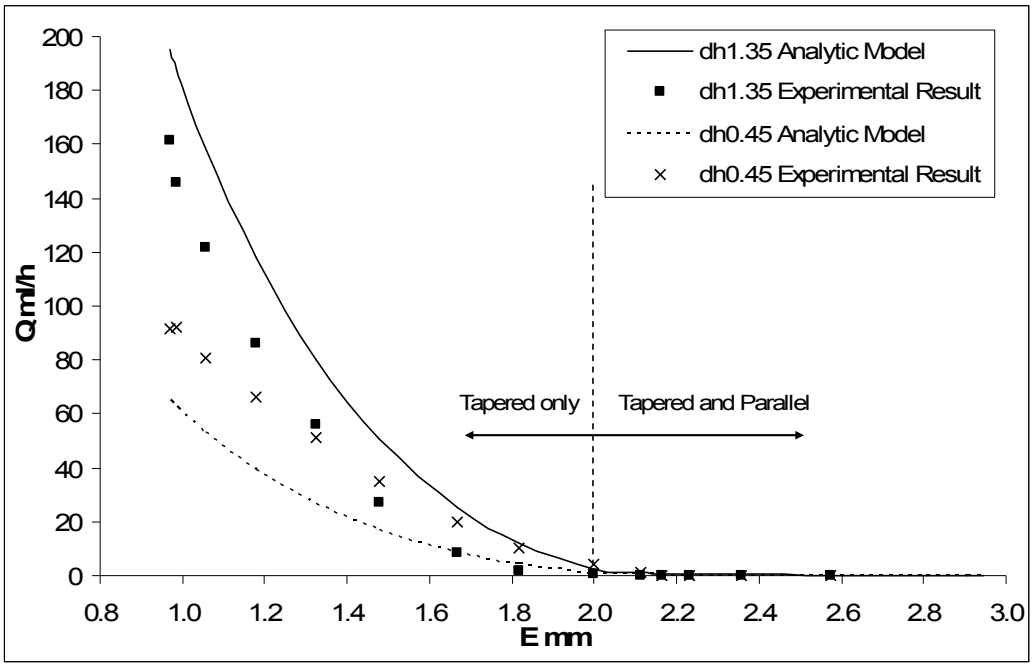

Figure 5-15 3° taper-angle. Transition from parallel to tapered section begins as E=2mm.

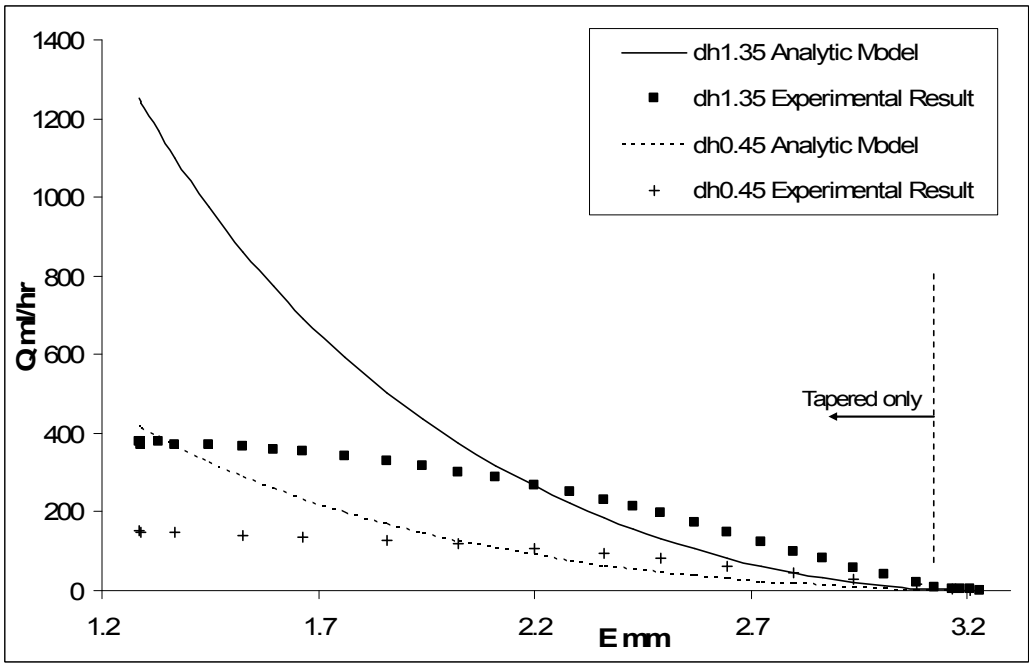

Figure 5-16 4° taper-angle. Transition from parallel to tapered section begins as E=3.12mm.

The natural scale used for flow rate Q gives an undue emphasis on the higher flow rates found at low E values, while the flow rates of interest are at the lower end of the scale. As these flow rates are orders of magnitude below the highest flow rates, it is difficult to determine their effect using a natural scale. In order to examine the accuracy of the model at the lower end of the scale, the same data can be viewed using a *log* scale for the flow rate Q as seen in Figure 5-17, Figure 5-18, Figure 5-19 and Figure 5-20.

From these new charts, it can be seen that there are a variety of flow characteristics displayed by the test data for the different needle profiles including concave, convex and s-shaped trends. Generally the overall test data trends are matched by the analytical model with the different curve characteristics generated by each needle profile being picked up in the analytical solution. Differences can be attributed to the difficulty in determining the channel geometry at these very small scales, but the trends are sufficiently close to have confidence that the analytical solution is functioning correctly.

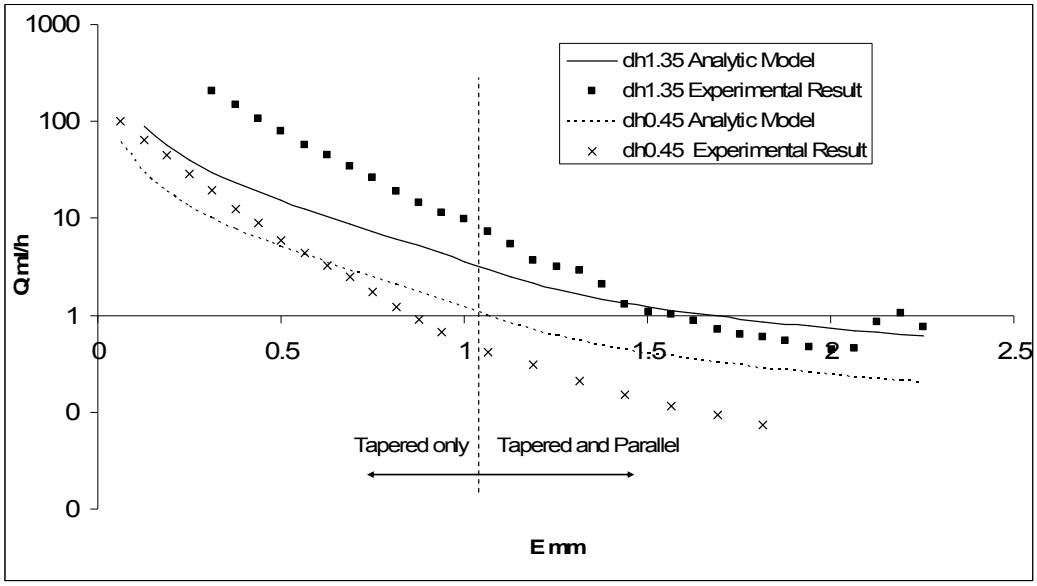

Figure 5-17 1° taper-angle. Transition from parallel to tapered section begins as E=1.08mm.

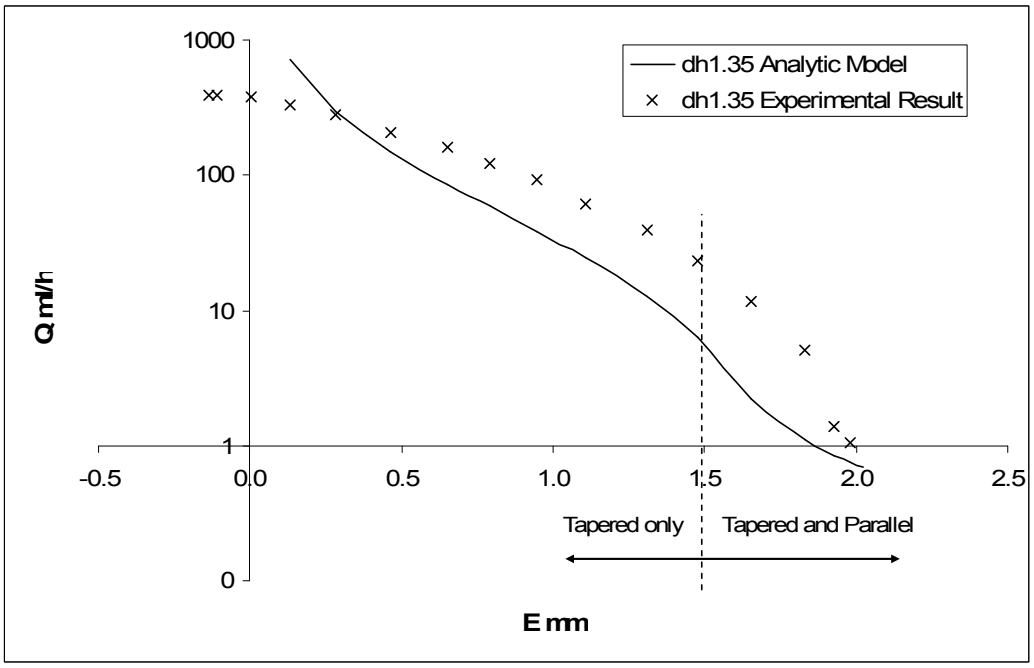

Figure 5-18 2° taper-angle. Transition from parallel to tapered section begins as E=1.5mm.

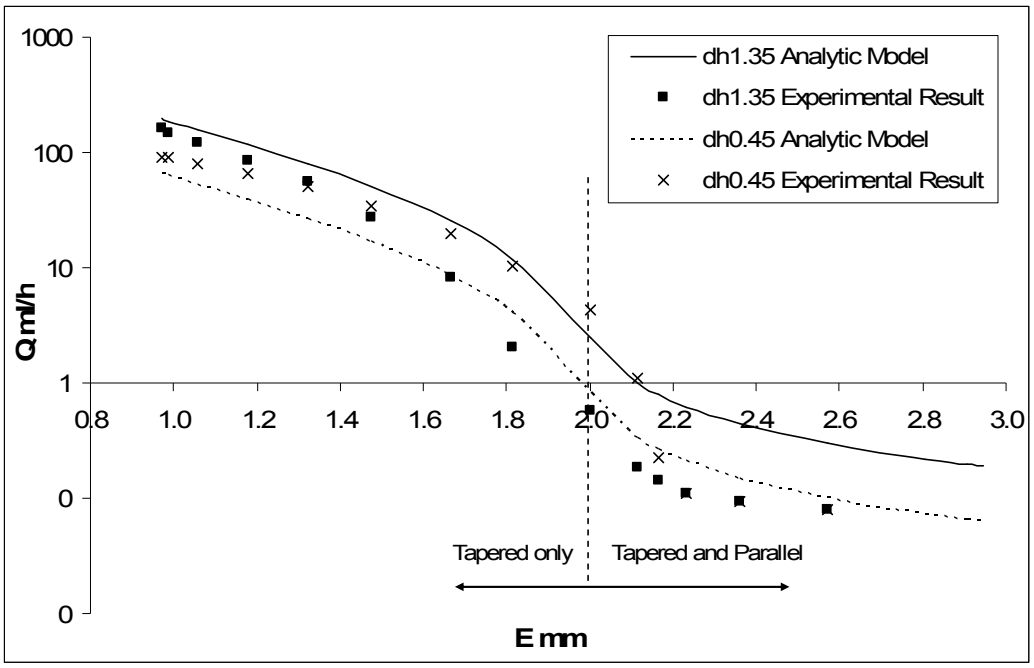

Figure 5-19 3° taper-angle. Transition from parallel to tapered section begins as E=2mm.

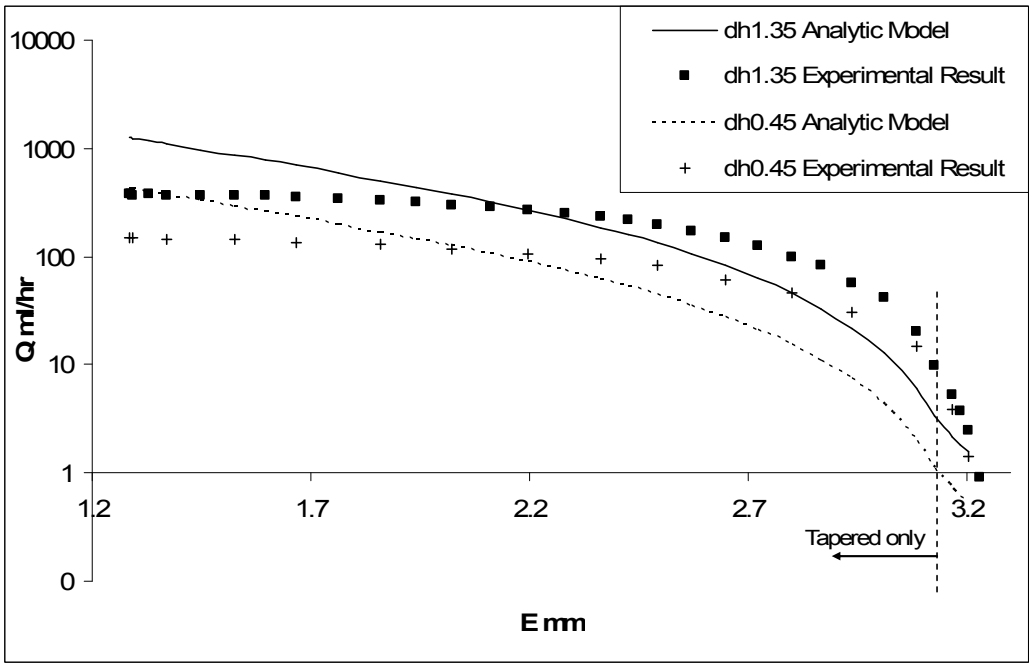

Figure 5-20 4° taper-angle. Transition from parallel to tapered section begins as E=3.12mm.

5.1.4 Ideal Flow

Central to the idea that flow rate can be controlled by variable geometry, such as found in a needle valve, is the characteristics of the flow variable in relation to the controlled variable. It is therefore necessary to understand how the needle geometry affects the flow characteristic. It is also necessary to understand and define the required flow characteristic. This could be defined as the maximum and minimum flow rate the valve can pass (range) and the characteristic of the curve between these two points. Various flow characteristics are known to the industrial control valve sector, including; fast acting, linear and equal percentage. The appropriate flow characteristic depends on the application requirements and must take into consideration the actuator and controller performance. The ideal flow characteristic is the one that most suits the application to hand and may be any of the above, none or some combination of characteristics. Skousen [15] describes an equal percentage flow characteristic as one in which "the change in flow per unit of valve stroke is directly proportional to the flow just before the change is made". This suits lubricant dispensing applications as it provides good rangeability matched to the ability to accurately control both high and low flow rates. One of the results of this thesis is the creation of an analytical model that can be used to interrogate needle geometries and therefore aid the designer to create and appropriate flow characteristic.

While this research is based largely on an existing design of needle valve that has been found to work well in the application for which it was developed, it was created through a process of trial and error and not subjected to detailed flow analysis. As such its flow characteristics have not been investigated in detail and the required characteristics have never been formally defined. In order to provide a context for the

following investigation, it is useful to define a suitable flow profile for the existing application. While the maximum available flow rate for a given valve is dependant on a number of factors including viscosity and pressure head, the flow characteristics are largely related to the needle profile. The difference in flow characteristics generated by different needle profiles can be clearly seen in the following example.

Figure 5-21 shows the measured flow profile for a tapered needle valve. Flow rate Q is shown as a function of the valve position VP. The ideal flow curve shows flow increments of 32%. This shows that the current valve profile operates in a similar manner to an equal percentage valve. The main benefit of this is that it allows fine adjustability of the flow rate at both high and low flow rates at the same time as providing a large range of flow rates. The equivalent graph using a natural log scale on the flow axis highlights the strength of the equal percentage characteristic. It clearly shows that there is a great deal of adjustment available above and below the nominal range of one drip every 30-60 seconds allowing good adjustability to suit a wide range of conditions. This could include a variety of oil viscosities at different temperatures.

An equivalent graph of the flow profile of a parallel needle (Figure 5-23) shows a very similar curve to that of the tapered needle in Figure 5-21, however the range is much smaller and although the equal percent curve looks similar it does not fit quite so well. This is confirmed by Figure 5-24 where it is clear that a parallel needle is not equal percentage. There is very little adjustment range above and below the nominal band, meaning it is less able to adapt to a range of operating conditions.

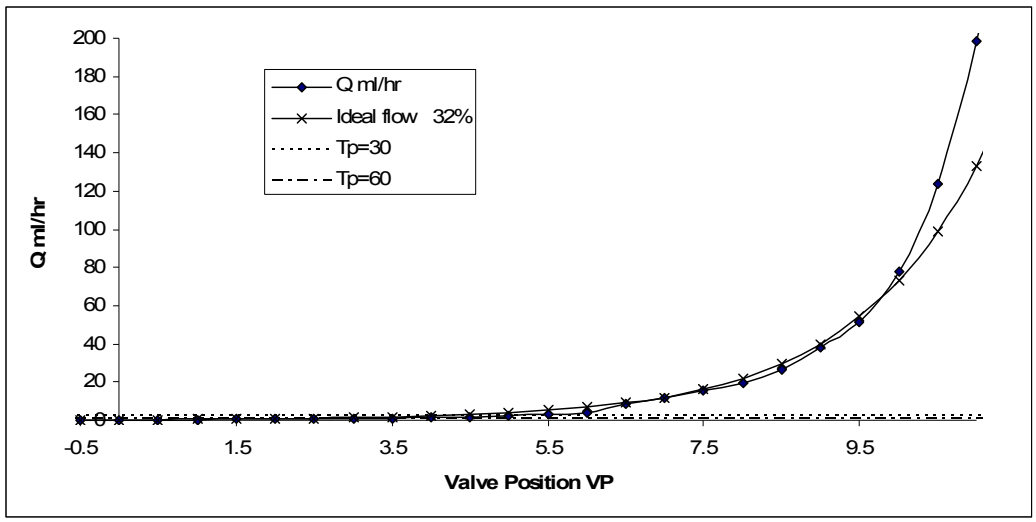

Figure 5-21 Tapered needle showing measured flow curve and 32% equal increment curve in natural form. This shows the large range of flow available.

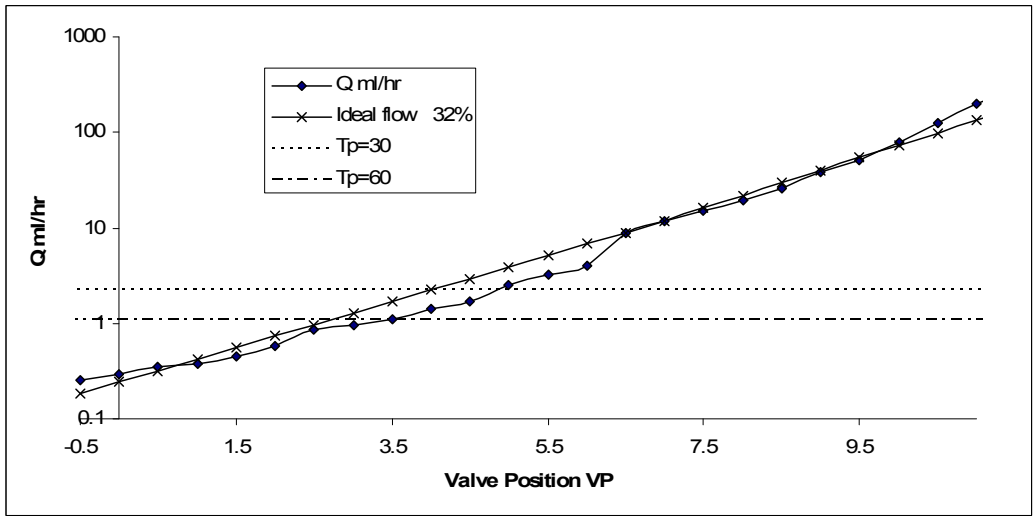

Figure 5-22 The same data as Figure 5-21 in natural log scale. The linear trend of the experimental data and an ideal, equal-percentage curve highlights the similarities.

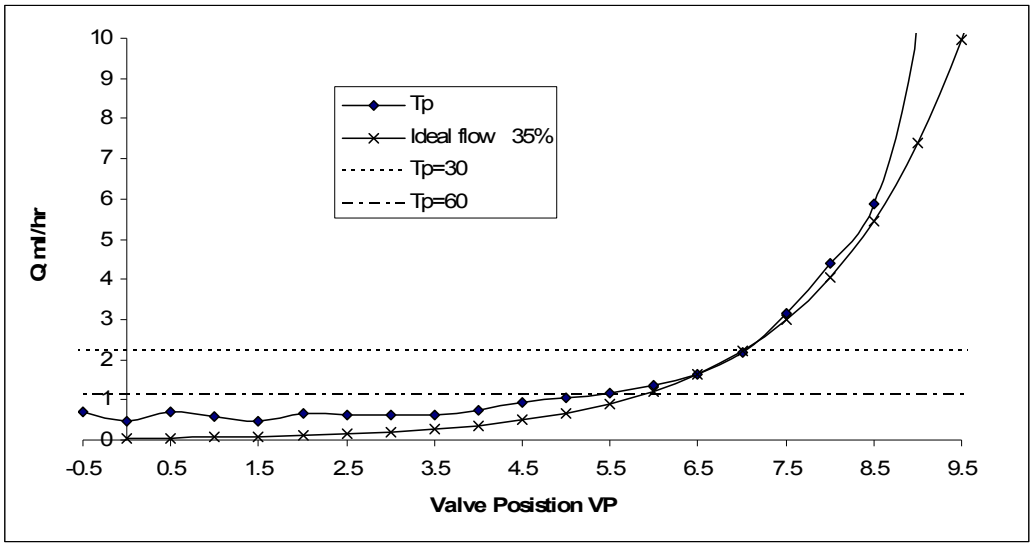

Figure 5-23 flow curve of a parallel needle and 35% equal increment curve.

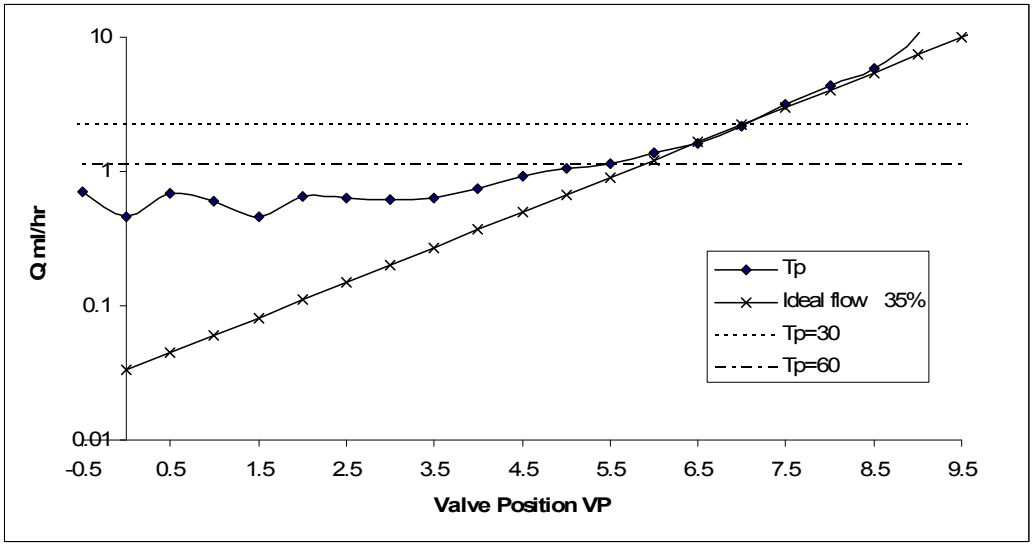

Figure 5-24 The natural log graph of Figure 5-23 shows that a parallel needle is not inherently equal percentage.

5.2 Conclusion

Predicting and characterising the flow through a valve is dependant on a number of factors, the most important of which are fluid viscosity, differential pressure and channel geometry. A valve flow model has been proposed based on these three elements including sub models that take into consideration secondary effects such as temperature effects on viscosity and valve geometry. The area of greatest uncertainty

involves the channel geometry and a number of model variants have been investigated to account for this. Analytical models have been verified by CFD and compared with test data. Until this point there is no reference in literature to studies that link valve geometry and the flow characteristic of a valve. The analytical solution presented here is a significant contribution in the development of understanding control of very low flow in microchannels.

The general equation developed for flow past a tapered needle has significant potential to aid the design and function of future control valves. The following chapter explores the mechanical and operational requirements of a mechatronic control valve. The implications of the valve flow model on the design characteristics of needle valves are considered in 7 in conjunction with the following 6 Mechatronic Developments.

6 Mechatronic Developments

6.1 Introduction

An integral objective of this research was to develop a mechatronic solution to a problem currently solved by purely mechanical means. While this suggests that the current mechanical solution is in some way deficient, this is not necessarily the case, but it is certainly normal to expect functionality and ease of use to be extended. The current valve has three basic functions, two of which are currently combined in a single operation.

1-Provide a means to Start/Stop oil flow: Currently performed by the vacuum connection to a motorcycle engine.

2-Provide logic control for when to Start/Stop oil flow: Also performed by the vacuum connection to a motorcycle engine.

3-Provide a means to regulate the volume of oil flow: Currently performed by the screw adjuster mechanism.

Mechatronic control would provide improved functionality by severing the link between valve actuation and the need for an engine activated vacuum, thus providing greater flexibility for use in different environments. It would also be able to regulate the flow to provide a flexible interface for controlling the required flow rate while at the same time being able to maintain the flow rate at the set level despite outside influences such as temperature fluctuation. This allows a much greater flexibility through being able to program the hardware to the requirements of a variety of situations. This could potentially replace the need to develop different needle and oil

viscosity grades as the integrated control system can compensate for this. It is also possible that oil viscosity grade could be varied according to the lubrication needs instead of as a means of overcoming temperature/viscosity issues.

However the interdisciplinary and integrated nature of a mechatronic system means that the design process must be considered from a number of standpoints. This includes (but is not limited to) understanding functional requirements, user requirements including user interaction, the physics of the systems to be controlled and the interaction of each of these systems. Each of these systems must be considered and understood in detail for the system to operate as a single entity to meet the end objective.

Two main projects were undertaken as part of the mechatronic development. The first was a fully functioning self contained oiler prototype for use in an industrial environment that automates functions 1 and 2 above. The second was a laboratory based prototype that replaces all three functions listed above.

6.2 Development of an Industrial Oiler

The aim of industrial testing is to prove the general architecture of the design. Problems encountered can be fed back into the design process to make improvements. Due to the nature of mechatronic products, the design has to reflect the role that it performs and the environment in which it is used. Hardware and software have to work in harmony in order to be able to produce the desired affect in response to the environment. An incorrect specification of the software or hardware, or an incorrect interpretation of the environment can result in an undesirable result. Due to this interdependency a problem in one area can have repercussions in the others, this in

turn can create knock on effects. Figure 6-1 describes the interrelated nature of a mechatronic system.

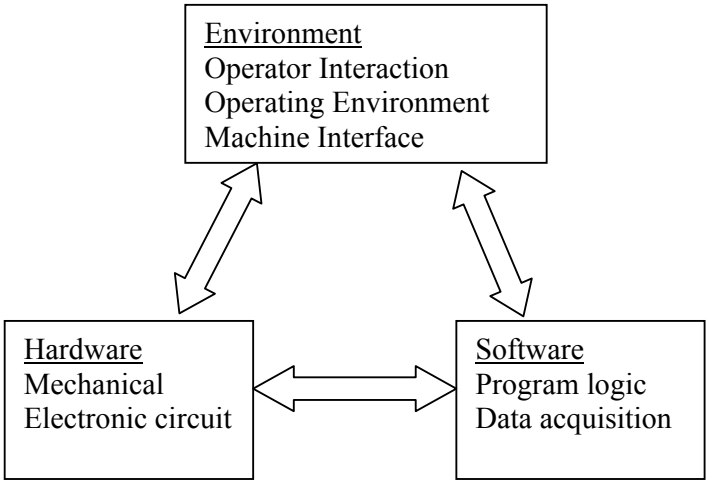

Figure 6-1 Interrelationship of factors that affect a mechatronic system design.

As the system architecture is heavily influenced by the environmental factors. It was necessary to test an oiler system in an operational environment. To this purpose a number of local manufacturing companies were assessed to identify a chain driven machine that would benefit from automated lubrication. The machine selected was a 'cooling tower' at a local biscuit manufacture (see 10.4 Appendix D: Prototype Oiler Images). It is a chain driven rack that transports biscuit wafers through a refrigerated tower. The application is characterised by an abrasive environment caused by broken and crushed biscuit wafers, interspersed with periods of high moisture due to the frequent high intensity cleaning regime.

6.3 Basic architecture

Two prototypes were built and commissioned through the course of this research, although their architecture was broadly the same, some modifications were made to the second prototype in response to operational requirements. This description will

focus on the first prototype with the differences to the second prototype explained after. Both prototypes were installed on the same chain driven wafer cooling machine. Aside from testing the functionality of the prototype oiler, the cooling machine was monitored for power use and potential benefits of continuous lubrication.

The functional requirements of the first prototype were based on an assumed mode of operation as a specific application and location had not yet been identified. The basic premise of the first prototype was that it should be a self-contained unit capable of activating the RMV valve when a machine or more specifically a chain, is operational. It should be easy to install with minimal interface requirements with the target machine. These assumptions defined the architecture of the first prototype.

From this, the following assumptions could be made:

- The unit would be battery powered to simplify installation.
- Energy consumption would have to be minimised for the purpose of extending battery life.
- All components would be housed in a case, including the oil reservoir.
- The only external input would be from an externally mounted motion sensor.
- The only output would be the regulated oil flow conduit.

At a later date, the requirement to count the chain run time was added, in order to be able to conduct chain lubrication and wear studies. At the initial stage it was assumed that a proprietary Scottoiler component would be able to split the oil flow to multiple locations.

Figure 6-2 shows the basic architecture of the first prototype, where the electrical and control system is shown in black and the lubricant handling system is shown in grey.

The solenoid acts as the interface between the electrical and mechanical systems, while the RMV is the interface between the mechanical and fluid systems.

Images of the prototypes and installation can be found in 10.4 Appendix D: Prototype Oiler Images.

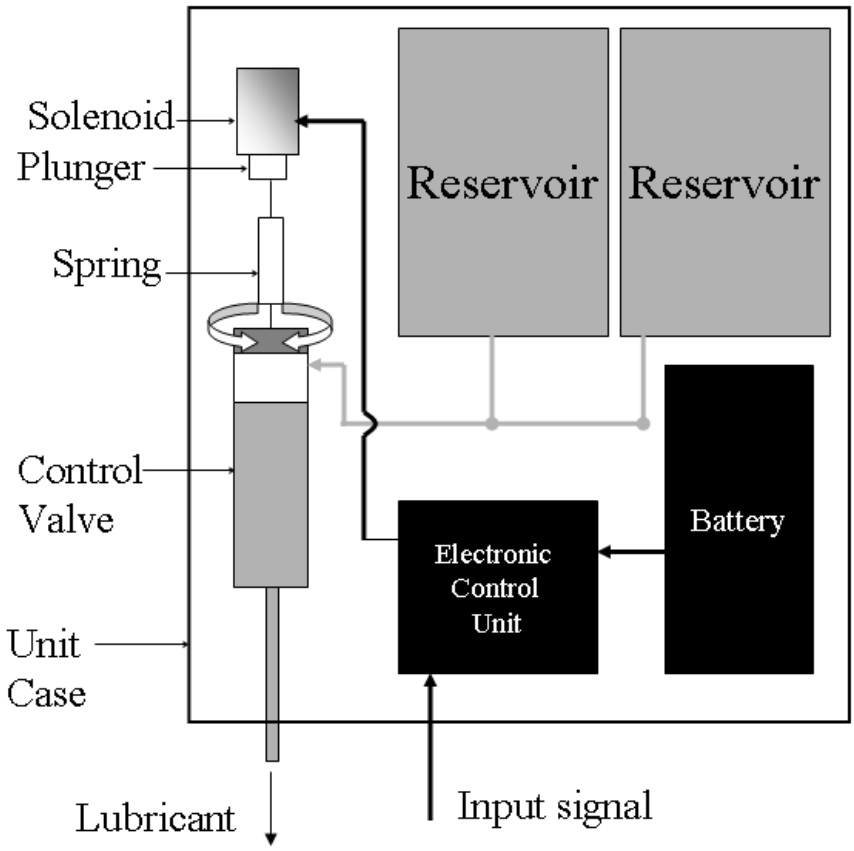

Figure 6-2 Prototype architecture showing electrical system in black and the lubricant system in grey.

6.3.1 Spring Solenoid Model

As the RMV was originally designed to be activated by a connection to the intake manifold of a motorbike engine, an alternative means of activation was required. It is possible to convert the RMV to cable operation so that the needle is lifted via a cable connected to the needle mount. This is relatively easy to achieve with minimal

interruption to the normal operation of the valve. The benefits of this are that it allows a much wider range of activation methods while avoiding the difficulty of generating a constant vacuum. Due to its simplicity and relatively low cost, the obvious choice for a mechatronic application is a solenoid. The use of a magnetically latching solenoid significantly reduces the power required compared to a regular solenoid, by removing the need to maintain current flow while the valve is open. This limits current draw to pulses when switching the flow on or off.

There are two important characteristics of latching solenoids that must be considered when incorporating them in a mechanical system. Firstly, by definition, a latching solenoid sits in one of two positions, with the plunger either *in* or *out*. In the *in* position the plunger is held by an internal magnet but must be stopped by an external mechanism to prevent the plunger from exiting the body completely when the current is reversed. As such, it is not designed or able to regulate the extent of plunger travel. Secondly, the ability of the solenoid to successfully pull the plunger decreases exponentially as the plunger exits the solenoid body. This means that it is able to exert a strong force in very short travel applications, but a very weak force when fully extended.

Because of these characteristics, there is an immediate problem when trying to interface a latching solenoid with the RMV. The RMV requires a range of travels corresponding to the amount of needle lift available as set on the adjuster dial. This is approximately 3mm, corresponding to the available travel of the needle between the closed and Prime positions of the valve. As can be seen from the basic architecture diagram in Figure 6-2, a spring must be inserted between the RMV and solenoid to allow the solenoid full travel while the RMV needle travel is restricted.

This now leads to the problem of matching the solenoid force and travel to the force and travel of the RMV. As can be seen from Figure 6-3, the total distance required to travel by the solenoid plunger, x_T, is:

$$x_T = x_{RMV} + x_C$$

Equation 39

Where x_{RMV} is the compression on the internal RMV spring, and x_C is the extension of the centre spring. RMV spring travel is limited by the adjustable stop, and the total travel of the solenoid is the sum of RMV spring compression and centre spring extension.

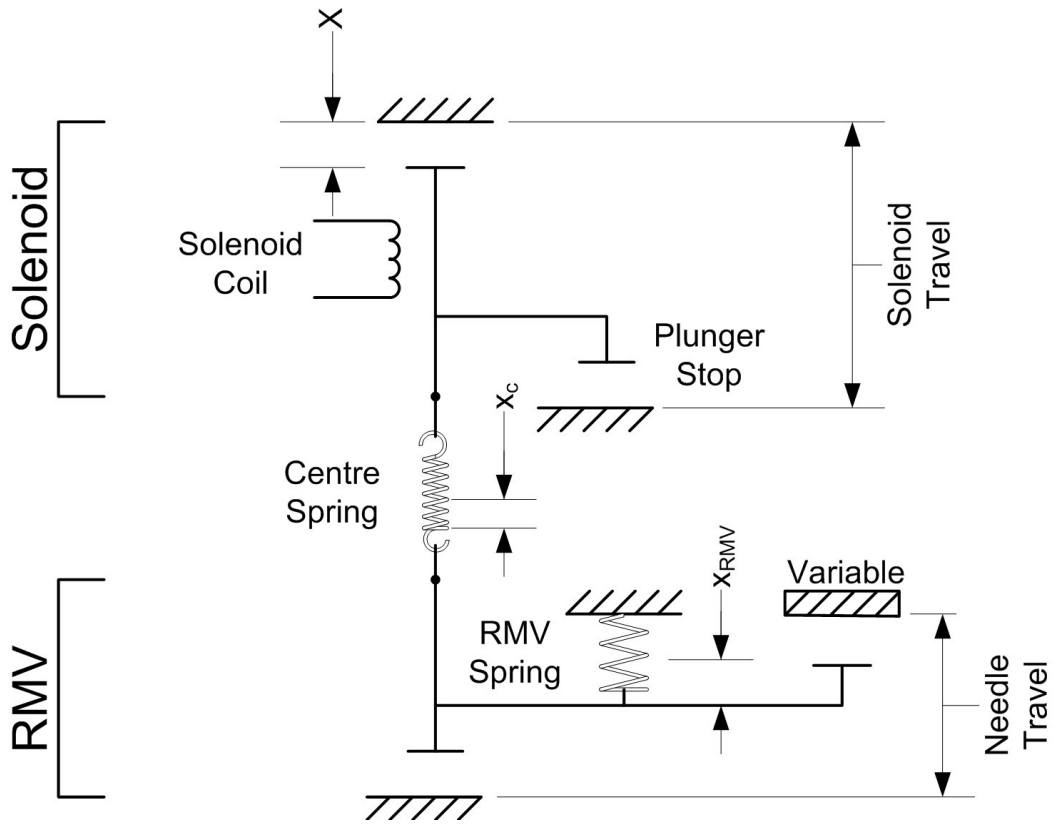

Figure 6-3 Mechanical system summary

As the spring constant k can be defined by $F=kx$, where F is the force applied and x is the spring extension, the total spring extension can be defined as:

$$x_T = F/k_{RMV} + F/k_C$$

Equation 40

Where k_{RMV} and k_C are the spring constants of the RMV and centre spring respectively. If the spring constants are known it is possible to plot the total extension against applied force. Combined with the pull force/stroke information provided by the solenoid manufacturers it is possible to see the effect of different spring constants.

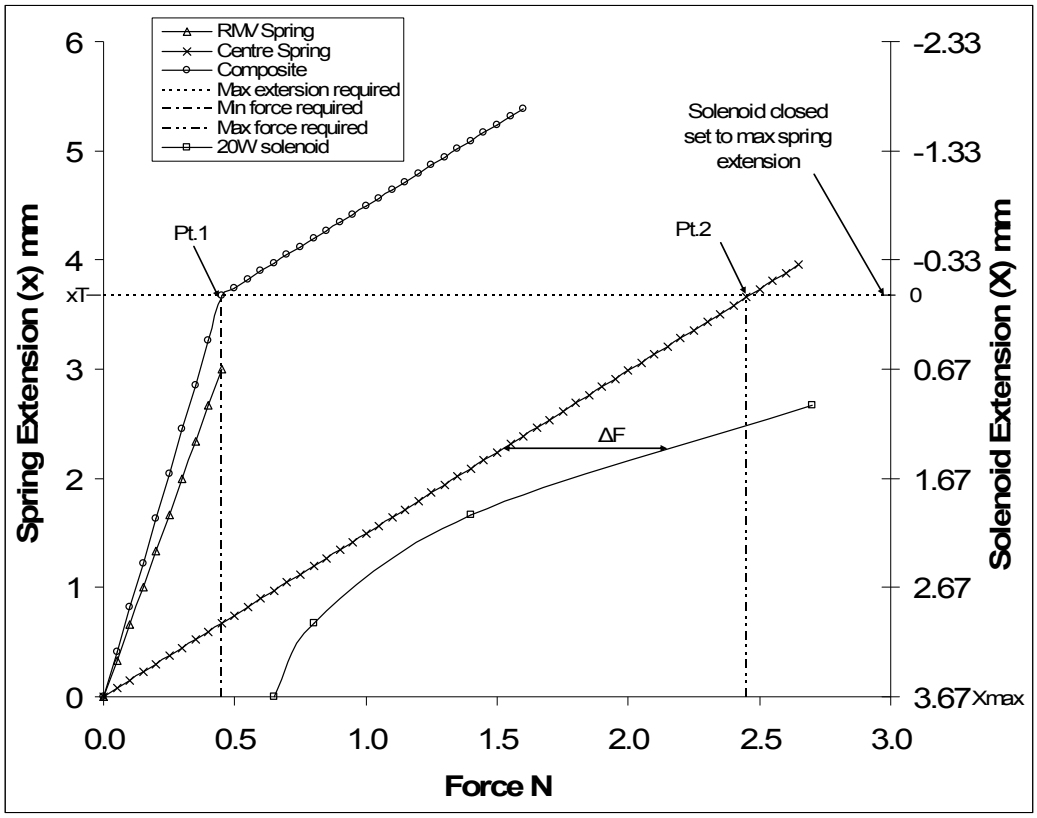

Figure 6-4 Spring extension and force in relation to solenoid force

Plotted in Figure 6-4 are the force/extension characteristics for the RMV spring on its own (RMV Spring), the centre spring on its own (Centre Spring) and the combined affects of the RMV spring and centre spring (Composite). Also shown is the force/ extension curve for a 20w solenoid as provided by the manufacturer. The minimum stroke required of the solenoid is equal to the maximum extension of the composite spring as per Equation 39. In the example given it can be seen that the minimum

stroke required of the solenoid to ensure the RMV has moved through the full amount of travel possible is 3.75mm as indicated by the change in angle of the composite curve and by the *Max extension* line. It is achieved with the RMV spring and centre spring in series and corresponds to the RMV spring reaching its limit of travel. The Centre Spring line represents the case when the RMV is closed and so allows no compression of the RMV spring. In this case all the force is through the centre spring and a much higher force is required to achieve the same travel. As the minimum solenoid stroke length is set by the minimum RMV stroke, this is the situation that places the highest load on the solenoid and it can be seen from the dashed lines that a force of 2.45N is required to pull the centre spring the minimum stroke of 3.75mm. As the valve travel adjustment is achieved by limiting the travel of the RMV spring, all possible force/extension combinations lie between the Composite and Centre Spring lines and so the force range is 0.45-2.45N. Changing either of the two spring constants alters the minimum stroke length required which in turn alters the maximum force required.

The solenoid data shown on Figure 6-4 is given relative to the plunger fully engaged position and has been converted from the force/stroke data supplied by the manufacturer. Taking this as a datum, the stroke=0 point is set to the maximum spring extension line. This means that for all spring force plots above the solenoid force line, the solenoid should be able to pull the spring. If the Centre Spring line (also the worst case) were to cross the solenoid curve, it would indicate that the solenoid would start to pull but then not be able to generate enough force to fully engage the plunger.

It can be seen from this example, the benefits of a relatively high k_C spring constant relative to k_{RMV}, as this limits the total extension required, which in turn reduces the total force required when the RMV is in the closed position.

However, there are knock on effects of changing the centre spring constant, as the solenoid power curve is linked to the total extension point. As the total extension reduces, so the total travel required by the solenoid reduces, putting it in a more favourable power band.

This interrelationship means that there is a range of spring constants that could be suitable for this application. In practice it was found that while the system was fairly insensitive to specific k_C, it was very sensitive to the particular position of the solenoid and plunger stop. This is because of conflicting positional requirements. The position of the solenoid is such that the following requirements must be fulfilled:

1. In the engaged position there is enough tension in the centre spring to be able fully lift the RMV needle while in Prime position.
2. There is enough tension in the centre spring to aid the disengagement of the solenoid plunger when the current is reversed. This is at a minimum when the RMV is at prime.
3. There is no residual tension in the centre spring when the plunger is disengaged, as this will prevent the valve from fully closing and allow it to leak.
4. When conditions 1-3 are achieved there remains enough power in the solenoid to pull the plunger when the RMV is in the closed position.

While it could be argued that condition 4 is unnecessary, it would be considered good practice, as the system needs to be able to operate when the RMV is ‘nearly closed’ and as this position is impossible to define, it is prudent to design the mechanism to activate when the RMV is closed.

The points above and Figure 6-4 can be formalised in terms of the difference between the force available from the solenoid and that required to open the valve, ΔF as marked on Figure 6-4.

The maximum force required to open the valve is determined by the position of Point 2 on the centre spring line, which in turn is determined by Point 1.If the needle and centre spring displacement is denoted by x, and the maximum displacement required of the RMV and the centre spring called x_T, x_T marks the position of Point 1. x_T and Pt.1 can be determined by:

$$x_T = x_{RMV} + \frac{F_{\min}}{k_C}$$

Equation 41

Where x_{RMV} is the needle movement required to fully open the valve, k_C is the spring constant of the centre spring and F_{min} is the minimum force required to close the valve taking in to account the opening force of the fluid pressure head. In this way the valve opening distance and the shut force of the valve determines the spring constant required of the RMV. The maximum force required to open the valve is determined by Pt.2;

$$F_{\max} = k_C x_T$$

Equation 42

If the force generated by a solenoid F_S is [79]:

$$F_S = \frac{1}{2}\frac{N^2 I^2}{X^2} A_a \xi$$

Equation 43

Where N is the number of turns of the solenoid coil, I is the current through the coil, ξ is the permeability of air, A_a is the cross-sectional area of the air gap and X is the displacement of the plunger. For ease, all the values other than the plunger

displacement can be amalgamated into a single term τ that can be considered as the solenoid coefficient.

The ΔF value is dependant on the position of the solenoid relative to the valve and X is a vector in the opposite direction to x (as represented by the opposing scales on Figure 6-4). However if the maximum travel of the solenoid is taken to be equal to the maximum travel required of the valve and centre spring;

$$|x_T| = |X_{\max}|$$

Equation 44

And therefore X can be converted to x as;

$$X = x_T - x$$

Equation 45

Using a combination of Equation 43 and Equation 45 it is possible to define ΔF in terms of valve displacement x;

$$\Delta F = \frac{\tau}{x_T - x} - k_C x$$

Equation 46

It is interesting to note that the solenoid curve moves as the solenoid is moved relative to RMV and that ΔF is smallest in mid-stroke. It was noticed during testing that the successful functioning of the system was particularly sensitive to the position of the solenoid relative to the RMV and that the solenoid would stall mid stroke if positioned too far from the RMV. This corroborates the theoretical analysis.

It becomes difficult to prescribe predetermined parameters for future manufacture, as there are a number of uncontrolled variables that mean each system has to be selectively assembled. Due to the manufacturing tolerances of the RMV components, the RMVs themselves are individually tuned to set the closed position relative to the

adjuster dial. This means that the total travel for each RMV is subtly different for each assembly. It has also been noted that there are notable differences in performance between solenoids, particularly for the plunger release force.

6.3.2 Electronic Control Unit

The primary purpose of the Electronic Control Unit (ECU) is to control the lubricant flow in response to chain operation. The ECU inputs and outputs are summarised in Figure 5-6.

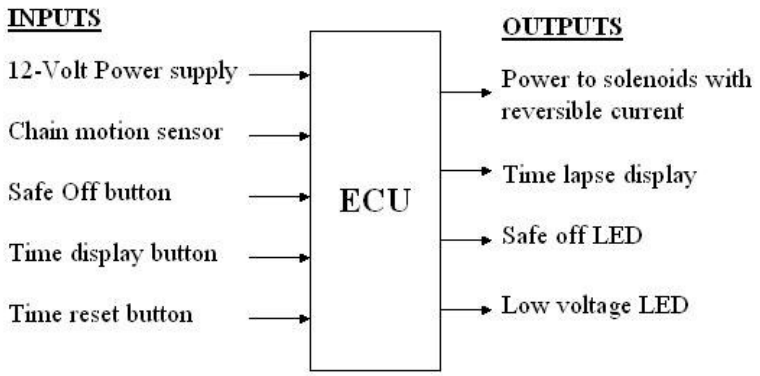

Figure 6-5 ECU inputs and outputs

This translates to the following input and outputs for the controller:

Primary Operations:

- Activate the lubricant flow when the chain is running and deactivate when the chain stops.
- Monitor the chain running time and display run time when requested

Secondary operations:

- Monitor battery level and display warning signal when low
- Provide a function to safely deactivate solenoids and store time counter to memory.

- Allow time counter to be reset.

6.3.2.1 Electronic Circuit

The ECU functionality is achieved through a combination of electronic circuit and microprocessor chips. The circuit can be split in two operational sections, defined by the voltage use. Circuit diagrams can be found in 10.5Appendix E: Prototype Oiler Control Circuit. There is the logic control circuit that runs from a 5-volt rail and comprises of two PIC microprocessor chips, logic input buttons, sensors and LED displays. This interfaces with the 12V power control circuit through the use of transistors to supply the current to the valve activation solenoid. It consists of two PIC triggered transistors and a relay. One of the transistors activates the relay, allowing the current direction to the solenoid to be reversed and the other transistor supplies the power for the solenoid when required. As the ECU is designed to run from a 12-volt input, there is a regulator to step down the voltage for the 5-volt circuit. The solenoid power circuit is supplied directly from the 12v rail.

6.3.2.2 Microprocessor function

The use of microprocessors allows the logic structure to be flexible within the limits of the hardware. It also allows a high level of functionality to be included at low cost. It is also relatively easy to update and allows the oiler to work as an independent unit. This means that bulky and expensive PC based controllers are not required and the oiler does not rely on the presence of a PLC controller.

The basic functionality was developed around a single PIC16F84 produced by Microchip Technology Inc. with the chain runtime functions using a second chip of the same type. The PIC16F84 microprocessor is an 8-bit CMOS EEPROM

microcontroller made by Microchip. It has 18 pins with 12 in/outs over two ports (4 on A and 8 on B). It can operate on 2-6 volts, at speeds up to 10MHz and sink 25mA per pin. In this case it is run on 5-volts and 2.4575MHz.

PIC1 Functions	**PIC2 Functions**
Monitor sensor signal, execute solenoid control logic and Activate solenoids	Monitor activation of PIC1 and count runtime.
Monitor and display low battery voltage	Monitor counter display button and activate 7-segment LED on demand.
Monitor safe off button, activate power shutdown sequence and display safe off LED	Monitor shut down request from PIC1 and store clock count in memory
	Monitor clock reset button at power-up and reset clock on demand.

6.3.2.3 PIC1 Functions

The main purpose of PIC1 is to control the solenoid functions. This is achieved by pulsing the solenoid on or off in response to the signal from a motion sensor mounted on the machine. The sensor is a reed switch that is closed by a magnet mounted on a moving part of the machinery. When the magnet passes the sensor, a low pulse (logic=0) is generated at Port A Bit3 as the sensor contact is closed and high pulse (logic=1) is generated when the contact is open. As always, the program needs to be tailored to take into account the specific hardware in use, particularly because a microprocessor is able to execute command logic many times faster than even very quick mechanical systems. For this reason certain lines of code are inserted to ensure the system works reliably. As can be seen in Figure 6-7, when querying the status of buttons and sensors, false positives and missed signals can be avoided by repeating the query with a pause in between queries. This AND system means that unintentional pulses cannot trigger a response and the pause ensures that signals are not missed due

to the contacts bouncing during the second poll. The pause must be short enough to ensure that the signal is not missed in situations where the pulse might be short, such as when the magnet moves past the sensor at high speed. The pause can also be used to ensure that buttons are not being pressed accidentally.

Although it could be considered unlikely that the magnet would stop directly in front of the sensor, it is important to take this into account to ensure reliable running of the system. From a program logic point of view, there is no difference between detecting a short low pulse or a long high pulse. This can be seen in Figure 6-7 represented by the parallel logic streams.

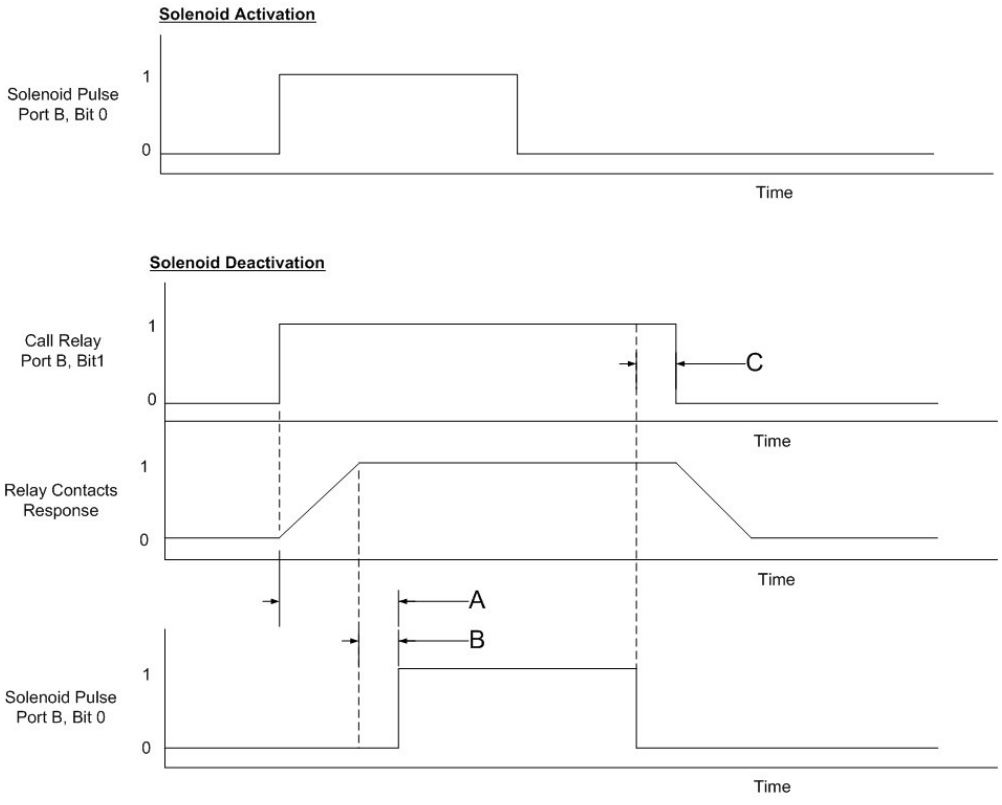

Figure 6-6 Deactivation of the solenoid requires a relay to reverse current. The solenoid pulse must be within relay settling time.

Port	Bit	Pin	I/O	Function
A	0	17	In	Battery low comparator input
A	1	18	In	Battery low comparator on
A	2	1	In	Shut down command
A	3	2	In	Motion sensor
B	0	6	Out	Solenoid pulse
B	1	7	Out	Relay coil pulse
B	2	8	Out	Green LED. OK to switch off
B	3	9	Out	Red LED. Low volt warning
B	4	10	Out	Stop count on PIC2
B	5	11	Out	Start count on PIC2
B	6	12	Out	Cause interrupt on PIC2
B	7	13	n/a	Not used

Table 6-1 PIC1 In/Out functions and pin numbers

Pulling, or activating the solenoid simply requires a pulse to Port B Bit 0. This pulse powers the solenoid via a transistor. A reversed current is required to release, or deactivate, the solenoid. This is achieved via a relay. Activating the relay while it is carrying current corrodes the contact terminals, so it is good practice to switch the relay before transmitting current via the transistor. In a similar fashion to the sensor, a delay is required to allow the relay terminals time to switch and settle. The solenoid can then be pulsed before the relay is allowed to return to its normal position. The sequence can be seen in Figure 6-6, where A represents the total time lag between relay pulse and solenoid pulse, B represents the time between the relay settling and the solenoid pulse and C represents the delay required to ensure the relay does not return while the solenoid is still being pulsed.

The In/Out functions of PIC1 with corresponding pin numbers are summarised in Table 6-1.

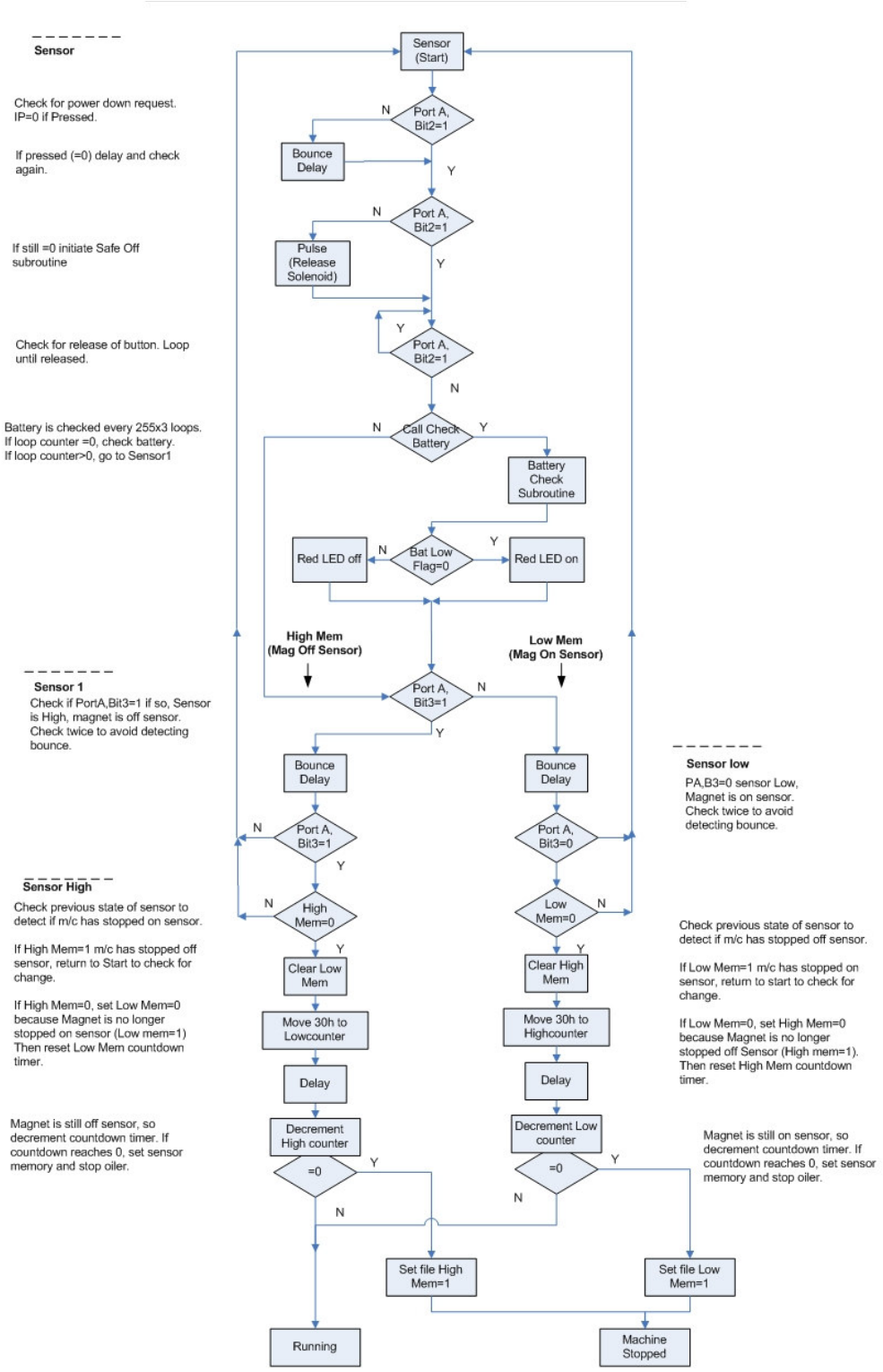

Figure 6-7 PIC1 program flow diagram. Includes shut down request monitoring, battery low check, motion sensor monitor and logic.

6.3.2.4 PIC2 Functions

The main function of PIC2 is to keep count and display the runtime of the oiler. The In/Out functions of PIC2 with corresponding pin numbers are summarised in Table 6-2. This allows the runtime of the chain to be cross referenced against chain wear and also oil use. The timer is activated and stopped by a signal from PIC1. The display is normally blank in order to conserve battery life and the user can request a readout of the timer at any time using a micro switch on the circuit.

Port	Bit	Pin	I/O	Function
A	0	17	In	Reset count
A	1	18	In	Start count
A	2	1	In	Stop count
A	3	2	In	Read out count
B	0	6	In	Interrupt
B	1	7	Out	LED segment 1
B	2	8	Out	LED segment 2
B	3	9	Out	LED segment 3
B	4	10	Out	LED segment 4
B	5	11	Out	LED segment 5
B	6	12	Out	LED segment 6
B	7	13	Out	LED segment 7

Table 6-2 PIC2 In/Out functions and pin numbers

The readout uses a single seven-segment display to scroll a four digit number corresponding to the number of hours the host machine has run for. The display scrolls the count starting with the most significant digit and is bracketed at either end to assist the reader in identifying the correct order. The display therefore reads as [ABCD]. Scrolling the display minimises the number of output pins required to display four digits. A single four-digit seven segment display unit would have

required an additional four pins in order to switch the seven segment's output between each of the digits.

6.3.2.5 Power use

An important consideration during the design of the circuit and program was the reduction of power use. The two main blocks of power use are the solenoid pulse where a high current is required for a short time and power use is largely dependent on the number of activation/deactivation cycles the circuit conducts. This is dictated by the duty cycle of the oiler system which is turn is dictated by the duty cycle of the machine being serviced. The other important factor is the background current the circuit draws while the machine is operational. Although this is much lower than the peak current draw, it can have a significant effect on battery life, as it is a constant current drain. Various measures were taken to reduce background current to a minimum. Large gains were made by replacing the regular solenoid with a magnetically latching version. This removed the need for a permanent current to keep the oiler activated. The activation LED that signalled the oiler is in operation was removed from the early prototype. The current drawn by the sensor was reduced from 10m/a to 7m/a by replacing the original hall-effect sensor with a reed switch. The hall-effect transducer relies on a relatively large current to be able to generate a signal from the disturbance of a magnetic field. The reed switch is a passive system that only requires the smallest current that is detectable by the PIC. The time-lapse display is only activated on request and uses a scroll function instead of an array of 4 seven-segment displays.

6.4 Revised Architecture

Due to the concurrent nature of the project, the first prototype was developed before a specific application was found. The original specification called for the regulation of a single fluid outlet with the expectation that it would be possible to divide the flow if required. However it was found during implementation of the first prototype that it was difficult to reliably divide the flow after the valve. It was found that when the RMV is in the closed position, the conduit downstream of the valve is effectively an inverted U-tube making it impossible to maintain an even pressure on both outlets, thus allowing the feeder tubes to drain. In order to allow power consumption testing on the biscuit cooling machine to continue with the minimum disruption to the plant, it was decided to modify the design of a second prototype, already under construction, to include a dual dispenser. This would use two RMVs to provide two regulated flows, one for each chain on the machine. There were several potential methods for activating two RMVs with one control system. The first option is to activate the two RMVs with a single solenoid. However, it was thought that this would require a complex mechanical system for balancing the force generated by the solenoid across the two RMVs, which have slightly different resistances. It was also found that it was necessary to overload the 12v solenoid with approximately 17v for it to be able to develop enough force to pull two RMVs. While it is not a problem to momentarily overload a solenoid on a low duty cycle, it is difficult to provide a suitable power source. The second option is to use a solenoid for each RMV with associated mechanics. One of the main advantages of this method is that is allows the solenoids to be positioned relative to their respective RMVs to take into account slight differences in RMV travel and spring tensions, thus optimising the solenoid performance. Due to the modular nature of the design, powering the two solenoids

was easily achieved by adding a second set of power circuitry to the ECU circuit board. This meant that the control software and 5V portion of the circuit remained unchanged. The greatest problem with using multiple solenoids is that the increased power requirements mean that it is no longer possible to achieve the required battery life from a suitably sized unit. It would be possible to use a larger battery unit but it would become unfeasibly large, heavy and costly. As the intended destination of the oiler unit was now known it was possible to convert the system to use a 12v power pack capable of running from 110-240v. See 10.5 Appendix E: Prototype Oiler Control Circuit. and 10.4Appendix D: Prototype Oiler Images.

6.5 Simulated Duty Cycle Testing

During initial development, before the final application of the prototype oiler was known, it was important to be able to gain an indication of its performance under different operational conditions. The main performance parameters to be investigated include; the reliability of the solenoid actuation system and battery voltage drop over time under operating conditions. To do this it was necessary to be able to simulate the signal inputs that represent the operating parameters of a factory based machine. This was achieved through the use of a 'dummy machine' that consists of a computer controlled motor that moved a magnet past the sensor in the same fashion as the actual machinery would. The use of a LabVIEW based computer control allowed duty cycles to be easily altered.

The duty cycle used was based on the working hours of the industrial partner. Their machines run twenty-four hours a day, five days a week, with the weekend shutdown used for machine maintenance. It was then necessary to estimate the number and frequency of machine stoppages during normal operational hours. This can depend

greatly on the specific machine. During planning a number of different machines were considered for the trial. This could be divided into two basic styles of machine. The first is the high-speed conveyor type as typically found in packaging lines. Here sorting operations lead to many short duration stoppages, where produce or wrapping can become jammed in the machine. These stoppages are typically of very short duration, less than ten seconds. The other is a slower moving type of conveyor used for transport of bulk material during the manufacture process. Since short duration stoppages should not affect the oiler, it is only necessary to make an assumption on the number of longer duration stoppages that may occur in a twenty-four hour period.

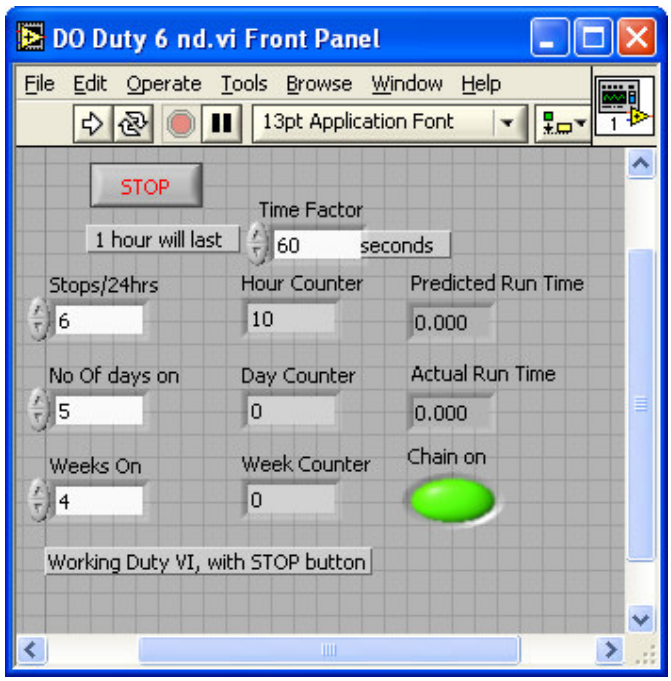

Figure 6-8 Duty Cycle front panel for control of the simulated machine interface.

The duty cycle interface can be seen in Figure 6-8. The main duty cycle functions can be seen with the number of stops required in a twenty-four hour period, the number of operational days in the week and the number of weeks the duty cycle is to last. The interface shows the count for each time unit as the duty cycle progresses. As it is not feasible to conduct real-time long-term endurance tests, it is important to be able to

compress the duty cycle. In this way it is possible to carry out a large number of solenoid activations following the prescribed work pattern in a short time period. It is for this reason the hours to be counted can be defined in seconds. The real-time actual run time is then calculated automatically. An indicator displays when the machine is operational.

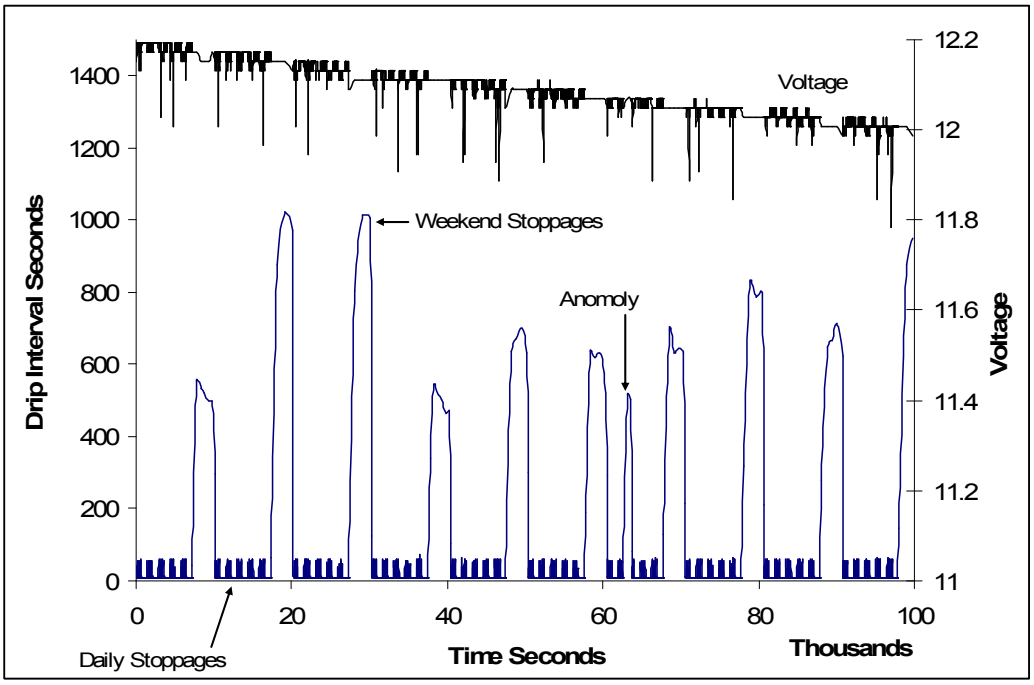

Figure 6-9 Duty cycle testing of the prototype oiler. The bottom line shows the drip interval response to the duty cycle and the top line is the corresponding drop in battery voltage.

In order to verify the prototype oiler's response to the duty cycle input, it is necessary to monitor the resulting oil flow from the oiler which can be done by analysing the drip times. Figure 6-9 shows the drip response to an early experiment and what can be read from the drip times. It shows a run of ten weeks, running five days a week with six stoppages per day. The ten high peaks represent the very long drip intervals generated by the machine stoppage over the weekend. The smaller peaks represent the six shorter stoppages during the day. It can easily be seen that there is an extraneous tall peak in week seven. This is an anomaly in the flow response that corresponds to a

mechanical failure which was subsequently rectified, thus showing the benefit of duty cycle testing. Also visible is the effect of the compressed duty cycle on battery life. The real-time duration of the test was 100000 seconds or nearly 28 hours with 300 solenoid activation and deactivation cycles corresponding to the equivalent of 10 weeks continuous running. The voltage drops 0.2 volts over this time period which is reasonable for the number of activation cycles.

6.6 Industrial Testing

Industrial testing of the two prototypes gave an indication of how well the mechanism and control reflected the operational requirements of the factory. It also showed how difficult it is to design and implement a stand-alone system in a complex working environment. To this effect, the oiler could not be 'stand-alone' as there is always some form of operational interaction from the host system. In this way, the first prototype has no interaction with the factory control systems, but as it was mounted inside the cooling tower, access became very limited, thus affecting how the oiler was maintained (Figure 6-10). It became, very difficult to access the oiler to check battery voltage levels, to change the battery or to refill the reservoir. In the same way, the second prototype solved some of the shortcomings of the first by distributing oil to multiple locations and using a mains power supply (Figure 6-11). This in turn, caused different problems through the factory system cutting power to the unit before it was able to deactivate the oil supply. While these problems are not insurmountable, they do require additional hardware and programming, thus reinforcing the requirement to fully understand the operational conditions in order to be able to create a successful system. Through this it was noted that it is particularly difficult to design a universal

solution and that for every installation, some form of customisation will probably be necessary.

Figure 6-10 Installation of the first oiler prototype inside the cooling tower.

Points to consider include, but are not limited to:

- Availability of power source and interaction of power source with the oiler unit.
- Number of oiling locations required.

- Height of the reservoir above the fluid outlet. This is often dictated by the availability of suitable mounting locations.
- Viscosity of lubricant. This affects the oil throughput which is tied in with the reservoir height and rangeability of the valve.
- How often the oiler unit is to be inspected and maintained. This affects the size of the reservoir and the battery if it is battery powered. If so, this has a knock on affect on the operational hardware due their effects on battery life.

Figure 6-11 Installation of the second oiler prototype on the same machine as the first. This time mounted on the outside for easier access.

The force stroke curve inherent in a solenoid means that it has a short effective stroke. The knock on effect is that the function of the system is extremely sensitive to the position of the solenoid relative to the load. Although the stroke of the RMV is relatively short and entirely compatible with the stroke typical of a solenoid, the varying load caused by altering the valve travel makes solenoid selection difficult and inefficient. The inefficiency arises due to the need to select a solenoid capable of activating when the valve is in the closed or nearly closed position which means that

the solenoid has to pull a high load through the full stroke while only creating a very small movement in the valve. The high loads placed on the solenoid also means that a high peak current is generated, in the region of 2.5-3 Amps per solenoid. This can put unnecessary strain on supply circuitry. In the case of the industrial testing performed here, it required up rating the factory control system circuit breaker. This seems entirely disproportionate considering the other high power machinery also operating on the same control system works using a lower rated circuit breaker.

6.7 Linear Actuated RMV (LARMV)

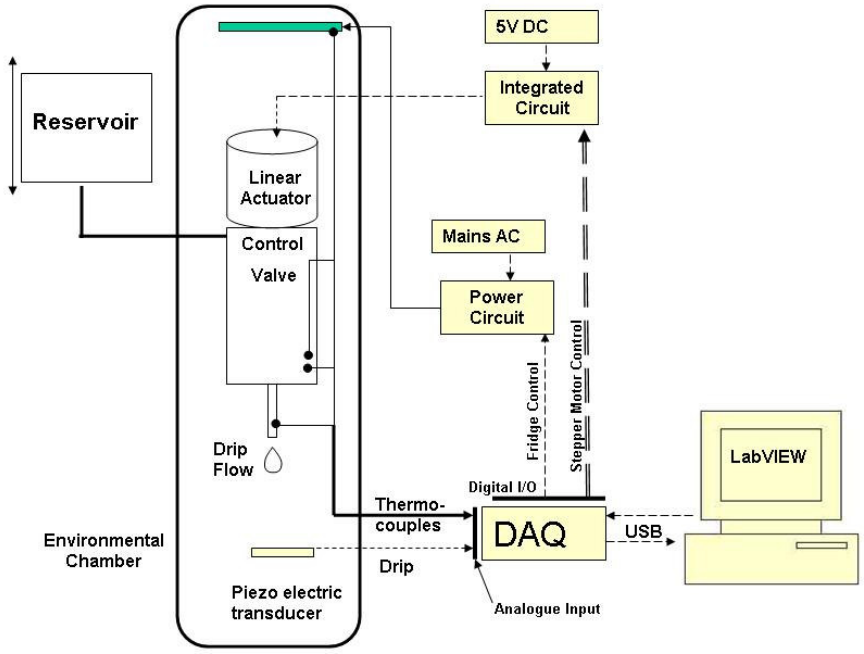

Figure 6-12 Experimental test rig incorporating linear actuated control of the valve.

Laboratory testing of the valve and the prototype oiler indicted that some form of dynamic control of the valve has many benefits. It increases the flexibility of the system and can improve the accuracy of flow control through the use of dynamic compensation of outside factors such as temperature and pressure head variations.

The modular test rig architecture shown in Figure 4-1 can be modified to incorporate the linear actuated valve as shown in Figure 6-12.

Numerous forms of linear actuator exist as discussed in the literature review and a micro linear actuator based on a rotational stepper motor was chosen for this application for the following reasons:

- They have a low cost performance ratio, with high performance available in a readily available package.
- It is easy to build and program stepper motors controllers, allowing easy integration with existing systems.
- Overall the micro linear actuator is commensurate with the RMV itself, meaning that they are equivalent technologies that work on similar scales in terms of accuracy, physical size and cost.

The actuator chosen was a Haydon Switch & Instrument, high resolution, 26000 Series linear actuator. A number of options were specified including captive shaft with M2 threaded spigot and end-stop switch. This bipolar 5V motor has a 7.5° step angle that translates to a linear step distance of 0.00643mm. Although it is possible to buy purpose built motor-controllers, wiring diagrams and phase sequences are provided allowing a custom motor controller to be built.

As with all mechatronic systems there must be a complete understanding of the intricacies of the system mechanics in order for the control program to be able to manage the system reliably. Any part of the program that is based on an assumption or theoretical working that does not reflect reality introduces the potential for the system to operate in an undesirable way. For this reasons a detailed program of performance measurement was undertaken on the linear actuated valve. Due to the nature of stepper motors, a particular problem can be ‘step loss’ [61]. As the motor

movement is characterised by a number of discrete steps, these steps can be counted as a means of determining specific positional locations. Any miscounting or interruption of the motor movement will cause ongoing positional errors due to the difference between the step count and actual position of the motor. Measures were taken to ensure this was not occurring, as this type of error is continuous and accumulative. As a precaution the control program automatically resets the step count or 'zeros' at a known physical location or datum. In this case the end-stop switch allows the control program to zero itself in order to know when to begin counting and can also be used as a reference point during program operation.

Ideally the linear actuator would be directly attached to the valve needle for the most positive connection between the actuator and the valve. However, as with all valves there is a trade off between direct control of the valve needle and creating a sealed unit. Direct attachment to the needle would require some form of seal on the moving shaft. In this case the shaft is splined and so almost impossible to seal effectively.

It is possible to make use of the existing valve architecture to maintain a sealed unit by connecting the linear actuator to the valve needle mount column. There are several ways in which this can be achieved, but the main design decision is whether to flexibly or rigidly connect the linear actuator to the needle mount column (see Figure 6-13). As it was, the first attempt at creating a linear actuated needle valve was created with a flexible coupling, similar to that used to connect the needle to the needle mount. This would allow for the flexible movement of the needle mount column caused by the diaphragm. It was not until after the movement characteristics had been defined and flow testing had begun that problems with this architecture became evident. It became apparent that the internal valve pressures acting on the

diaphragm at large gravity heads are sufficient to compress the flexible coupling and so alter the needle position and therefore change the fundamental flow characteristics of the valve.

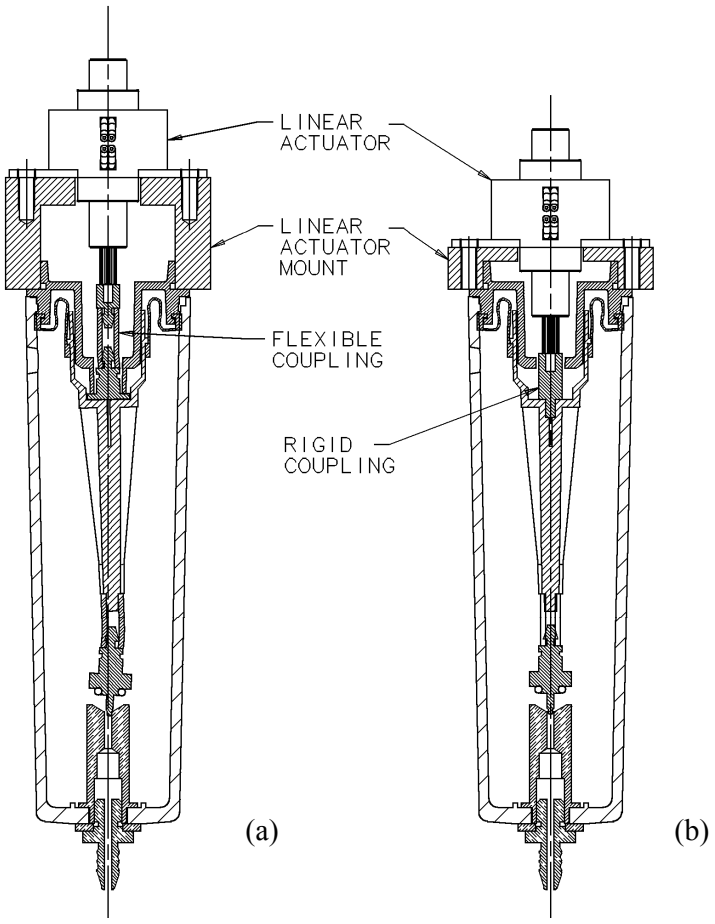

Figure 6-13 (a) Original LARMV including flexible coupling to allow for needle misalignment. Flexible coupling compresses at a high pressures causing inconsistent flow characteristics. (b) Modified design uses a direct link.

Alternatively, a rigid connection could put greater strain on the linear actuator through radial forces caused by the diaphragm, particularly if the connection is not perfectly concentric with the needle mount. It also means that any slight misalignment of the linear actuator would translate into a large radial displacement of the needle putting further strain on the assembly. It is for this reason the first option was to use the

flexible coupling. As this was found not to work, there was little option but to pursue the rigid connection solution.

Each mounting method has repercussions on the valve flow characteristics and therefore on the control program. Although the needle movement characteristics of both assembly methods were investigated in full, only the rigid version is described in detail as this is what was used for flow experiments.

6.7.1 Valve Actuator Control Program

There are two levels of valve control program; the stepper motor driver and the valve driver. The motor driver is required to control the motor such that the correct binary outputs are sent to each phase of the motor so that it extends or retracts. This is essentially a simple four step counter outputting a binary signal at each count. The counter can be reversed to count upwards or downwards.

The next level up is the valve driver that allows the valve to reach a requested set point in a controlled manner without exceeding predefined motion limits. It does this by counting the number of steps taken by stepper motor (x_a) and comparing that value with the requested position (x_d). It is independent of the high level smart programs that are able to determine the desired set point for a given situation. At this level, the valve can be control manually or through the use of a smart program. Figure 6-14 shows the valve driver logic, including a number of safety checks and functions.

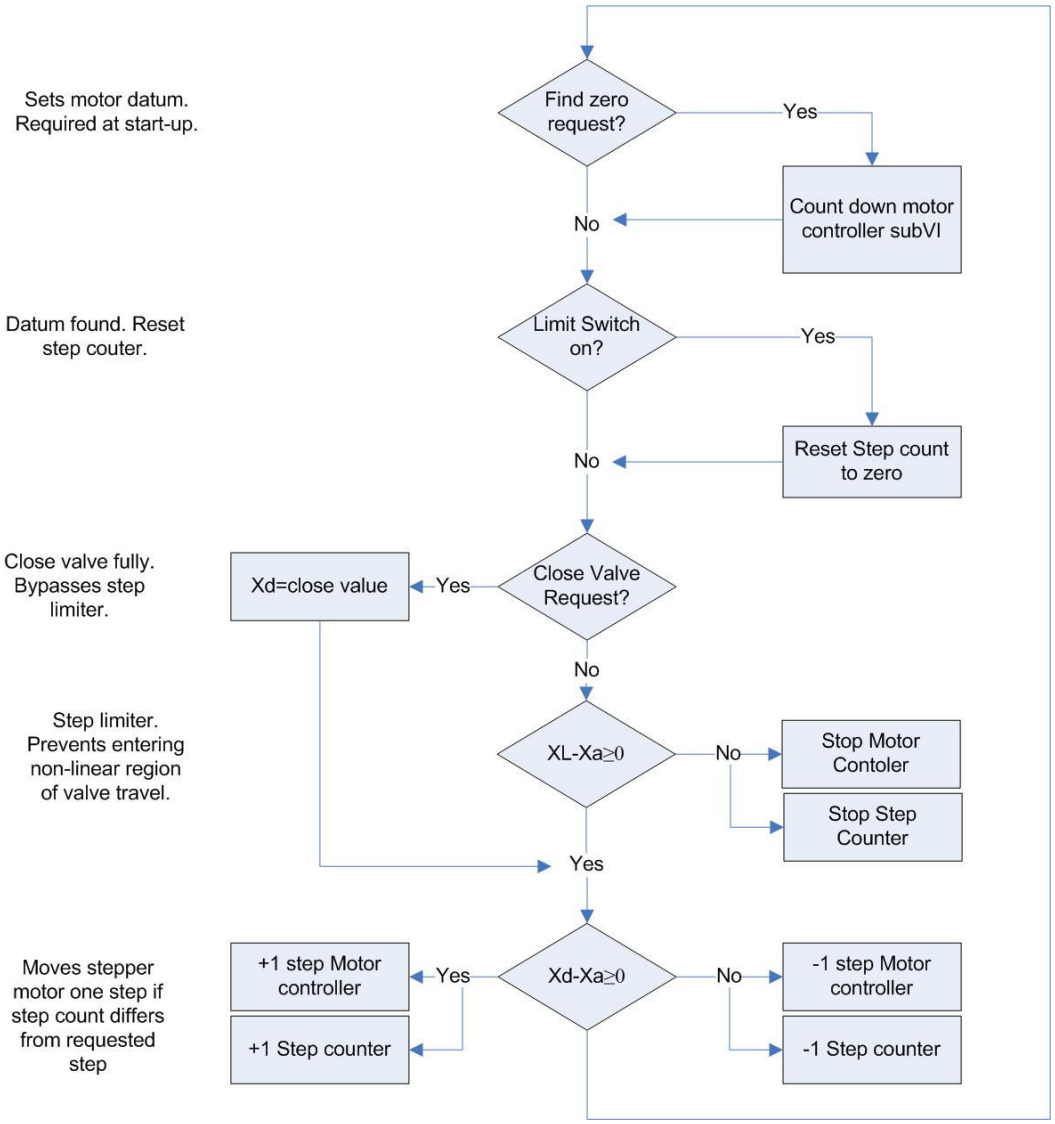

Figure 6-14 Valve Driver logic. x_d =requested step position. X_a =actual step position. x_L =step limit.

The main functions are:

- Set motor datum: Starts a sub-routine that continuously counts down the motor driver to retract the motor spindle until the limit switched is reached. Required to define the motor position in real space. Required on start up, but can also be requested at other times if necessary, for instance if a high motor load has caused the motor to skip steps and therefore move out of synchronisation with the step counter.

- Limit switch on: The motor driver is automatically cut if the limit switch is reached to prevent damage to the motor once it has reached the end of its stroke.
- Upper step limit: As there is no physical switch at the other end of the stroke, a programmed limit is put in place to prevent the motor from driving the needle into the valve seat. This is set at a point before the loads on the motor become high and may need to be re-zeroed using the datum switch.
- Close valve request: A step value higher than the step limit is required to ensure the valve is fully sealed shut so the upper step limit must be by-passed. The close valve request will move the needle to a set point above the upper step limit, but below the level at which undue load is placed on the motor.
- If none of the previous checks are active, the valve controller compares the requested step position with the actual step position and if there is a discrepancy is able to move the motor drive one step in the appropriate direction. It then repeats the loop.

With a functioning valve driver it is necessary to characterise the valve actuation performance so that an appropriate smart controller can be built. The aim is for the intelligent valve controller to request the appropriate valve position in terms of step number in response to a request for a particular flow rate from the user. Ultimately it would then be possible to have an even higher level of control and have intelligent requests for the desired flow rate without the need of human intervention.

6.7.2 Valve Actuation Performance

Control performance relies on a complete understanding of the physical system to be controlled, so a thorough investigation of the valve travel was undertaken.

The main points to be quantified were:

- Confirmation of step size
- Determine step loss if any and under what conditions.

- Repeatability of datum
- Backlash

Step size is of critical importance as it is used to determine the position of the needle relative to the valve orifice. With an engagement length (*E*) of 1.84mm, and a total travel of 2.75mm, the number of steps required to cover each distance is approximately 290 and 430 respectively, depending on the exact step size. Setting the datum at the fully retracted position in contact with the end stop switch, means that any error in the step size is multiplied by this number of steps. Therefore at full travel, a 0.1µm error in step size becomes a 43µm positional error in the needle. This level of positional change is easily detected using the flow measurement equipment developed for this study.

Measuring step size and step positions is not easily achieved due to the scales involved. The quoted step size of the linear actuator is 0.00643mm (6.43µm), the quoted resolution and accuracy of the vision measuring machine (VMM) used throughout this study is 0.5µm and 2.5µm respectively. Experience has shown that it is possible to reliably define the same point on an object to within 2µm. Therefore with a minimum of 4.5µm variation on each measurement it is not possible to directly confirm the quoted step size of 6.43µm. In practice, the measurement variation is actually even larger as the needle position is not measured directly, but via a gauge rod as used for the manual RMV and described in section 4.4.3.

As expected, the displacement of the needle is generally very linear in relation to the number of steps taken by the actuator. See Figure 6-15. This contrasts with the manual valve, an example of which can be seen in Figure 4-16.

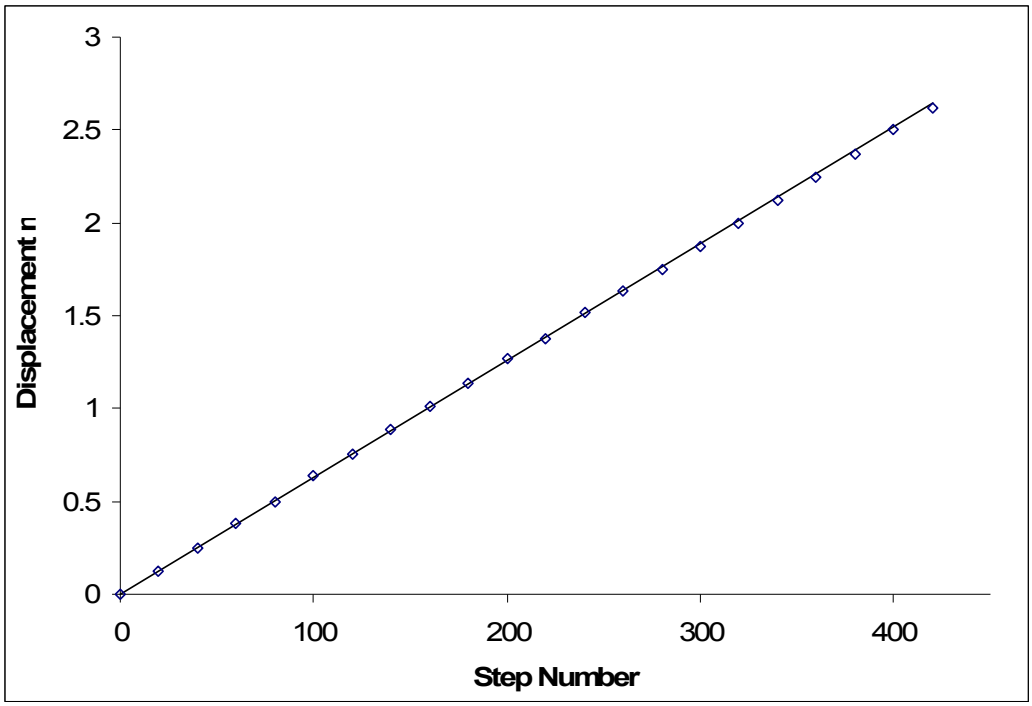

Figure 6-15 LARMV needle displacement in relation to step number.

The step size is calculated by dividing the needle displacement by the number of steps taken.

$$Step\ Size\ (S_d) = \frac{Needle\ Displacement\ (X)}{Step\ Number\ (S_n)}$$

Equation 47

It can be seen from Figure 6-16 that the actual measured step size is well below that of the manufactures specification of 0.00643mm. It can also be seen that despite the relatively high amount of scatter in the points, the two data sets reflect each other quite closely. Data Set 1 was measured in the close direction and Data Set 2 is reversed, in the open direction. This suggests there is a trend rather than simply measurement scatter and also indicates a relatively low amount of backlash, although this is investigated in detail later.

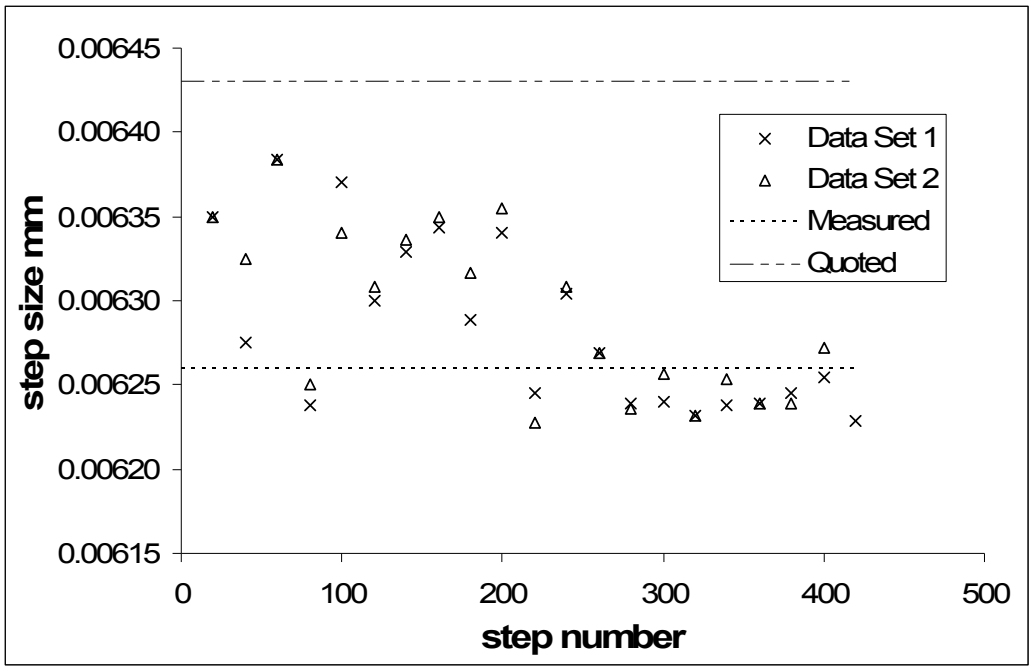

Figure 6-16 Measured step size of needle displacement. A comparison can be seen with the manufacturer's quote step size and actual measured. Data Set 1 was measured in the close direction and Data Set 2 is reversed, in the open direction.

Using regression it is possible to minimise the error between the predicted position and measured position for a given step size. This suggests a step size of 0.00626mm and reduces the error to 2% of the maximum engagement length, *E* (Figure 6-17).

$$Prediction\ Error\ \%\ (Er_p) = \frac{Predicted\ Position - Measured\ Position}{Maximum\ Engagement}.100$$

Equation 48

Also worth noting for its affect on future analysis is the positional error as a percent of actual engagement length.

$$Postional\ Error\ \% = \frac{Er_p}{Engagement\ (E)}.100$$

Equation 49

From Figure 6-18 it is clear that the step error becomes more significant as the channel length reduces. As the error value becomes large in proportion to the engagement length the uncertainty increases. This is of particular significance when

trying to correlate the modelled flow rate with measured flow rate at low engagement values.

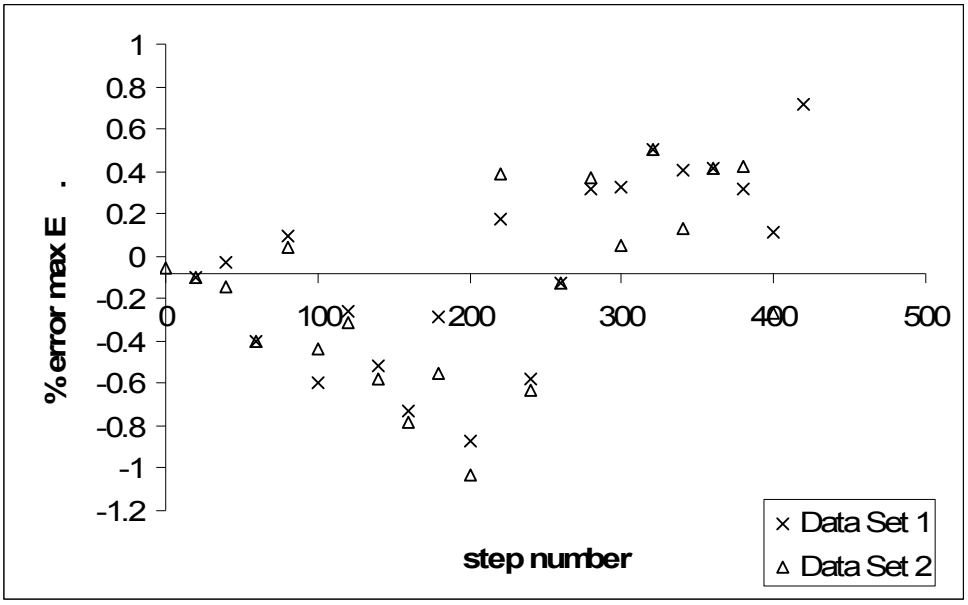

Figure 6-17 Percent error of maximum engagement length E.

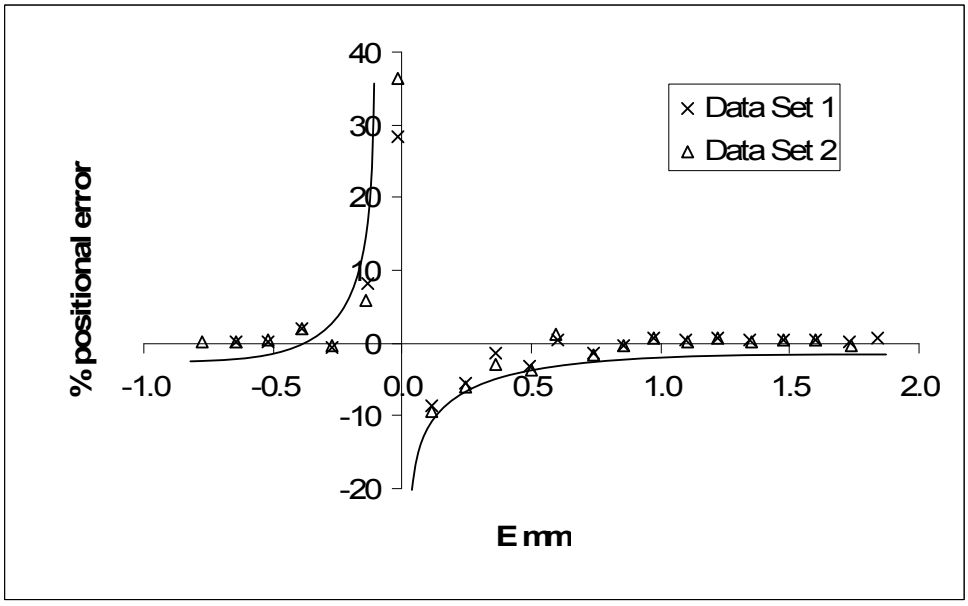

Figure 6-18 The positional error becomes more significant as the engagement length reduces. As such low engagement length brings greater uncertainty.

Needle displacement and step size are useful performance parameters for the general function of the valve and can be correlated with valve position and the mechanical

function of the valve. For example it may be possible to make inferences between the needle entering the valve orifice with the corresponding effect on step size. Far more obvious is the effect of the valve closing on the needle displacement and step size, as can clearly be seen from Figure 6-19 and Figure 6-20. They show that displacement and step size start to decrease above step number 420 and that the return values (Data Set 2) shows significant hysteresis effects. It is to be expected that the displacement would tend towards a fixed value once the valve reaches the fully closed position. This occurs over a number of steps as the 'soft' o-ring seal deforms as the back-force builds up until a full seal is achieved. This is also clearly visible in the change in step size.

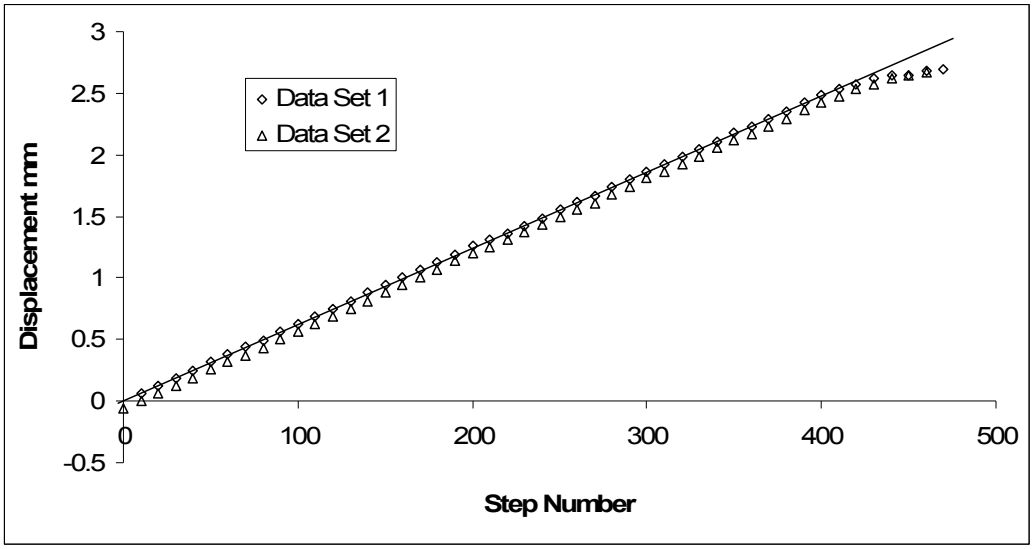

Figure 6-19 Hysteresis effects on needle displacement caused by closing of the valve.

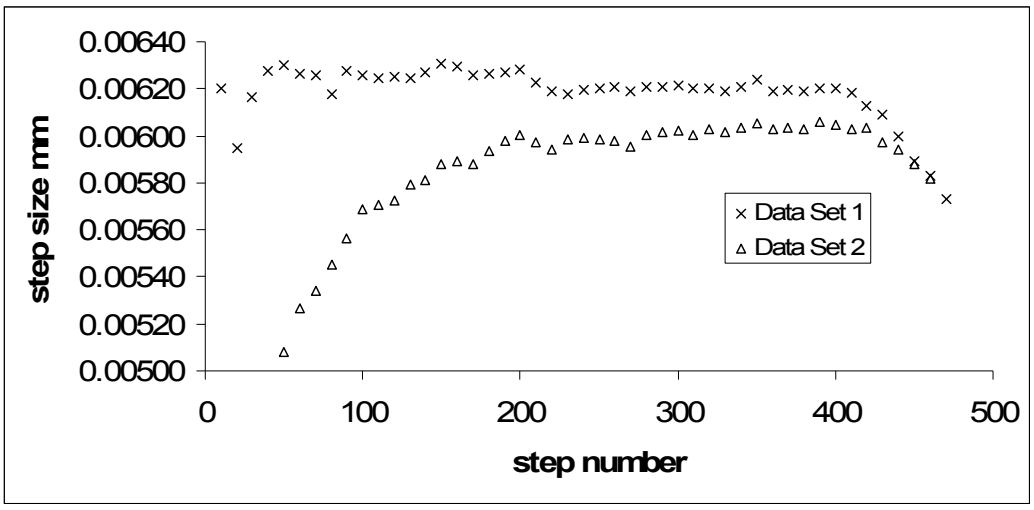

Figure 6-20 The corresponding effect on step size.

Further investigation revealed that the hysteresis effects are caused by the compression of the needle mount assembly, the most likely source of which is the flexible coupling used to mount the needle. It was found that higher step numbers and also longer periods in the closed or partially closed position caused greater hysteresis and that this would recover if the valve was left in the open position indicating the flexible coupling returns to its natural length. Incidentally, it is during the closing of the valve that step loss is most likely to occur due to the change in loading and it also happens that the hysteresis effects experienced after valve closing are very similar to what one might expect to see as a result of step loss. The differentiating characteristic being that step loss will not recover over time as is the case here.

The result of this means that it is not possible to predict the valve needle position for some period of time after it has been in the closed or nearly closed position and so valve travel should be limited to 420 steps unless full valve shut off is required. This retains an engagement length E=1.84mm. It was found that full closure was achieved at step 467 (E=1.979).

In order to gain a level of confidence in the overall operation of the linear actuated valve other important characteristics were also investigated. Throughout the range of experiments on the initial valve and the modified valve, attention was paid to how consistent valve position is, particularly over repeated cycles. An attempt was made to quantify the repeatability of the positioning and to highlight any backlash in the system.

Datum Repeatability: It is important to determine the location of the needle relative to the orifice, or at the very least to be able to accurately and repeatably place the needle in a known location. The end stop switch on the linear actuator provides a known location for the actuator movement but it is not known if this translates to a repeatable needle position. The needle position relative to the actuator is affected by its previous history, but as it has been found, this normally returns to a natural position. Repeatedly setting the positioning control program to seek the datum showed that even at high speeds the seek program would define the same spot repeatedly without overshooting the switch point.

Backlash and return to zero: A trial was run to determine the level of backlash and the ability to return to the datum point. To do this, the valve was cycled through a close-open loop four times, while measuring the following step positions on each cycle; 0, 140, 240 & 340 (the relatively low top step number avoids hysteresis effects caused by compressing the needle mount column on closing). This should highlight any difference in positional accuracy between opening and closing for step positions 140 & 240 and a comparison with repeatably reaching the fixed points 0 & 340. Table 6-3 shows the maximum and minimum recorded values of each step position with a distinction between values recoded during valve closing (up) and valve opening

(down). The range for each value was found to be less than 0.005mm showing excellent repeatability and there was very little difference between the range of the opening and closing values (total Range) indicating negligible backlash.

Step Number	Min Value	Max value	Range	Total Range
0	0.003	0.008	0.005	N/A
140 up	0.870	0.875	0.005	0.006
140 down	0.871	0.876	0.005	
240 up	1.479	1.481	0.002	0.005
240 down	1.476	1.480	0.004	
340	2.089	2.092	0.003	N/A

Table 6-3 Backlash and return to zero results. All results in mm.

Through a combination of measurement interpretation and visual inspection, the valve state can be summarised at step values as follows:

Step Number	Valve State
0-80/100	Prime position. Only nipple end (section D) is located in orifice
80/100-120/140	Transition. Control surface of needle (Section B) is now located in needle orifice but normal orifice aperture is not established as the taper has not fully engaged the orifice bore.
400+	o-ring begins to contact valve seat
420	Step size begins to decrease, indicating resistance due to o-ring contact with valve seat. Hysteresis effects begin
467	Valve sealed shut.

Table 6-4 Valve state summary

These interpretations were also confirmed by the flow results.

6.7.3 Valve Programming

There are two levels of program required for use with the linear actuated valve. First there is the basic low level program required to place the needle reliably in the desired

location and respond to commands in an appropriate manner in terms of speed and accuracy taking into account all of the physical limitations of the hardware as investigated in the previous sections. The second allows for the automatic control of the valve by intelligently selecting the appropriate valve position in response to user requirements and other external inputs. The following functions must be incorporated into the system control program and are listed in order of implementation.

First level functions:

1. Motor driver. Generates digital signal to turn motor at various speeds in both directions.
2. Find datum. Locates real world reference point from which to start counting step positions.
3. Keep count of current step to keep track of linear actuator position.
4. Stop Limits. Prevent over-closing ie crashing the needle into the valve seat or the non-linear zone of movement. Conversely the motor must be stopped once actuator has reached position zero (or below). This can only be achieved if the correct step number and datum is known.
5. Manual close. As the valve travel is limited to the linear travel region, a manual override is required to close the valve fully.

Extended functions for a closed-loop automated control system include:

6. Count drip interval
7. Adjust step position to achieve desired flow rate.

Or for an open-loop system

8. Adjust step according to predefined parameters (eg temperature, viscosity, pressure head) to achieve desired flow rate.

In terms of program complexity, integrating the essential peripheral functions can be as challenging as the core control algorithm.

6.7.4 Closed Loop Control

A simple proportional control was implemented by adjusting the output (number of steps) in proportion to the error value K_c between the desired time internal T_pd and measured time interval T_pa. While there are several types of control philosophy that can be applied to valves, such as PID (Proportional Integral Derivative) and Neural Networks, a simple control algorithm was found to produce good results. It is important to tailor the control system to fit the physical components that make up that system. In this case the two primary components to be considered that make up the closed loop system are the linear actuated valve and the drip interval based flow measurement. Any control system has to be sympathetic to the characteristics of these devices. Although the feedback mechanism is the drip time interval, T_p, conversion to flow rate inputs and outputs can easily be added using the system described in Section 0. The closed loop control was implemented as follows and uses the variables:

Actual flow: T_pa
Desired flow: T_pd
Actual step number: S_na
Desired step number: S_nd
Step correction: S_nk
Gain: G

It must conform to the following equations and conditions.
$S_nd = S_na + S_nk$
$S_nk = G(T_pd - T_pa)$
Where
$G = 11.01 T_p^{-0.7768}$
Unless
$S_nk \geq 50$ then $S_nk = 50$
Or

$S_nk \leq$-50 then S_nk=-50

A suitable level of G to produce a T_pa close to that of T_pd without unstable fluctuations was found by trial and error. The resulting data points were then modelled using regression to give a continuous gain range that was easily implemented in the control program.

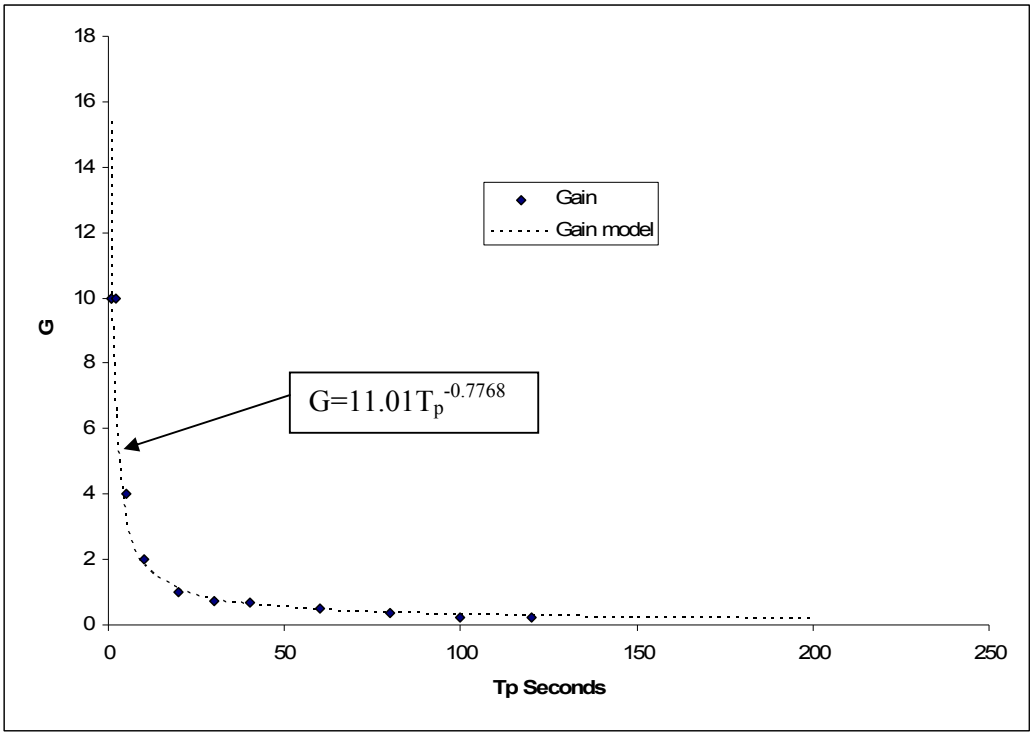

Figure 6-21 Closed loop control program gain model.

The step correction number S_nk must be limited to damp the system in the case where large step numbers are required. If there is a sudden change in T_p demand, the resulting large step change can cause unstable oscillations. The automatic gain controller means that there is normally sufficient damping when moving from low T_pa to high T_pd (gain is in the region of 0.25 at T_pd=100), however any overshoot could inadvertently cause the valve to close and therefore stop responding. Conversely when moving from high T_pa to low T_pd, there is a high gain of 15, this would cause a step

correction number well in excess of permissible travel. As such, the step correction number is limited to approximately 25% of full travel. There are also additional interference affects of the valve itself. Moving the valve needle causes a pumping action within the valve from the diaphragm, this causes a sudden peak or dip in flow rate before normal flow is established. The control program obviously reacts to the sudden change in flow, but as the peak or trough is normally in the opposite direction to the one requested, this normally just increases the step correction slightly, and speeds up reaction times.

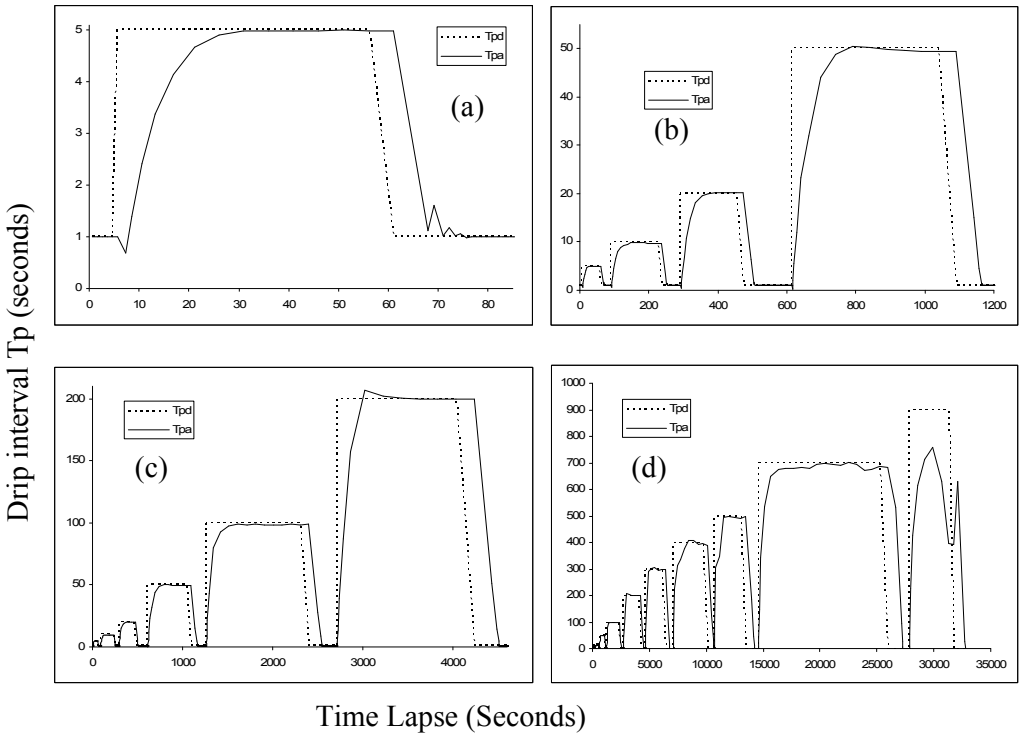

Figure 6-22 Drip interval response compared with demand. (a), (b) and (c). show enlarged portions of the full plot (d)

There are two performance criteria that the automated valve control must fulfil. The first is the ability to reach any given flow rate requirement under a specified set of operating conditions. Whist high speed dynamic response is not a critical requirement at this stage, it is still important for the system to be able to reach a specified flow rate

within a reasonable amount of time and without unstable fluctuations. The second is the ability to maintain a given flow rate under the influence of outside disturbances such as temperature fluctuations and pressure changes.

A test was devised to investigate the ability of the control system to reach a specified target. It consists of reaching an ever increasing drip interval whilst returning to a low set point between each increment; in this case the low set point is T_p=1sec (Figure 6-22). The challenge is to be able to cope with large changes in demand at the same time as reduced feedback intervals. Very long feedback intervals can be a cause of instability if the control algorithm is not robust. Figure 6-22 (a) shows the T_pa response to a demand of T_pd=5; it is fairly typical of a T_pd demand.

Points to note are: the system is critically damped and so overshoot is minimal or nonexistent. The downward response is much faster than upwards where damping is more evident. The small dip in flow rate just after an upwards demand is clearly evident and is due to the pump effect of the diaphragm. There is a similar effect on the downwards stroke, but it is not clear if this is also due to pumping effects. The response lag after the demand is equal to the drip interval, i.e. 1second at T_p=1 and 5seconds at T_p=5. Through Figure 6-22 (b) and (c) it can be seen that the trend is consistent through ever increasing demand levels. The difference being that at higher T_pd levels, the trajectory is not as smooth, although ultimately a good match with T_pa is achieved. This is due to the increased feedback intervals and the accumulation of disturbing factors over the extended period. From Figure 6-22 (d) it can be seen that by T_p=700 the fluctuations about the set-point are more pronounced and that by T_p=900 the control becomes ineffective. Table 6-4 shows that above step number 400, the O-ring begins to contact the valve seat and that at step number 470, the valve

should be closed. However, odd effects have been observed after this point, where the flow rate can actually increase despite further closing of the valve. This is possibly due to deformation of the o-ring under load while not being fully concentric with the valve seat. In this case step numbers greater than 400 occurred at T_pd=700 resulting in a less stable flow and increase flow effects occurred at T_pd=900. Despite this, satisfactory control was achieved at Tp=700, equal to a flow rate of 0.09ml/hr or 1 litre per 15 months. Table 6-5 shows the percentage error for each T_pd. The greatest error was 2.11% while the average error was only 1.11%, well within the levels required for a lubrication application and of potential use in high accuracy applications.

T_pd	1	5	10	20	50	100	200	300	400	500	700	Avg.
% Error T_pa	0.27	0.26	2.11	0.61	0.71	1.65	0.18	0.95	1.69	1.08	1.61	1.11

Table 6-5 Response error as a percentage of demand for each drip interval demand T_pd.

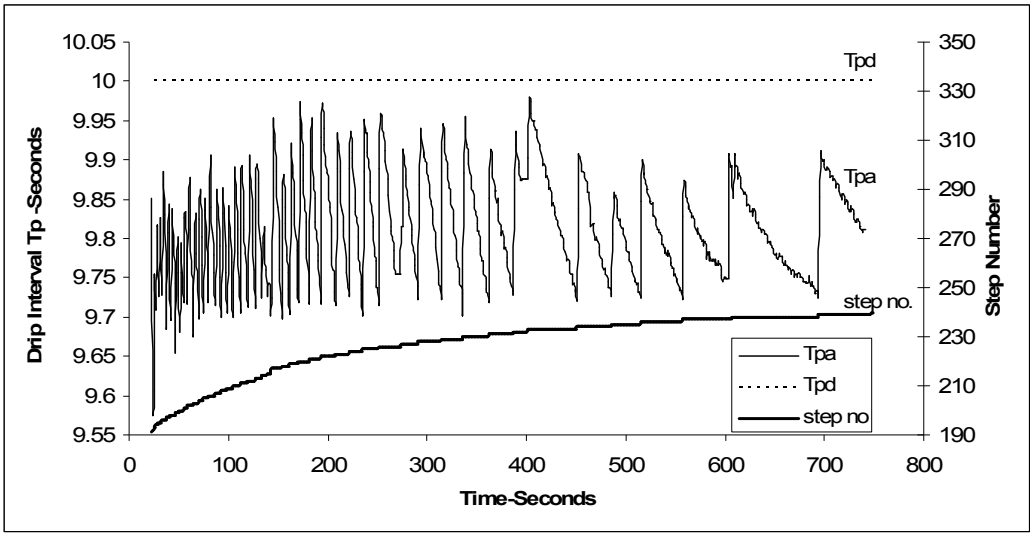

Figure 6-23 Automatic adjustment of needle position in response to a continuous increase in temperature. The drip interval is kept within 3% of the set point.

Once a desired flow rate is achieved, it is important to be able to maintain that level while the system is under the influence of outside factors, the main one being

temperature. Figure 6-23 shows the valve self-adjusting to compensate for a temperature rise from 5°C to 20°C. The saw tooth pattern of T_pa is caused by the reduction in drip interval caused by the rising temperature and the corresponding step up as the valve self compensates. The step number can be seen rising, closing the valve to compensate for the reduction in viscosity of the fluid and the expansion of the valve body. The flow is maintained within 3% of desired flow rate.

6.7.5 Graphic Model Based Open Loop Control

Closed loop control relies on the feedback provided by the flow sensor. However it is not always possible or practical to incorporate an inline flow sensor in a system. In these cases it may be possible to implement an open loop system.

There are two general reasons for developing a model of valve flow. The first is to generate insights into the design of valve geometry in order to generate different flow characteristics; the second is to provide the basis of an open loop control system. As an analytical model is of most use for the design phase, they are often not suitable for control purposes as they tend to describe general characteristics rather than the specific characteristics of the actual valve to be controlled. There are different ways in which the test data can be implemented in a control program. One method would be to use a form of look up table where the required needle position for a desired flow rate is measured under each condition it is likely to operate in, such as variations in pressure head and temperature. However even with a small number of factors, this would create a huge number of permutations requiring not only a large memory in the control device, but a very significant amount of testing. It is also particularly inflexible requiring a large amount of testing for any change in valve design. A Neural Network as described by Thananchai in *Flow-sensorless control valve: Neural*

computing approach [139] is a method that reduces the size of the data base required as the Neural network is able to actively interpolate between a wide range of input functions with complex interrelationships. While this has been proven to work, training the neural network to react reliably can be problematic due to issues with the number of data points used for training and over fitting of data.

A more direct form of flow mapping exists, that increases the flexibility somewhat by reducing the number of data readings to be taken. This is made possible by understanding the inherent flow characteristics of the valve which allows simple relationships to be made between the factors that affect flow rate. Understanding and simplifying the interrelationship between the flow factors allows us to define equations that represent the flow characteristics from just a few data points. The method used here uses a relatively small number of experimental readings to capture the valve flow characteristic which is then represented in the form of a graph. This graphical representation of the valve flow characteristic can in turn be represented by a mathematical equation using regression. In this way it is possible to summarise the valve flow in a single equation that can easily be incorporated into a relatively simple microprocessor for onboard control.

The experimentally derived valve coefficient, C_v [38-40], used to describe the flow characteristic of industrial control-valves is a means of defining flow rate in terms of differential pressure, but there is no indication how this is to be used for control purposes. Thananchai [43] also uses a similar experimental procedure to characterise the flow properties of a ball valve in terms of orifice area by plotting the flow rate in terms of pressure differential and orifice area. This was used as part of a study to alter

the low characteristics of a valve and not used in the implementation of a control system.

The method described below is similar to Thananchais in that flow rate is plotted in terms of valve position, but in this case the valve position is represented by linear position rather than orifice area. Two methods of defining the relationship between flow rate and valve position were investigated through the course of this research. The first is similar to that used by Thananchai where firstly; *lndh* is plotted against *lnQ* for a range of valve positions. This produces nominally parallel, straight lines for each valve position, from which the intersect with the ordinate can then be plotted against the valve position to define a relationship between flow rate and valve position. The alternative is to make use of the very reliable relationship between pressure head and flow rate and first plot *dh* against *Q* for a range of valve positions (Figure 6-24). This produces a series of straight lines converging on the origin where each line represents the flow at different valve positions. In this way it is the gradient rather than the intercept that is used as the defining parameter. This second method requires fewer data points and has generally been found to be the more accurate method during comparisons with test data. As such it was used as the basis of the valve control algorithm.

In the following valve model description, Q is replaced by the mathematically equivalent value of $1/T_p$. The reasons for this is that the drip time interval is the main working parameter in this experiment and as such working directly with T_p removes any added uncertainty converting to and from Q. It can be shown that $1/T_p$ behaves in an equivalent manner to Q for modelling purposes and can be used as a substitute when convenient. Depending on the flow measurement system, the method used in

these experiments could be repeated equally well using Q. However for the purposes of user interface of the control system developed as a result of this flow model, T_p can be expressed in terms of Q using the model described in Section 0. Differential pressure is expressed as fluid head height dh.

The following results relate to the model generated for the purpose of controlling the linear actuated valve. The model was successfully converted into an open loop control algorithm for controlling the flow of the valve for a user specified flow rates for a given differential pressure under constant temperature conditions. The technique was developed using the manual control-valves and applied to the linear actuated valve.

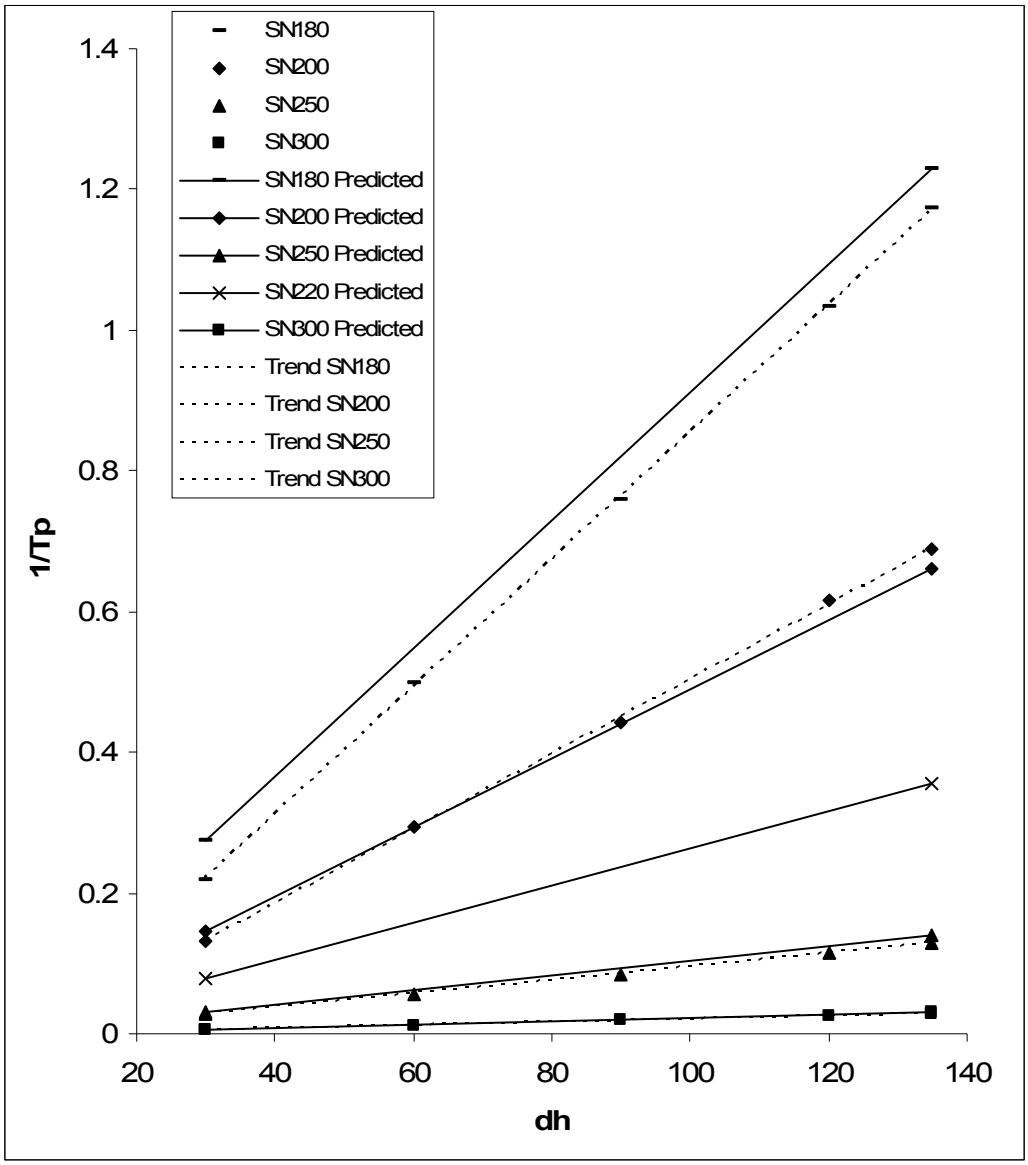

Figure 6-24 This figure clearly shows the linear relationship between the flow variable $1/T_p$ and pressure head dh for a variety of valve needle positions (Step Number, SN). Also shown is a selection of predicted flow rates based on the flow model.

Flow measurements readings were taken for a variety of step number positions (SN) and differential pressure heads. The step number is used in place of the valve number of the manual valve used in previous experiments. Whilst there is no discernable relationship between drip interval *Tp* and pressure head *dh*, it can be seen from Figure 6-24 that there is a very linear relationship between the inverse of the drip interval

1/Tp and pressure head. This is in line with Bernoulli's principle which states that potential energy in the form of pressure is converted to kinetic energy in the form of fluid velocity which is directly proportional to flow rate for a given cross sectional area. Incidentally it was at this stage of the development of the first linear actuated valve that a problem was first noticed. As explained in section 6.7, pressure induced compression of the needle position mechanism caused the needle to move. This was clearly visible as a non-linear response indicating an additional variable was at work. This was rectified by modifying the valve design.

If the gradient of each step number series is calculated and called the gravity fed needle valve coefficient G_v:

$$1/T_p = Gv.dh + j$$

Equation 50

where j=0 as all lines cross at the origin, then each value can be plotted against the step number in natural log form as shown in Figure 6-25. This graph is the defining characteristic of the valve and as long as it can be modelled in some form it is possible to predict the flow rate for any combination of valve position and pressure differential within the bounds of the initial training data. As can be seen in this example, the model is particularly straight forward due to the linear relationship between G_v and the valve position when using a natural log scale. It takes the form:

$$lnG_v = m.SN + k$$

Equation 51

Where *m* is the gradient of the line and *k* is the intercept. Using Equation 50 and Equation 51 it is possible to predict flow rate for any given valve position and pressure head, a selection of which are shown in Figure 6-24. Conversely it is possible to combine Equation 50 and Equation 51 and rearrange for the step number

as shown in Equation 52. In this way the needle position can be defined for any desired flow rate for a given pressure head. This is particularly useful for an open loop control system.

$$SN = \frac{\ln\left[\frac{(1/T_p) - j}{dh}\right] - k}{m}$$

Equation 52

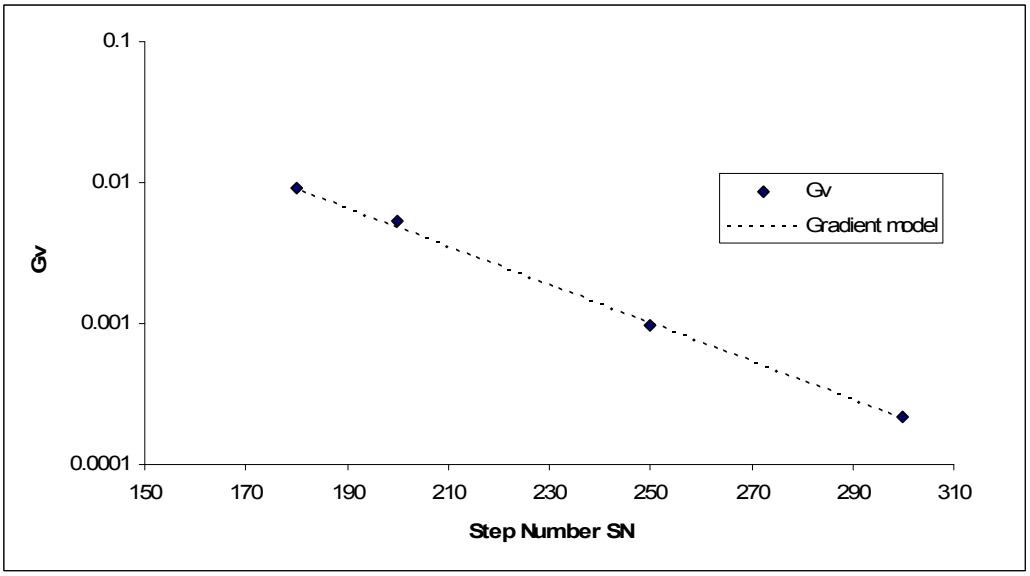

Figure 6-25 Valve coefficient profile, G_v.

A number of discrete values were predicted and checked by re-measuring flow rate and a comparison made. Table 6-6 shows a comparison of predicted and measured flow rates. Average error is approximately 10% with a maximum of 25%. Although 25% may seem significant, when looked at in the context of the overall available flow rate which is over three orders of magnitude greater than the smallest flow rate, this is well within the required accuracy for most lubrication applications.

Pressure head *dh*	Valve Position *SN*	Predicted $1/T_p$	Measured $1/T_p$	Absolute Error	Relative Error %
105	200	0.514385	0.578035	-0.06365	-11.01
105	300	0.023113	0.022222	0.000891	4.01
105	220	0.276569	0.296736	-0.02017	-6.80
105	270	0.058626	0.05531	0.003316	6.00
105	250	0.109038	0.118343	-0.00931	-7.86
105	180	0.956695	1.098901	-0.14221	-12.94
45	200	0.220451	0.201207	0.019244	9.56
45	300	0.009906	0.00885	0.001056	11.93
45	220	0.11853	0.106724	0.011806	11.06
45	270	0.025125	0.02	0.005125	25.63
45	250	0.04673	0.042017	0.004714	11.22
45	180	0.410012	0.380228	0.029784	7.83
				RMS	**10.49%**

Table 6-6 A comparison of predicted and measured flow rates. RMS of realitve error is approximately 10% with a maximum of 25%.

For development purposes the method described here uses a relatively large number of data points, but as the valve coefficient profile G_v (as in Figure 6-25) is a straight line, in theory, it can be plotted from two points which in turn can be generated from four data points, meaning that the whole valve flow range can be defined using only four experimental data points. It is conceivable that certain valve types may require more points if the valve coefficient profile graph does not produce a straight line, but the number of points required can be restricted to the minimum required to define the G_v curve. Other factors that affect flow rate, such as temperature can also be accounted for by modelling their effects on the valve coefficient profile G_v.

6.8 Conclusion

The mechatronic means by which very low flow can be accurately controlled has been investigated. This has involved building and commissioning two prototype oiler

systems in an industrial location. This process has provided insights into the operational requirements of the fluid handling system and the associated control program all of which has a bearing on the hardware and software of future systems.

With critical channel dimensions in the region of 17-250μm and step sizes in the order of 6.25μm, the linear actuated valve (LARMV) can be considered a macro scale technology with micro scale features [4].

A high accuracy intelligent control system has been demonstrated that uses a closed loop control program and makes use of the linear actuated valve and low flow measurement device developed for this research. The control system has good response characteristics and is able to reach set points with large differentials in good time without overshoot despite the low feedback intervals inherent of the drip interval flow measurement device. An automatic gain controller ensures a robust response without instabilities for T_p>700. Accuracy is in the region of 1% of set point for drip intervals of 1-700 seconds (0.1-80ml/hr). This system enables an automatic response to a requested change of set point, but is also able to maintain a set flow rate under changing environmental conditions such as large changes in temperature. The closed loop control system is able to mitigate or entirely remove many of the inherent shortcomings of a very low flow needle valve, particularly its sensitivity to ambient temperature.

An open loop control system has also been developed for the event that a suitable flow sensor is not available. This system uses knowledge of inherent valve flow properties to efficiently plot a valve's flow characteristic using the minimum amount of physical testing. While it is not as accurate as the closed loop system it is nevertheless able to reach set points accurately enough for many lubrication

applications. There is also scope for expanding the systems to cope with changes in ambient temperature.

Isermann characterises a mechatronic system as one in which feedback (closed loop) control systems are prevalent as opposed to feedforward (open loop) and that mechanical non-linearities of components are compensated for through intelligent control rather than by expensive mechanical solutions [146]. The development of the drip interval measurement device has allowed closed loop control of the valve and therefore created a highly flexible and adaptable control system.

As has been stressed previously, when creating a mechatronic system it is necessary to develop the mechanical and control aspects simultaneously due to the high interdependence of the two. In this way there are many diverse and interrelated factors that affect the performance and design of any low flow control valve. Of particular importance is the flow channel geometry, but also the valve actuator, operational environment, control system including any feedback transducers and cost considerations.

7 Low Flow Control-valve Design Synthesis

One of the results of attempting to accurately reproduce analytical results by experimentation, is that it highlights the difficulties of working at such small physical scales and that small variations in physical parameters can have significant effects on performance. In this case it would be wise to avoid trying to tighten the specification beyond the process capability and instead allow the specification to be relaxed while still achieving the desired performance. This philosophy is at the heart of the Taguchi approach to design for quality [140].

"*A product's (or process') performance variation can be reduced by exploiting the nonlinear effects of the product (or process) parameters on the performance characteristic*" [147]. There are several factors that affect the performance of low flow viscous fluids though a needle valve, and understanding them allows the design of the valve to be altered to account for different operational conditions. An analytical model allows areas of high sensitivity to noise factors to be avoided, while nonlinearities can be used to increase stability.

This chapter includes a synthesis of the knowledge gained throughout the research project and comprises of understanding derived from a large variety and number of experiments involving valve flow and operation and also from the interrogation of the analytical model developed.

7.1 Model Use

There are differences between the analytical model predictions and the test data results. It is not possible to determine if this is due to a deficiency in the analytical model or because the test conditions have been misrepresented in the model solution.

Separating the two sources of error is difficult because the channel geometry test conditions are defined indirectly through the use of the valve and valve measurements. A specific study of the relationship between channel geometry and the analytical solution would perhaps clarify the model's use. This would require conducting flow trials on some form of geometrically stable and well defined flow channel built specifically for the purpose of channel flow prediction. This could consist of an annular flow channel where the core is concentrically located extremely accurately, or an alternative would be to create a flattened flow channel similar to that of the analytical solution. However, even if further insights into the relationship between the channel geometry and flow were such that precise flow predictions could be made, these conditions would be difficult and expensive to recreate in a working valve. As such it would still fail to accurately predict actual valve flow performance. From this it can be taken that there are two significant factors in precisely controlling micro flows with needle valves:

1. The accuracy of the prediction model is closely linked to the accuracy of the valve mechanism such that, as the valve mechanism accuracy is increased, so to does the ability to predict and control its performance. If it is assumed that there is a link between mechanism complexity/component precision and cost, that there would also be a corresponding rise in unit cost, creating a direct link between cost and performance.

2. The need to precisely control the needle geometry and alignment can be removed entirely by introducing a flow feedback mechanism to create a closed loop control system. In this way complexity and cost is transferred to the system as a whole, a significant portion of which would be due to the addition

of a flow measurement module. Although adding a module to the system adds cost and complexity, it removes the need to add significant complexity to the valve subsystem and so overall creates a more robust system.

From this it can be concluded that as long as the general form of the needle valve is appropriate, a closed loop system can be used to maintain accurate control, or where this is not possible an open loop system can be used to compensate for some of the deficiencies in an uncontrolled valve. It is worth noting though, that a poorly designed mechanical system will never provide good performance even with a sophisticated controller [78]. The general flow profile would need to be adapted to account for different applications. For example, if a higher flow rate is required with a particularly viscous liquid or vice versa. To this purpose the following section details the effects on valve performance to changes in all of the main influencing factors. This is of particular use when designing new valves, adapting existing valves to new applications and also trouble shooting the performance of valves not behaving as expected. One of the most important aspects when considering the effects of influencing factors is the degree to which they affect valve performance. Understanding the sensitivity of performance to changes in factor effects is important in creating robust designs.

The examples in the following sections are based on the nominal dimensions of a 1° tapered needle valve. This is used as a benchmark from which design variations can be discussed.

7.2 Channel Geometry and Sizing

Orifice and needle diameter tolerance. An inspection of Equation 13 or Equation 38 shows that flow rate is related to the geometric parameters W, h_1 and l, (see Figure 5-3) where W is the circumference of the mid-point of the channel ($\pi[r_o+r_a]$), h_1 is the channel height (r_o-r_a) and l is the length of the channel or the equivalent of engagement length E for a parallel needle. Regarding flow rate Q, there is a direct relationship with W, an inverse relationship with l, but most importantly a cubic relationship with h_1. This means that any change in the h_1 parameter has a significant effect on flow rate.

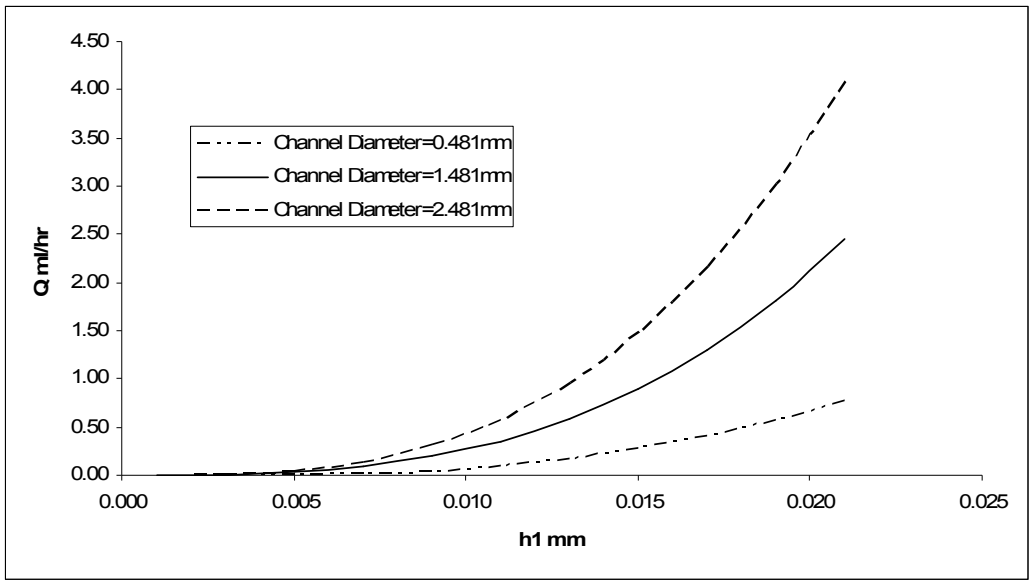

Figure 7-1 The effect on flow rate of changing gap size (h_1) for constant channel diameters (equivalent to constant channel widths, W).

This can be directly attributed to the theory of laminar flow where it is assumed that the fluid velocity at the channel wall is zero and the point of maximum velocity is the mid point of the channel. This makes the distance between channel walls particularly important. The effect of varying the gap size between the needle and orifice (h_1) while maintaining a constant channel diameter can be seen in Figure 7-1. Maintaining the

channel diameter means the channel circumference remains constant and therefore the equivalent channel width (*W*) also remains constant. Various channel circumference values are shown. As an example of the effects of valve tolerance on flow rate, a one micron reduction in needle radius from nominal, increases flow rate by 25%.

Taper-angle. From the analytical model based simulations in Figure 7-2, it can be seen that increasing the taper-angle significantly increases the maximum flow rate, while the minimum flow rate is affected to a much lesser extent. This means that it is possible to significantly increase the range through the use of taper-angle. The knock on effect is that there may be a reduction in controllability as the change in flow per needle position increment is significantly increased. This would make an automatic flow control system susceptible to instability.

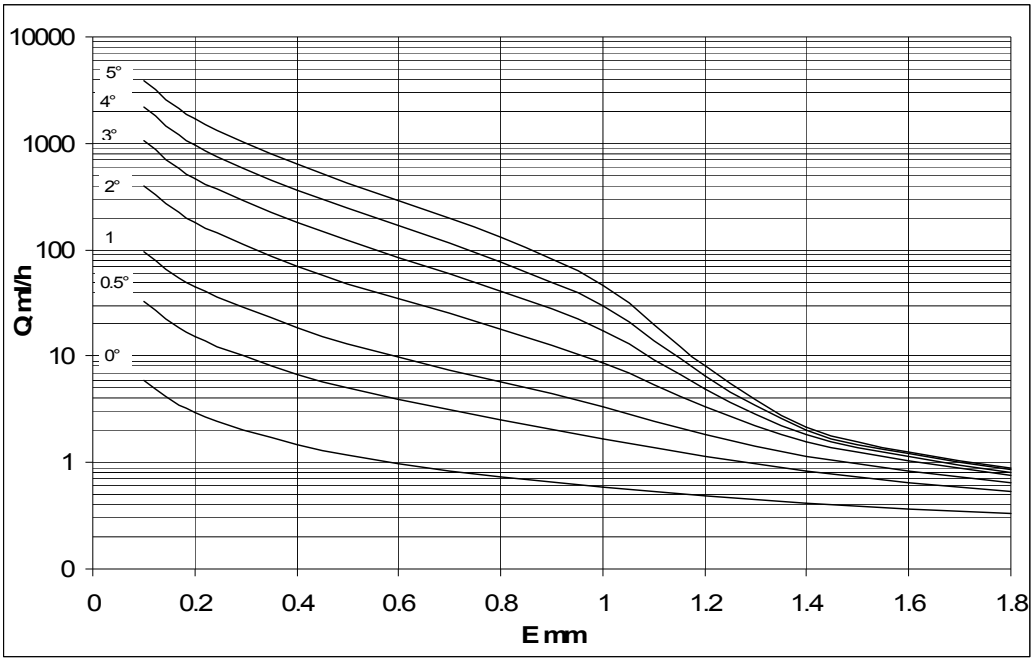

Figure 7-2 Flow range is linked to taper-angle. The transition from composite profile to taper only occurs at E=1.2mm.

The transition from a composite (parallel and tapered) to tapered only, occurs at E=1.2mm and although increasing the taper-angle interrupts the smoothness of the

response curve, this is only visible using a logarithmic plot for *Q*. As such, the transition from the parallel to tapered portion of the needle profile should not have an adverse affect on controllability of the valve by creating sudden changes in flow conditions.

The controllability of the 5° valve can be improved by increasing the orifice diameter and maximum engagement. The flow range generated by the 5° taper is maintained but the flow rate is less susceptible to small changes in needle engagement. Enlarging the orifice counteracts the effects of increased fluid friction caused by increasing the maximum engagement length. The increased engagement and similar range are clearly visible in Figure 7-3.

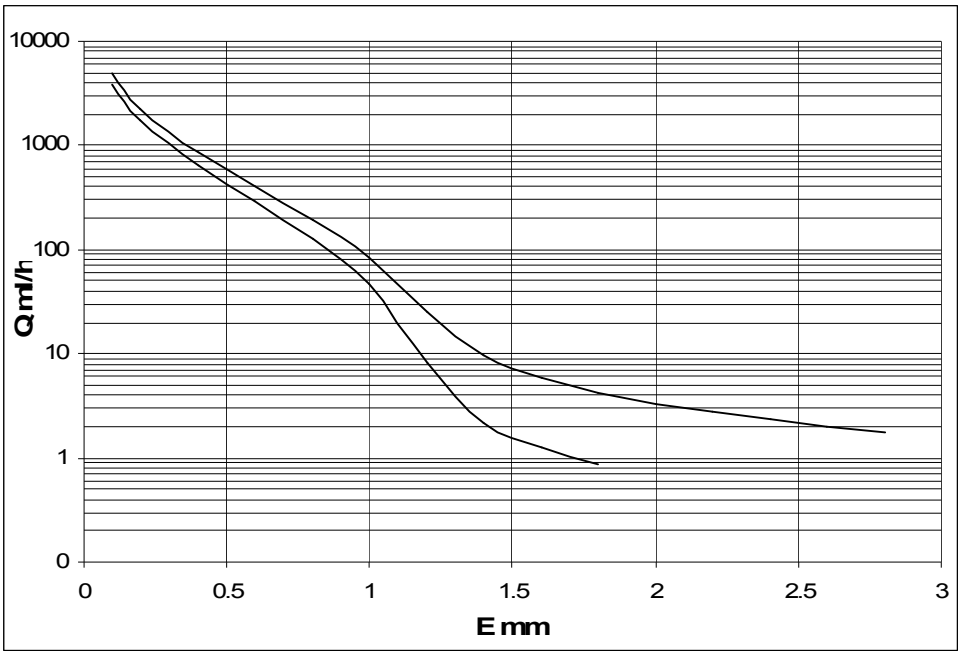

Figure 7-3 the flow characteristics of two valve geometries with similar ranges but different levels of controllability. The upper curve is less sensitive to variations in *E*, whilst maintaining maximum flow rate.

Eccentricity. The effects of an eccentric annulus on the flow rate of a parallel needle are quite clear and are discussed in Sections 2.3.2.2 and 5.1.3.6, where an increased effect would show as increased flow rate and a minimal effect would be similar to a

concentric core. However there is no existing theory for the effects of eccentricity on a tapered annulus. From the literature [92, 94], it is known that the effects of eccentricity are greatest when the core and pipe diameters are of similar size, that is to say a small channel height equivalent to h_1, and that when the core is significantly smaller and completely offset, the flow is almost uninterrupted. From this behaviour, it is possible to surmise what effect an eccentric tapered needle would have on flow rate.

Two flow scenarios should be considered. Firstly when some portion of the parallel section of the needle is engaged in the orifice, and secondly when only the tapered portion is engaged. In the first case, eccentricity effects could be assumed to be significant as the channel height is generally small and eccentricity effects are large in proportion to the flow in the channel. The eccentricity effects would generally decrease as the flow passes the tapered section as the channel height increases. As the taper is located relatively centrally by the non tapered section, the effects may still be significant, especially if low taper-angles are used. Secondly, as the needle is retracted to leave only the tapered portion engaged in the orifice, this produces an ever reducing core located against the orifice wall which has less effect on flow rate. At this point, the increase in the flow area is likely to be more significant than eccentricity effects.

7.3 Viscosity Effects

The geometry effects on valve flow can be significant, as discussed in the previous section, however, viscosity is also known to affect valve flow rate. In a similar fashion to the previous section it can be seen from Equation 13 and Equation 38 that while the viscosity term μ has an inversely proportional affect on flow rate it is still small compared to the geometric affects. Perhaps more significant, is the relationship

between temperature and viscosity, where a change in temperature generates a relatively large change in viscosity (Figure 5-2), especially at lower temperatures. Viscosity values may also be altered intentionally through the selection of the oil ISO grade, either as a means of compensation for temperature induced viscosity effects or for use in different lubrication applications. From Appendix H: Viscosity Comparison Charts, it can be seen that the increase in absolute viscosity is much more marked for higher ISO grades than lower grade oils. The flow rate is inversely proportional to the viscosity (Equation 13 and Equation 38) indicating that changing viscosity will create a directly proportional change in flow rate. Figure 7-4 demonstrates the effects of temperature on viscosity. All the oils show a similar trend, where a 1°C change in temperature at 90°C will cause a change of approximately 3% in viscosity (and therefore flow rate) while a 1°C change in temperature at 15°C will cause a change in viscosity of around 5.5%. As can be seen from Equation 13 and Equation 38 the viscosity effects on flow rate are independent of channel and valve geometry, which means the values given in Figure 7-4 are applicable to all valve geometries and valve types while the flow is laminar.

This means that there may be additional issues relating to controlling the valve at low temperatures when using high viscosity oils. A closed loop control system should be able to compensate for temperature induced changes in viscosity within the flow limits of the valve. This may require specialised needle geometries designed specifically to cope with low viscosity fluids and with a particularly high range to allow for the large changes in viscosity. Conversely ISO grade fluids have a lower viscosity range and therefore do not require such a large valve flow range.

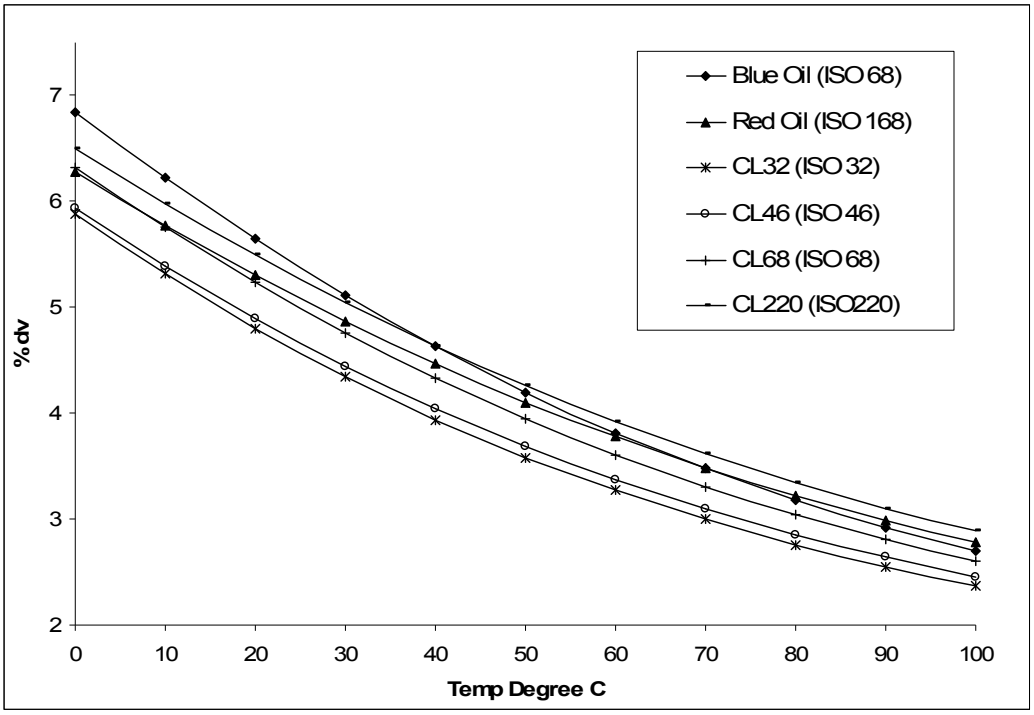

Figure 7-4 The percentage change in viscosity (%*dv*) for 1°C change in temperature. This indicates that the effects of temperature change are greater at lower temperatures.

An oil is considered to conform to the ISO standard grade if the viscosity is within 10% of the nominal value. See Table 7-1. It is worth considering the effects of a ±10% tolerance. The viscosity comparisons in Appendix H: Viscosity Comparison Charts, was calculated using values supplied by the manufacturer on their material information and data sheet. These are clearly nominal viscosities. If the 10% tolerance that can be used when defining an oil viscosity is applied to the two data points supplied, the effects can be significant when deriving viscosities at other temperatures. This is particularly true when using adjacent high and low values as can be seen from Figure 7-5. At 0°C, the error becomes –37%, +66%, although this reduces significantly as the temperature increases. This is clearly a worst case scenario and it is unlikely that a reputable oil manufacturer would be working to the limits of allowable tolerances, but it does highlight the importance of the manufacturer's stated ISO grade on viscosity and therefore valve flow rate.

ISO Viscosity Grade	Mid-point Kinematic Viscosity mm^2/s (cSt) at 40°C	Kinematic Viscosity Limits. mm^2/s (cSt) at 40°C	
		Minimum	Maximum
ISO32	32	28.8	35.2
ISO46	46	41.4	50.6
ISO68	68	61.2	74.8
ISO220	220	198	242

Table 7-1 ISO viscosity grades

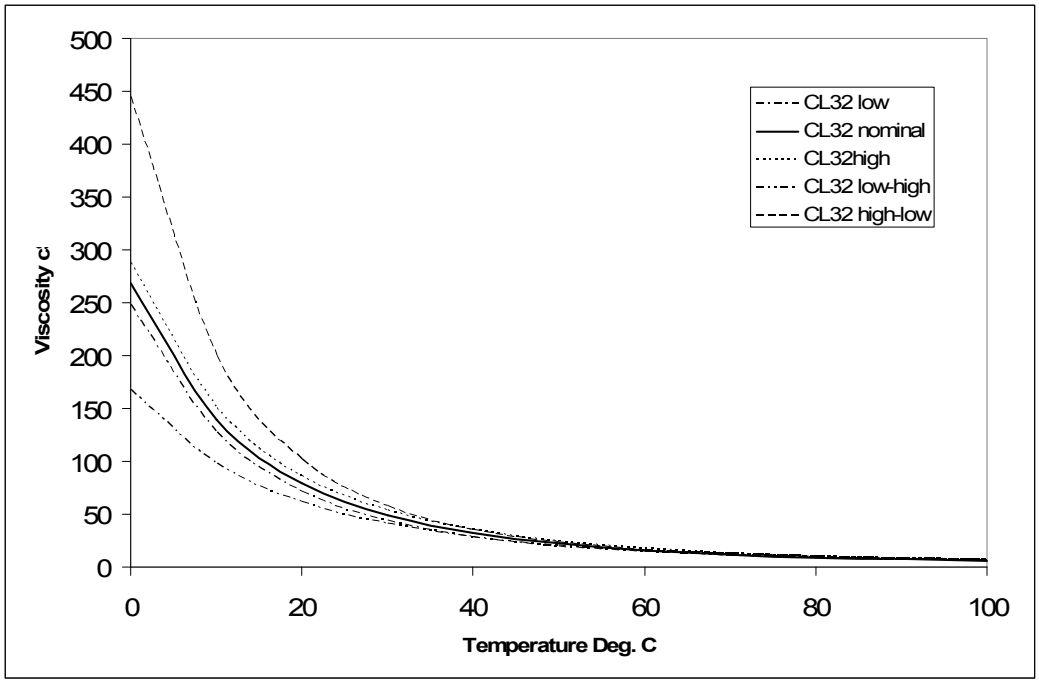

Figure 7-5 Tolerance effects when calculating kinematic viscosity temperature relationships from two known viscosity values. The largest variations occur when the opposite tolerances are applied to each value.

7.4 Thermal Effects

As discussed in 7.2 and 7.3, the valve geometry and the fluid viscosity can potentially have a significant effect on the flow rate of the valve. As changes in ambient temperature can affect both the channel geometry and the viscosity of the fluid, it has a profound effect on the stability of the valve flow.

7.4.1 Valve Expansion

Most engineering materials experience a certain amount of expansion during heating. The valve body in this study is no exception and it means that due to the configuration of the valve, any expansion or contraction of the valve body causes the valve needle to move a corresponding amount, and so alters the engagement length. Of course if the needle mount were to expand by exactly the same amount, there would be no net change in the engagement length. This is highly unlikely due to the different material properties of the needle mount and the insulating effects of the fluid within the valve. This means that there is a dynamic relationship between ambient temperature and the effect on flow rate. Experience has proved that the valve is affected by changes in the ambient temperature and if this could be defined by a simple linear relationship, it could be incorporated into a control algorithm with relative ease.

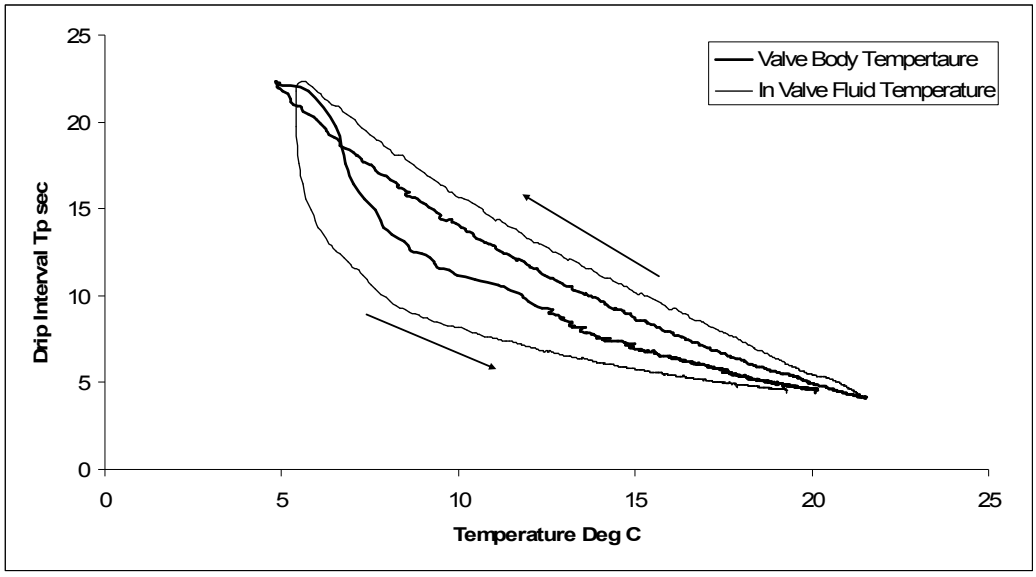

Figure 7-6 Temperature induced hysteresis effects on drip interval (flow rate). The chart shows the temperature plots for the outer valve body temperature and the fluid temperature inside the valve.

Unfortunately the dynamic relationship between ambient temperature and flow rate causes significant hysteresis effects, illustrated by the example in Figure 7-6.

Although the complexity of the system makes it unfeasible to precisely model the interaction between flow rate and valve expansion, certain calculations can be made to quantify the effects of temperature and give an insight in to the workings of flow control.

While the expansion of the valve body can be easily calculated, the actual effect on the engagement length is dependant on the relative temperature of the needle mount. The following calculation explains the effects of temperature on the valve body assuming there are no hysteresis effects associated with the valve body alone:

•The coefficient of linear thermal expansion of valve body material, Diakon is $8x10^{-5}$-$12x10^{-5}$m/°C, i.e. 0.00008mm expansion per mm per °C.

•Assuming ambient temperature changes of 20°C are possible and the valve body is 119mm long results in 0.00008x119x20= 0.1904mm expansion of the valve body for a 20°C increment in temperature.

•One position on the adjuster scale on the RMV is 0.17mm and so makes a 20°C change in temperature equivalent to turning the adjuster dial one position, equivalent to about $1/10^{th}$ of total travel.

•Varying needle position has different effects on flow rate depending on the engagement length.

Having measured the flow rate of a valve over its range of needle movement, it is possible to see flow rate as a function of needle position. If the effects of temperature on needle position are also known (as has been calculated above) it is possible to cross reference the effect of temperature on flow rate.

Assuming the above rates of expansion it is possible to calculate the possible effect of temperature change based on a set of measured flow results and extrapolating flow rates between data points. Figure 7-7 shows the calculated change in flow rate for a temperature change of 1°C when the above rates of expansion are applied to existing flow data (CL32 oil, 0.6m pressure head and 18.5°C ambient temperature).

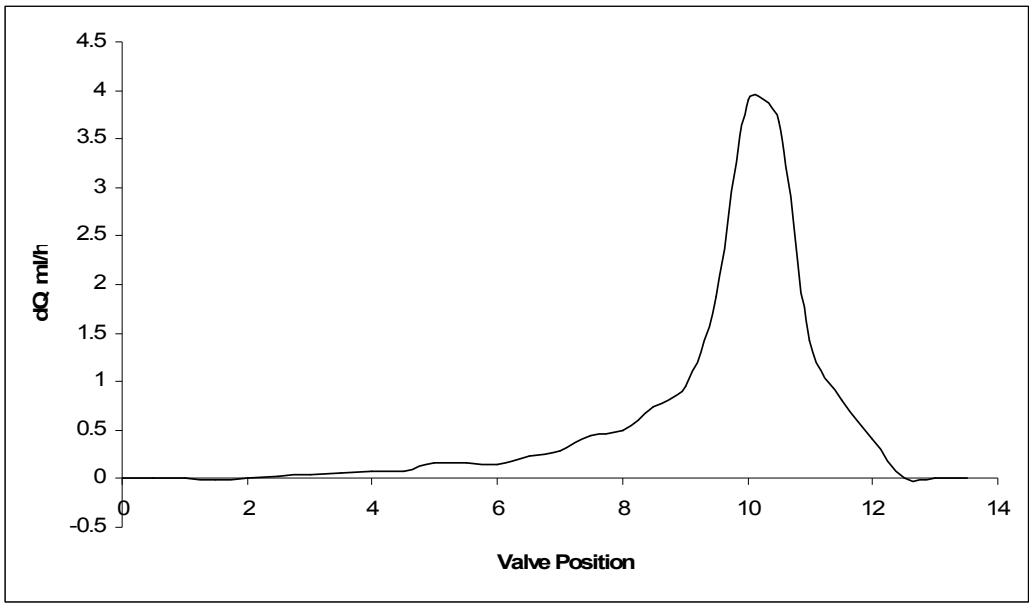

Figure 7-7 Calculated change in flow rate *Q* for 1°C change in RMV temperature.

It can be seen from Figure 7-7 that the effect of temperature change varies depending on the position of the needle in the valve orifice. However if the change in flow rate is expressed as a percentage of the original flow rate as in Figure 7-8, it can be seen that flow rate change is generally in the region of 2-5% per °C. This calculation is valid for small fluctuations in temperature over a short period that can be expected while a valve is in use. The small temperature gradient over a short period means that any rise in needle mount temperature will be small and can be neglected. Higher temperature differentials over a long period will see a rise in the needle mount temperature and therefore the expansion effects of the needle mount would need to be accounted for also.

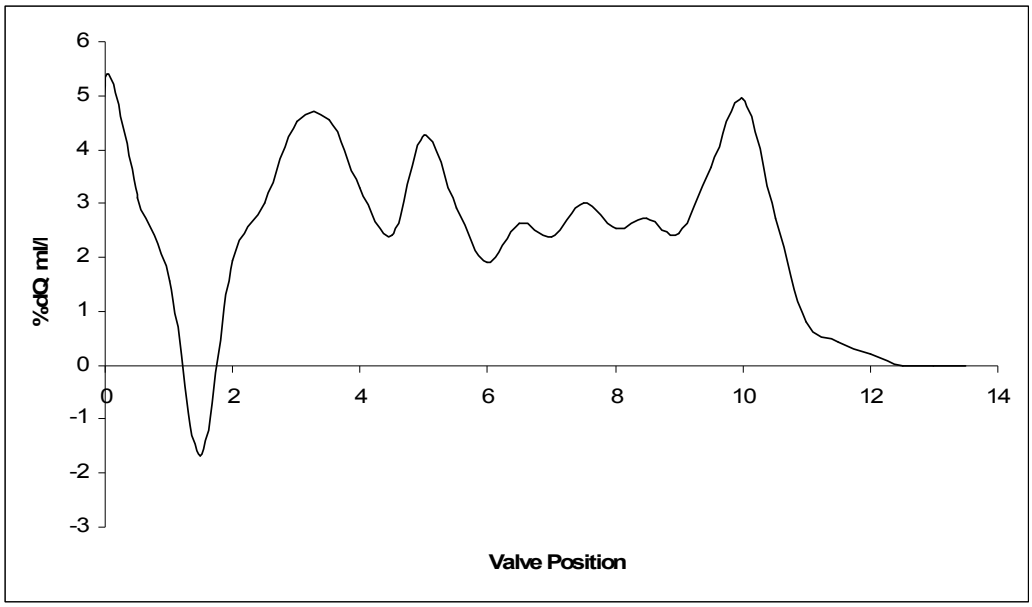

Figure 7-8 Percentage change to flow rate for 1°C change in temperature

7.4.2 Combined Effects

It can be seen from Equation 13 for flow past a parallel needle and Equation 38 for flow past a tapered needle, that flow rate is directly proportional to fluid viscosity. However, the effect of temperature on viscosity and therefore flow rate is also significant. The effect of temperature on viscosity has already been explained in Section 5.1.1, and this can be related to flow rate using Equation 13 or Equation 38. However, observation has shown that viscosity is not the only temperature related factor affecting flow rate. It has been shown in Section 4.3 that material expansion also influences flow rate. By modelling the temperature effects on the valve geometry, it is possible to include it in the flow equation. Figure 7-9 shows the effects of temperature on flow rate for a parallel needle and Figure 7-10 for a 1° tapered needle. The broken line shows only the effects of temperature driven viscosity effects on valve flow, while the solid line incorporates viscosity and valve expansion. The horizontal lines represent the flow range of a typical motorcycle chain lubrication

application. The valve expansion and viscosity models are calculated from a 20°C starting temperature. The expansion model assumes that the needle mount remains at a temperature of 20°C. In reality, the valve core temperatures will follow the body temperature (ie by the time the valve body temperature drops from 20°C to -10°C, the needle mount will normally have reached an intermediate temperature). This means that the graph shows the best and worst case for change in flow rate due to temperature, therefore the actual flow trend will lie between the dashed and solid line for each valve position. It is clear that thermal expansion of the valve can significantly aggravate the effects of temperature induced viscosity change. The steep gradient of the curve at low engagement lengths indicates a high sensitivity to temperature change compared to higher engagement lengths. At E=0.2mm the acceptable flow range for the parallel needle can be crossed by a 10°C change in temperature while for the tapered needle this is significantly less. As a design parameter, it would be best to tune a needle valve flow range to higher engagement lengths. The higher flow rates and greater sensitivity of the tapered needle to changes in E, mean it is significantly more prone to temperature induced flow changes than a parallel needle.

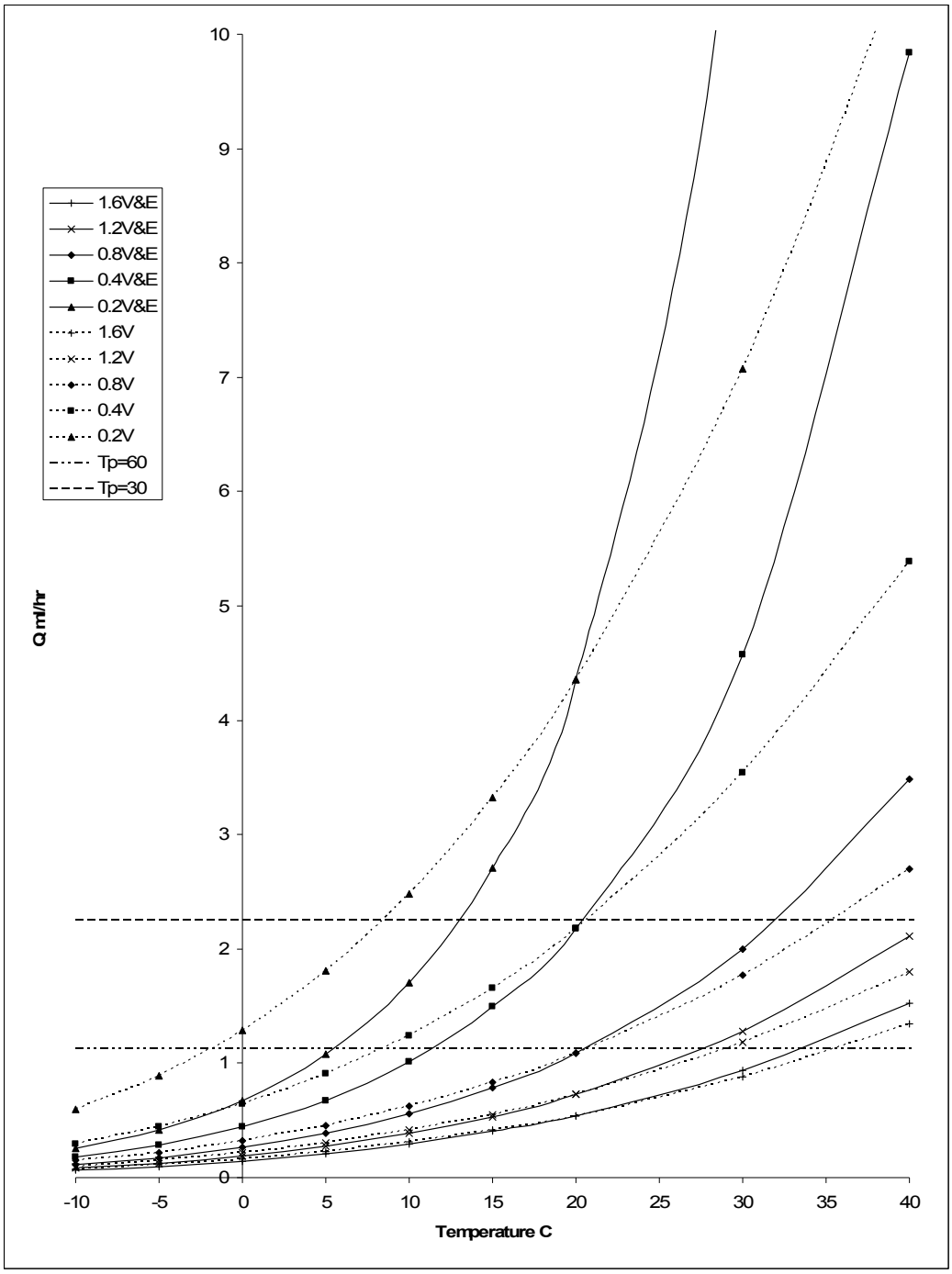

Figure 7-9 Parallel needle: Valve flow rate in response to temperature from a 20°C starting temperature. The dotted line (V) models effects of viscosity only, and the solid line (V&E) incorporates valve expansion effects. Horizontal lines indicate normal flow range for a motorcycle chain lubrication application.

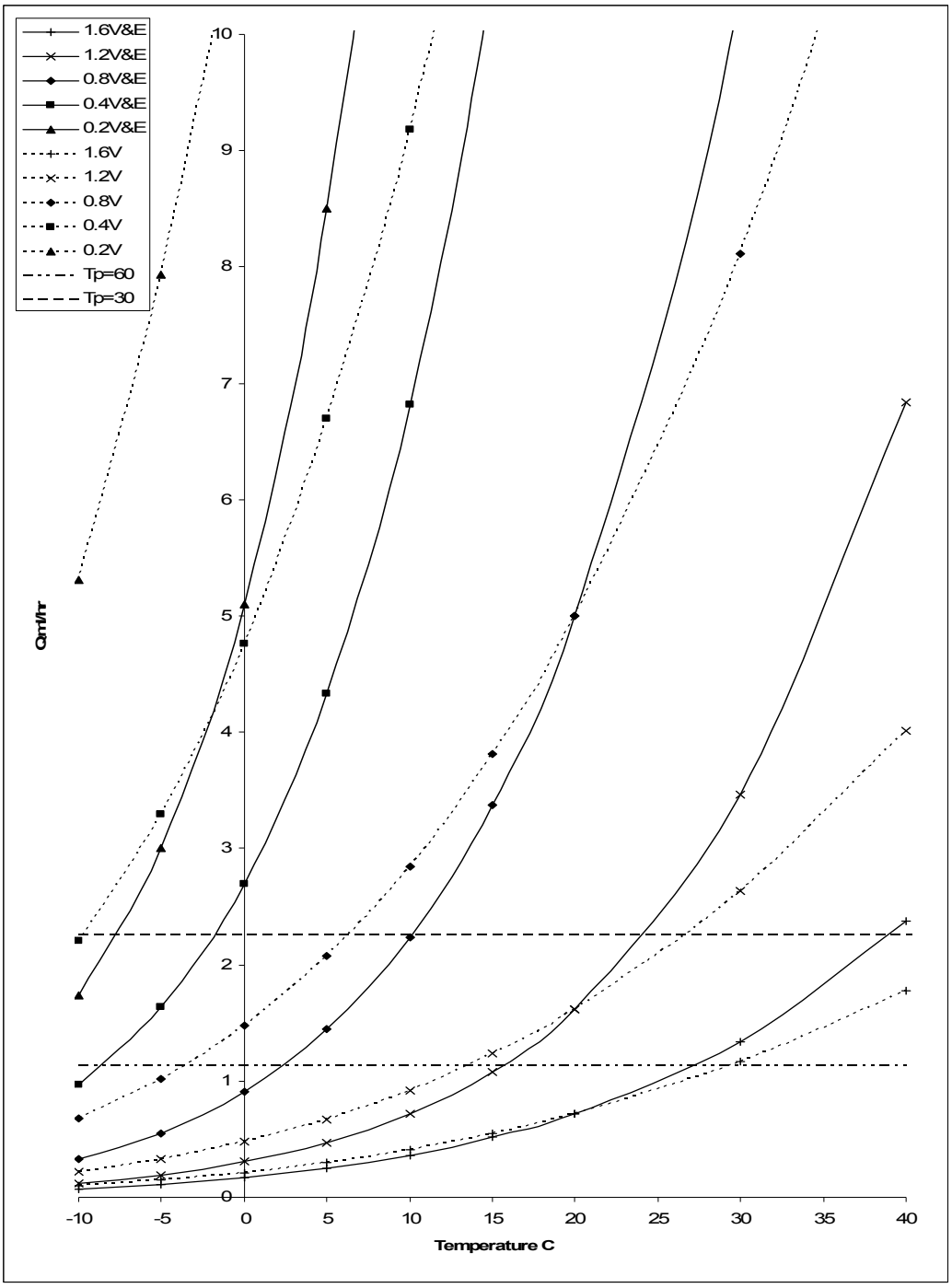

Figure 7-10 1° Tapered needle: Valve flow rate in response to temperature from a 20°C starting temperature. The dotted line (V) models effects of viscosity only, and the solid line (V&E) incorporates valve expansion effects. Horizontal lines indicate normal flow range for a motorcycle chain lubrication application.

Ideally it would be possible to chart flow rate against temperature for a given valve, needle position, and oil type. This would allow temperature effects to be incorporated into a control algorithm with relative ease. However as the valve expansion is affected by considerable hysteresis effects caused by the temperature differential between the inner part of the valve and the valve body, this is not possible. The dynamic effects of the temperature on flow rate mean that it is preferable to have some form of dynamic control such as the closed loop system described in Section 6.7.4, although it should be possible to compensate for steady state temperature effects using the modelling method described in Section 6.7.5. Even though this control method would not fully compensate for temperature effects, it should increase accuracy to somewhere between that of an uncompensated system and a dynamic control system.

7.5 Pressure Differential

Flow rate is directly proportional to the pressure differential across the valve (Equation 13 and Equation 38) which in turn is directly proportional to the fluid column height *dh* (Equation 23) which can be adjusted by altering the height of the fluid reservoir. As such the sensitivity of flow rate to reservoir height carries the same weight as changing the viscosity grade of the oil. The reservoir dimensions are important for maintaining a constant pressure head. Reservoirs with a large fluid surface area will lose a smaller amount of pressure head per volume flow than one with a small fluid surface area. It is for this reason that level drop indicators are not a suitable means of flow measurement for gravity fed needle valves as the inherent fluid level drop causes a change in flow rate. Conversely the reservoir position can be used as a means of tuning the valve flow and so can be used to compensate for different fluid viscosities if the installation allows.

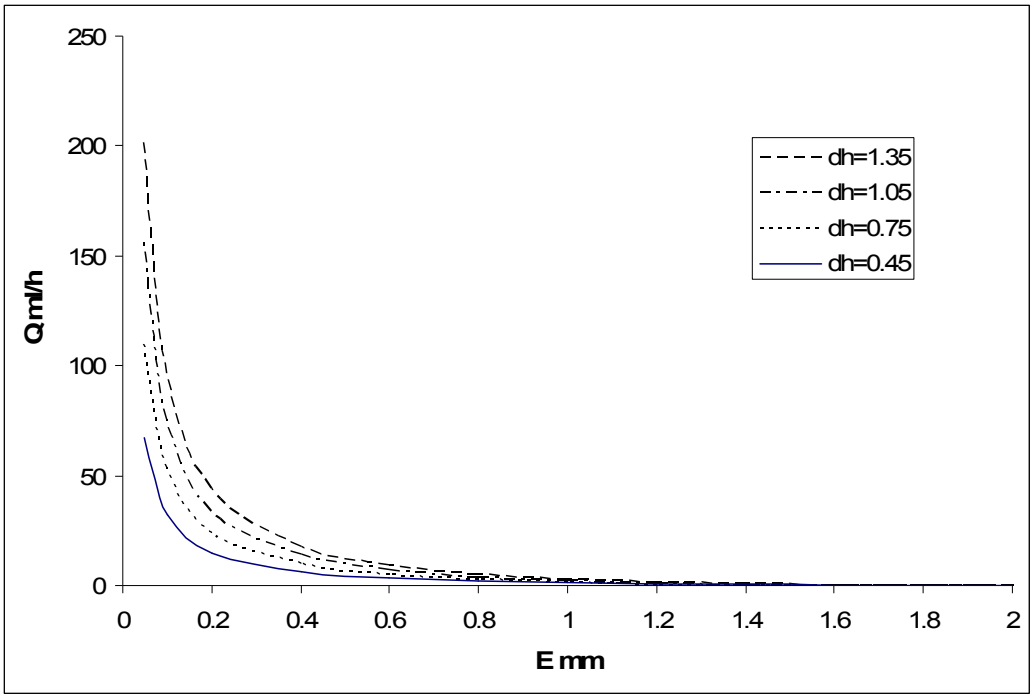

Figure 7-11 The effect of fluid column height (dh) on the flow characteristics of a valve.

Figure 7-11 shows the relationship between flow rate and needle engagement for various fluid column heights. It can been seen that the change in flow rate in terms of volume is much greater at low E values compared to high E values, however, due to the linear response of flow rate to changes in pressure, there is a constant 200% change between the dh=1.35 and dh=0.45 values for flow rate.

The universally consistent relationship between flow rate and pressure head is a useful benchmark when developing flow models and used as the basis of the model that was developed into an open loop control algorithm for valve control.

Control valves function by restricting the flow of fluid in controlled manner and in so doing creates a pressure differential between the entrance and the exit of the active channel. Different parts of the flow channel profile will cause different pressure gradients. Equation 37 can be used to give an indication as to which parts of the flow channel profile contribute most to the pressure differential.

Figure 7-12 shows the pressure drop along the length of a needle channel for a 1° taper angle at a flow rate of 2.2ml/hr, the equivalent to one drop per minute. It shows that low *E* values of a tapered needle has very little effect on pressure differential (and therefore flow rate) but that there is an exponential increase as the needle engages to the point where the tapered portion is fully engaged. At this point the parallel section starts to take effect and there is a linear increase in pressure differential as it engages.

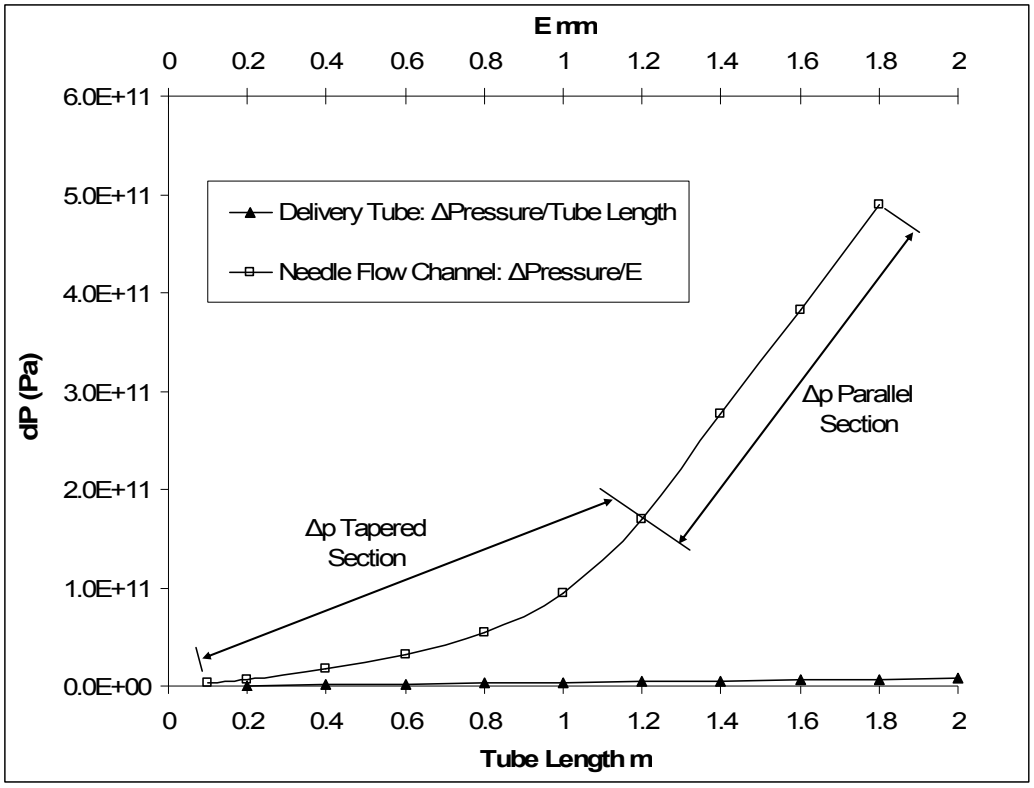

Figure 7-12 The pressure drop along the length of the needle channel is shown for a 1° taper needle (top horizontal scale: E mm). The effects of the tapered and the parallel sections are also shown for comparison purposes. Also shown for comparison is the pressure drop due to conduit length (bottom horizontal scale: Tube Length m).

From the same figure it can also be seen that the pressure drop due to the fluid flowing along a length of conduit is very small in comparison to the pressure reduction effects of the needle valve. This is important as is justifies neglecting tube friction from the flow calculations. This may become significant for installations with conduit tubing of several meters. This assumption is still valid for high viscosity

fluids because, the valve channel will have a correspondingly higher effect for high viscosity fluids.

7.6 Factor Analysis

An important part of determining the critical factors affecting valve flow control performance is to establish the relative importance of each of the contributing factors. This is essential for developing a robust design and follows the principles of Taguchi by not increasing accuracy by reducing tolerances but by desensitising the design to outside factors [140].

A method described by Lochner and Mata [140] based on the Taguchi principles was used to determine the strength of the influencing factors and combination effects. A 2^5 (five factors at two levels) two factorial orthogonal array type experiment was conducted using analytical model. The factors and designations are listed in Table 7-2 where a high and low value representative of the range of each of the factors was chosen. The high and low values were chosen as being towards the top and bottom range of those used within this study without being at either extreme and corresponded to approximately the 20% and 80% of full range. This was to avoid any possible effects caused by being close to the limits of normal operating range. While factors such as temperature may undoubtedly reach values far in excess of those used here this would bring it outside of the range of the practical experiments conducted in the lab. It is also true to say that the choice of upper and lower values is subjective and has the potential to affect the results. For example, choosing an extreme range of temperatures would undoubtedly show as a strong factor effect.

The results are displayed following the format described by Lochner and Mata and as used by Kackar and Sheomaker [148] and are shown in Figure 7-13. The Response Value represents the average flow rate in ml/hr attributable to the factor in question. As such the value itself is somewhat arbitrary and it is the relative value of each factor effect that is important; the larger values having the greatest effect at increasing flow rate.

It can be seen from Figure 7-13 that the factor effect with the greatest response value is the needle position (C). This is to be expected, and desirable, as this is the factor that is used as the means of actively controlling flow rate. Likewise the taper-angle (D) also has a particularly strong effect and taken in conjunction with the valve position (C) effect shows that the flow rate is particularly sensitive to channel geometry. This is valuable as this is what is used to control the flow characteristics of the valve. The oil type (A) also has a significant effect on flow rate, although slightly less than the previous two factors. The implications of this are both positive and negative, depending to the application. Valve ISO grade is currently used to compensate for viscosity changes due to extreme climate variations. As such, higher grade oil can be used in hot climates and low grade oils work better at colder regions especially in winter. In this way oil grade is a useful way of tuning the flow characteristic. However, this is an undesirable trait when the viscosity grade is dictated by the lubrication task and not simply for tuning flow characteristics. For example, heavy duty lubrication applications may dictate a high ISO grade oil and if this happens to be in a cold climate there may be significant implications on the flow characteristics of the valve.

The situation with the differential pressure head (D) effect is similar to that of oil type (A), although the effect is smaller. Pressure head can be used to tune the flow rate characteristics, however if the position of the reservoir relative to the flow outlet is limited by the installation then this option no longer exists.

Perhaps somewhat surprisingly, the temperature effects (B) on the oil seem to be the smallest perhaps because valve expansion was not included in the analysis. It could be argued that a 15°C spread does not represent the full working range of a lubricant dispensing valve in a motorcycle application, which conceivably could be in the range of -20°C to 40°. This is true when considering the lifetime of valve operation however, 15° is representative of temperature range likely to be found in normal daily use. This argument aside, it is clear that the temperature induced viscosity effects are small in relation to oil type and valve position. This is encouraging as it indicates that where applicable the temperature effects can be mitigated by the selection of oil ISO grade. However, the strong needle position effect means that if the needle position is effected by temperature, such as through the expansion of the valve body, this is likely to have a significant effect on flow rate.

			Level		
Factors	**Control Item**	**Designation**	**1**	**2**	**Units**
Oil Type	ISO Grade	**A**	Red	CL32	n/a
Oil Temperature	Fluid Temperature	**B**	20	5	°C
Needle Position	Engagement (E)	**C**	0.4	1.8	mm
Taper-angle	Taper-angle	**D**	1°	4°	Degrees
Differential Pressure	Reservoir height	**E**	0.3	1.35	M

Table 7-2 Factor analysis levels

The combination factor effects can also be analysed in the same way. Unsurprisingly the greatest combination factor is the needle position and taper-angle (CD) and all factors that are combined with either C or D are also quite large. Also unsurprisingly, combining the two smallest factors, oil temperature (B) and differential pressure (E) to give the combined factor (BE), give the smallest result. Again this shows that flow channel geometry has the largest affect of flow while the flow rate can be manipulated by the pressure head to fine tune flow rate. It should be noted that these results are only relative and that large changes in the upper and lower values for any of the factors would change the relative importance according to this method. However, as the ranges chosen are within the normal working range, this gives a good indication of system sensitivity and gives a good basis for developing a robust design.

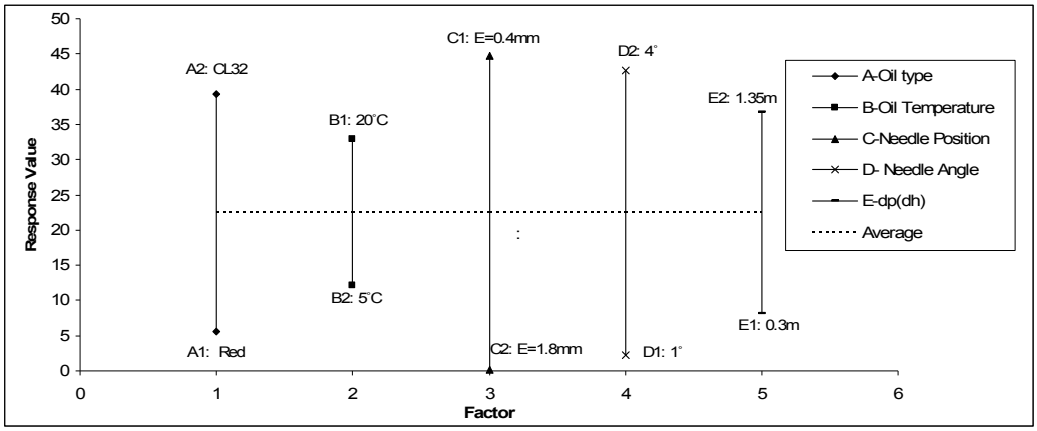

Figure 7-13 Factor effects

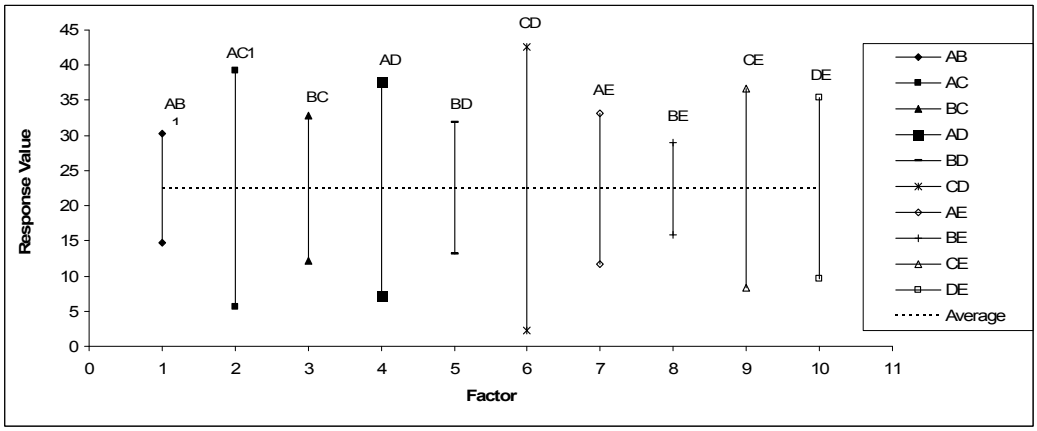

Figure 7-14 Combination factor effects

Normal plots are a useful means of visualising the factor effects relative to the mean response value [149]. Figure 7-15 shows a normal plot of the above data. The horizontal axis is P_i=100(i-0.5)/m, where i is the order of position of the effect when ranked in ascending order. The vertical axis is simply the effect value. Any values that stray from the mean line indicate significant factor effects. In this case it can be seen that there is a significant dichotomisation of the results. This can be explained by noting that factors in the group including BC and D (top right group on the Figure 7-15) were all set at Level 2 when the highest response value was observed.

Aside from the dichotomisation, it is clear to see that C and D both deviate from the generally fitted line and as such are significant factor effects. It can also be noted that

many of the combination effects combined with D and particularly C also deviate further indicating the factor effect of C.

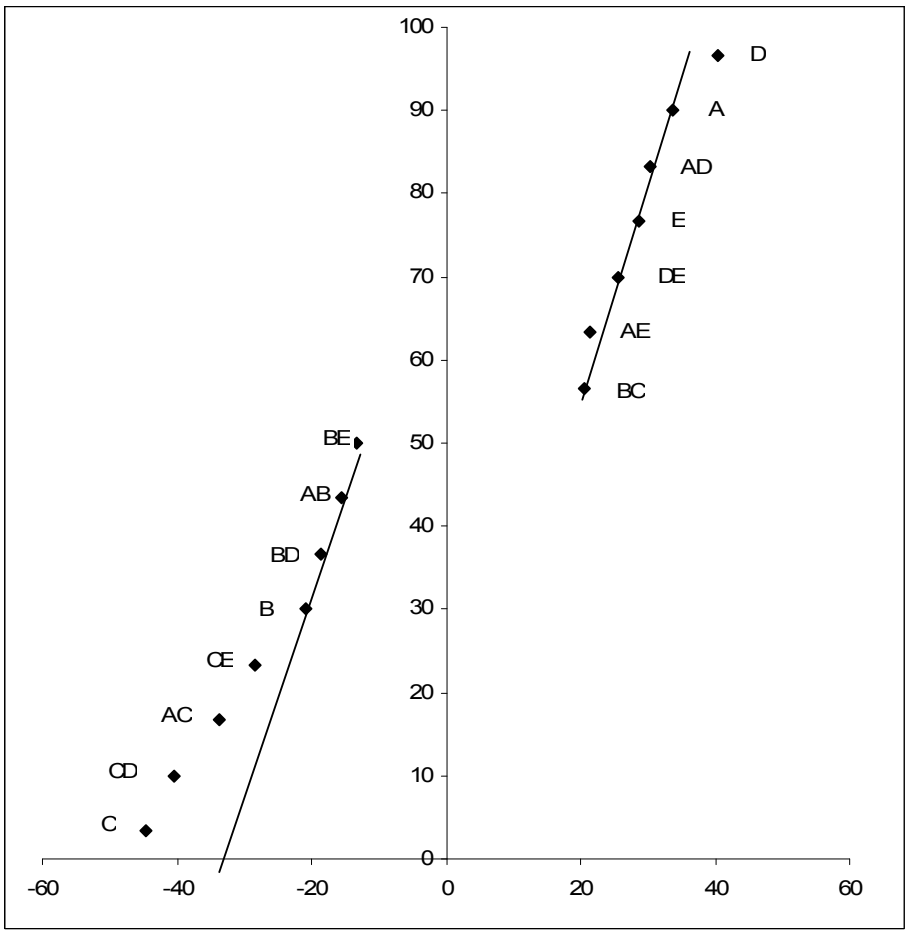

Figure 7-15 Normal Plot of factor effects. Points deviating from the fitted line indicate significant factors.

From this analysis it can be concluded that engagement length C and taper-angle have the greatest effect on flow rate while other factors have a lesser, but contributory effect on flow rate.

7.7 Conclusion

To increase predictability, maximise r_o-r_a (as per Figure 5-3) as this reduces the effects of eccentricity, reduces the effects of non-parallel flow when coupled with a larger taper-angle and reduces the likelihood of the flow channel becoming blocked

by contaminants. Increase the needle travel while maintaining the required flow range to reduce the need for a precision needle positioning mechanism.

To minimise thermal effects: The effects of small changes of needle position on the flow rate are large, so it is important to minimise thermal expansion effects. To do this, minimise valve body length and use a body material of low thermal expansion coefficient. Optimise valve geometry to desensitise the valve to changes in engagement length by increasing needle travel (increase max E) while maintaining the required flow range. This is particularly important as this works in conjunction with reducing the need for a high precision positioning system. This in turn allows tolerances on the positioning system or linear actuator specification to be relaxed. Thermal effects are dynamic and so can only be mitigated through the use of a dynamic control system. This in effect means the use of a closed loop control system however; reducing the thermal effect would also reduce the burden of charting the thermal effects for the purpose of an open loop control system. A closed loop system is much more flexible than the open loop system in terms of automatically compensating for uncharted factors that affect flow rate and also in terms of coupling the valve to an intelligent flow command system.

It can be concluded that the accuracy of the actuator and the total travel length of the valve is interchangeable; in that if the valve geometry is highly sensitive to axial displacement (high gain), a short travel is required but that a correspondingly accurate positioning device is required. It is possible to desensitise the valve though the use of appropriate geometry in which case a longer travel is required but less positional accuracy is required of the actuator mechanism.

Pressure change is a useful means of altering the flow rate and can be achieved by the position of the reservoir. It is important that the reservoir dimensions are chosen carefully in order to reduce the effects of dropping fluid levels. The constant relationship between flow rate and pressure head and the ease of adjustability makes it a useful parameter for developing a control model.

Despite the investigation by Du [13], there is no indication that altering the valve channel geometry will have any effect at desensitising it to viscosity changes; either from ISO grade changes or temperature induced viscosity changes. Temperature induced viscosity changes can only be accounted for via the control system. While it seems feasible to develop a single needle geometry that will account for a range of ISO grades at a range of temperatures, it is likely that should the need arise for a high viscosity low temperature application a specific geometry would have to be developed for the purpose.

8 Conclusions

8.1 Introduction

Whilst there are various means by which very low flow control can be achieved, the restriction of a gravity fed flow is perhaps the simplest and most efficient. Regardless of the source of pressure differential, some form of mechanical obstruction of the flow conduit is required to regulate flow. Where there is a control requirement of a mechanical system, it is logical to apply mechatronic principles where appropriate. A needle valve is one of the most common means of restricting the flow for very small flow rates and so is an ideal subject for mechatronic control. In light of this, a modelling based methodology coupled with a mechatronic approach has been identified as a suitable means of researching the areas where literature is deficient.

8.2 Research Outcomes and Contributions

Mechatronic systems by nature include components from multiple domains. This traditionally includes mechanical and electronic aspects; however in this case the mechanical and electronic systems interface with the fluid dynamics domain. As such there is a wide range of disciplines and applications that can be brought to bear to solve this particular problem. The review section of this thesis collates this information so that it may be applied to create a flow control solution. The review also highlights the areas in which the existing literature is deficient and where there is scope for new research areas.

Existing literature does not cover the scale of flows between industrial control-valves and MEMS type microvalves which leaves a gap corresponding to the control of

microflows using macro-scale technology. In addition to the lack of specific valve theory relating to this scale of valve, there is no literature relating to the general design aspects of creating and controlling small valves able to control micro flows.

There are unique problems faced when controlling very low flow viscous fluids with a variable geometry valve such as a needle valve. Two points in particular have been addressed by this work with regards to furthering valve flow theory. The first advancement is the creation of an analytical model based on the flow channel rather than the flow orifice as is applicable to higher flow rate valves. The second is to establish the link between valve geometry and the flow characteristics of the valve and is implemented through the use of the analytical model. Verification of the analytical model has been achieved through comparisons with numerical models and test data. While extensive measures were taken to ensure the test conditions were fully understood in order to be able to make a true comparison with the analytical model, the geometric uncertainties of working at the micro scale are such that it is very difficult to be sure of the actual flow channel profile. This is a potential source of the difference between the theoretical models and the test data. However the results are sufficiently close to indicate that the model is correct within the bounds of experimental error. The analytical model created is an important tool for the development of valve channel profiles which in turn has implications for the mechatronic system as a whole.

The mechatronic content of this research is in the form of the test apparatus developed specifically for this research and in the form of working prototypes for controlling lubricant flow. Generating the test data used in the development of the analytical model required the design and build of dedicated laboratory test equipment. Of

particular note is the development of a novel highly sensitive very low flow measurement device. The linear relationship between volumetric flow rate and drip interval is a critical part of the functionality of the drip interval measurement device when used for control purposes and as far as the author is aware is previously unpublished. The large range, high sensitivity and low cost of the device make it ideal for use in laboratory based experiments investigating flow characteristics. The ability to place the piezo transducer in a remote location allows flow measurements to be made in harsh environments such as an environmental chamber without risk of interrupting the function of electronic equipment or mechanical linkages.

Other laboratory equipment comprises of the integration of the temperature controlled chamber with valve temperature acquisition and valve activation. Activation methods include solenoid control for on/off functionality and as a development of this, a linear actuator with micro-steps for dynamic adjustability and the development of active control systems. The sum of these tools enables a complete environment for testing and developing valve flow characteristics.

A holistic view of valve development looks at each valve subsystem (flow channel geometry, actuator and control) as well as the whole valve control system. It also takes into consideration the valve's operational environment. Important insights into the operational requirements of a mechatronically controlled lubricant dispensing system were gathered from the installation of two prototype oilers in an industrial location. Initial testing was conducted on a laboratory based simulator able to simulate and compress the duty cycle of an industrial environment. The simulator was able to aid in improving the reliability and endurance of the oiler system while field

testing provided insights into the interface requirements of a factory based machine and of the human interface requirements.

The stepper-motor actuated valve allowed the valve needle to be positioned with a 6.25μm resolution and allowed precise and flexible control of the valve and valve flow rate. As mechatronic systems are characterised by the need for simultaneous design of the mechanical components and control system, the lower order functions of the control systems were developed alongside the hardware. Once this was achieved, the linear actuated valve could be used in conjunction with the other laboratory equipment to develop intelligent valve control systems to suit different environments.

Using the new flow measurement device as part of a closed loop system with the linear actuated valve, it was possible to achieve highly accurate and dynamic control of the flow rate. One of the main points to note is that a closed loop system is probably the most effective means of achieving reliable and highly accurate controlled flow rates of a continuous stream. This in turn requires a suitable flow measurement device that is able to match the control device in terms of precision and range. While it may be possible to develop a measurement system based on other principles, the drip interval based method presented here has been shown to function well and is well matched to the flow range of the valve. Whilst the use of a linear actuator for the control of a needle valve is undoubtedly not novel, it is felt a minor contribution can be attributed to the detailed description of the implementation of such a system, particularly in conjunction with a novel flow measurement device. This is especially true when taken in the wider context of the design implications on a mechatronic system.

Currently the low flow sensor is only suitable for a laboratory environment and as such is not available for industrial applications. There are also situations in which it is unlikely to ever function well, such as on a motorbike. For this reason, an open loop variant was also developed making use of the knowledge gained of valve flow characteristics to describe an efficient system for characterising valve flow rates. A minor contribution can be claimed from the process by which the valve is characterised in the form of a model. In theory the model can be generated using only four data points whilst further points are likely to increase accuracy. The simplicity of the model makes it ideal for integration in an embedded control system as the calculation requirements are small and there is no need for large databases or look-up tables. This also makes it flexible and easy to adjust if necessary. The author is not aware of this method of modelling the valve flow characteristics for the purpose of valve control being previously published in the public domain.

All the knowledge gained from theoretical and practical work has been consolidated into a low flow control valve design synthesis describing the important factors affecting the creation and control of very low flow control-valves. Much of this is derived from the analytical model and its description of flow behaviour in relation to channel geometry and needle movement. When the analytical model is considered in conjunction with the experience gained through the mechatronic developments, the implications of needle profile on the mechanical and control aspects can be understood.

In conjunction with the analytical model, the design synthesis forms the major contribution of this work. All the relevant factors affecting very low flow control using needle valves have been explored in detail and discussed. The design synthesis

produced is relevant to many forms of variable geometry valves. The relationships between the channel geometry and flow characteristics described here are independent of size and flow volume and are applicable to variable channel flows with low Reynolds numbers and parallel flow. Likewise, the relationship between the linear actuation of the valve and the alteration of the valve geometry is independent of the length scales involved, making the findings here applicable to the MEMS and micro actuator domain. Of particular importance to mechatronic control is the significance of the simultaneous effects of flow channel geometry on the valve flow characteristics and linear actuator requirements and associated control system.

Scottoiler has recently been awarded a prestigious SMART award by the Scottish Executive to develop a commercial product based on the knowledge derived from this research.

8.3 Future Work

While a good level of conformance was achieved between the analytical model and the experimental flow data, higher accuracy levels could be achieved through further refinement of the analytical model. This would be possible by addressing the area of greatest uncertainty: matching the model to the actual experimental geometry. This would involve either, further refinement of the experimental equipment such that the needle and therefore the channel geometry is more accurately defined or secondly, explore other, more complicated analytical models and seek a match with the test data. The first option would be preferable as it eliminates the uncertainty at source rather than trying to account for it, which would almost certainly involve the greater effort.

In a practical sense, it is always going to be difficult to accurately centre the needle within the orifice and while there are undoubtedly a number of possible solutions, perhaps a better method is to avoid it altogether and develop a flow channel that mimics the form of the analytical model. i.e. a flat structure. This has a number of advantages: it would mean the model is a direct representation of the actual flow channel, it would remove the need to centralise the needle and the form would be conducive to the manufacturing methods common to current MEMS devices. If this were feasible it would then be possible to actuate the valve by means of macro sized linear actuator as used in this study or some form of microscale actuator such as those reviewed in Section 2.3.1.5 Valve Actuation and Control. A MEMS scale actuator would have the advantage of significantly reducing the overall size of the valve package. Also if the displacement resolution of the actuator were high it would allow for accurate control with a small stroke valve as discussed in Section 7.2 as actuator displacement and accuracy are interchangeable.

The analytical model of valve flow is currently formulated to predict the valve flow characteristic for a given valve geometry. It should however be possible to reverse the process such that it is possible to derive the required channel geometry to achieve the desired flow characteristics. This would be of great value to the design process.

An integral part of the closed loop control system is the low flow sensor. Currently this is only suitable for a laboratory environment. It would be of great value to develop the concept such that it could be used in either static or mobile locations such as an industrial environment or even a motorbike.

The current open loop model demonstrates a method for characterising the flow rate of a valve in terms of valve needle position and pressure differential with just a few

data points. It should be feasible to extend this concept such that temperature fluctuations can also be accounted for. One trial conducted as part of this study to incorporate temperature effects had a small amount of success but in general, the results of the temperature compensated version were no more accurate than the non-compensated version. Further study should be able to refine this concept to successfully include temperature compensation.

This research has attempted to provide solutions to the problems associated with controlling very low flows of viscous fluids. Many of the problems are caused by the sensitivity of the system to very small changes in physical parameters. One way of mitigating these effects is to reconsider if the application requires a constant feed. In the case of lubrication applications, most lubrication requirements would be equally well served by timed bursts of a higher flow rate. In this way, the level of control afforded by an automatically actuated needle valve is maintained, but as the needle geometry can be optimised for higher flow rates, it would become less sensitive to small noise effects thus producing a more robust design solution.

9 References

[1] M. D. Kidd, "Bicycle Chain Efficiency," in *Department of Mechanical and Chemical Engineering*, vol. Doctor of Philosophy. Edinburgh: Heriot-Watt University, 2000, pp. 238.

[2] M. Gad-el Hak, *The MEMS Handbook*: CRC, 2001.

[3] P. J. Lee, P. J. Hung, R. Shaw, L. Jan, and L. P. Lee, "Microfluidic application-specific integrated device for monitoring direct cell-cell communication via gap junctions between individual cell pairs," *Applied Physics Letters*, vol. 86, pp. 223902, 2005.

[4] D. J. Laser and J. G. Santiago, "A review of micropumps," *Journal of Micromechanics and Microengineering*, vol. 14, pp. 35, 2004.

[5] J. Judy, D. Maynes, and B. W. Webb, "Characterization of frictional pressure drop for liquid flows through microchannels," *International Journal of Heat and Mass Transfer*, vol. 45, pp. 3477, 2002.

[6] G. Hetsroni, A. Mosyak, E. Pogrebnyak, and L. P. Yarin, "Fluid flow in micro-channels," *International Journal of Heat and Mass Transfer*, vol. 48, pp. 1982, 2005.

[7] W. Dieterle, "Mechatronic systems: Automotive applications and modern design methodologies," *Annual Reviews in Control*, vol. 29, pp. 273, 2005.

[8] J. Hollingum, "How are we doing in mechatronics?" *Assembly Automation*, vol. 19, pp. 25, 1999.

[9] R. Isermann, "Mechatronic systems-Innovative products with embedded control," *Control Engineering Practice*, vol. 16, pp. 14, 2008.

[10] S. Centinkunt, *Mechatronics*: Wiley, 2007.

[11] S. Crosson, "Final Report," in *DMEM*. Glasgow: University Of Strathclyde, 2002.

[12] M. R. Casey, "An Experimental and Computational Investigation of the Scottoiler Motorcycle Chain Lubrication System," in *DMEM*, vol. MSc. Glasgow: University Of Strathclyde, 2002, pp. 107.

[13] Y. Du, "A Numerical Investigation of A Motorcycle Chain Lubrication System for Redesign," in *DMEM*, vol. MSc. Glasgow: University of Strathclyde, 2003, pp. 99.

[14] B. T. Stojkov, *the Valve Primer*: Industrial Press Inc., 1997.

[15] P. L. Skousen, *Valve Handbook*, 2nd ed: McGraw-Hill Professional, 2004.

[16] H. E. Merritt, *Hydraulic Control Systems*: Wiley-Interscience, 1967.

[17] B. Munson, R, D. Young, F, and T. Okiishi, H, *Fundamentals of fluid mechanics*, 3rd ed: John Wylie & Sons, inc, 1988.

[18] C. Schaschke, *Fluid Mechanics: Worked Examples For Engineers*: Institution of Chemical Engineers (IChemE), 2005.

[19] J. R. Backhurst, J. H. Harker, J. F. Richardson, and J. M. Coulson, *Chemical Engineering Volume 1: Fluid Flow, Heat Transfer and Mass Transfer*: Butterworth-Heinemann; 6 edition (19 Oct 1999), 1999.

[20] B. S. Massey, *Mechanics of Fluids*: Taylor Francis, 1998.

[21] R. A. Bryant, "Characteristics of small needle valves," *Australian Mechanical Engineering*, vol. 49, pp. 40, 1962.

[22] M. M. Takemura, "Precision control of a small flow," *Energie Fluide*, vol. 14, pp. 55-61, 1975.

[23] H. Xi, H. Xu, and R. Tang, "Experimental study of the flow in the gap of needle valve," *Qinghua Daxue Xuebao/Journal of Tsinghua University*, vol. 41, pp. 68, 2001.

[24] G. F. Stiles, "Cavitation in control valves," *Instruments and Control Systems*, vol. 34, pp. 2086, 1961.

[25] G. F. Stiles, "Liquid viscosity effects on control valve sizing," 1964.

[26] G. F. Stiles, "Analyzing cavitation in high-recovery valves," *Instrumentation Technology*, vol. 14, pp. 49, 1967.

[27] G. F. Stiles, "Cavitation in control valves," *Control & Instrumentation*, vol. 6, pp. 20, 1974.

[28] G. F. Stiles, "International control valve standards-a status report," Anaheim, CA, USA, 1977.

[29] H. D. Baumann, "Introduction of critical flow factor for valve sizing," *Instrument Society of America -- Transactions*, vol. 2, pp. 107, 1963.

[30] H. D. Baumann, "Viscosity flow correction for small control valve trim," *Journal of Fluids Engineering, Transactions of the ASME*, vol. 113, pp. 86, 1991.

[31] H. D. Baumann, "Control-valve sizing improved," *InTech*, vol. 46, pp. 54, 1999.

[32] H. D. Baumann, "Control valves-a practical guide to their selection and application. II," *Instrument Practice*, vol. 22, pp. 845, 1968.

[33] H. D. Baumann, "Important trends in control valves and actuators," *Instruments and Control Systems*, vol. 48, pp. 21, 1975.

[34] H. D. Baumann, "Control valve vs. variable-speed pump," *Chemical Engineering*, vol. 88, pp. 81, 1981.

[35] H. D. Baumann, "Solve valve noise and cavitation problems," *Hydrocarbon Processing*, vol. 76, pp. 5, 1997.

[36] W. Rahmeyer and L. Driskell, "CONTROL VALVE FLOW COEFFICIENTS," *Journal of Transportation Engineering*, vol. 111, pp. 358, 1985.

[37] J. A. George, "Sizing and selection of low flow control valves," *InTech*, vol. 36, pp. 46, 1989.

[38] "Industrial-process control valves - Part 1: Control valve terminology and general considerations," BS EN 60534-1:2005, 2005.

[39] "Industrial-process control valves - Part 2-1: Flow capacity - Sizing equations for fluid flow under installed conditions," BS EN 60534-2-1:1999, 1999.

[40] "Industrial-process control valves - Part 2-3: Flow capacity - Test procedures," BS EN 60534-2-3:1998, 1998.

[41] H. S. Sondh, S. N. Singh, V. Seshadri, and B. K. Gandhi, "Design and development of variable area orifice meter," *Flow Measurement and Instrumentation*, vol. 13, pp. 69, 2002.

[42] S. N. Singh, B. K. Gandhi, V. Seshadri, and V. S. Chauhan, "Design of a bluff body for development of variable area orifice-meter," *Flow Measurement and Instrumentation*, vol. 15, pp. 97, 2004.

[43] L. Thananchai, "Design factors for “linear” ball valve: theoretical and experimental studies," *Songklanakarin J. Sci. Technol.*, vol. Vol.27 No.2 Mar., 2005.

[44] M. Borghi, "Hydraulic locking-in spool-type valves: Tapered clearances analysis," *Proceedings of the Institution of Mechanical Engineers. Part I: Journal of Systems and Control Engineering*, vol. 215, pp. 157, 2001.

[45] B. Eryilmaz and B. H. Wilson, "Unified modeling and analysis of a proportional valve," *Journal of the Franklin Institute*, vol. 343, pp. 48, 2006.

[46] J. Ruan, P. Ukrainetz, and R. Burton, "Frequency. Domain Modeling and Identification of 2D Servo Valve," *International Journal of Fluid Power*, vol. 1(2), pp. 76-78, 2000.

[47] J. Ruan, S. Li, X. Pei, R. Burton, P. Ukrainetz, and D. Bitner, "2D digital simplified flow valve," *Chinese Journal of Mechanical Engineering (English Edition)*, vol. 17, pp. 311, 2004.

[48] E. Thielicke and E. Obermeier, "Microactuators and their technologies," *Mechatronics*, vol. 10, pp. 431, 2000.

[49] A. R. Gamboa, C. J. Morris, and F. K. Forster, "Improvements in fixed-valve micropump performance through shape optimization of valves," *Journal of Fluids Engineering, Transactions of the ASME*, vol. 127, pp. 339, 2005.

[50] K. Ki Hoon and Y. Sang Silk, "Fabrication and test of an electromagnetic micro actuator with a planar coil on a parylene diaphragm," Orlando, FL, USA, 2000.

[51] N. T. Nguyen, S. Schubert, S. Richter, and W. Dotzel, "Hybrid-assembled micro dosing system using silicon-based micropump/valve and mass flow sensor," *Sensors and Actuators A (Physical)*, vol. A69, pp. 85, 1998.

[52] J. D. Zahn, A. Deshmukh, A. P. Pisano, and D. Liepmann, "Continuous on-chip micropumping for microneedle enhanced drug delivery," *Biomedical Microdevices*, vol. 6, pp. 183, 2004.

[53] X. Yang, C. Grosjean, Y.-C. Tai, and C.-M. Ho, "MEMS thermopneumatic silicone membrane valve," Nagoya, Jpn, 1997.

[54] B. Bae, H. Kee, S. Kim, Y. Lee, T. Sim, Y. Kim, and K. Park, "In vitro experiment of the pressure regulating valve for a glaucoma implant," *Journal of Micromechanics and Microengineering*, vol. 13, pp. 613, 2003.

[55] C. Jin-Woo, Y. W. Oh, A. Han, N. Okulan, C. Ajith Wijayawardhana, C. Lannes, S. Bhansali, K. T. Schlueter, W. R. Heineman, H. B. Halsall, J. H. Nevin, A. J. Helmicki, H. Thurman Henderson, and C. H. Ahn, "Development and characterization of microfluidic devices and systems for magnetic bead-based biochemical detection," Columbus, OH, USA, 2001.

[56] K. W. Oh, R. Rong, and C. H. Ahn, "Miniaturization of pinch-type valves and pumps for practical micro total analysis system integration," *Journal of Micromechanics and Microengineering*, vol. 15, pp. 2449, 2005.

[57] K. W. Oh and C. H. Ahn, "A review of microvalves," *Journal of Micromechanics and Microengineering*, vol. 16, pp. 13, 2006.

[58] S. C. Terry, J. H. Jerman, and J. B. Angell, "GAS CHROMATOGRAPHIC AIR ANALYZER FABRICATED ON A SILICON WAFER," *IEEE Transactions on Electron Devices*, vol. ED-26, pp. 1880, 1979.

[59] G. Waibel, J. Kohnle, R. Cernosa, M. Storz, M. Schrmitt, H. Ernst, H. Sandmaier, R. Zengerle, and T. Strobelt, "Highly integrated autonomous microdosage system," *Sensors and Actuators, A: Physical*, vol. 103, pp. 225, 2003.

[60] T. Goettsche, J. Kohnle, M. Willmann, H. Ernst, S. Spieth, R. Tischler, S. Messner, R. Zengerle, and H. Sandmaier, "Novel approaches to particle tolerant valves for use in drug delivery systems," *Sensors and Actuators, A: Physical*, vol. 118, pp. 70, 2005.

[61] J. Peirs, D. Reynaerts, and H. Van Brussel, "Design of miniature parallel manipulators for integration in a self-propelling endoscope," The Hague, Netherlands, 2000.

[62] K. W. Oh, R. Rong, and C. H. Ahn, "In-line micro ball valve through polymer tubing," presented at microTAS 2001, 2001.

[63] N. Vandelli, D. Wroblewski, M. Velonis, and T. Bifano, "Development of a MEMS microvalve array for fluid flow control," *Journal of Microelectromechanical Systems*, vol. 7, pp. 395, 1998.

[64] J. Collier, D. Wroblewski, and T. Bifano, "Development of a rapid-response flow-control system using MEMS microvalve arrays," *Journal of Microelectromechanical Systems*, vol. 13, pp. 912, 2004.

[65] E. Stemme and G. Stemme, "Valveless diffuser/nozzle-based fluid pump," *Sensors and Actuators, A: Physical*, vol. 39, pp. 159, 1993.

[66] M. C. Carrozza, N. Croce, B. Magnani, and P. Dario, "Piezoelectric-driven stereolithography-fabricated micropump," *Journal of Micromechanics and Microengineering*, vol. 5, pp. 177, 1995.

[67] A. Olsson, G. Stemme, and E. Stemme, "Valve-less planar fluid pump with two pump chambers," *Sensors and Actuators, A: Physical*, vol. 47, pp. 549, 1995.

[68] H. Q. Li, D. C. Roberts, J. L. Steyn, K. T. Turner, J. A. Carretero, O. Yaglioglu, Y.-H. Su, L. Saggere, N. W. Hawgood, S. M. Spearing, M. A. Schmidt, R. Mlcak, and K. S. Breuer, "A High Frequency High Flow Rate Piezoelectrically Driven MEMS Micropump," presented at IEEE Solid State Sensors and Actuators Workshop, Hilton Head, 2000.

[69] R. L. Bardell, N. R. Sharma, F. K. Forster, M. A. Afromowitz, and R. J. Penney, "Designing high-performance micro-pumps based on no-moving-parts valves," Dallas, TX, USA, 1997.

[70] B. G. Lipták, *Instrument Engineers' Handbook: Process Control and Optimization*: CRC Press, 2005.

[71] K. F. Elmer and C. R. Gentle, "A parsimonious model for the proportional control valve," *Proceedings of the Institution of Mechanical Engineers, Part C: Journal of Mechanical Engineering Science*, vol. 215, pp. 1357, 2001.

[72] N. D. Vaughan and J. B. Gamble, "Modelling and simulation of a proportional solenoid valve," Dallas, TX, USA, 1990.

[73] Z. Q. Yu, M. J. Hu, X. Pei, and J. Ruan, "Actuation and Control of a Micro Electrohydraulic Digital Servo Valve," presented at International Symposium on Instrumentation Science and Technology, 2006.

[74] B. C. Murphy, "Design and construction of a precision tubular linear motor and controller," in *Mech Eng*, vol. Master of Science. Texas: Texas A&M University, 2003.

[75] S. Zappe, M. Baltzer, T. Kraus, and E. Obermeier, "Electrostatically driven linear micro-actuators: FE analysis and fabrication," *Journal of Micromechanics and Microengineering*, vol. 7, pp. 204, 1997.

[76] M. Baltzer, T. Kraus, and E. Obermeier, "Linear stepping actuator in surface micromachining technology for low voltages and large displacements," Chicago, IL, USA, 1997.

[77] R. A. Miller, G. W. Burr, T. Yu-Chong, D. Psaltis, H. Chih-Ming, and R. R. Katti, "Electromagnetic MEMS scanning mirrors for holographic data storage," Hilton Head Island, SC, USA, 1996.

[78] J. Van Amerongen and P. Breedveld, "Modelling of physical systems for the design and control of mechatronic systems," *Annual Reviews in Control*, vol. 27 I, pp. 87, 2003.

[79] D. A. Bradley, D. Dawson, N. C. Burd, and A. J. Loader, *Mechatronics; Electronics in products and processes*. London: Chapman & Hall, 1993.

[80] K. Warwick, *An Introduction to Control Systems*: World Scientific, 1996.

[81] C. L. Nachtigal, *Instrumentation and Control: Fundamentals and Applications*: Wiley-IEEE, 1990.

[82] G. F. Stiles and C. W. Sheldon, "Liquid viscosity effects on control valve sizing," *ISA Transactions*, vol. 9, pp. 316, 1970.

[83] K. V. Sharp, R. J. Adrian, J. G. Santiago, and J. I. Molho, "Liquid Flow In Microchannels," in *The MEMS Handbook*, vol. 6 1-38, M. Gad-El-Hak, Ed. Boca Ranton: CRC Press, 2001.

[84] C.-M. Ho and Y.-C. Tai, "Micro-Electro-Mechanical-Systems (MEMS) and Fluid Flows," *Annual Review of Fluid Mechanics*, vol. 30, pp. 579-612, 1998.

[85] J. Pfahler, J. Harley, H. Bau, and J. N. Zemel, "Gas and liquid flow in small channels," Atlanta, GA, USA, 1991.

[86] M. Gad-El-Hak, "Flow Physics," in *The MEMS Handbook*, vol. 4 1-38, M. Gad-El-Hak, Ed.: CRC, 2001.

[87] N. P. Migun and P. P. Prokhorenko, "Measurement of viscosity of polar liquids in microcapillaries," *Colloid Journal USSR*, vol. 49, pp. 894, 1987.

[88] J. Pfahler, J. Harley, H. Bau, and J. Zemel, "Liquid transport in micron and submicron channels," Montreux, Switzerland, 1990.

[89] J. Reese, "Beyond Navier-Stokes. The complex fluid mechanics of hypersonic aerodynamics and micro-and nano-scale," Seminar. Department of Mechanical Engineering. University of Strathclyde, 2008.

[90] H. Struchtrup, *Macroscopic Transport Equations for Rarefied Gas flows*. Berlin: Springer-Verlag, 2005.

[91] J. F. Douglas, J. M. Gasiorek, and J. A. Swaffield, *Fluid Mechanics*, 4th ed. Harlow, Essex: Pearson Education Limited, 2001.

[92] N. A. V. Piercy, M. S. Hooper, and H. F. Winny, "Viscous flow through pipes with cores," *London, Edinburgh, Dublin Philosophical Magazine and Journal of Science*, vol. 15, pp. 647, 1933.

[93] J. F. Heyda, " Heat transfer in turbulent flow through nonconcentric annuli having unequal heat release from the walls," vol. APEX-391: General Electric Co. Aircraft Nuclear Propulsion Dept., Cincinnati, 1957, pp. Pages: 29.

[94] P. J. Redberger and M. E. Charles, "Axial laminar flow in circular pipe containing fixed eccentric core," *Canadian Journal of Chemical Engineering*, vol. 40, pp. 148, 1962.

[95] W. T. Snyder and G. A. Goldstein, "An analysis of fully developed laminar flow in an eccentric annulus.," *AIChE Journal*, vol. 11, pp. 462-467, 1965.

[96] H. Schlichting, *Boundary-Layer Theory*, vol. 7th ed: McGraw-Hill, 1979.

[97] D. F. Rogers, *Laminar Flow Analysis*: Cambridge University Press, 1992.

[98] B. G. Lipták, *Flow Measurement*: CRC Press, 1993.

[99] J. Eggers, "Nonlinear dynamics and breakup of free-surface flows," *Reviews of Modern Physics*, vol. 69, pp. 865, 1997.

[100] O. E. Rossler, "Synergetics: a workshop: proceedings of the workshop on synergetics at schloss elmau, bavaria, may 2-7, 1977," pp. P174, 1977.

[101] X. Wu, E. Tekle, and Z. A. Schelly, "Dripping faucet apparatus with temperature and high-resolution timing and flow rate controls," *Review of Scientific Instruments*, vol. 60, pp. 3779-82, 1989.

[102] B. Ambravaneswaran, S. D. Phillips, and O. A. Basaran, "Theoretical analysis of a dripping faucet," *Physical Review Letters*, vol. 85, pp. 5332, 2000.

[103] B. Ambravaneswaran, H. J. Subramani, S. D. Phillips, and O. A. Basaran, "Dripping-jetting transitions in a dripping faucet," *Physical Review Letters*, vol. 93, pp. 034501, 2004.

[104] E. Bonabeau, G. Theraulaz, J. L. Deneubourg, A. Lioni, F. Libert, C. Sauwens, and L. Passera, "Dripping faucet with ants," *Physical Review E (Statistical Physics, Plasmas, Fluids, and Related Interdisciplinary Topics)*, vol. 57, pp. 5904, 1998.

[105] R. F. Cahalan, H. Leidecker, and G. D. Cahalan, "Chaotic rhythms of a dripping faucet," *Computers in Physics*, vol. 4, pp. 368, 1990.

[106] A. D'Innocenzo and L. Renna, "Dripping faucet," *International Journal of Theoretical Physics*, vol. 35, pp. 941, 1996.

[107] A. D'Innocenzo and L. Renna, "Analytical solution of the dripping faucet dynamics," *Physics Letters A*, vol. 220, pp. 75, 1996.

[108] N. Fuchikami, S. Ishioka, and K. Kiyoko, "Simulation of a dripping faucet," *Journal of the Physical Society of Japan*, vol. 68, pp. 1185, 1999.

[109] W. M. Goncalves, R. D. Pinto, J. C. Sartorelli, and M. J. de Oliveira, "Inferring statistical complexity in the dripping faucet experiment," *Physica A*, vol. 257, pp. 385, 1998.

[110] T. Katsuyama, K. Kiyono, and N. Fuchikami, "Chaos in a dripping tap," Tokyo, Japan, 2002.

[111] H. N. Nunez-Yepez, S. Brito, C. A. Vargas, and L. Vicente, "Chaos in a dripping faucet," *European Journal of Physics*, pp. 99-105, 1989.

[112] H. N. Nunez-Yepez, C. Carbajal, A. L. Salas-Brito, C. A. Vargas, and L. Vicente, "Nonlinear behaviour in a dripping faucet," Santiago, Chile, 1991.

[113] R. D. Pinto, W. M. Goncalves, J. C. Sartorelli, I. L. Caldas, and M. S. Baptista, "Interior crises in a dripping faucet experiment," *Physical Review E (Statistical Physics, Plasmas, Fluids, and Related Interdisciplinary Topics)*, vol. 58, pp. 4009, 1998.

[114] R. D. Pinto, J. C. Sartorelli, and W. M. Goncalves, "Homoclinic tangencies and routes to chaos in a dripping faucet experiment," *Physica A*, vol. 291, pp. 244, 2001.

[115] A. D'Innocenzo, F. Paladini, and L. Renna, "Experimental study of dripping dynamics," *Physical Review E (Statistical, Nonlinear, and Soft Matter Physics)*, vol. 65, pp. 056208, 2002.

[116] A. D'Innocenzo, F. Paladini, and L. Renna, "Effects of geometrical parameters on dripping from cylindrical nozzles," *Physica A*, vol. 338, pp. 272, 2004.

[117] Z. Neda, B. Bako, and E. Rees, "The dripping faucet revisited," *Chaos*, vol. 6, pp. 59, 1996.

[118] D. M. Henderson, W. G. Pritchard, and L. B. Smolka, "On the pinch-off of a pendant drop of viscous fluid," *Physics of Fluids*, vol. 9, pp. 3188, 1997.

[119] X. Zhang and O. A. Basaran, "An experimental study of dynamics of drop formation," *Physics of Fluids*, vol. 7, pp. 1184, 1995.

[120] H. Honda, "CFD visualization of drop generation from a nozzle," Honolulu, HI, United States, 2003.

[121] E. D. Wilkes, S. D. Phillips, and O. A. Basaran, "Computational and experimental analysis of dynamics of drop formation," *Physics of Fluids*, vol. 11, pp. 3577, 1999.

[122] A. Tufaile, R. D. Pinto, W. M. Goncalves, and J. C. Sartorelli, "Simulations in a dripping faucet experiment," *Physics Letters A*, vol. 255, pp. 58, 1999.

[123] T. Schmidt and M. Marhl, "A simple mathematical model of a dripping tap," *European Journal of Physics*, vol. 18, pp. 377, 1997.

[124] H. J. Shore and G. M. Harrison, "The effect of added polymers on the formation of drops ejected from a nozzle," *Physics of Fluids*, vol. 17, pp. 33104, 2005.

[125] E. D. Wilkes and O. A. Basaran, "Drop ejection from an oscillating rod," *Journal of Colloid and Interface Science*, vol. 242, pp. 180, 2001.

[126] C. Cramer, P. Fischer, and E. J. Windhab, "Drop formation in a co-flowing ambient fluid," *Chemical Engineering Science*, vol. 59, pp. 3045, 2004.

[127] G. F. Scheele and B. J. Meister, "Drop formation at low velocities in liquid-liquid systems," *A.I.Ch.E. Journal*, vol. 14, pp. 9, 1968.

[128] T. N. Buch, W. B. Pardo, J. A. Walkenstein, M. Monti, and E. Rosa, Jr., "Experimental issues in the observation of water drop dynamics," *Physics Letters A*, vol. 248, pp. 353, 1998.

[129] T. Zhang, K. Chakrabarty, and R. B. Fair, *Microfluidic Systems. Modeling and Simulation*: CRC Press, 2000.

[130] J. A. Davis and M. Stewart, "Predicting globe control valve performance. I. CFD modeling," *Transactions of the ASME. Journal of Fluids Engineering*, vol. 124, pp. 772, 2002.

[131] J. A. Davis and M. Stewart, "Predicting globe control valve performance. II. Experimental verification," *Transactions of the ASME. Journal of Fluids Engineering*, vol. 124, pp. 778, 2002.

[132] R. J. Townsend, M. Hill, N. R. Harris, N. M. White, S. P. Beeby, and R. J. K. Wood, "Fluid modelling of microfluidic separator channels," *Sensors and Actuators, B: Chemical*, vol. 111-112, pp. 455, 2005.

[133] F. Iancu and N. Muller, "Efficiency of shock wave compression in a microchannel," *Microfluidics and Nanofluidics*, vol. 2, pp. 50, 2006.

[134] I. Kobayashi, K. Uemura, and M. Nakajima, "CFD study of the effect of a fluid flow in a channel on generation of oil-in-water emulsion droplets in straight-through microchannel emulsification," *Journal of Chemical Engineering of Japan*, vol. 39, pp. 855, 2006.

[135] A. S. W. Ng, W. L. W. Hau, Y.-K. Lee, and Y. Zohar, "Electrokinetic generation of microvortex patterns in a microchannel liquid flow," *Journal of Micromechanics and Microengineering*, vol. 14, pp. 247, 2004.

[136] T. Maruyama, T. Kaji, T. Ohkawa, K.-i. Sotowa, H. Matsushita, F. Kubota, N. Kamiya, K. Kusakabea, and M. Goto, "Intermittent partition walls promote solvent extraction of metal ions in a microfluidic device," *The Analyst*, vol. 129, pp. 1 0 0 8 – 1 0 1 3, 2004.

[137] H. Klank, G. Goranovic, J. P. Kutter, H. Gjelstrup, J. Michelsen, and C. H. Westergaard, "PIV measurements in a microfluidic 3D-sheathing structure with three-dimensional flow behaviour," *Journal of Micromechanics and Microengineering*, vol. 12, pp. 862, 2002.

[138] F. R. Giordano, M. D. Weir, and W. P. Fox, *A first course in mathematical modeling*, 2nd ed. ed: Brooks/Cole Pub. Co., 1997.

[139] L. Thananchai, "Flow-sensorless control valve: neural computing approach," *Flow Measurement and Instrumentation*, vol. 14, pp. 261, 2003.

[140] R. H. Lochner and J. E. Matar, *Design For Quality.*, 1990.

[141] G. E. P. Box and N. R. Draper, *Empirical model-building and response surfaces*, 1987.

[142] Fang Lin Luo, Hong Ye, and M. H. Rashid, *Digital Power Electronics and Applications*: Academic Press, 2005.

[143] A. K. Singh, P. S. Mukherjee, and N. M. Mishra, "Interrelationship among viscosity, temperature and age of lubricant," *Industrial Lubrication And Tribology*, vol. 58, pp. 50-55, 2006.

[144] Standard, "BS 4231:1992 Viscosity grades of industrial liquid lubricants," 1992.

[145] F. Kreith, *Fluid Mechanics*: CRC Press, 2000.

[146] R. Isermann, "Modeling and design methodology for mechatronic systems," *IEEE/ASME Transactions on Mechatronics*, vol. 1, pp. 16, 1996.

[147] R. N. Kackar, "TAGUCHI'S QUALITY PHILOSOPHY: ANALYSIS AND COMMENTARY," *Quality Progress*, vol. 19, pp. 21, 1986.

[148] R. N. Kackar and A. C. Shoemaker, "Robust Design: A cost-effective method for improving manufacturing processes," *AT&T Technical Journal*, vol. 65, pp. 39, 1986.

[149] C. Daniel, "Use of half-normal plots in interpreting factorial two-level experiments," *Technometrics*, vol. 1, pp. 311, 1959.

[150] R. C. Zante and X.-T. Yan, "AN INVESTIGATION INTO THE USE OF NEURAL NETWORKS IN THE DESIGN OPTIMISATION OF A GRAVITY FED NEEDLE VALVE," presented at ICDM06, Bristol, 2006.

[151] R. C. Zante and X.-T. Yan, "A MECHATRONIC SOLUTION TO INVESTIGATING A GRAVITY-FED OIL DISPENSING NEEDLE VALVE," presented at MX2006, Penn State, Philadelphia, 2006.

[152] R. C. Zante, "Piezo-electric transducer based very low flow, large range, measurement method.," *Submitted to Flow Measurement and Instrumentation*, 2007.

10 Appendices

10.1 Appendix A: BS EN 60534-2-1 Sample Calculation

The procedure is adapted from an example given in EN 60534-2-1:1998 and uses typical values for the application being studied. It is an iterative process that requires the calculation of an estimated *C* value called C_i. The process out-line is as follows:

1. Estimate C_i using generic flow equation.

$$C = \frac{Q}{N_1}\sqrt{\frac{\rho_1}{\rho_0}\Delta p}$$

Equation 53

Where:

C_i=C_v for iterative purposes
Q= 1.38x10^{-6} m^3/hr
N_1=0.08650 (constant from standard)
ρ_1=830 kg/m^3
ρ_0=1000 kg/m^3
Δp=1.22 kPa
C=1.314x10^{-5}
C_i=1.3.C for C_v=1.70918x10^{-5}

2. Use this C_i value to calculate valve style modifier F_d.

$$F_d = \frac{N_{19}\sqrt{C.F_L}}{D_o}$$

Equation 54

Where:

C_i =1.70918x10^{-5}

F_L=0.95 (table 2 from standard) Liquid pressure recovery factor

N_{19}=1.3 (table 1 from standard) Numerical constant

D_o=0.5 mm Orifice diameter

F_d=0.01047

3. Use F_d to calculate valve Reynolds number Re_v.

$$Re_v = \frac{N_4 F_d Q}{v\sqrt{C_i F_L}}\left(\frac{F_L^2 C_i^2}{N_2 D^4}+1\right)^{1/4}$$

Equation 55

Where:

N_4=0.076 (table 1 from standard) Numerical constant

N_2=0.00214 (table 1 from standard) Numerical constant

v= 0.000032 m^2/s kinematic viscosity

D=1.5 mm Internal diameter of piping

Re_v= 0.00851409 (note Re_v<10000 is non turbulent)

4. Determine correct Reynolds factor (F_R) equation to use and use solve using Re_v.

If $\frac{C}{d^2} < 0.016 N_{18}$

where N_{18}=1 use:

$$F_R = 1+\left(\frac{0{,}33F_L^{1/2}}{n_2^{1/4}}\right)\log_{10}\left(\frac{Re_v}{10000}\right)$$

Where:

$n_2 = 1 + N_{32}\sqrt{C_i/d^2} = 1.35$

N_{32}=127 (table 1 from standard)

F_R= -0.834

Calculate C_v using appropriate equation. In this case, for non-turbulent fluid flow.

$$C = \frac{Q}{N_1 F_R}\sqrt{\frac{\rho_1/\rho_o}{p_1 - F_F.p_v}}$$

C_i= -1.097

5. Compare C_i with C_v to determine correctness. If not, increment C_i by 30% and repeat calculation.

Check $C/F_R<C_i$

C/F_R= -1.5753

C_i= -1.0972

Is true so *should* be the correct value of C_v.

However as can be seen from the above calculation, the negative F_R value results in a negative C_v value which is clearly impossible. The cause of the negative value can be traced to the extremely low Re_v value. Assuming the F_L and n_2 are constant Re_v would need to be above 5.21 to generate a positive C value. Therefore the C_v calculation method described in EN 60534-2-1:1998 is only valid for Reynolds Valve numbers above 5.21.

10.2 Appendix B: RMV Build Procedure

1-Make thermocouples, test and calibrate

2-Measure needle geometry. **Number & Record**

3-Measure orifice diameter and z-axis distance from orifice aperture to top surface of jetpost. **Number & Record**

4-Fit jetpost. Flatten end of nozzle to be used as datum.

5-Measure orifice position. **Number & Record**

- Place measuring gauge in orifice. Align gauge with top surface of jetpost using flat surface inserted into valve body.
- Place on VMM using VMM-RMV fixture and measure gauge end position.
- Remove gauge measure nozzle end position.
- Find difference and subtract from gauge length.
- Nozzle is now reference position for orifice.

6-Drill holes for thermocouples in RMV body. Close together and some bellow. This stops them spreading out and creating a constrictive band with the adhesive which can promote cracking.

7-Unwind TC and rewind in place. X3

8-Glue TCs in place. Use combination of super glue and fixer.

9-Use 2-part epoxy glue to seal RMV body holes.

10-When set apply super glue to TC entry points to fix wires into epoxy and create seal.

11-Heat RMV, Fit cap and test airtight:

- Seal RMV outlet and use connector block and empty fill bottle.
- Submerge in water and pressurise with bottle.
- Check for bubbles.

If airtight, it is possible to complete adjuster mechanism assembly.

12-Align thermocouples in body

13- Ensure flexible hose in top of valve adjuster assembly is trimmed to size before insertion of spring tree.

14- Fit needle to tree

15-Heat RMV. Fit cap to body, ensure dial is in prime position. Take care not to allow Pin to lodge in orifice. This damages the pin surface.

16-Test closing and seal action of assembly. If ok mark close position. If not follow work instruction for needle fitting corrective actions.

17-Loosen screw action by moving back and forth several times.

18- Fit adhesive scale to RMV. Align 0 to closed position.

19-Fit crimp loop to RMV cable. Ensure valve is in PRIME position. This ensures the crimp does not obstruct the movement of the screw adjuster.

20-Measure needle displacement on VMM. **Number & Record**

10.3 Appendix C: Surface Measurement

In order to fully benchmark the needles to be used in flow testing, it is important to understand their initial condition. Part of this is to account for the surface finish of the needles to discount any effects it may have on flow rate. A Mitutoyo Quick Scope 359 3D CNC Vision Measuring Machine (VMM) was used to make two types of surface measurement; surface roughness including Ra, Ry and Rt values and the surface profile. The surface profile allows better visualisation of the surface of the needle, as it does not compensate for surface features. As such the one degree taper of the needle should be clearly visible (see Figure 10-1 b). The surface roughness values are defined as:

Ra= Arithmetic mean

Rt=Absolute max Peak (Rp) – max valley (Rv)= Total Max Peak to valley

Ry=average of Rt sectors

It was found that surface roughness was consistent across all the samples with some exceptions. The arithmetic mean Ra was found to be approximately 0.3μm and Ry values representing the maximum peak to trough distance for a given sector were in the 1.5-2μm range. See Figure 10-1 (a) for a typical reading. It should be noted that the minimum theoretical clearance around the needle is 3μm although the minimum actual clearance was found to be in the region of 17μm. This means that for minimum needle clearance the surface finish may have significant effects on the orifice profile.

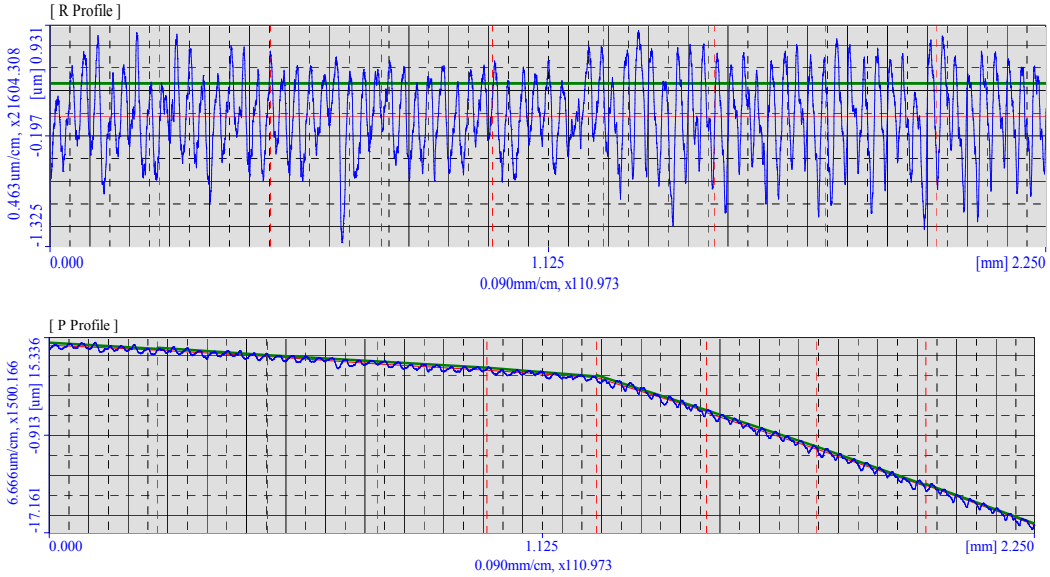

Figure 10-1 a) Normal roughness reading. b) Normal profile reading

As with the used needle described earlier it was found that some of the needles had markings similar to those in Figure 4-14. Due to the small scale it can be difficult to ascertain the nature of surface markings, even using heavy magnification. Surface examination of these markings showed that despite their high visibility, there was mixed results in terms of the effect on the surface roughness and profile. While some large and clearly visible dents had a moderate impact on the surface roughness (Rt up to 4.1µm) and was clearly visible on the profile chart, other markings had a much more significant effect with Rt values up to 38.1µm. This brings the surface roughness into the same scale as the orifice clearance. The different effects of damage to the surface of the needle can clearly be seen in Figure 10-2 and Figure 10-3. The examples of heavy surface damage were measured early in the research project and it was subsequently discovered that much of the pin damage to new needles was due to the valve build process. As a consequence the assembly procedure was changed to avoid damaging the needle.

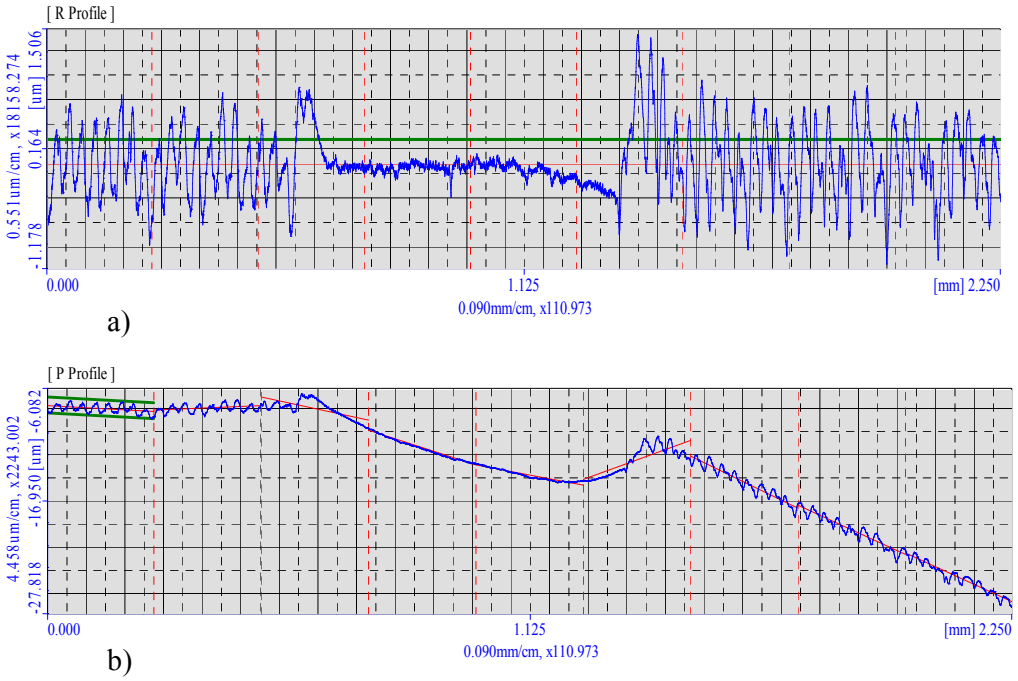

Figure 10-2 Dented needle a) Minor surface roughness effects. The damages has actually smoothed the surface of the needle b) Clear damage as shown in the profile.

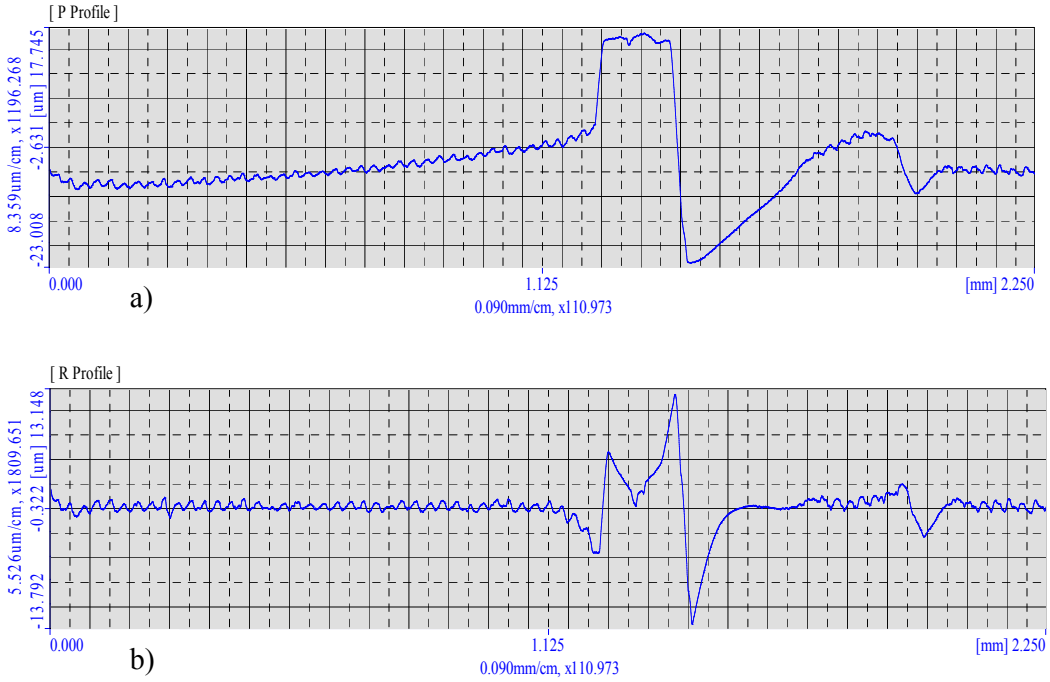

Figure 10-3 Surface damage a) Large scale variations in surface readings. b) Corresponding profile damage

10.4 Appendix D: Prototype Oiler Images

Prototype I

Prototype I Installation

Prototype I Installation

Prototype I Installation

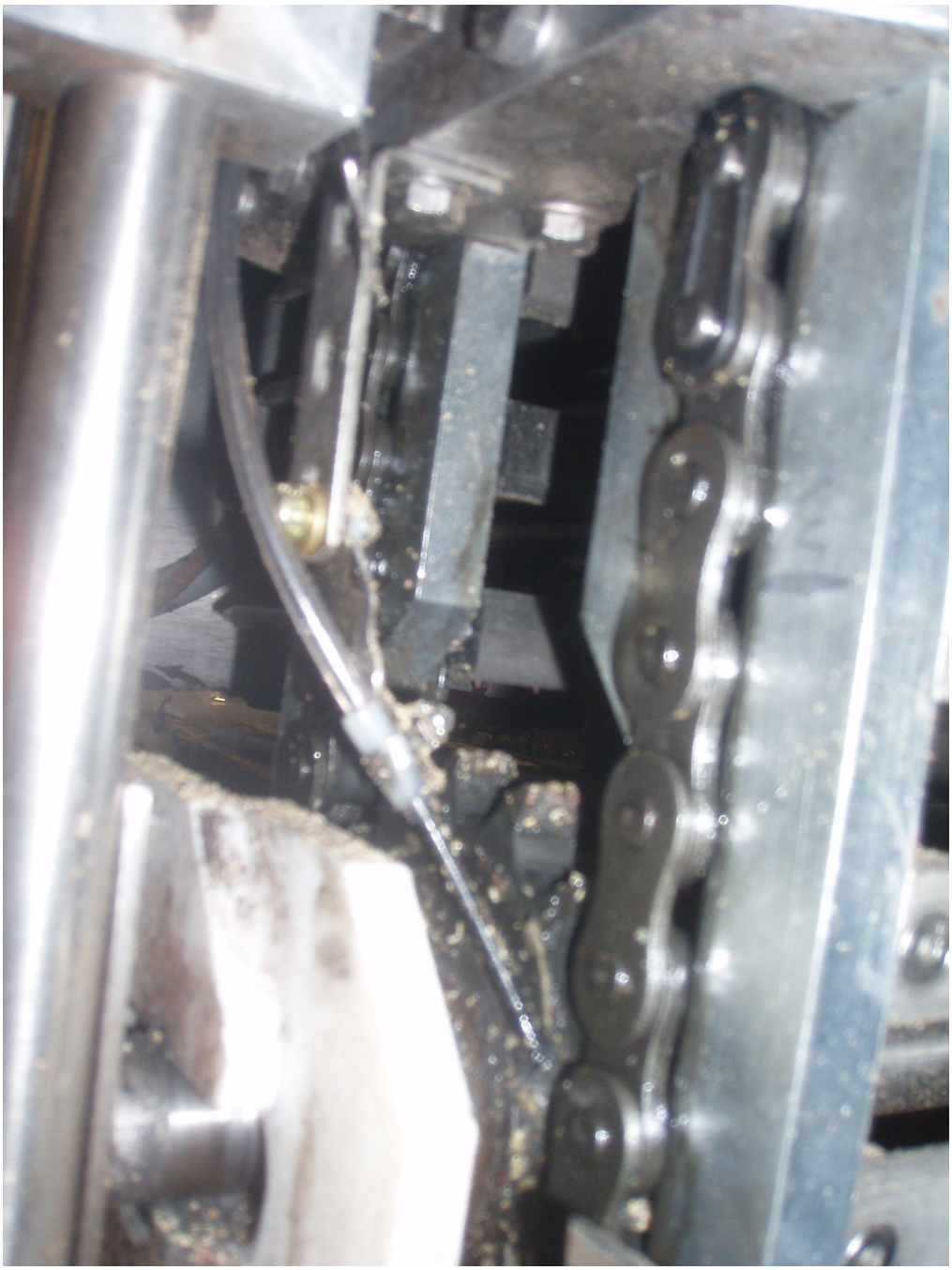

Lubricant feed nozzle

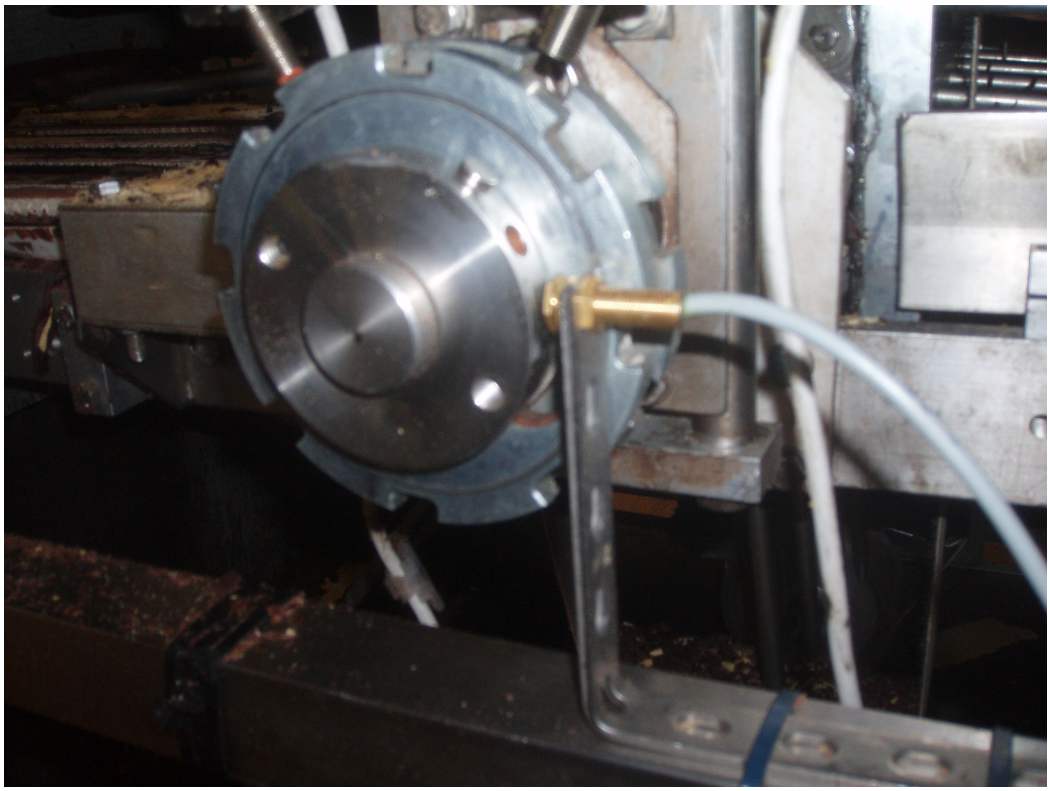

Chain Movement Sensor. Note the brass reed switch and magnets bonded to the shaft.

Prototype II in installed position

Prototype II in installed position

10.5 Appendix E: Prototype Oiler Control Circuit.

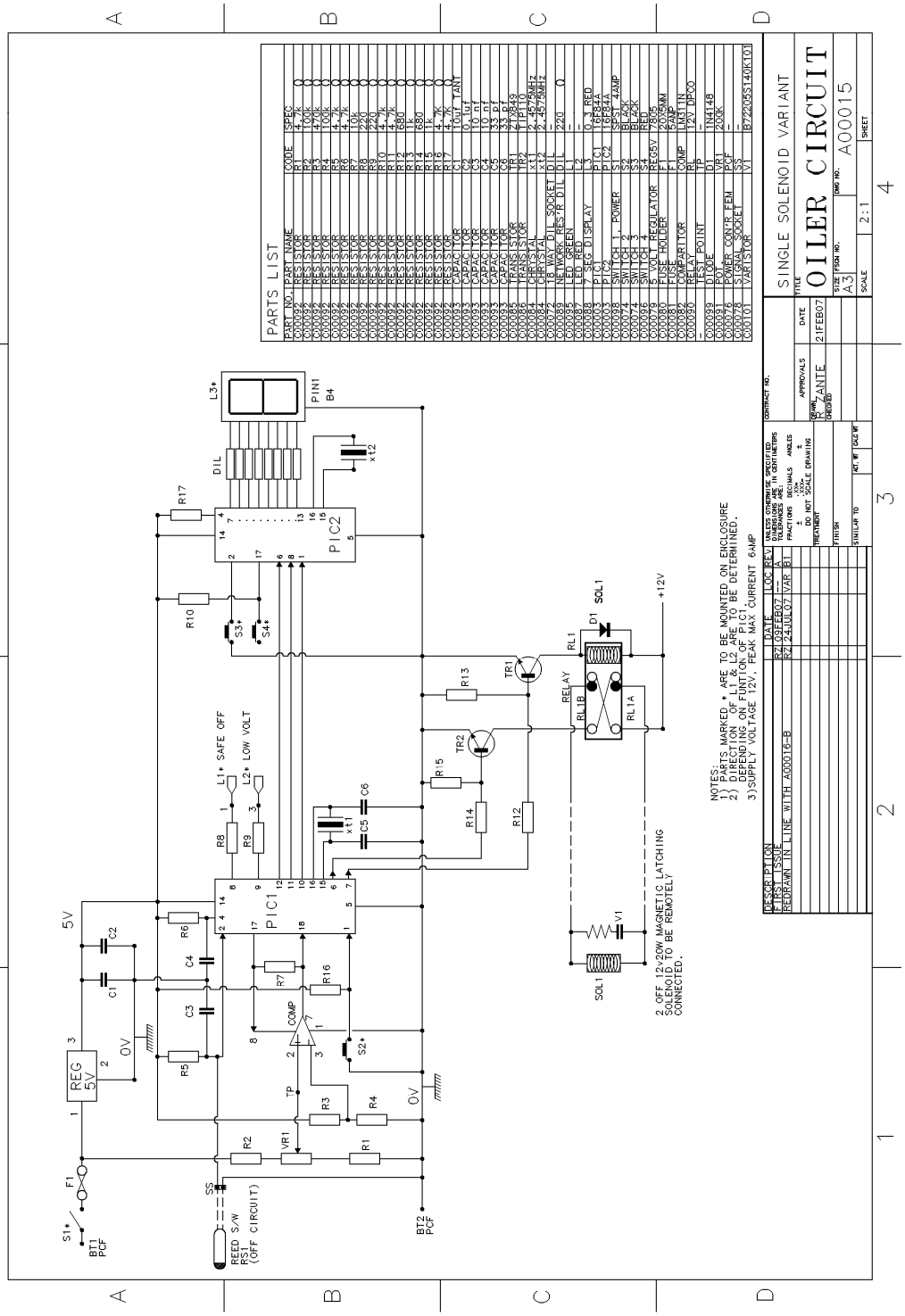

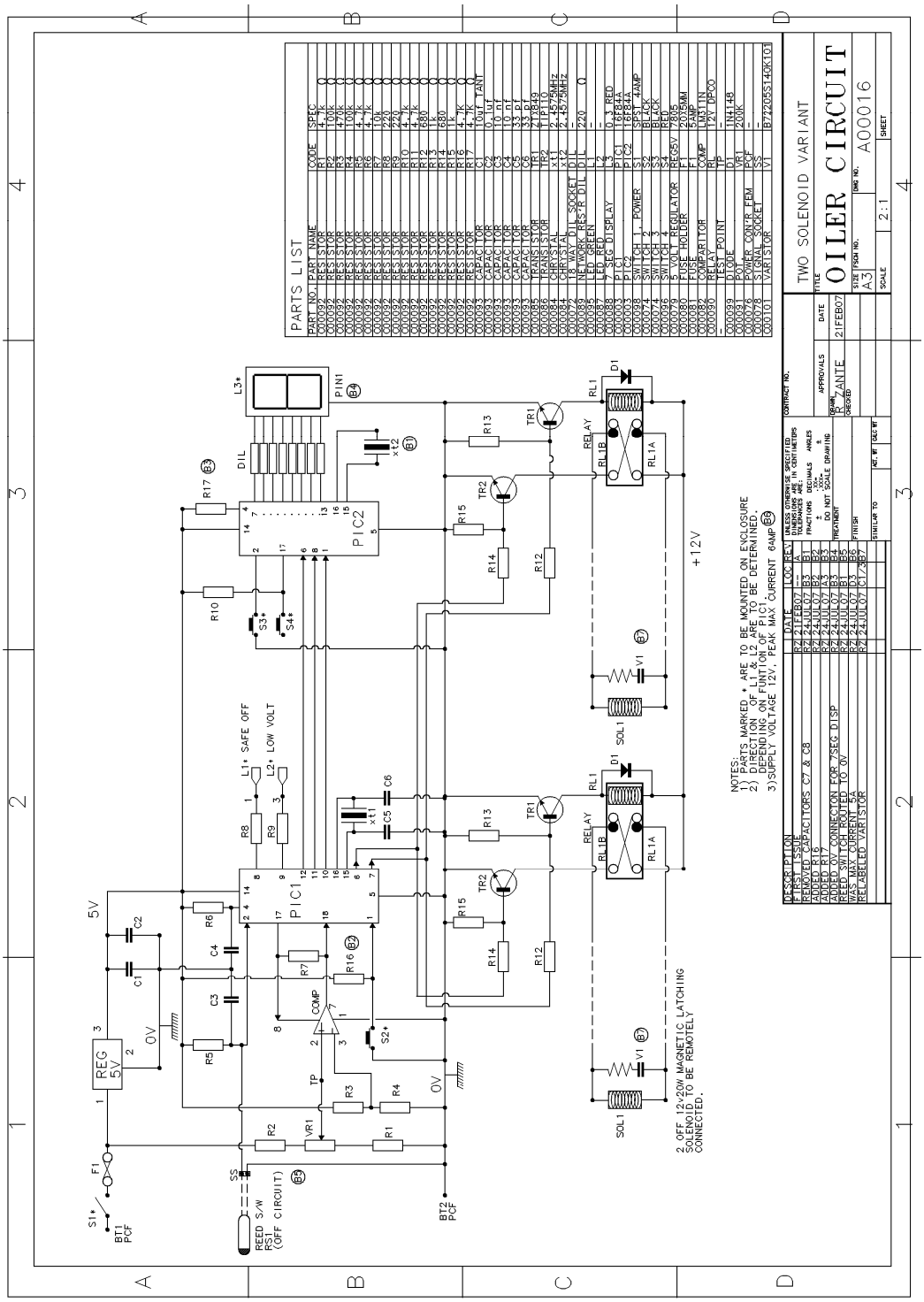
PARTS LIST
PART NO | PART NAME | CODE | SPEC
C00092 | RES STOR | R1 | 4.7K
C00092 | RES STOR | R2 | 100K
C00092 | RES STOR | R3 | 470K
C00092 | RES STOR | R4 | 470K
C00092 | RES STOR | R5 | 4.7K
C00092 | RES STOR | R6 | 4.7K
C00092 | RES STOR | R7 | 22K
C00092 | RES STOR | R8 | 220
C00092 | RES STOR | R9 | 220
C00092 | RES STOR | R10 | 4.7K
C00092 | RES STOR | R11 | 680
C00092 | RES STOR | R13 | 1K
C00092 | RES STOR | R14 | 680
C00092 | RES STOR | R15 | 1K
C00092 | RES STOR | R16 | 4.7K
C00092 | RES STOR | R17 | 4.7K
C00093 | CAPACITOR | C1 | 10uF TANT
C00093 | CAPACITOR | C2 | 10 nf
C00093 | CAPACITOR | C3 | 10 nf
C00093 | CAPACITOR | C4 | 10 nf
C00093 | CAPACITOR | C5 | 33 pf
C00093 | CAPACITOR | C6 | 33 pf
C00084 | CRYSTAL | X1 | 2.4576MHz
C00084 | CRYSTAL | X2 | 2.4576MHz
C00041 | 16 WAY DIL SOCKET | DIL | –
C00089 | NETWORK RES 9 PR DIL | DIL | 220 Ω
C00095 | LED GREEN | L1 | –
C00088 | LED RED | L2 | –
C00003 | DISPLAY | L3 | 0.3 RED
C00003 | PIC | PIC1 | 16F84A
C00003 | PIC | PIC2 | 16F84A
C00078 | SWITCH 1 POWER | S1 | SPST 4AMP
C00078 | SWITCH 2 | S2 | BLACK
C00074 | SWITCH 3 | S3 | BLACK
C00096 | SWITCH 4 | S4 | RED
C00089 | REGULATOR | REG5V | 7805
C00089 | FUSE HOLDER | F1 | 20MM
C00081 | FUSE | F1 | 6AMP
C00082 | COMPARITOR | COMP | LM311N
C00090 | RELAY | RL | 12V DPCO
– | POINT | TP | –
C00099 | DIODE | D1 | 1N4148
C00091 | POT | VR1 | 200K
C00078 | EXTRA LOW VOLT FEM | ELVF | –
C00041 | 8 WAY DIL SOCKET | V1 | –
C00101 | VARISTOR | V1 | B72205S140K101
DESCRIPTION | DATE | LOC | REV
REMOVED 22PACITORS C7 & C8 | R2 21JUL07 | B1 | A1
ADDED R16 | R2 21JUL07 | B2 | A2
ADDED R17 CONNECTION FOR 7SEG DISP | R2 21JUL07 | B3 | A3
REED SWITCH ROUTED TO 0V | R2 21JUL07 | B4 | A4
WAS MAX CURRENT 5A | R2 21JUL07 | B5 | A5
RELABELED VARISTOR | R2 21JUL07 | C1 | A6
CONTRACT NO.
APPROVALS | DATE
DRAWN R.V.ZANTE | 21FEB07
CHECKED
TITLE
TWO SOLENOID VARIANT
OILER CIRCUIT
SIZE | FSCM NO. | DWG NO. | A00016
A3
SCALE | 2:1 | SHEET
FINISH | MATERIAL
SIMILAR TO | NEXT ASSY | USED ON
UNLESS OTHERWISE SPECIFIED DIMENSIONS ARE IN MILLIMETRES TOLERANCES ARE: FRACTIONS ±1/64 DECIMALS ±0.1 ANGLES ±1
DO NOT SCALE DRAWING
TREATMENT
NOTES:
1) PARTS MARKED * ARE TO BE MOUNTED ON ENCLOSURE
2) DIRECTION OF L1 & L2 ARE TO BE DETERMINED.
DEPENDING ON FUNTION OF PIC1
3)SUPPLY VOLTAGE 12V. PEAK MAX CURRENT 6AMP
2 OFF 12-20W MAGNETIC LATCHING SOLENOID TO BE REMOTELY CONNECTED.
+12V
5V
0V
REG 5V
PIC1
PIC2
DIL
COMP
RELAY
SOL1
TR1
TR2
REED S/W (OFF CIRCUIT)
BT1 PCF
BT2 PCF
L1* SAFE OFF
L2* LOW VOLT
L3*

10.6 Appendix F: Reynolds Number Calculation for Concentric Annular Flow

The Reynolds number for an annular flow channel can be calculated from a combination of Equation 2 and Equation 16, in which d_o is replaced by d_m giving:

$$\mathrm{Re} = \frac{4Q_m}{\pi\mu(d_o - d_a)}$$

Equation 15

Mass flow rate at an equivalent value of the nominal maximum and minimum volumetric flow rate is:

	Q		***Q_m***
	ml/hr	**m3/s**	**kg/s**
Min	0.45	1.25x10-10	1.03 x10-7
Max	400	1.11 x10-7	9.16 x10-5

Table 10-1 Volumetric flow rate to mass flow rate conversion

Similarly, dynamic viscosity as an equivalent of kinematic viscosity is:

	Kinematic viscosity *v*		**Dynamic viscosity μ**
	cSt	**St**	**Ns/m^2**
CL32	70	0.7	0.05768
CL220	688	6.88	0.566912

Table 10-2 Kinematic to dynamic viscosity conversion

Using the nominal values for valve dimensions as d_o=0.0015m and d_a=0.001475m gives:

Q ml/hr	CL32 70cSt	CL220 688 cSt
0.45	0.0909	0.0093
400	80.8406	8.2251

Table 10-3 Re_c values for maximum and minimum valve flows.

As boundary between the turbulent and laminar regime for flow in pipe occurs at Reynolds numbers of approximately 2300, this application is firmly in the laminar regime.

10.7 Appendix G: Eccentric Annular Profile Derivation

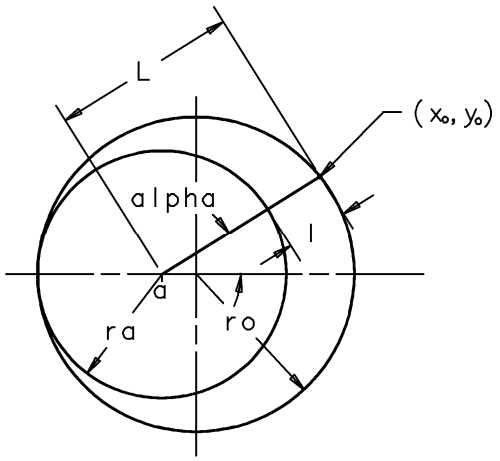

Figure 10-4 Needle orifice geometry

$$x_o^2 + y_o^2 = r_o^2$$

$$y_o = \sqrt{r_o^2 - x_o^2}$$

$$for - r_o < x < r_o$$

$$L = \sqrt{(x+a)^2 + y^2}$$

$$l = L - r_a$$

$$\sin\alpha = \frac{y_o}{L}$$

Where x_o,y_o is a point on the orifice circumference, r_o is the radius of the orifice, r_a is the radius of the cylindrical section of the needle, a is the distance from the centre of the needle to the point on the orifice diameter and is equal to r_o-r_a, l is the distance between the needle and the orifice and represents the channel height and α is the angle between the x-axis and the line L.

10.8 Appendix H: Viscosity Comparison Charts

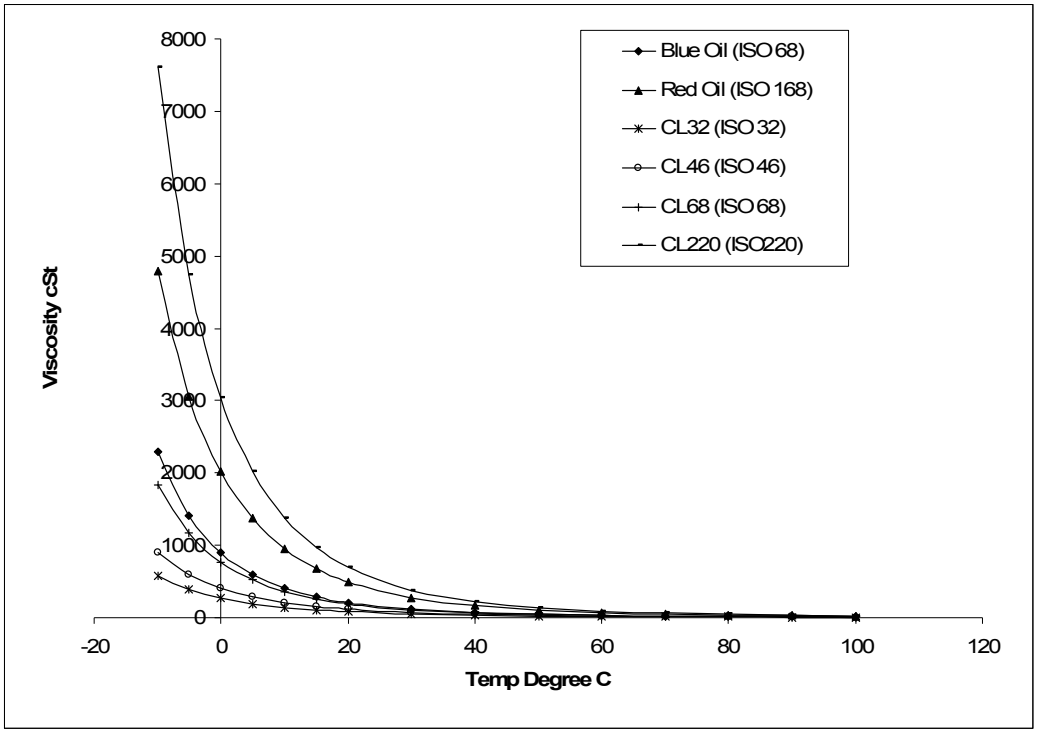

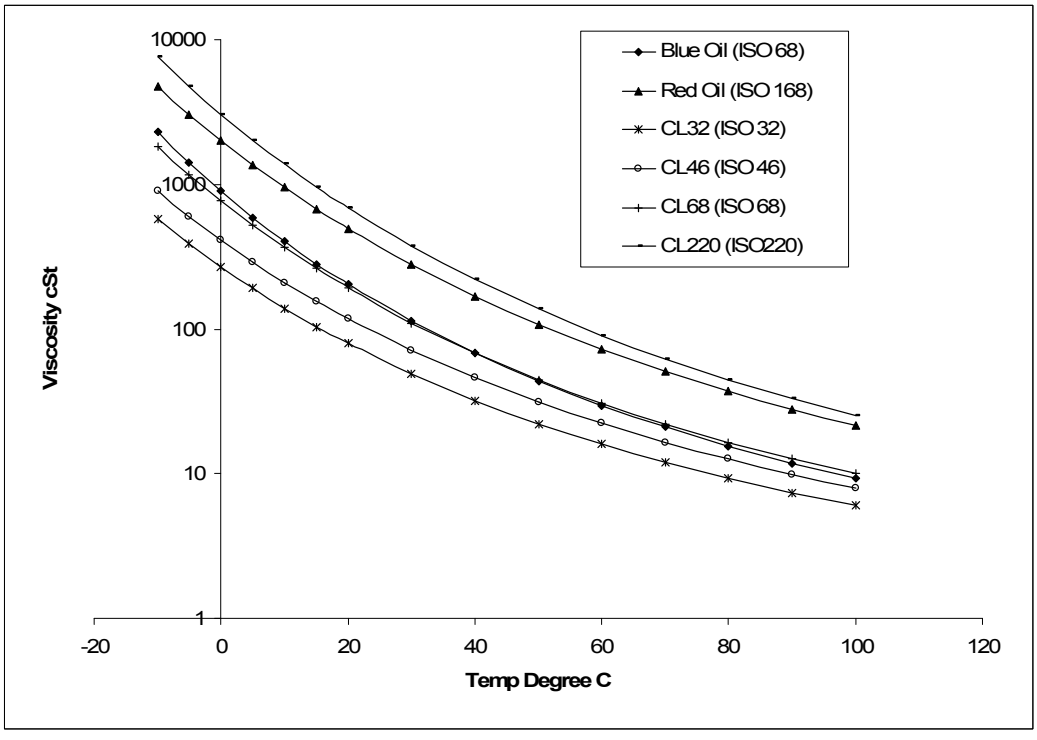

10.9 Appendix I: List of Publications

[150] R. C. Zante and X.-T. Yan, "AN INVESTIGATION INTO THE USE OF NEURAL NETWORKS IN THE DESIGN OPTIMISATION OF A GRAVITY FED NEEDLE VALVE," presented at ICDM06, Bristol, 2006.

[151] R. C. Zante and X.-T. Yan, "A MECHATRONIC SOLUTION TO INVESTIGATING A GRAVITY-FED OIL DISPENSING NEEDLE VALVE," presented at MX2006, Penn State, Philadelphia, 2006.

[152] R. C. Zante, "Piezo-electric transducer based very low flow, large range, measurement method." *Under review by Flow Measurement and Instrumentation*, September 2007.